Anaerobic biodesulfurization of thiophenes

Chris Marcelis

Anaerobic biodesulfurization of thiophenes

Chris Marcelis

Proefschrift

Ter verkrijging van de graad van doctor

Op gezag van de rector magnificus

van Wageningen Universiteit,

Prof. dr. ir. L. Speelman,

in het openbaar te verdedigen

op maandag 16 december 2002

des namiddags te half twee in de Aula

Aan Sandra

Table of contents   page

CHAPTER 1

INTRODUCTION

BACKGROUND

Oil-refining industries have to cope with more stringent specifications on the sulfur content that are driven by environmental concerns (Anabtawi *et al.*, 1996). During the last decade, clean air considerations have led to drastic reductions on the allowable sulfur content for gas oil, as depicted in Table 1. The stricter regulations on the sulfur content for gas oil are an impetus to perform research on deep desulfurization to obtain gas oils with low sulfur concentrations (Table 1). To give an outline; 75% of the refractory sulfur compounds must be converted, without altering the remaining hydrocarbons in the gas oil that constitute more than 98% of the gas oil (Segawa *et al.*, 2000).

Table 1: Product specification requirements for gas oil.

Year	Sulfur content
Prior 1990	0.3 – 0.5 wt.% world wide
1990 - 1994	0.2 wt.% EC* and Japan
1994	0.05 wt.% USA
1996	0.05 wt.% EC and Japan
2000	0.035 wt.% EC
2005	0.005 wt.% EC

*European Community

The use of insufficiently desulfurized distillates as fuels results in the formation of sulfur oxides. These sulfur-containing emissions contribute to the acid deposition ('acid rain') and were the impetus to announce stringent legislation. Future restrictions on the sulfur content are mainly driven to reduce the amount of particulates formed during the burning of the fuel and to improve the applicability of exhaust catalysis. Apart from legislative constraints, downstream catalytic requirements have an impact on the allowable sulfur content in oil fractions, *e.g.* catalytic reforming processes are more efficient in the absence of organic sulfur compounds.

Unfortunately, there is a trend towards higher sulfur contents of the crude oil reserves. Easily accessible and relatively low sulfur oil-reserves are being depleted; consequently reserves with higher sulfur contents must be used as feedstock for refining processes.

SULFUR COMPOUNDS IN OIL

The sulfur content of crude oil from different sources ranges from 0.03 wt.% to values as high as 8 wt.%, which was demonstrated in a previous study on 78 different crude oil types (Rall *et al.*, 1972). Organic sulfur compounds are the most important constituents, but inorganic sulfur *i.e.* elemental sulfur, hydrogen sulfide and pyrites can also be present (Tissot *et al.*, 1984). An overview concerning the ranges of organic sulfur contents as present in crude oils found in different countries over the world is given in Table 2.

Table 2: Organic sulfur contents in crude oils (De Krom, 2002).

source	wt.% sulfur
Argentina	0.06 - 0.42
Australia	0 - 0.1
Canada	0.12 - 4.29
Cuba	7.03
Denmark	0.2 - 0.25
Egypt	0.04 - 4.19
Indonesia	0.01 - 0.66
Iran	0.25 - 3.23
Iraq	2.26 - 3.3
Italy	1.98 - 6.36
Kuwait	0.01 - 3.48
Libya	0.01 - 1.79
Mexico	0.9 - 3.48
Nigeria	0.04 - 0.26
Norway	0.03 - 0.67
Russia	0.08 - 1.93
Saudi Arabia	0.04 - 2.92
United Kingdom	0.05 - 1.24
USA	0.29 - 1.95
Venezuela	0.44 - 4.99

In addition to the data depicted in Table 2 it should be mentioned that the Middle East and Venezuela have the most oil reserves with high organic sulfur contents (De Krom, 2002). More than 200 sulfur-containing organic compounds have been identified from crude oils, these compounds include sulfides, mercaptanes and thiophenes. Some molecular structures are presented in Fig. 1. The distribution and amount of organic sulfur compounds reflect the source and maturity of the crude oil (Ho *et al.*, 1974). Chemically immature oils are rich in sulfur and often have a high content in non-thiophenic sulfur compounds. During

maturation labile non-thiophenic compounds are degraded and the sulfur content decreases (Payzant *et al.*, 1986). Mature oils contain mainly high molecular weight alkylated benzo- and dibenzothiophene derivates, the benzothiophene:dibenzothiophene ratio decreases with maturity (Tissot *et al.*, 1984). Because of the ubiquity of alkylated benzo- and dibenzothiophenes in practically all crude oils, these compounds represent the bulk of sulfur. The majority of the alkylated benzothiophenes can be found in the boiling point range of 220 up to 300ºC, then alkylated dibenzothiophenes are found with boiling points up to approximately 350ºC (Schultz *et al.*, 1999).
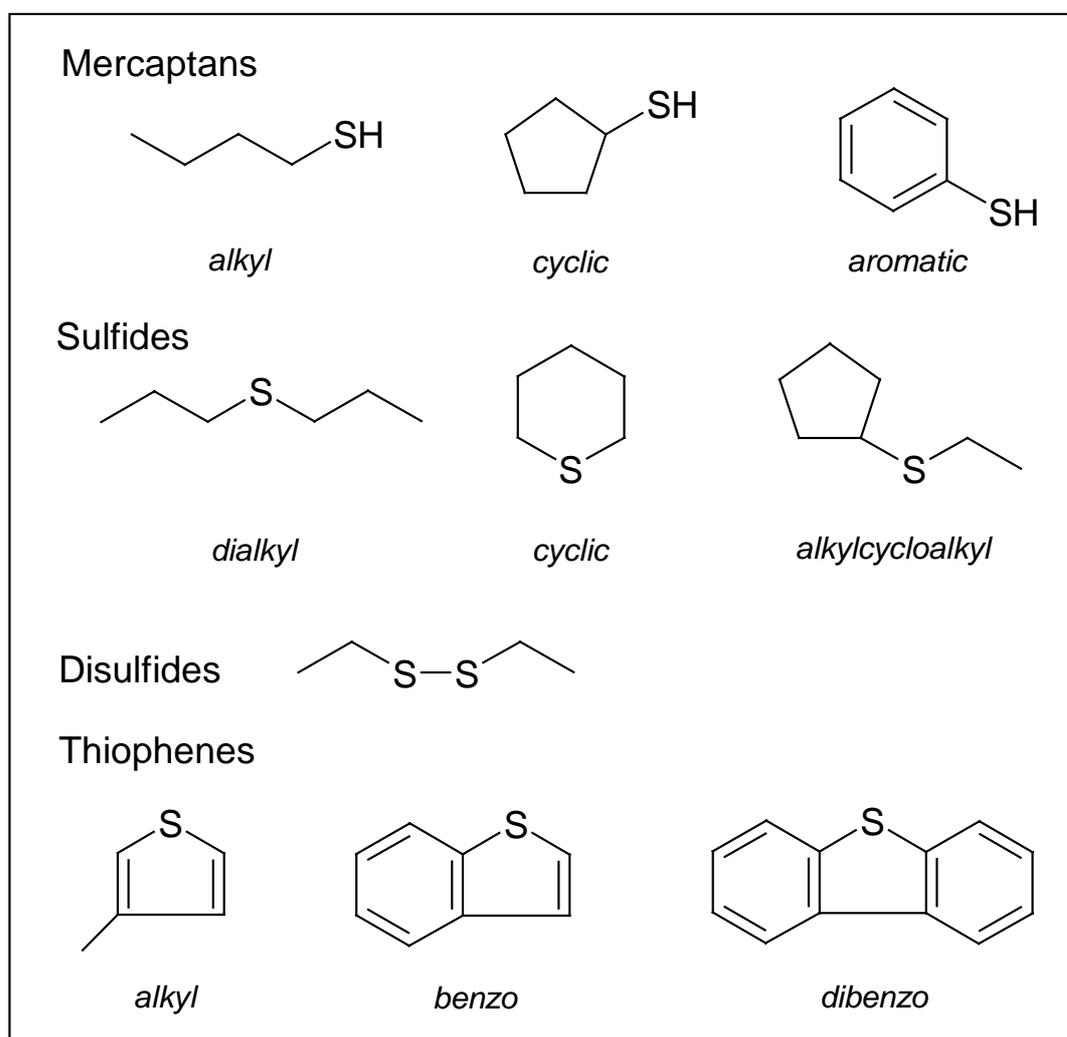

Fig. 1: Chemical structures of organic sulfur compounds present in crude oils.

PHYSICO-CHEMICAL HYDRODESULFURIZATION

Conventional hydrodesulfurization

Hydrodesulfurization (HDS) is an established physico-chemical technology to remove organically bound sulfur down to specified levels (Speight, 1981). The desulfurization of organic sulfur compounds as present in the boiling point range typical for gas oil (260 up to 350°C) is of particular importance (Schulz *et al.*, 1999). The removal of the bulk of sulfur present in gas oil is conventionally performed by hydrotreatment with cocurrent downward flow of hydrogen gas and hydrocarbon over a catalyst bed, known as the trickle-flow concept. In the presence of a catalyst, hydrogen gas reacts with the sulfur compounds to produce gaseous hydrogen sulfide. Typical HDS conditions are temperatures between 200 and 350°C and pressures from 5 up to 10 MPa, depending on the desulfurization severity required.

Unfortunately, the conventional technique is not suitable to meet the future specified deep desulfurization levels. Important aspects that play a role to achieve these levels are the application of novel catalyst types and innovations on HDS process configurations.

HDS reaction mechanism and catalyst performance

Reaction pathways for benzothiophene and dibenzothiophene

For the desulfurization of benzothiophene (BT) two different parallel reactions with H_2 are catalyzed, known as the hydrogenation and the hydrogenolysis pathway (Fig. 2). In the hydrogenation pathway the thiophene ring is hydrogenated prior to desulfurization, while in the hydrogenolysis pathway the thiophene ring is split due to the attack of surface adsorbed hydrogen at the sulfur atom (Van Parijs *et al.*, 1986). For BT desulfurization the hydrocarbon products are styrene and ethylbenzene. The H_2S formed inhibits the hydrogenolysis but not the hydrogenation reactions.
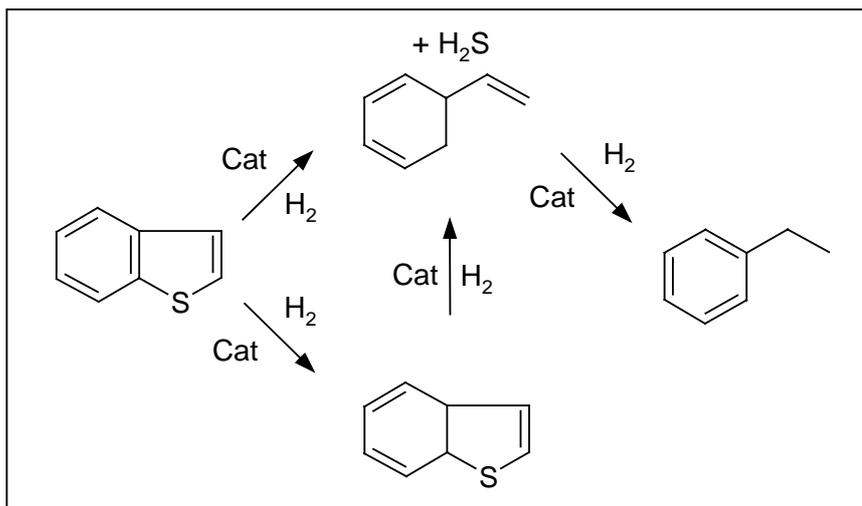
Fig. 2: HDS reaction mechanism for benzothiophene (Cat = catalyst).

Houalla *et al.* (1980) proposed the HDS reaction network for DBT as depicted in Fig. 3. According to this mechanism the conversion proceeds via the path of minimal H_2 consumption, the hydrogenation of biphenyl and cyclohexylbenzene (CHB) proceeds slowly. The rate of DBT hydrogenation increased at higher H_2S concentrations at the expense of hydrogenolysis. Furthermore, the CHB concentrations depend on the catalyst type applied.
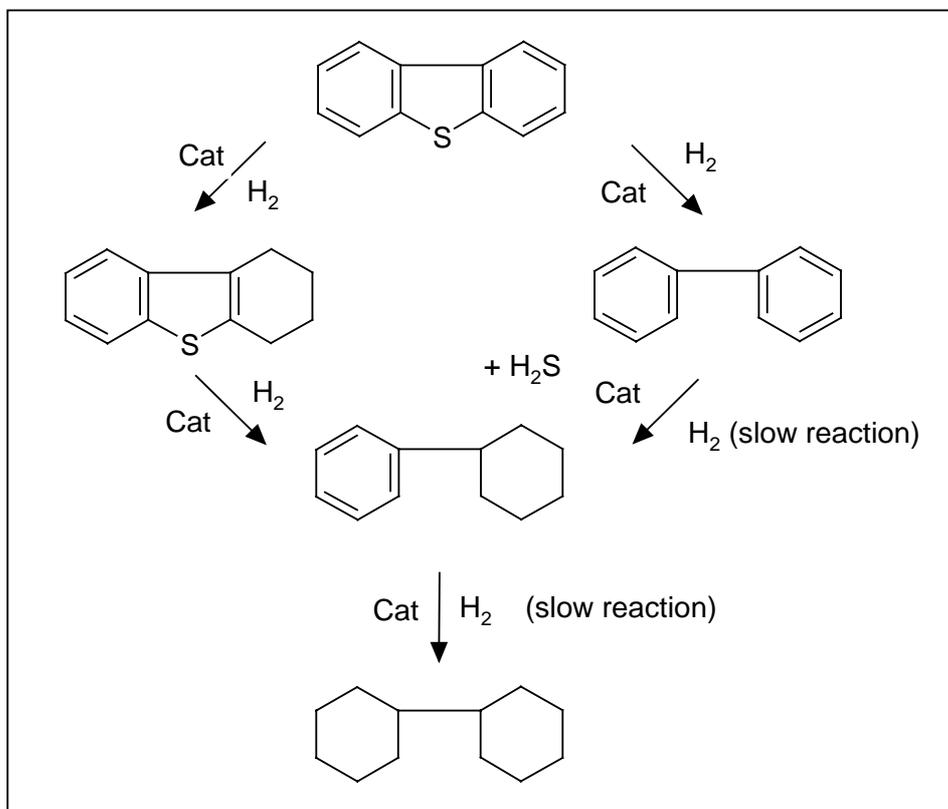
Fig. 3: Proposed reaction mechanisms for DBT hydrodesulfurization (Cat = catalyst).

The presence of alkyl substituents on (di)benzothiophene molecules might favor one of the possible HDS routes, this will depend on the alkyl substituent position and thus to what extent the electron density is altered by the electron donating effect of alkyl groups (Schulz *et al.*, 1999). In addition, substituents in the vicinity of the sulfur atom cause steric hindrance and influence the HDS route (Kabe *et al.*, 1992), as will be discussed below.

Catalysts

Dibenzothiophene (DBT) and alkyl derivatives substituted adjacent to the sulfur atom are refractory to HDS using conventional catalysts. The key sulfur compounds present in gas oil fractions after conventional HDS are 4-methyldibenzothiophene (4-MDBT) and 4,6-dimethyldibenzothiophene (4,6-DMDBT), as depicted in Fig. 4.
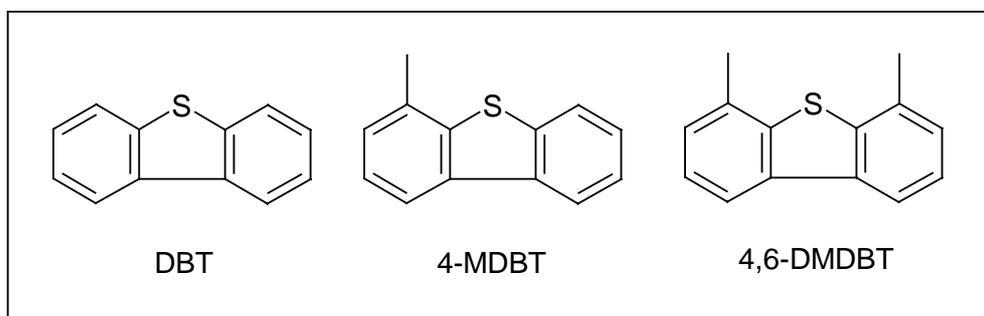
Fig. 4: Structural formulas of refractory methylated dibenzothiophenes.

The γ-alumina (γ-Al$_2$O$_3$) supported molybdenum oxide catalysts promoted with cobalt or nickel have been widely used in conventional HDS processes (Segawa *et al.*, 2000). Active sites are formed when MoO$_3$ changes to MoS$_2$ by sulfurization (Arnoldy *et al.*, 1985). The question arises if these catalyst types are the most optimal to use for deep desulfurization. The hydrogenation route is the most important pathway in the HDS of DBT molecules with substituents on the 4- and 6-postition (Kabe *et al.*, 1993). The direct hydrogenolysis route is less favourable due to the steric hindrance (Robinson *et al.*, 1999a). The molecule becomes more flexible upon hydrogenation of (one of) the aromatic rings and the steric hindrance is relieved (Kabe *et al.*, 1993; Landau *et al.*, 1996). Consequently, catalysts with a relatively high hydrogenation activity must be considered. Nickel promoted mixed sulfide catalysts are known for their high hydrogenation activity (Van Veen *et al.*, 1993). Furthermore, noble catalysts (containing Pt or Pd) are attractive to use, because of their high hydrogenation activity (Robinson *et al.*, 1999b). Kabe *et al.*

(2001) reported that under deep desulfurization conditions, the H_2S partial pressure has a strong inhibitory effect on the catalytic activity and product selectivity of HDS reactions of dibenzothiophene and 4,6-DMDBT. The inhibiting effect is the result of the more strongly adsorption of H_2S compared to DBT and 4,6-DMDBT on the catalyst and thus dependent on the catalyst type. Noble catalysts are characterized by a sensitivity for elevated H_2S levels (Stanislaus *et al.*, 1994). If deep desulfurization is performed in a separate process stage, *i.e.* after initial removal of the bulk of organic sulfur, alternative catalyst types can be applied, because high H_2S concentrations are minimized. Robinson *et al.* (1999a) evaluated the role of the catalyst support in deep HDS. When NiMo was supported on amorphous silica-alumina (ASA) instead of alumina (γ-Al_2O_3), hydrogenation of 4-MDBT and 4E6M-DBT (4-ethyl,6-methyl-dibenzothiophene) could be increased. Based on the level of 4E6M-DBT desulfurization, this study demonstrated that CoMo and NiMo catalysts are inappropriate to apply in deep desulfurization processes (Robinson *et al.*, 1999a). On the contrary ASA supported NiW and Pt catalysts showed a much better performance in 4E6M-DBT desulfurization because of their high hydrogenation activity, especially at low H_2S levels (Robinson *et al.*, 1999b). However, when pre-hydrotreated gas oils are subjected to deep desulfurization, other competing reactants are present which complicate the interpretation of single component model studies (Reinhoudt *et al.*, 1999). In the study of Reinhoudt *et al.* (1999) it was shown that ASA supported Pt/Pd catalysts are very promising to apply in deep desulfurization, provided that H_2S is removed efficiently. A major drawback is the price of the noble metals.

During HDS, the catalysts will age and deactivate as the result of coke and metal deposition on the catalyst (Seki *et al.*, 2001). The deposition severity in greatly influenced by the feedstock properties. As asphalthenes are precursors for coke formation higher boiling point fractions increase the deactivation. Next to that the HDS reaction conditions, temperature (regarding coke formation) and pressure (regarding metal deposition), enhance the deactivation.

Developments in HDS reactor configurations

Apart from the catalyst type involved, optimal process configurations to minimize the suppression of H_2S on the catalyst activity are important. The H_2S produced from sulfur compounds with higher reactivity in the early stage of desulfurization, negatively influences HDS of less reactive sulfur compounds. To circumvent this problem a two-stage principle carried out in conventional cocurrent trickle-flow reactor can be applied. After removal of the bulk of easily convertible sulfur compounds in the first step, the more refractory compounds are removed in the second step with pure hydrogen (Ma *et al.*, 1994; Reinhoudt *et al.*, 1999). This approach also enables the use of the most appropriate catalyst types in different stages (Reinhoudt *et al.*, 1999). A more favorable H_2S profile during HDS can be achieved with countercurrent flow. Unfortunately, using liquid velocities at a practical scale, flooding prevents the down flow of liquid against up flowing gas (Sie, 1999). To operate below the flooding limit, the catalyst particle diameter must be increased leading to unacceptable pore diffusion limitations (Hanika *et al.*, 1992).

Reactors using monolithic catalyst supports may be an attractive alternative to conventional multi-phase reactors (Kapteijn *et al.*, 2001). Instead of a catalyst trickle-bed, monolithic channels are present were bubble-train (or Taylor) flow occurs. Gas bubbles and liquid slugs move with constant velocity through the monolith channels approaching plug flow behavior. Gas is separated from the catalyst by a very thin liquid film and during their travel through the channels the liquid slugs show internal recirculation. These two properties result in optimal mass transfer properties (Kapteijn *et al.*, 2001). Apart from that very sharp residence time distributions for gas and liquid compared to trickle flow can be achieved (Nijhuis *et al.*, 2001). Currently, the application of monoliths in various forms and applications is an object of research (Kapteijn *et al.*, 2001). Larger channel geometries ('internally finned monolith channels') might allow countercurrent flow at a relevant industrial scale and the scale up properties are promising.

BIODESULFURIZATION AS COMPLEMENTARY TECHNIQUE FOR HDS

The use of microorganisms might offer an alternative way to remove sulfur specifically from hydrocarbon fractions without altering the carbon skeleton. Biodesulfurization is considered as an environmentally benign process because of the mild process conditions (low pressure and temperature). However, conversion rates are expected to be lower than the aforementioned HDS technique. Therefore, biodesulfurization can be considered as a complementary process, after the bulk sulfur is removed using HDS techniques. The cleavage of carbon-sulfur bonds can be performed either with an aerobic or an anaerobic mechanism. Based on the bond strengths summarized in Table 3 the C-S bonds in the sulfur heterocycles (thiophene, benzo- and dibenzothiophene) will be broken preferentially (Bressler *et al.*, 1998). The C-C bond strengths are greater compared to the C-S bond strengths. As can be seen from Table 3, the addition of oxygen to a carbon atom adjacent to the sulfur atom weakens the bond strengths making the C-S bond more susceptible to cleavage. This is a common feature in the aerobic microbial conversion of sulfur compounds, where enzymes (dioxygenases) introduce oxygen molecules to facilitate C-S cleavage. According to the bond strengths (Table 3) the C-S bonds will also be attacked preferentially in the anaerobic reaction mechanism that is similar as the metal-catalyzed HDS reaction mechanism. The role of enzymes to enable an attack on the C-S bond in the anaerobic route is currently unknown.

Table 3: Bond strengths of various C-S, C-C and C-H bonds (adapted from Bressler *et al.*, 1998).

C-S bonds	(kJ/mol)	C-C bonds	(kJ/mol)
C-S in thiophene	341	H_3C-CH_3	376
C-S in benzothiophene	339	$H_2C=C_2H$	733
C-S in dibenzothiophene	338	C-C in benzene	505
$HS-CH_3$	312	$H_3C-CH_2CH_3$	330
H_3C-SCH_3	308	$H_3C-COCH_3$	290
$H_3C-SO_2CH_3$	280	C-H bonds	(kJ/mol)
$H_3C-SCH_2C_6H_5$	257	$H-CH_3$	438
$H_3C-SO_2CH_2C_6H_5$	221	$H-CH_2OH$	410
		H-CHO	364

AEROBIC BIOLOGICAL DESULFURIZATION

Mechanism of aerobic desulfurization

A vast amount of research is performed on the development of aerobic microbiological desulfurization. Dibenzothiophene (DBT) is the key heterocylic sulfur compound used in most biodesulfurization studies.

Kodama *et al.* (1973) were the first to report on the aerobic conversion of DBT. The transformation of DBT with the 'Kodama' pathway results in ring cleavage of one of the aromatic DBT rings, while the sulfur is not released. Also *Brevibacterium* sp. performs an aspecific pathway using DBT as the sole source of carbon, sulfur and energy (Van Afferden *et al.*, 1990). Because of the degradation of C-C bonds the caloric value is altered, consequently this route is not desirable in biodesulfurization.

The first sulfur selective *Rhodococcus erythropolis* strains were isolated by Kilbane *et al.* (1989). This species is able to carry out a stepwise selective oxidation of the hetero sulfur atom, while the carbon skeleton is not metabolized. *Rhodococcus* strain IGTS8 appeared to be able to utilize a wide range of organic sulfur compounds as the sole source of sulfur, *i.e.* thiophenes, sufides, disulfides, mercaptans, sulfoxides and sulfones (Kayser *et al.*, 1993). In particular sulfur is removed from DBT to give the end-product 2-hydroxybiphenyl (Gallagher *et al.*, 1993). The sulfur specific metabolic pathway for DBT desulfurization involves four enzymatic steps and is designated the 4S-pathway. The 4S-pathway is presented in Fig. 4. *Rhodococcus* strain IGTS8 desulfurizes DBT using three enzymes DszA, DszB and DszC, which are localized at the plasmid-encoded (dsz) operon. Denome *et al.* (1993; 1994) and Piddington *et al.* (1995) provided insight in the sequence of reactions by identifying and cloning the responsible desulfurization dszA, dszB and dszC genes. Oldfield *et al.* (1997) succeeded in the conclusive elucidation of the 4S-pathway by analyzing the intermediates and products of the 4S-pathway.

As depicted in Fig. 5, a mono-oxygenase (DszC) catalyses the stepwise S-oxidation of DBT, first to dibenzothiophene 5-oxide (DBTO) and then to dibenzothiophene 5,5-dioxide (DBTO$_2$). The second mono-oxygenase (DszA) catalyses the conversion of DBTO$_2$ to 2-(2'-hydroxyphenyl)benzene sulfinate (HBPS). The last step is catalyzed by a sulfinase (DszB) and yields 2-hydroxybiphenyl (2-HBP) and sulfite as the end-products.
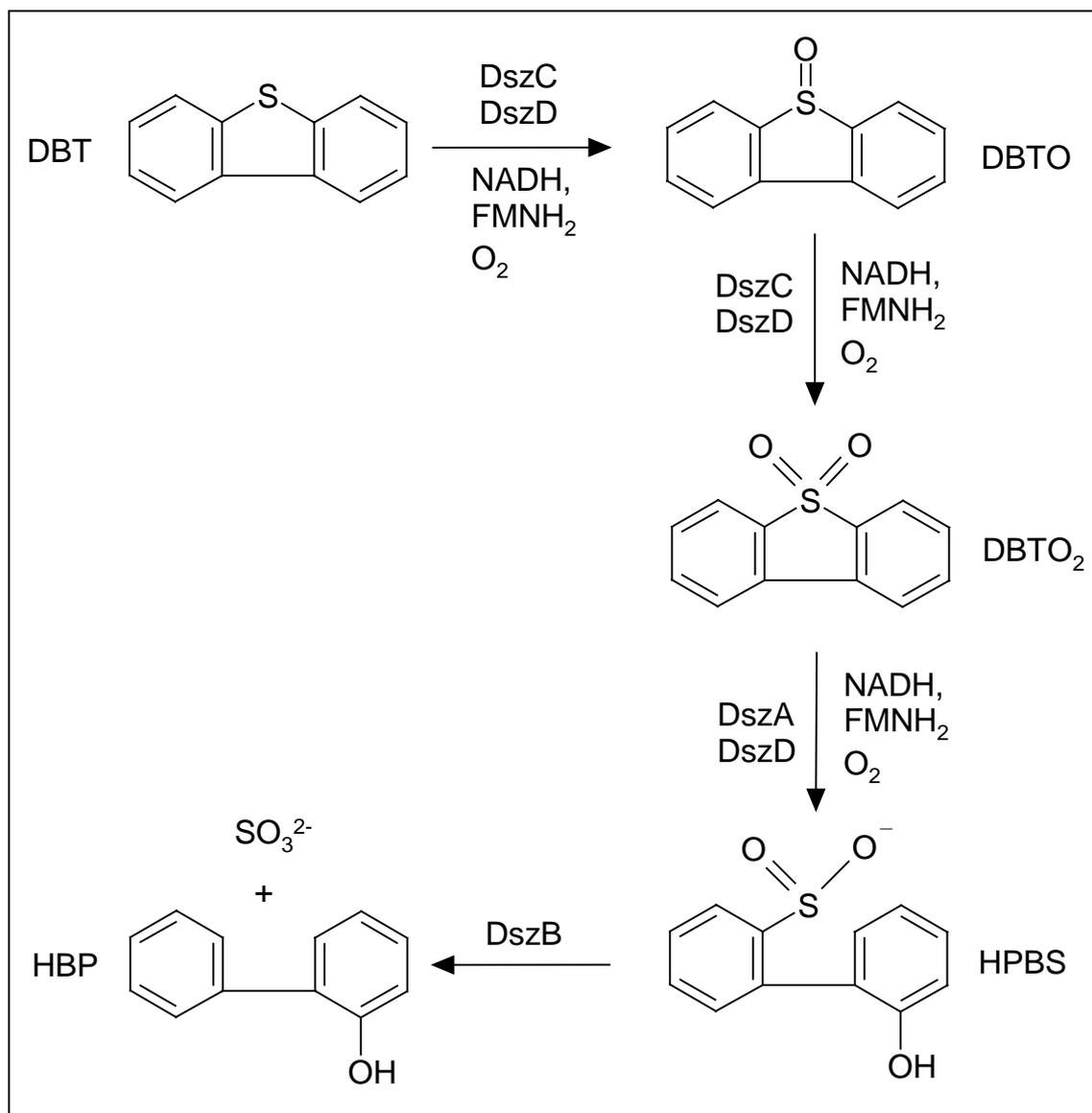
Fig. 5: 4S-pathway as performed by *R. erythropolis* IGTS8.

Enzymatic studies on *R. erythropolis* strain D-1 revealed the essential role of NADH as cofactor (Izumi *et al.*, 1994; Ohshiro *et al.*, 1994; Ohshiro and Izumi, 1999). It appeared that both oxygenases (DszA and DszC) require a flavin-oxidoreductase (DszD) for the catalytic actvity encoded by the dszD gene (Xi *et al.*, 1997; Gray *et al.*, 1996). The role of NADH and reduced FMN (FMNH$_2$) from flavin reductase in the DszA-catalyzed oxygenation of DBTO$_2$ (see Fig. 5) is presented schematically in Fig. 6.
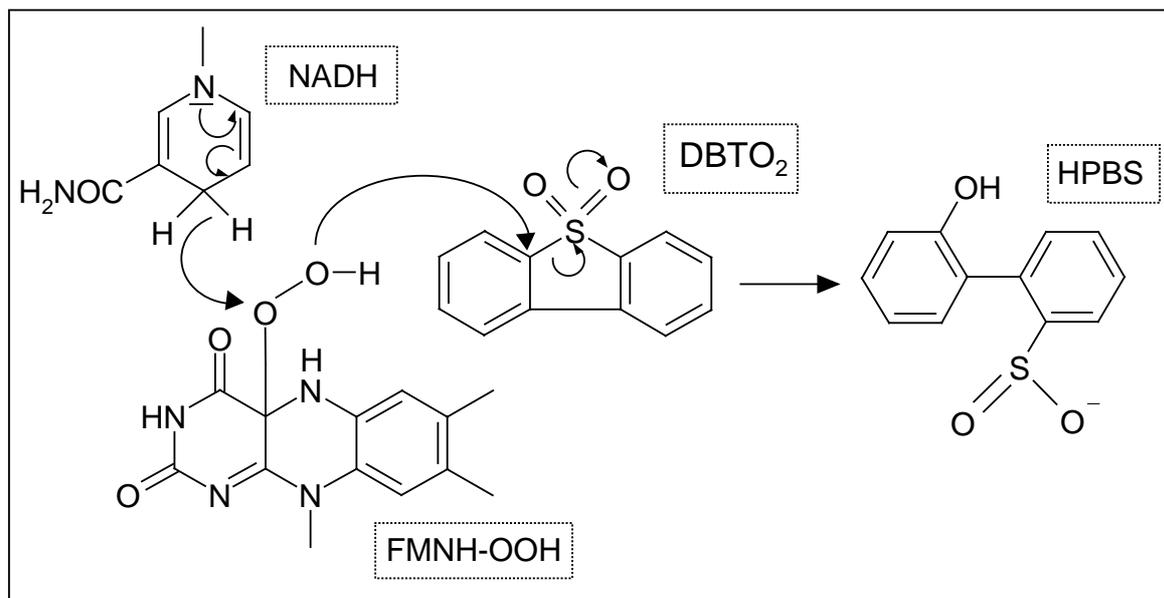
Fig. 6: Simplified reaction mechanism for the DszA-catalysed conversion of $DBTO_2$. Oldfield *et al*. (1997) propose the binding of $DBTO_2$ and $FMNH_2$ with DszA. After the reaction of $FMNH_2$ with O_2, an attack on the C-S carbon bond of $DBTO_2$ occurs resulting in HPBS. The DszD (NADH-FMN) flavin-oxidoreductase is utilized to supply free $FMNH_2$ to the oxygenase (Xi *et al.*, 1997). Only the relevant nicotinamide moiety of NADH and isoalloxazine moiety of FMNHOOH are shown.

Xi *et al.* (1997) suggest that the flavin is not a cofactor of the DszA or DszC enzyme, but the reduced form of flavin serves as a substrate, neither oxygenase uses NAD(P)H directly. The desulfination of HPBS to 2-HBP catalyzed by DszB was found to be the rate-limiting step (Gray *et al.*, 1996).

The end-product of the 4S-pathway is sulfite, which is released in the cytoplasm and assimilated (Fig. 5). However, to enable technological applications, the flux through this pathway must be enlarged considerably. Therefore, genetic and metabolic engineering efforts are applied currently (Arensdorf *et al.*, 2002; Hirasawa *et al.*, 2001; Matsui *et al.*, 2001a; Kertesz and Wietek, 2001; Li *et al.*, 1996).

Rate and extent of aerobic biodesulfurization

The majority of the studies conducted on the selective removal of organosulfur compounds use *R. erythropolis* as the biological catalyst, but other microorganisms are applied as well. All of these strains use the 4S-pathway and produce a stoichiometric amount of biphenyl from DBT. The 4S-pathway can proceed when the cells are not growing. However, essential co-factors to sustain the oxidation-reduction reactions are

required. An overview of a selection of DBT converting species using the 4S-pathway is presented in Table 3.

Table 3. Overview of reported aerobic degradation rates using the sulfur selective 4S-pathway at resting cell reaction conditions.

strain / microorganism	Specific Rate	Reference
R.. erythropolis KA2-5-1	120 mmol 2-HBP/(kg DCW·h) [1] Attacks alkylated forms of DBT and BT [1], [2]	Kobayashi *et al.* (2001) [1] Kobayashi *et al.* (2000) [2] Onaka *et al.* (2001a) [2]
R.. erythropolis rKA2-5-1*	196 mmol 2-HBP/(kg DCW·h) [1] Attacks alkylated forms of DBT and BT [3]	Kobayashi *et al.* (2001) [1] Hirasawa *et al.* (2001) [3]
Mycobacterium Strain G3	Activity on DBT at 37ºC was 46 mmol/(kg DCW·h) with 1 mM DBT as the sole S-source and 0.23 g DCW/L [4]. Attacks alkylated DBT's, initial activity on diesel fuel: 25 mmol/(kg DCW·h) [5].	Okada *et al.* (2001) [4] Okada *et al.* (2002) [5]
Rhodococcus Strain P32C1 **	43.5 mmol 2-HBP/(kg DCW·h) diesel fuel 303 ppm S: 49% efficiency at a VFO of 25%. diesel fuel 1000 ppm S: 24% efficiency at a VFO of 25%.	Maghsoudi *et al.* (2001) Maghsoudi *et al.* (2000)
R.. erythropolis I-19 (contains overexpressed key *Dsz* enzymes)	300 mmol 2-HBP/(kg DCW·h) diesel fuel 1850 ppm S: 150 mmol S/(kg DCW·h), 67% efficiency at a VFO of 25%. Attacks alkyl DBT's	Folsom *et al.* (1999)
Gordona Strain CYSK1	8.9 mmol 2-HBP/(kg DCW·h) diesel fuel 0.15 wt% S: 5.3 mmol S/(kg DCW·h), 70% efficiency at a VFO of 10% diesel fuel 0.3 wt% S: 4.7 mmol S/(kg DCW·h) 50% efficiency at a VFO of 10%	Rhee *et al.* (1998) Chang *et al.* (2000)
R. erythropolis IGTS8	30 mmol 2-HBP/(kg DCW·h) [6] 16.1 mmol 2-HBP/(kg DCW·h) [7]	Kaufman *et al.* (1998) [6] Honda *et al.* (1998) [7] Kayser *et al.* (1993)

*Genetically improved recombinant strain of KA2-5-1; **Formerly identified as *Corynebacterium* strain P32C1; DCW = dry cell weight; VFO = volume fraction oil.

A resting cell reaction system is used frequently (Izumi *et al.*, 1994; Ohshiro *et al.*, 1994, 1995; Lee *et al.*, 1995; Chang *et al.*, 1998). In this approach cells are pre-grown in the presence of a readily available carbon source (*e.g.* glucose) and DBT as the sole sulfur source. After harvesting and concentrating the cells a batch reaction is performed.

Harvesting cells in the exponential growth phase instead of the late log phase results in the best specific desulfurization rate (Chang *et al.*, 2000).

The performance of various aerobic strains under growing conditions is presented in Table 4.

Table 4. Overview of reported aerobic degradation using a sulfur selective pathway, results were obtained at growing conditions.

strain / organism	Organic S content decrease (%)	Reference
Paenibacillus sp. A11-2 Thermophilic (55°C)	DBT > 95% conversion to 2-HBP [1]. Attacks alkylated DBT's model compounds: ±25% conversion, in diesel fuel: ±11% conversion [1][2]. Converts BT analogous to the 4S-pathway [3].	Konishi *et al.* (1997) [1] Onoka *et al.* (2001b) [2] Ishii *et al.* (2000) Konischi *et al.* (2000) [3]
Rhodococcus Strain T09	This BT desulfurizing microorganism can assimilate various alkyl BT's, but cannot use DBT as the sole sulfur source [4]. When genetically modified, strain T09 also utilized alkylated BT's and DBT's [5].	Matsui *et al.* (2000) [4] Matsui *et al.* (2001a) [5] Matsui *et al.* (2001b) [5]
Rhodococcus Strain WU-K2R	Desulfurizes naphthothiophene (80% in 7 days) and benzothiophene (57% in 5 days) starting from a sulfur concentration of 0.27 mM.	Kirimura *et al.* (2002)
Rhodococcus Strain ECRD-1	Attacks alkyl DBT's in distillates of the diesel range. Diluted diesel fuel with 20 ppm S: approx. 30% efficiency at a VFO of 0.1% [6]. Diluted light cycle oil with 669±40 ppm S is reduced to 56±4 ppm S, at a VFO of 2% [7].	Grossman *et al.* (1999)[6] Grossman *et al.* (2001)[7] Lee *et al.* (1995)
Nocardia Strain CYSK2	DBT: 0.28 mg S/(L dispersion · h) at a VFO* of 10% In case of 0.3 wt% S Diesel fuel: 0.91mg S/(L dispersion · h); 20% efficiency at a VFO of 10% 0.99mg S/(L dispersion · h); 33% efficiency at a VFO of 5%	Chang *et al.* (1998)
Gordona sp. Strain 213E	Desulfurizes BT (but not DBT), during growth a phenolic compound accumulates.	Gilbert *et al.* (1998)
R. erythropolis N1-36	Batch reaction wit DBT $\mu = 0.153$ h^{-1} 2-HBP production: 1.8 µM·h^{-1} $\mu_{max} = 0.235$ h^{-1}	Wang *et al.* (1996a; 1996b)
Corynebacterium SY1	Batch DBT depletion during exponential growth phase: approx. 5 µM·h^{-1}	Omori *et al.* (1992)

*VFO = volume fraction oil.

To apply biodesulfurization to achieve deep desulfurization sufficient activity with the rather recalcitrant alkyl substituted dibenzothiophenes is of great importance. The first reported DBT desulfurizing bacterium that could grow on DBT derivates as the sole sulfur

source was *R. erythropolis* H-2 (Ohshiro *et al.*, 1995). The ability to attack alkyl-DBT's is also mentioned in Table 3 and 4. Generally, alkyl DBT's (or Cx-DBT's) are characterized by the carbon numbers of alkyl substituent groups (Kobayashi *et al.* 2001). Consequently, C1-DBT contains one methyl group at any position, while C2-DBT is dimethylated or contains one ethyl group. Genetically improved recombinant strains of *R. erythropolis* containing multiple copies of the *dsz*-genes were used to study the conversion of Cx-DBT's in more detail (Kobayashi *et al.*, 2001; Folsom *et al.*, 1999). Kobayashi *et al.* (2001) assessed the relevance of steric hindrance of Cx-DBT's by comparing the desulfurization of C2-DBT (4,6-dimethylDBT) and C3-DBT (3,4,6-trimethylDBT) to DBT. It was concluded that the desulfurization activities were fully dependent on the carbon number of the alkyl substituents. Neither the position nor the form of the alkyl substituent groups influenced the activity. The desulfurization activity against Cx-DBT's decreased inversely with an increment in the carbon number of the alkyl substituent groups. Furthermore, the desulfurization activity in mixtures of Cx-DBT's compared to the activity against the compounds solely was reduced, as is the case when distillate fractions are desulfurized.

On the other hand, Folsom *et al.* (1999) found that the overall rate kinetics was affected by the concentration and distribution of Cx-DBT's according to the number and/or lengths of alkyl groups attached. The *Dsz* system of *R. Erythropolis* I19 selectively and sequentially transformed Cx-DBT's in a middle distillate. DBT and C1-DBT's were attacked preferentially, followed by the more highly alkylated DBT's.

Apart from research on the desulfurization of specific Cx-DBT molecules also a lot of the efforts in aerobic desulfurization were aimed at the reduction of the total sulfur content of crude oil and distillates thereof. The results obtained in terms of total sulfur conversion at the specified conditions are summarized in Table 3 and 4.

Recently, Furuya *et al.* (2001) reported the thermophilic microorganism *Mycobacterium phlei* Strain WU-F1 that is able to grow at 50ºC. The DBT conversion speed using resting cells was 0.54 mM/h, producing 2-HBP according to the 4S- pathway. Alkylated forms of DBT (*i.e.* 2,8-dimethylDBT, 4,6-dimethylDBT) were converted with a speed of 0.1 mM/h (Furuya *et al.*, 2001). This strain was also used in a study on the conversion of naphthothiophenes (NTH), which can be formed in diesel fuel during severe physico-chemical hydrodesulfurization (Furuya *et al.*, 2002). Resting cells of Strain WU-F1 converted 67% and 83% of 0.81 mM NTH and 2-ethylNTH, respectively, within 8h.

Naphthothiophenes are converted with a selective cleavage of the C-S bonds, similar to the 4S-desulfurizing pathway (Furuya *et al.*, 2002).

ANAEROBIC DESULFURIZATION

In contrast to aerobic biodesulfurization, evidence for the anaerobic conversion of organic sulfur compounds is equivocal. Kim *et al.*, (1995) reported significant conversion of various model compounds under anaerobic conditions, accompanied with the concomitant formation of H_2S. The conversions were measured using an enzyme essay with a concentrated cell suspension of *Desulfovibrio desulfuricans* M6 in the presence of the artificial electron donor methyl viologen. *D. desulfuricans* M6 is a sulfate reducing bacterium isolated from soil and was selected for its high hydrogenase activity. Biphenyl was found as the major reaction product when dibenzothiophene was reductively converted, as depicted in Fig. 7.
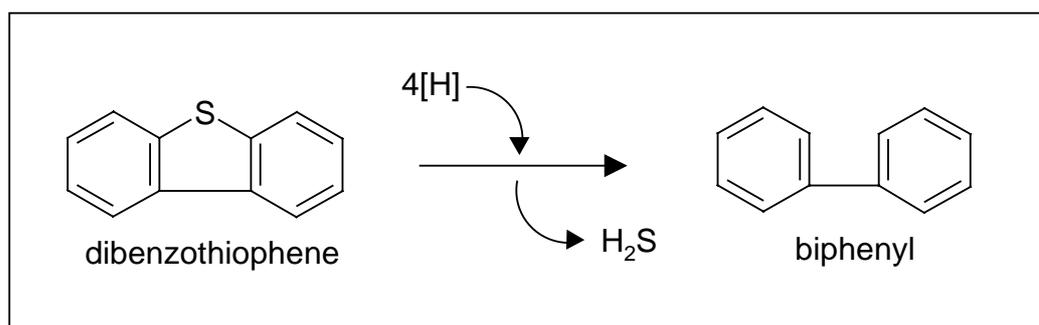
Fig. 7: Principle of reductive DBT desulfurization.

During the reductive conversion, DBT is used as the sole electron acceptor and sulfur is removed selectively (Kim *et al*., 1990a). Using the enzyme assay the same organism was able to desulfurize Kuwait crude oil in an electrochemical cell. The sulfur content of the crude oil was decreased by 21% with release of H_2S (Kim *et al*., 1990b). *D. desulfuricans* M6 also removed the organic sulfur compounds from other crudes and distillates (Kim *et al*., 1995). Although the principle of the anaerobic conversion was demonstrated, these results only show that *D. desulfuricans* M6 has enzymes with the capability to cleave C-S bonds. Desulfurization activity while growing with thiophenes as the alternative electron acceptor (instead of sulfate) in the absence of methyl viologen is necessary to go to practical applications. Reported attempts to desulfurize DBT using microorganisms in the exponential growth phase were not successful. Linzama *et al.* (1995) cultivated

Desulfotomaculum orientis, *D. desulfuricans* and *Thermodesulfobacterium commune* with lactate and citrate, while DBT served as the sole source of sulfur. A slight sulfide formation was demonstrated, but the formation of biphenyl was not demonstrated. Also Armstrong *et al.* (1997) could not demonstrate a significant amount of sulfide production using various sulfate reducing pure cultures or mixed sulfate reducing consortia at growing conditions. Neither DBT nor hydrocarbon fractions were significantly desulfurized. Recently, Bahrami *et al.* (2001) reported on the anaerobic degradation of DBT. However, no correlation of DBT disappearance with sulfide formation could be demonstrated. Furthermore, biphenyl could not be detected, indicating that an aspecific reaction occurred. This leaves the specific anaerobic desulfurization of DBT to be proven.

COMPARISON OF AEROBIC AND ANAEROBIC DESULFURIZATION OF ORGANIC SULFUR COMPOUNDS

The anaerobic route is a potentially attractive biodesulfurization route to apply, because of its sulfur specificity. From Fig. 7, it follows that the caloric value is maintained because C-C bonds are not altered. Furthermore, the reaction pattern is similar to HDS. However, growth under anaerobic conditions proceeds slowly, especially when organic molecules (like thiophenes) are involved in the conversion. When thiophenes are used as the sole electron acceptor, the conversion of thiophenes should be coupled to microbial growth.

From a process point of view, the aerobic route has some major drawbacks. Sulfur is used in the assimilatory metabolism of aerobic bacteria. Considering that the sulfur content of biomass is approximately 0.03 wt%, the yield of biomass per mole sulfur removed in the aerobic route is high. Approximately 50% of the energy produced by aerobic microorganisms will be used for growth, while anaerobic microorganisms use approximately 10% of their energy for assimilation. At high biomass concentrations down stream processing is complicated, because proteins originating from the biomass emulsify the oil/water mixture. In addition the mixing efficiency and O_2 availability is less optimal in emulsions with a high biomass concentration. Furthermore, diluted sulfate is formed as the end-product of the aerobic route that also must be removed, while H_2S that is formed in the anaerobic route can be treated with existing refinery desulfurization plants (*e.g.* Claus process). In the aerobic sulfur specific route oxygen molecules are added to the hydrocarbon skeleton. This is not desirable, because 2-hydroxybiphenyl is involved in the formation of viscous oil sludge ('gum') in the fuel. Furthermore, product inhibition 2-

hydroxybiphenyl might play a role. The 2-hydroxybiphenyl formed in the cells eventually will diffuse back into the oil phase, but the phenolic molecule is known as a potent biocide. Based on the aforementioned considerations the anaerobic route is chosen in this thesis.

ANAEROBIC BIODESULFURIZATION IN MULTIPLE PHASE SYSTEMS

Besides suitable anaerobic biomass to convert thiophenes also technological implications of using hydrocarbon-water systems must be studied. Volumetric productivities depend not only on the biocatalyst activity but also on the fluxes of apolar substrates (*e.g.* DBT) and metabolites (*e.g.* biphenyl) from the aqueous to the carrier phase and vice versa. In two-phase liquid-liquid systems the volumetric rate of apolar substrate transfer from the organic phase to the cells can be limiting (Lilly, 1982; Lilly *et al.*, 1987). A clear advantage of using liquid-liquid systems is the smaller influence of inhibitory effects because toxic apolar products partition back into the organic phase, provided that the solvent is not toxic for the bacteria (de Smet *et al.*, 1981). The maximal attainable mass transfer rate of apolar substrates across the liquid-liquid boundary to cells depends on: (*i*) the properties of microorganism, (*ii*) the mechanism of substrate transport, (*iii*) the measure of apolarity of the organic solvent and (*iv*) the mixing characteristics of the bioreactor (Schmid *et al.*, 1998).

Pseudomonas species have been observed to take up substrate dissolved in the aqueous phase requiring continuous mass transfer from the organic to the aqueous phase (Collins *et al.*, 1995; Woodley *et al.*, 1991) or via direct cell-droplet interaction (Goswami and Singh, 1991). Direct cell-droplet interactions predominate in systems containing hydrophobic substrates and solvents (Cameotra and Singh, 1990; Reddy *et al.*, 1982). Direct cell-droplet interactions are also claimed for the aerobic biodesulfurization process using *R. erythropolis*, because dibenzothiophene and analogs thereof are hardly soluble in the aqueous phase (Borole *et al.*, 2002; Shennan, 1996).

The requirement of an intimate biomass-substrate contact is the key factor in the preliminary bioreactor design suitable to anaerobically convert apolar organic sulfur compounds. However, also favorable carbon and energy sources are necessary to convert thiophenes. From a process point of view H_2 gas is the best option as electron donor for converting sulfur compounds, because of its low costs for application at relatively large scale (in case of oxidized inorganic sulfur compounds, see Van Houten *et al.*, 1996) and

the availability of H_2 gas at refineries (Gary and Handwerk, 1994). Small amounts of acetate and bicarbonate required for growth can be supplemented as carbon source to the aqueous phase. Besides H_2 also H_2S is involved as reaction product (see Fig. 7). Consequently, the use of this approach results in a three-phase gas-water-hydrocarbon system. To optimize the availability of organic sulfur compounds it is proposed to disperse the hydrocarbon phase as very fine droplets in the aqueous phase. In order to be able to supply H_2 gas to the dispersion without severe foaming, the hydrocarbon phase is saturated with H_2 gas before introduction in the bioreactor. Then the hydrocarbon phase is used as carrier phase for H_2 gas. This approach combines the requirements of a high specific surface area to maximize the availability of both apolar organic sulfur compounds and H_2 gas. A bioreactor system equipped with a nozzle to disperse the hydrocarbon phase is the most appropriate device to generate fine hydrocarbon droplets, while the mixing energy is only imparted on the hydrocarbon phase.

In order to favor the conversion of organic sulfur compounds the sulfide concentration must be as low as possible to avoid inhibition. The H_2S produced in turn dissolves in the hydrocarbon phase and is stripped off during the H_2 saturation. In this way any sulfide inhibition is avoided.

OUTLINE OF THIS THESIS

The main objective of this thesis is to develop a new bioprocess to desulfurize organic sulfur compounds using anaerobic bacteria and H_2 as the electron donor. A systematic approach was followed to reveal insight in this complex bioprocess. Both microbiological and engineering aspects were considered.

In Chapter 2, a mathematical model is presented to compare the mass transfer rate of DBT to the hydrocarbon/water interface for different hydrocarbon fractions with reported aerobic desulfurization rates. Chapter 3 addresses the biological experiments that demonstrate the reductive conversion of dibenzothiophene to biphenyl and sulfide, using anaerobic consortia obtained from oil fields. In Chapters 4 and 5 the focus is on the use of H_2 gas as electron donor in complex gas/water/hydrocarbon systems. An onset to study the applicability of a three-phase system using hydrocarbon as a carrier phase for H_2 is made in Chapter 4 by the determination of the H_2 mass transfer coefficients involved in the process using physical methods in the absence of biomass. In Chapter 5 the determination of the H_2 mass transfer coefficient between hydrocarbon and water is assessed using sulfate reducing bacteria. In addition, the applicability of using dispersed hydrocarbon as carrier phase for H_2 mass transfer was evaluated by measuring sulfate reduction in a dispersion system and the determination of the hold-up and droplet sizes attained in a defined dispersion system. A mathematical model describing the partitioning of H_2S over gas/water/hydrocarbon systems is presented in Chapter 6. With the results insight is provided in the H_2S concentration present in each phase involved in the biodesulfurization process. Finally, a summary and concluding remarks concerning the implications of the anaerobic biodesulfurization process is presented in Chapter 7.

REFERENCES

Anabtawi J.A., Ali S.A., Ali M.A. 1996. Impact of gasoline and diesel specifications on the refining industry. Energ. Source 18: 203-214.

Arensdorf J.J., Loomis A.K., DiGrazia, P.M., Monticello, D.J., Pienkos P.T. 2002. Chemostat approach for the direct evolution of biodesulfurization gain-of-function mutants. Appl. Environ. Microbiol. 68: 691-698.

Armstrong S.M., Sankey B.M., Verdouw, G. 1997. Evaluation of sulfate reducing bacteria for desulfurizing bitumen or its fractions. Fuel process. Technol. 76: 223-227.

Arnoldy P., Van den Heikant J.A.M., De Bok G.D., Moulijn. J.A. 1985. Temperature-programmed sulfiding of molybdenum(VI) oxide/alumina catalysts. J. Catal. 92: 35-55.

Bahrami A., Shojaosadati S.A., Mohebali G. 2001. Biodegradation of dibenzothiophenes by thermophilic bacteria. Biotechnol. Lett. 23: 899-901.

Borole A.P., Kaufman E.N., Grossman M.J., Minak-Bernero V., Bare R., Lee M.K. 2002. Comparison of the emulsion characteristics of *Rhodococcus erythropolis* and *Escherichia coli* SOXC-5 cells expressing biodesulfurization genes. Biotechnol. Progr. 18: 88-93.

Bressler D.C., Norman J.A., Fedorak P.M. 1998. Ring cleavage of sulfur heterocycles: how does it happen? Biodegradation 8: 297-311.

Cameotra S.S., Singh H.D. 1990. Uptake of volatile *n*-alkanes by *Pseudomonas* PG-1. J. Microb. Biotechnol. 5: 47-57.

Chang J.H., Chang Y.K., Cho K-S, Chang H.N. 2000. Desulfurization of model and diesel oils by resting cells of *Gordona* sp. Biotechnol. Lett. 22: 193-196.

Chang J.H., Rhee S-K, Chang Y.K., Chang H.N. 1998. Desulfurization of diesel oils by a newly isolated dibenzothiophene degrading *Nocardia* sp. Strain CYKS2. Biotechnol. Progr. 14: 851-855.

Collins A.M., Woodley J.M., Liddell J.M. 1995. Determination of reactor operation for the microbial hydroxylation of toluene in a two-liquid phase process. J. Ind. Microbiol. 14: 382-388.

De Krom H. 2002. Shell Global Solutions International B.V. (Amsterdam). Personal communication.

Denome S.A., Olson E.S., Young K.D. 1993. Identification and cloning of genes involved in specific desulfurization of dibenzothiophene by *Rhodococcus* sp. strain IGTS8. Appl. Environ. Microbiol. 59: 2837-2843.

Denome S.A., Oldfield C., Nash L.J., Young K.D. 1994. Characterization of the desulfurization genes from *Rhodococcus* sp. strain IGTS8. J. Bacteriol. 176: 6707-6716.

De Smet M-J, Wynberg H., Witholt B. 1981. Synthesis of 1,2-epoxyoctane by *Pseudomonas oleovorans* during growth in a two-phase system containing high concentrations of 1-octene. Appl. Environ. Microbiol. 42: 811-816.

Folsom B.R., Schieche D.R., DiGrazia P.M., Werner J., Palmer S. 1999. Microbial desulfurization of alkylated dibenzothiophenes from a hydrodesulfurized middle distillate by *Rhodococcus erythropolis* I19. Appl. Environ. Microbiol. 65: 4967-4972.

Furuya T., Kirimura K., Kino K., Usami S. 2002. Thermophilic biodesulfurization of naphthothiophene and 2-ethylnaphthothiophene by a dibenzothiophene-desulfurizing bacterium, *Mycobacterium phlei* WU-F1. Appl. Microbiol. Biotechnol. 58: 237-240.

Furuya T., Kirimura K., Kino K., Usami S. 2001. Thermophilic biodesulfurization of dibenzo-thiophene and its derivatives by *Mycobacterium phlei* WU-F1. FEMS Microbiol. Lett. 204: 129-133.

Gallagher J.R., Olson E.S., Stanley D.C. 1993. Microbial desulfurization of dibenzo-thiophene: a sulfur specific pathway. FEMS Microbiol. Lett. 107: 31-36.

Gary J.H., Handwerk G.E. 1994. Introduction to petroleum refining. Marcel Dekker, New York.

Gilbert S.C., Morton J., Buchanan S., Oldfield D., McRoberts A. 1998. Isolation of a unique benzothiophene-desulfurizing bacterium, *Gordona* sp. strain 213E (NCIMB 40816), and characterization of the desulfurizing pathway. Microbiol.-UK 144: 2545-2553.

Goswami P., Singh H.D. 1991. Different modes of hydrocarbon uptake by two *Pseudomonas* species. Biotechnol. Bioeng. 37: 1-11.

Gray K.A., Pogrebinsky O.S., Mrachko T., Xi L., Monticello D.J., Squires C.H. 1996. Molecular mechanisms of biocatalytic desulfurization of fossil fuels. Nat. Biotechnol. 14: 1705-1709.

Grossman M.J., Lee M.K., Prince R.C., Minak-Bernero V., George G.N., Pickering I.J. 2001. Deep desulfurization of extensively hydrodesulfurized middle distillate oil by *Rhodococcus* sp. Strain ECRD-1. Appl. Environ. Microbiol. 67: 1949-1952.

Grossman M.J., Lee M.K., Prince R.C., Garrett K.K., George G.N., Pickering I.J. 1999. Microbial desulfurization of a crude oil middle-distillate fraction: analysis of the extent of sulfur removal and the effect of removal on remaining sulfur. Appl. Environ. Microbiol. 65: 181-188.

Hanika J., Sporka K. 1992. Catalyst particle shape and dimension effects in gas oil hydro-desulfurization. Chem. Eng. Sci. 35: 2739-2744.

Hirasawa K., Ishii Y., Kobayashi M., Koizumi K., Maruhashi K. 2001. Improvement of desulfurization activity in *Rhodococcus erythropolis* KA2-5-1 by genetic engineering. Biosci. Biotech. Biochem. 65: 239-246.

Ho T.Y., Rogers M.A., Drushel H.V., Koons C.B. 1974. Evolution of sulfur compounds in crude oils. Am. Assoc. Pet. Geol. Bull. 58: 2338-2348.

Honda H., Sugiyama H., Saito I., Kobayashi T. 1998. High cell density culture of *Rhodococcus rhodochrous* by pH-stat feeding and dibenzothiophene degradation. J. Ferment. Bioeng. 85: 334 - 338.

Houalla M., Broderick D.H., Sapre A.V., Nag N.K., De Beer V.H.J., Gates B.C., Kwart H. 1980. Hydrodesulfurization of methyl-substituted dibenzothiophene catalyzed by sulfided Co-Mo/γ-Al$_2$O$_3$. J. Catal. 61: 523-527.

Isshi Y., Konishi J., Okada, H., Hirasawa, K., Onaka T., Susuki, M. 2000. Operon structure and functional analysis of the genes encoding thermophilic desulfurizing enzymes of *Paenibacillus* sp. A11-2. Biochem. Biophys. Res. Commun. 270: 81-88.

Izumi Y., Oshiro T., Ogino H., Hine Y., Shimao M. 1994. Selective desulfurization of dibenzothiophene by *Rhodococcus erythropolis* D-1. Appl. Environ. Microbiol. 60: 223-226.

Kaufman E.N., Harkins J.B., Borole A.P. 1998. Comparison of batch-stirred and electro-spray reactors for biodesulfurization of dibenzothiophene in crude oil and hydrocarbon feedstocks. Appl. Biochem. Biotechnol. 73: 127-144.

Kabe T., Aoyama Y., Wang D., Ishihara A., Qian W., Hosoya M., Zhang Q. 2001. Effects of H$_2$S on hydrodesulfurization of dibenzothiophene and 4,6-dimethyldibenzothiophene on alumina-supported NiMo and NiW catalysts. Appl. Catal. A-Gen. 209: 237-247.

Kabe T., Ishihara A., Zhang Q. 1993. Deep desulfurization of light oil. 2. Hydrodesulfuri-zation of dibenzothiophene, 4-methyldibenzothiophene and 4,6-dimethyldibenzo-thiophene. Appl. Catal. A-Gen. 97: L1-L9.

Kabe T., Ishihara A., Tajima H. 1992. Hydrodesulfurization of sulfur-containing polyaromatic compounds in light oil. Ind. Eng. Chem. Res. 31: 1577-1580.

Kapteijn F., Nijhuis T.A., Heiszwolf J.J., Moulijn J.A. (2001) New non-traditional multiphase catalytic reactors based on monolithic structures. Catal. Today 66: 133-144.

Kayser K.J., Bielaga-Jones B.A., Jackowski K., Odusan O., Kilbane J.J. 1993. Utilization of organosulfur compounds by axenic and mixed cultures of *Rhodococcus rhodochrous* IGTS8. J. Gen. Microbiol. 139: 3123-3129.

Kertesz M.A., Wietek C. 2001. Desulfurization and desulfonation: applications of sulfur-controlled gene expression in bacteria. Appl. Microbiol. Biotechnol. 57: 460-466.

Kilbane J.J. 1989. Desulfurization of Coal: the microbial solution. Trends Biotechnol. 7: 97-101.

Kim H.Y., Kim T.S., Kim, B.H. 1990a. Degradation of organic sulfur compounds and the reduction of dibenzothiophene to biphenyl and hydrogen sulfide by *Desulfovibrio desulfuricans* M6. Biotechnol. Lett. 12: 761-764.

Kim T.S., Kim H.Y., Kim B.H. 1990b. Petroleum desulfurization by *Desulfovibrio desulfuricans* M6 using electrochemically supplied reducing equivalent. Biotechnol. Lett. 12: 757-760.

Kim B.Y., Kim H.Y., Kim T.S., Park D.H. 1995. Selectivity of desulfurization activity of *Desulfovibrio desulfuricans* M6 on different petroleum products. Fuel Process. Technol. 43: 87-94.

Kirimura K., Furuya T., Sato R., Ishii Y., Kino K., Usami S. 2002. Biodesulfurization of naphthothiophene and benzothiophene through selective cleavage of carbon-sulfur bonds by *Rhodococcus* sp. Strain WU-K2R. Appl. Environ. Microbiol. 68: 3867-3872.

Kobayashi M., Horiuchi K., Yoshikawa O., Hirasawa K., Ishii Y., Fujino K., Sugiyama H., Maruhashi K. 2001. Kinetic analysis of microbial desulfurization of model and light gas oil containing multiple alkyl dibenzothiophenes. Biosci. Biotech. Biochem. 65: 298-304.

Kobayashi M., Onaka T., Ishii Y., Konishi J., Takaki M., Okada H., Ohta Y., Koizumi K., Suzuki M. 2000. Desulfurization of alkylated froms of both dibenzothiophene and benzothiophene by a single bacterial strain. FEMS Microbiol. Lett. 187: 123-126.

Kodama K., Umehara K., Shimizu K., Nakatanni S., Minoda Y., Yamada K. 1973. Identification of microbial products from dibenzothiophene and its proposed oxidation pathway. Agr. Biol. Chem. 37: 45-50.

Konishi J., Onaka T., Ishii Y., Suzuki M. 2000. Demonstration of the carbon-sulfur bond targeted desulfurization of benzothiophene by thermophilic *Paenibacillus* sp. strain A11-2 capable of desulfurizing dibenzothiophene. FEMS Microbiol. Lett. 187: 151-154.

Konishi J., Ishii Y., Onaka T., Okumura K., Suzuki M. 1997. Thermophilic carbon-sulfur-bond targeted biodesulfurization. Appl. Environ. Microbiol. 63: 3164-3169.

Landau M.V., Berger D., Herskowitz M. (1996) Hydrodesulfurization of methyl-substituted dibenzothiophenes: Fundamental study of routes to deep desulfurization. J. Catal. 159: 236-245.

Lee M.K., Senius J.D., Grossman M.J. 1995. Sulfur-specific microbial desulfurization of sterically hindered analogs of dibenzothiophene. Appl. Environ. Microbiol. 61: 4362-4366.

Li M.Z., Squires C.H., Monticello D.J., Childs J.D. 1996. Genetic analysis of the dsz promoter and associated regulatory regions of *Rhodococcus erythropolis* strain IGTS8. J. Bacteriol. 178: 6409-6418.

Lilly M.D. 1982. Two liquid phase biocatalytic reactions. J. Chem. Tech. Biotech. 32: 162-169.

Lilly M.D., Brazier A.J., Hocknull M.D., Williams, A.C., Woodley J.M. 1987. Biological conversions involving water-insoluble organic compounds. In: Laane C., Tramper J. and Lilly M.D. eds. Biocatalysis in organic media. Amsterdam: Elsevier Science Publishers 3-17.

Lizama H.M., Wilkins L.A., Scott T.C. 1995. Dibenzothiophene sulfur can serve as the sole electron acceptor during growth by sulfate-reducing bacteria. Biotechnol. Lett. 17: 113-116.

Ma X., Sakanishi K, Mochida I. 1994. Hydrodesulfurization reactivities of various sulfur compounds in diesel fuel. Ind. Eng. Chem. Res. 33: 218-222.

Maghsoudi S., Vossoughi M., Kheirolomoom A., Tanaka E., Katoh S. 2001. Biodesulfurization of hydrocarbons and diesel fuels by *Rhodococcus* sp. Strain P32C1. Biochem. Eng. J. 8: 151-156.

Maghsoudi S., Kheirolomoom A., Vossoughi M., Tanaka E., Katoh S. 2000. Selective desulfurization of dibenzothiophene by newly isolated *Corynebacterium* sp. Strain P32C1. Biochem. Eng. J. 5: 11-16.

Matsui T., Hirasawa K., Konishi J., Tanaka Y., Maruhashi K., Kurane R. 2001a. Microbial desulfurization of alkylated dibenzothiophene and alkylated benzothiophene by recombinant *Rhodococcus* sp. strain T09. Appl. Microbiol. Biotechnol. 56: 196-200.

Matsui T., Hirasawa K., Koizumi K., Maruhashi K., Kurane, R. 2001b. Effect of dszD gene expression on benzothiophene degradation of *Rhodococcus* sp. Strain T09. Process Biochem. 37: 31-34.

Matsui T., Onaka T., Tanaka Y., Tezuka T., Suzuki M., Kurane, R. 2000. Alkylated benzothiophene desulfurization by *Rhodococcus* sp. Strain T09. Biosci. Biotechnol. Biochem. 64: 596-599.

Nijhuis T.A., Kreutzer M.T., Romijn A.C.J., Kapteijn F., Moulijn J.A. 2001. Monolithic catalysts as more efficient three-phase reactors. Catal. Today 66: 157-165.

Ohshiro T., Hine Y., Izumi Y. 1994. Enzymatic desulfurization of dibenzothiophene by a cell-free system of *Rhodococcus erythropolis* D-1. FEMS Microbiol. Lett. 118: 341-344.

Ohshiro T., Hirata T., Izumi Y. 1995. Microbial desulfurization of dibenzothiophene in the presence of hydrocarbon. Appl. Microbiol. Biotechnol. 44: 249-252.

Ohshiro T., Izumi Y. 1999. Microbial desulfurization of organic sulfur compounds in petroleum. Biosci. Biotech. Biochem. 63: 1-9.

Okada H., Numura N., Nakahara T., Muruhashi K. 2002. Analysis of substrate specificity of the desulfurizing bacterium *Mycobacterium* sp. G3. J. Biosc. Bioeng. 93: 228-233.

Okada H., Numura N., Nakahara T., Muruhashi K. 2001. Cultivation of a desulfurizing bacterium, *Mycobacterium* sp. G3. Biotechnol. Lett. 23: 2047-2050.

Oldfield C., Pogrebinsky O., Simmonds J., Olson E.S., Kulpa C.F. 1997. Elucidation of the metabolic pathway for dibenzothiophene desulfurization by *Rhodococcus* sp. Strain IGTS8 (ATCC 53968). Microbiology 143: 2961-2973.

Omori T., Monna L., Saiki Y., Kodama T. 1992. Desulfurization of dibenzothiophene by *Corynebacterium* sp. Strain SY1 Appl. Environ. Microbiol. 58: 911-915.

Onaka T., Kobayashi M., Ishii Y., Konishi J., Maruhashi K. 2001a. Selective cleavage of the two C-S bonds in assymetrically alkylated dibenzothiophenes by *Rhodococcus Erythropolis* KA2-5-1. J. Biosci. Bioeng. 92: 80-82.

Onaka T., Konishi J., Ishii Y., Maruhashi K. 2001b. Desulfurization characteristics of thermophilic *Paenibacillus* sp. Strain A11-2 against asymmetrically alkylated dibenzothiophenes. J. Biosci. Bioeng. 92: 193-196.

Payzant J.D., Montgomery D.S., Strausz O.P. 1986. Sulfides in petroleum. Org. Geochem. 9: 357-369.

Piddington C.S., Kovavevich B.R., Rambosek J. 1995. Sequence and molecular characterization of a DNA region encoding the dibenzothiophene desulfurization operon of *Rhodococcus* sp. Strain IGTS8. Appl. Environ. Microbiol. 61: 468-475.

Rall H.T., Thompson C.J., Coleman H.J., Hopkins R.L. 1972. In: Bulletin 659, Sulfur compounds in crude oil, U.S. Dept. of Interior, Bureau of Mines.

Reddy P.G., Singh H.D., Roy P.K., Baruah J.N. 1982. Predominant role of hydrocarbon solubilization in the microbial uptake of hydrocarbons. Biotechnol. Bioeng. 24: 1241-1269.

Reinhoudt H.R., Troost R., Van Langeveld A.D., Sie S.T., Van Veen J.A.R., Moulijn J.A. 1999. Catalysts for second-stage deep hydrodesulfurization of gas oils. Fuel Process. Technol. 61: 133-147.

Rhee S-K., Chang J.H., Chang Y.K., Chang H.N. 1998. Desulfurization of dibenzothiophene and diesel oils by a newly isolated *Gordona* strain, CYKS1. Appl. Environ. Microbiol. 64: 2327-2331.

Robinson W.R.A.M., Van Veen J.A.R., De Beer V.H.J., Van Santen R.A. 1999a. Development of deep hydrodesulfurization catalysts I. CoMo and NiMo catalysts tested with (substituted) dibenzothiophene. Fuel Process. Technol. 61: 89-101.

Robinson W.R.A.M., Van Veen J.A.R., De Beer V.H.J., Van Santen R.A. 1999b. Development of deep hydrodesulfurization catalysts II. NiW, Pt and Pd catalysts tested with (substituted) dibenzothiophene. Fuel Process. Technol. 61: 103-116.

Schmid A., Sonnleitner B., Witholt B. 1998. Medium chain length alkane solvent-cell transfer rates in two-liquid phase, *Pseudomonas oleovorans* cultures. Biotechnol. Bioeng. 60: 10-23.

Schulz H., Böhringer W., Ousmanov F., Waller P. 1999. Refractory sulfur compounds in gas oils. Fuel Process. Technol. 61: 5-41.

Segawa K., Takahashi K., Satoh S. 2000. Development of new catalysts for deep hydrodesulfurization of gas oil. Catal. Today 63: 123-131.

Seki H., Yoshimoto M. 2001. Deactivation of HDS catalyst in two-stage RDS process II. Effect of crude oil and deactivation mechanism. Fuel Process. Technol. 69: 229-238.

Shafi R., Hutchings G.J. 2000. Hydrodesulfurization of hindered dibenzothiophenes: an overview. Catal. Today 59: 423-442.

Shennan J.L. 1996. Microbial attack on sulfur-containing hydrocarbons: implications for the biodesulfurization of oils and coals. J. Chem. Tech. Biotechnol. 67: 109-123.

Sie S.T. 1999. Reaction order and role of hydrogen sulfide in deep hydrodesulfurization of gas oils: consequences for industrial reactor configuration. Fuel Process. Technol. 61: 149-171.

Speight J.G. 1981. The Desulfurization of Heavy Oils and Residua (Heinz Hienemann, ed.). Marcel Dekker, New York.

Stanislaus A., Cooper B.H. 1994. Aromatic hydrogenation catalysis - a review. Catal. Rev. Sci. Eng. 36: 75-123.

Tissot B.P., Welte D.H. 1984. Petroleum formation and occurrence, 2nd edn. Springer-Verlag, Berlin.

Van Afferden M., Schacht S., Klein J., Trüper H.G. 1990. Desulfurization of dibenzothiophene by *Brevibacterium* sp. DO. Arch. Microbiol. 153: 324-328.

Van Houten R.T., Lettinga G. 1996. Biological sulfate reduction with synthesis gas: microbiology and technology, p. 793-799 In: Wijffels R.H., Buitelaar, R.M., Bucke C., Tramper J. (Ed.) Progress in Biotechnology. Vol. 11. Elsevier, Amsterdam.

Van Parijs I.A., Hosten L.H., Froment G.F. 1986. Kinetics of the hydrodesulfurization on a Co-Mo/γ-Al$_2$O$_3$ catalyst. 2. Kinetics of the hydrogenolysis of benzothiopene. Ind. Eng. Chem. Proc. Res. Dev. 25: 437-443.

Van Veen J.A.R., Colijn H.A., Hendriks P.A.J.M., Van Welsenes A.J. 1993. On the formation of type-I and type-II NiMos phases in NiMo/Al$_2$O$_3$ hydrotreating catalysts and its catalytic implications. Fuel Process. Technol. 35: 137-157.

Wang P., Krawiec S. 1996a. Kinetic analysis of desulfurization of dibenzothiophene by *Rhodococcus erythropolis* in batch and fed-batch cultures. Appl. Environ. Microbiol. 62: 1670-1675.

Wang P., Humphrey A.E., Krawiec S. 1996b. Kinetic analysis of desulfurization of dibenzothiophene by *Rhodococcus erythropolis* in continuous cultures. Appl. Environ. Microbiol. 62: 3066-3068.

Woodley J.M., Brazier A.J., Lilly M.D. 1991. Lewis cell studies to determine reactor design data for two-liquid-phase bacterial and enzymatic reactions. Biotechnol. Bioeng. 37: 133-140.

Xi L., Squires C.H., Monticello D.J., Childs J.D. 1997. A flavin reductase stimulates DszA and DszC proteins of *Rhodococcus erythropolis* IGTS8 *in vitro*. Biochem. Biophys. Res. Commun. 230: 73-75.

MODEL DESCRIPTION OF DIBENZOTHIOPHENE MASS TRANSFER IN OIL/WATER DISPERSIONS WITH RESPECT TO BIODESULFURIZATION

ABSTRACT

A mathematical model was developed in order to describe the mass transfer rate of dibenzothiophene within the oil droplet to the oil/water interface of droplets created in a stirred tank reactor. The mass transfer rate of dibenzothiophene was calculated for various complex hydrocarbon distillates and model solvents in the temperature range of 20 up to 60°C, at volume fractions of oil of 10 and 25% (v/v). The viscosity of the various oil phases used appeared to be the most critical physical parameter governing the dibenzothiophene mass transfer rate, while density and interfacial tension were found to be of minor importance. Based on the model calculations, we estimated that the mass transfer rate of dibenzothiophene within the oil droplet to the oil/water interface is at least a factor 10 up to 10^4 higher compared to experimentally determined specific dibenzothiophene conversion rates. Due to the prevailing mass transfer resistance from the oil/water interface to the bacterium it is essential to maximize the specific surface area to enhance the surface contact between the bacteria and the oil droplets. The microbial desulfurization rate is the overall rate-limiting process step.

KEYWORDS

Bacteria; Biodesulfurization; Bioreactor; Dibenzothiophene; Mass Transfer; Mixing; Modeling; Viscosity

INTRODUCTION

Crude oils frequently contain significant quantities of organically bound sulfur, ranging typically between 0.05 and 5.0 wt.%, although values as high as 8 wt.% have been reported (Rall *et al.*, 1972). In general, the distribution of organically bound sulfur in crude oil is such that the proportion of organic sulfur increases along with the boiling point of the distillate fraction. Distillates such as diesel and fuel oil may contain significant amounts of benzothiophenes and dibenzothiophenes. Without a suitable sulfur-removing step, their use as a fuel results in the formation and emission of polluting sulfur dioxide during combustion (Speight, 1981). Due to stricter environmental legislation, the desulfurization of crude oil and its distillates is becoming increasingly important. In Europe the allowable level of the sulfur content in diesel fuel already has been reduced from 3000 ppm to 500 ppm S in the past decade and a further restriction down to 50 ppm S by 2005 has been announced (Anabtawi *et al.*, 1996; E.U. directive, 1998).

Hydrodesulfurization (HDS) is the current method used by the petroleum/oil industry for reducing the sulfur content. HDS involves the catalytic reaction of hydrogen and the organic matter in the feed, at pressures ranging from 5 up to 10 MPa and temperatures between 300 and 350°C, depending on the oil fraction and the required level of desulfurization (Shafi and Hutchings, 2000; Gary and Handwerk, 1994). Thiols, sulfides and thiophenes are readily removed by HDS. However, benzothiophenes, dibenzothiophenes and especially derivates bearing alkyl substitutions, are considerably more resistant to HDS. Alkyl derivates from dibenzothiophenes, which are substituted adjacent to the sulfur atom, represent a significant barrier to obtain very low sulfur levels in fuels because of steric hindrance (Shafi and Hutchings, 2000; Kabe *et al.*, 1992). Due to the high costs and inherent chemical limitations associated with HDS, alternatives for this technology are of great interest to the petroleum industry.

Microbiological methods to desulfurize hydrocarbon streams might represent an attractive alternative. Biological processes require relatively mild conditions (low pressures and low temperatures), which could be a major advantage of biodesulfurization. Until the present time numerous attempts to develop biological desulfurization processes have been reported in literature (Okada *et al.*, 2002; Kobayashi *et al.*, 2001; Onaka *et al.*, 2001; Maghsoudi *et al.*, 2001; Folsom *et al.*, 1999; Grossman *et al.*, 1999). The efficiency of a biodesulfurization process largely depends on a sufficient oil/water (o/w) contact, because the reactions proceed mainly at the interface (Kaufman *et al.*, 1998; Shennan, 1996). Bacteria prevail in the water phase, consequently the organic sulfur compounds *e.g.* benzo- and dibenzothiophenes must be transferred from the oil bulk phase to the o/w-interface.

Stirred tank reactors (STR) are frequently used to create fine dispersions, since high-energy inputs can be achieved (Zhou and Kresta, 1998). Furthermore, general relationships describing the dispersion process is a STR are known. In an agitated medium the drop size distribution of the dispersed phase depends on droplet breakage and coalescence (Hinze, 1955). Reactor operating conditions, physical properties and the volume fraction of dispersed phase, are the factors affecting the average droplet size (Calabrese *et al.*, 1986; Wang and Calabrese, 1986).

In this Chapter, we present a mathematical model to enable a comparison of the mass transfer rate of dibenzothiophene (DBT) within the oil droplet and the biological desulfurization rate. Different hydrocarbon fractions were simulated in the model, ranging

from simple model fractions (*i.e.* DBT dissolved in a clean solvent) to complex distillates with a much less defined composition. The work presented describes the estimation of the DBT mass transfer rate, expressed by a time constant as a function of the energy capacity (W/kg) at different o/w-ratios (*viz.* 10 and 25% v/v) and temperatures (*viz.* 20, 40 and 60°C). The calculated mass transfer rates are compared to reported biological DBT desulfurization rates in order to assess the overall process-limiting step.

MODEL CALCULATION OF THE TIME CONSTANT FOR DBT MASS TRANSFER TO THE O/W-INTERFACE

Correlations and assumptions used in the model

Outline of the model

In order to enable a comparison between the mass transfer rate of dibenzothiophene (DBT) in the oil droplet to the o/w-interface and the biological desulfurization rate, a time constant (τ_o) for the DBT mass transfer in a dispersed phase to the o/w-interface is estimated using a newly developed mathematical model. The time constant (or characteristic time) is composed of the reciprocal product of (*i*) the mass transfer coefficient (k_o) and (*ii*) the specific surface area (a_{ow}) of the oil phase and gives an indication of the mass transfer rate. The time constant is calculated from (de Gooijer *et al.*, 1991; Sweere *et al.*, 1987):

$$\tau_o = \frac{1}{k_o \cdot a_{ow}} \tag{1}$$

Fig. 1 shows a schematic representation of the relevant parameters necessary to describe the dispersion process and to estimate k_o and a_{ow} in an ideally mixed STR.
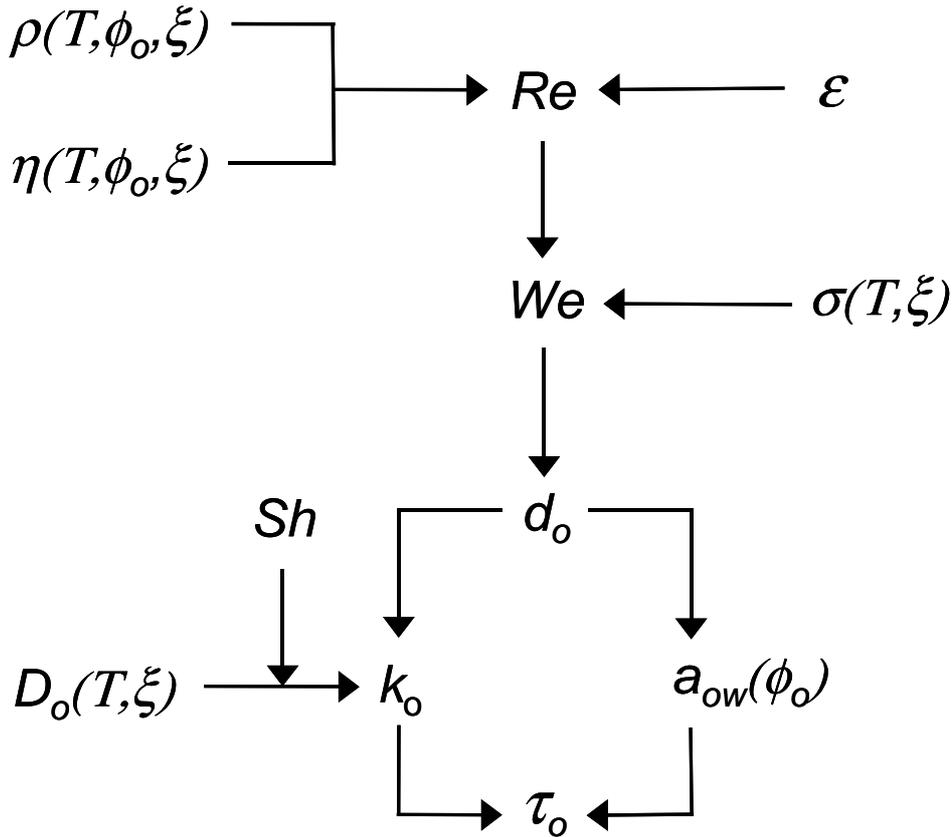
Fig. 1. Schematic representation of the interrelation between the parameters and variables necessary to estimate the DBT mass transfer rate.

The backbone of the dispersion model consists of three dimensionless numbers: Reynolds (*Re*), Sherwood (*Sh*) and Weber (*We*). The Reynolds number expresses the hydrodynamics of the liquid phase, using the input variables density (ρ_l), dynamic viscosity (η_l) and energy capacity (ε). The Sherwood number gives the characteristics for the mass transfer in the system based on the estimation of the diffusion coefficient (D_o) as input variable. The Weber number is used to estimate the diameter of the droplets (d_o) and depends on the interfacial tension (σ_{ow}) as input variable. The property input variables ρ_l, η_l, D_o and σ_{ow} are a function of temperature (*T*), volume fraction of the oil phase (ϕ_o) and type of organic phase (ξ), as shown in Fig. 1. Furthermore, the relation between the parameters used is presented. The following sections describe the most relevant mathematical relationships applied in the model (see also Fig.1), together with the prevailing conditions.

The model was written in Mathcad 6.0 using vector expressions, which contain the data for the various oil fractions.

Energy capacity

To disperse the oil phase in the aqueous bulk phase energy is required. The energy capacity (ε) is defined as the amount of mechanical energy input (P) into the system per kg reactor content. This variable depends on the liquid density (ρ_l) and the vessel geometry and can be calculated according to (Perry and Green, 1997):

$$\varepsilon = \frac{P}{\rho_l \cdot V_l} = N_p \cdot \frac{\rho_l N^3 D^5}{\rho_l \frac{\pi}{4} T_s^2 H} \tag{2}$$

Here: V_l, denotes the liquid volume in the STR; N_p, the power number; N, the stirrer speed; D, the impeller diameter; T_s, the tank diameter and H, the liquid height in the tank. The overall density of the total mixed liquid phase (ρ_l) depends on the volume fraction of the oil phase (ϕ_o) and is a linear combination of the densities of the oil and water phase. It can be calculated according to Eq. 3 (Zuiderweg, 1988).

$$\rho_l = \phi_o \rho_o + (1 - \phi_o) \rho_w \tag{3}$$

To calculate a suitable range of values for ε where the mixture is homogeneously dispersed, the following numbers and characteristics were used: $V_l = 2 \times 10^{-3}$ m^3, $D = T_s/3.3$, $N_p = 5$ (Rushton turbine impeller) and a range in N of 8 up to 25 s^{-1}. However, the mixing performance depends on the type and amount of impellers, while N_p is influenced by the gas hold-up of oxygen (Gogate *et al.*, 2000). Nevertheless, the calculated range of ε-values using the values mentioned above is the same as the range used in studies on gas-liquid dispersions (Moucha *et al.*, 1995; Pinelli *et al.*, 1994; Nocentini *et al.*, 1993). For practical operational conditions an optimal energy capacity must be found between droplet breakage and energy consumption. It has to be taken into consideration that operating at high mixing intensities will result in high shear forces, which may negatively influence the biomass.

Viscosity relationships of oil in water dispersions

Bacteria thrive in the aqueous phase and it is assumed that the bacteria convert DBT on the interface of the oil droplets and aqueous phase in the o/w dispersion. The conversion rate is limited by the availability of the o/w surface. The o/w surface can be maximized by minimizing the droplet diameter and by increasing the volume fraction of oil (ϕ_o). When the volume fraction of oil in the o/w dispersion increases, the viscosity of the total mixture

will also increase. Therefore, a relation between volume fraction of oil and dispersion viscosity has to be known. In order to select a maximally acceptable fraction dispersed phase (ϕ_o) to apply in the model, the following two criteria must be met:

- As the volume fraction of oil in water exceeds 40%, a phase inversion from o/w to w/o is possible. The inversion point is usually uncertain and a transition region may exist. Therefore, ϕ_o should remain well below 40% (v/v) in order to be able to describe the behavior of an o/w dispersion accurately (Polderman, 1999).

- The dispersion should remain Newtonian, otherwise a correction for non- Newtonian behavior is necessary. Consequently, ϕ_o may not be higher as 25% (Polderman, 1999).

According to these two criteria the maximal value for ϕ_o is 25% (v/v). The influence of biomass on the dispersion viscosity is neglected in this work, because in the aerobic biodesulfurization systems free resting cells are used and no growth occurs (Chang *et al.*, 2000; Maghsoudi *et al.*, 2000, 2001).

The relative viscosity (η_r) is defined as the ratio of the dispersion viscosity (η_{ow}) to that of the continuous aqueous phase (η_w). The relative viscosity can be estimated using Eq. 4:

$$\eta_r = \frac{1}{(1-\phi_o)}\left(1+\frac{1.5 \cdot \eta_o \cdot \phi_o}{\eta_o + \eta_w}\right) \tag{4}$$

In principle Eq. 4 is only valid for dilute dispersions, where $\phi_o < 15\%$ (v/v). Under these conditions the relative viscosity (η_r) increases linearly with an increasing ϕ_o (Zuiderweg, 1988). At $\phi_o = 25\%$ (v/v) also Eq. 4 is applied because a more accurate calculation method is not available. Measurements of the dispersion viscosity for each oil fraction applied in the model were found to be not feasible. The viscosity of the dispersion also depends on the size of the oil droplets. During the measurement the same droplet size distribution must be present as in the STR, while the droplet size attained during the viscosity measurement depends on the shear rate applied. This results in droplet sizes that are not representative for the situation in the STR and consequently experimental errors will be obtained (Polderman, 1999).

Calculation of the average oil droplet size

Generally, droplets in the reactor are subject to turbulent conditions, variations in shear forces and pressure. These processes deform the droplets and break them up into smaller droplets, if disruptive forces exceed the interfacial tension forces. The ratio between these forces is expressed in the *We* number in Eq. 5 (Zhou and Kresta, 1998).

$$We = \frac{c_1 \cdot \rho_w \cdot \varepsilon^{2/3} \cdot d_{max}^{5/3}}{\sigma_{ow}} \tag{5}$$

The interfacial tension (σ_{ow}) in the denominator counteracts the disruptive forces in the numerator. After rearrangement the *We* number in the STR can be defined by Eq. 6, which can be used for the calculation of maximum attainable droplet diameter (d_{max}) (Hinze, 1955). Appendix I shows the derivation of Eq. 5 and Eq. 6 together with the underlying assumptions.

$$\frac{d_{max}}{D} = c_2 \left(We_{STR} \right)^{-3/5} \tag{6}$$

The droplet diameter is also affected by the volume fraction of oil (ϕ_o), since higher coalescence rates occur at larger volume fractions of oil. Coalescence does not dominate over droplet break-up because ϕ_o is below 25% (v/v), thus droplet break-up will determine the average drop size. Due to uncertainties in the drop size distribution, it is not possible to relate the Sauter mean diameter (d_{32}) accurately to physical parameters, as is the case for d_{max} (Appendix I). However, it has been found that d_{32} is proportional to d_{max} (Zhou and Kresta, 1998). Commonly, a linear function of the volume fraction oil is used to find d_{32}, as depicted in Eq. 7.

$$\frac{d_{32}}{D} = c_3 \left(1 + c_4 \cdot \phi_o \right) \left(We_{STR} \right)^{-3/5} \tag{7}$$

Available literature values for the constants c_3 and c_4, measured under defined experimental conditions, *i.e.* volume fraction oil phase (ϕ_o), energy capacity (ε) and standard STR geometry, are summarized in Table 1.

Table 1. Possible values of c_3 and c_4 in Eq. 7.

c_3	c_4	reference
0.051	3.14	Brown and Pit, 1970
0.047	2.5	Van Heuven and Beek, 1971
0.058	5.4	Mlynek and Resnick, 1972

Van Heuven and Beek (1971) determined the coefficients (c_3 and c_4) in Eq. 7 under the widest range of experimental conditions (*i.e.* ϕ_o and ε), consequently these values were applied in our model initially.

Estimation of the mass transfer coefficient

The mass transfer coefficient can be calculated using the Sherwood number for the dispersed oil phase, according to:

$$k_o = \frac{Sh_o \cdot D_o}{X} \qquad (8)$$

The characteristic length (X) of the oil droplet is assumed to be equal to d_{32}. The diffusion coefficients (D_o) of dibenzothiophene in the different organic phases at various temperatures were estimated using the Wilke Chang equation (see Appendix II) (Wilke and Chang, 1955). The Sherwood number for rigid and spherical particles was applied (see Appendix III) (Aris, 1969).

Specific surface area

The specific surface area (a_{ow}) is the total surface area of the oil droplets per m^3 dispersion and is given by (Zuiderweg, 1988):

$$a_{ow} = \frac{6\phi_o}{d_{32}} \qquad (9)$$

Data of the applied organic phases

The most relevant characteristics and physical properties of a variety of hydrocarbon fractions (HCF) applied as solvent for DBT are summarized in Table 2a and 2b.

Table 2a. Characteristics of the applied organic phases*.

solvent	BP [a]-range	API [b] gravity	\<MW\>	H/C ratio	MeABP [c]
	[°C]	[-]	[g/mole]	[-]	[°C]
iso-octane	-	-	114	2.25	126
n-dodecane	-	-	170	2.17	215
benzene	-	-	78.11	1	80
HCF 1	139 - 358	36.55	145.4	1.58	184
HCF 2	116 - 291	44.71	164	1.93	204
HCF 3	153 - 459	30.21	280	1.74	330
HCF 4	135 - 396	18.86	196	1.33	269
HCF 5	134 - 427	33.1	209	1.84	263

[a] boiling point, [b] American Petroleum Institute, [c] Mean Average Boiling Point. The API gravity, average molecular weight and mean average boiling point are calculated according to the appropriate API procedures (API handbook, 1997).

Table 2b. Measured properties of the applied organic phases at 20 and 60°C.*

Solvent	Temperature 20°C			Temperature 60°C		
	ρ	η	σ	ρ	η	σ
	[kg.m^{-3}]	10^{-3} [Pa.s]	[N.m^{-1}]	[kg m^{-3}]	10^{-3} [Pa s]	[N m^{-1}]
iso-octane	741.9	0.544	0.0480	706.2	0.373	0.043
n-dodecane	750.6	1.52	0.0480	722.5	0.832	0.043
benzene	872.9	0.645	0.0350	832	0.386	n.a.
HCF 1	838.7	1.38	0.0389	806.4	0.625	0.0348
HCF 2	799.9	1.58	0.0381	769.4	0.977	0.0342
HCF 3	872.3	13.2	0.0377	846.4	3.92	0.0337
HCF 4	937.9	5.05	0.0376	907.7	2.22	0.0336
HCF 5	856.8	3.55	0.0378	828.5	1.80	0.0338

* Data were kindly supplied by Shell Global Solutions International B.V. (Amsterdam).

RESULTS AND DISCUSSION

Comparing the diffusivity of DBT in various organic phases

The results in Fig. 2 present the calculated time constant values of the DBT transfer at a variable energy capacity in different types of organic phases ($\phi_o = 10\%$) at 20°C.
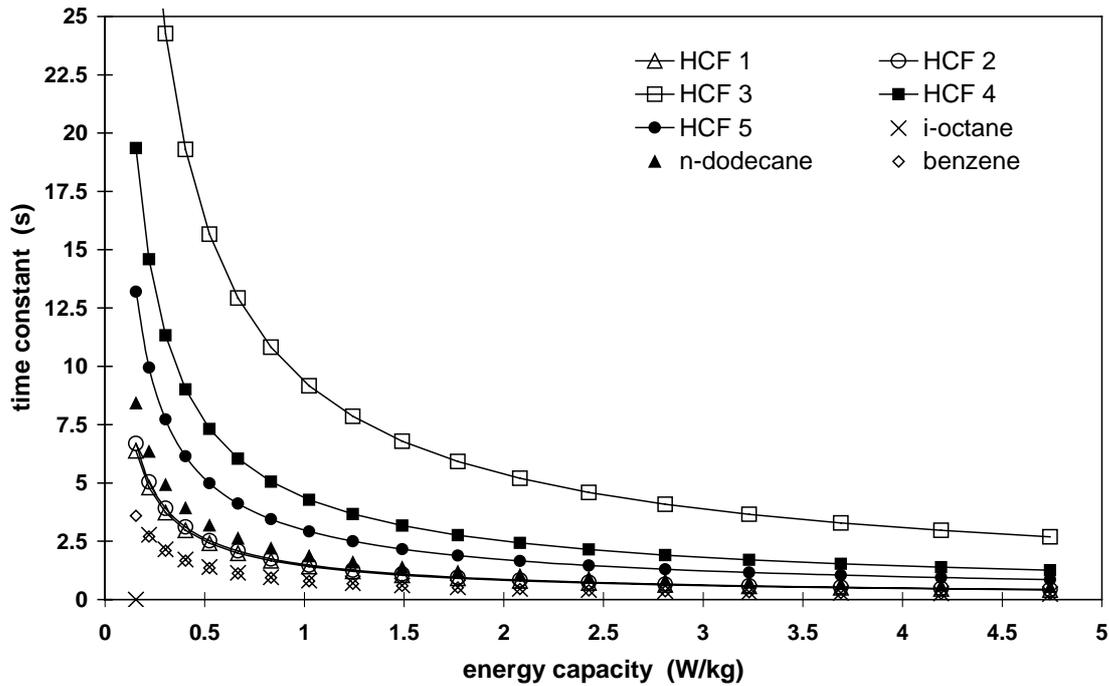

Fig. 2. Time constant of DBT mass transfer in various organic phases vs. energy capacity at a temperature of 20°C and $\phi_o = 10\%$.

It can be seen that the simulated time constants (τ_0) for DBT diffusion in the solvents benzene and *iso*-octane (model solvents) are smaller compared to the values calculated for complex oil distillates, *e.g.* at $\varepsilon = 1.5$ W/kg: $\tau_0 = 0.6$ s for both benzene and *iso*-octane, while $\tau_0 = 6.8$ s or 3.2 s for HCF 3 or HCF4, respectively. The considerably lower viscosities of the model solvents explain these results (Table 2b). Obviously, these model solvents are not representative for DBT diffusion in complex hydrocarbon fractions. Benzene and *iso*-octane are not abundant in complex hydrocarbon fractions because the boiling points are lower (Table 2a). Because of the comparable characteristics (boiling points and viscosities, see Table 2a/b) between *n*-dodecane, HCF 1 and HCF2, the estimated time constants are in the same order, *e.g.* at $\varepsilon = 1.5$ W/kg: $\tau_0 = 1.4$ s for *n*-dodecane, 1.1 s for HCF 1 and HCF 2, respectively. The selected hydrocarbon fractions (HCF 1 up to HCF 5) can be considered as suitable representatives for complex

hydrocarbon fractions. Fig. 2 shows that HCF 3 and HCF 1 present the upper and lower boundary limits of estimated time constants.

Differences in the mass transfer of DBT result from variations in physical properties. An appropriate physical parameter needs to be found to enable a comparison of the mass transfer in different oil distillates. For this purpose, the API gravity in the characterization of oil distillates is frequently used. This parameter is directly derived from the density (API handbook, 1997). However, from the comparison of the physical parameters in Table 2a/b with the results of the time constant analysis, it can be concluded that the API gravity as such is not a suitable parameter to compare oil distillates. A clear relationship between the calculated time constant and the values for the density was not found. Therefore, we attempted to assess a relationship between the viscosity of the applied oil distillate fractions and the estimated time constants. The results are shown in Fig. 3.
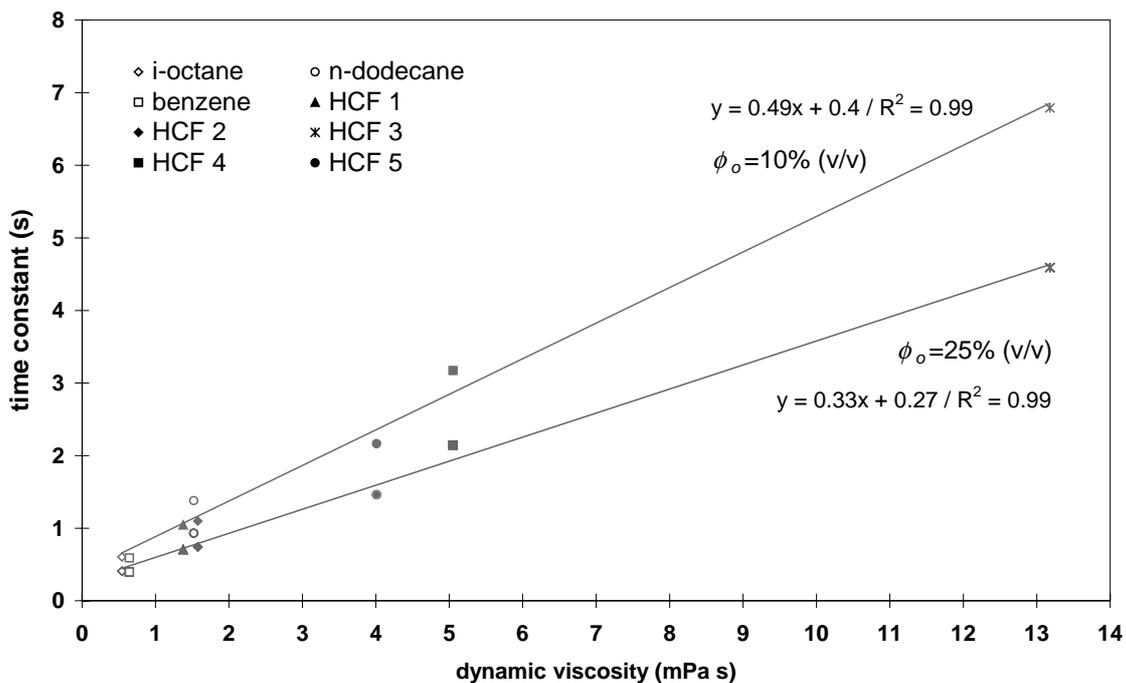
Fig. 3. Time constant of the DBT mass transfer in various organic phases vs. the dynamic viscosity at 20°C. The energy capacity is 1.5 W/kg and ϕ_o is 10 or 25% (v/v).

For both the oil distillates and model solvents it appears that the time constant depends linearly on the dynamic viscosity. The viscosity seems to be the predominant physical parameter: it has a clear impact on the DBT mass transfer rate. A similar relation of density and interfacial tension compared to the time constant cannot be found. The influence of these physical parameters is considered to be of minor importance on the

DBT mass transfer rate. As the time constant is composed of the mass transfer coefficient (k_o) and the specific surface area (a_{ow}), we investigated the effect of the energy capacity (ε) on both parameters. The results are shown in Fig. 4.
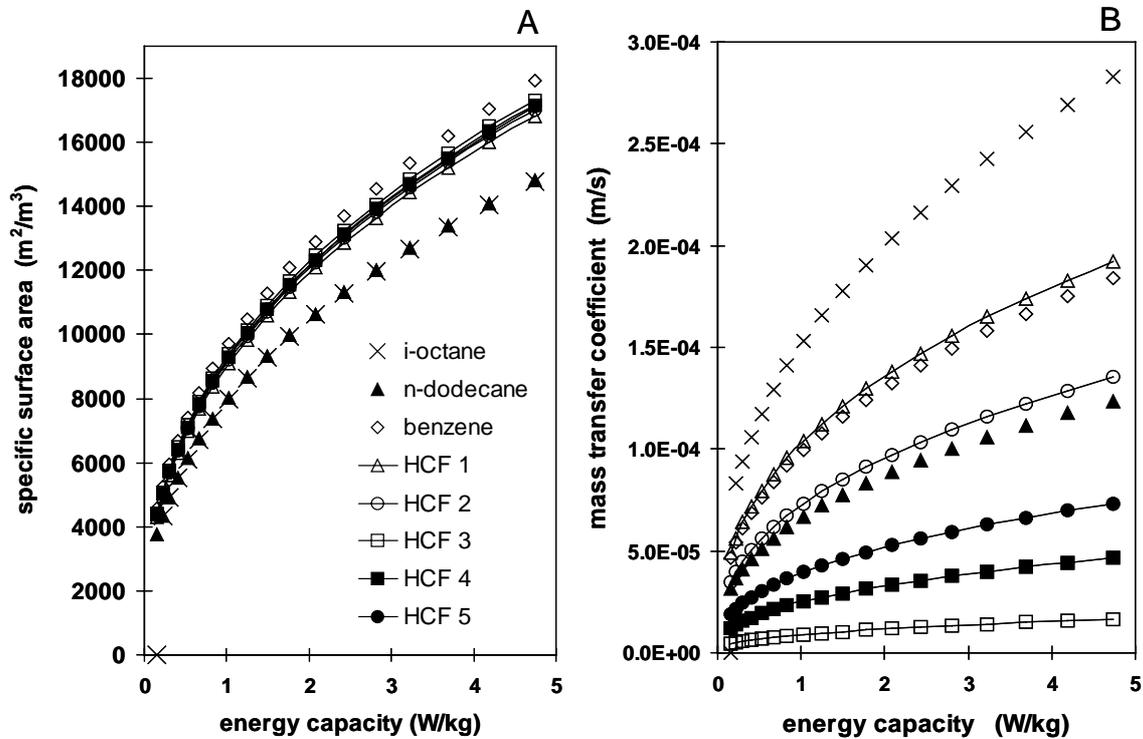

Fig. 4. Specific surface area of various organic phases (Fig. 4A) and DBT mass transfer coefficient in various organic phases (Fig. 4B) vs. the energy capacity at $\phi_o = 10\%$ (v/v) and 20°C (same key for both Figs. 4A and 4B).

The results depicted in Fig. 4A indicate that the specific surface area only slightly depends on the type of HCF. The specific surface areas of the oil distillates are between the values found for the model solvents. These results can be explained by comparing the interfacial tensions (σ_{ow}, Table 2b), of the hydrocarbon fractions. The interfacial tensions of alkanes are relatively high, while those of aromatic compounds are relatively low (Table 2b). The interfacial tension of a complex fraction is the sum interfacial tensions of its individual pure organic compounds (σ_i) multiplied by the weight fraction (x_i) in the hydrocarbon, thus: $\sigma_{ow} = \sum \sigma_i \cdot x_i$.

Therefore, the variation in the time constants between complex fractions must be contributed to differences in the mass transfer coefficients (k_o). The viscosity has a profound influence on the diffusion coefficient (Wilke and Chang, 1955) and consequently

on k_o. The influence of the viscosity on k_o is clearly demonstrated in Fig. 4B. HCF 3 has the highest viscosity ($\eta = 13.2 \times 10^{-3}$ mPa.s at 20°C) and consequently the lowest mass transfer coefficient ($k_0 = 0.1 \times 10^{-4}$ m/s at $\varepsilon = 1.5$ W/kg), while for HCF 1 ($\eta = 1.4 \times 10^{-3}$ mPa s at 20°C) the opposite is found ($k_0 = 1.2 \times 10^{-4}$ m/s at $\varepsilon = 1.5$ W/kg).

Influence of temperature and the amount of organic phase

The fluid properties (density, viscosity and interfacial tension) of the water and oil phases all are more or less temperature dependent and consequently the temperature influences the value of the time constant. The question therefore arises, which of the two parameters (k_o and a_{ow}) would be the most temperature sensitive and therefore exerts the greatest influence upon the time constant. To illustrate the influence of temperature on k_o this parameter was plotted versus the energy capacity as shown in Fig. 5A. In order to give an outline, only the least viscous (HCF 1) and most viscous (HCF 3) hydrocarbon distillates are presented.

The effect of the temperature on the mass transfer coefficient clearly manifests for both complex fractions. This effect mainly originates from the influence of temperature on the diffusion coefficient. Apart from a direct temperature dependency on mass transfer, an indirect temperature effect via the viscosity exists, which is non-linear and most profound at low temperatures. As the interfacial tension hardly depends on the temperature, it is not taken into account (data not shown).

Refinery operations require high temperatures and therefore application of a biodesulfurization at thermophilic (55-65°C) temperatures might be economically favorable. From a process point of view a mesophilic (30-37°C) bioprocess has high cooling demands. With respect to the calculated DBT mass transfer coefficients, an advantage of a thermophilic process conditions can be noticed: *e.g.* for HCF 1 at $\varepsilon = 1.5$ W/kg: k_0 at 40°C $= 14 \times 10^{-5}$ m/s and k_0 at 60°C $= 24 \times 10^{-5}$ m/s, while for HCF 3 at $\varepsilon = 1.5$ W/kg: k_0 at 40°C $= 2.7 \times 10^{-5}$ m/s and k_0 at 60°C $= 5.3 \times 10^{-5}$ m/s. This advantage could be used if high rate desulfurizing thermophilic bacteria are available.
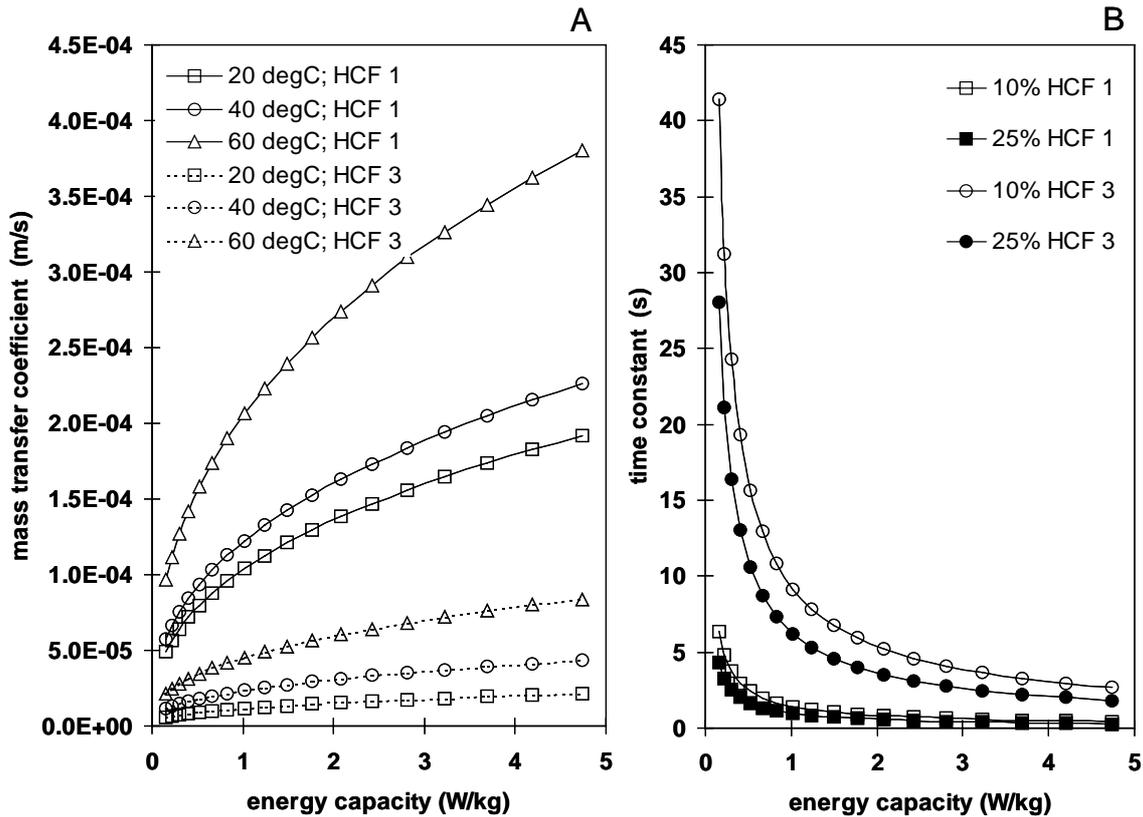
Fig. 5. 5A: Influence of the temperature on the DBT mass transfer coefficient in HCF 1 and HCF 3 as function of the energy capacity at $\phi_o = 10\%$ (v/v). 5B: Time constant of DBT mass transfer for diffusion in HCF 1 and HCF 3 at 20°C vs. the energy capacity at $\phi_o = 10$ or 25% (v/v).

The o/w-ratio should be as high as possible in order to optimize the load of organic sulfur compounds that must be converted by the bacteria. Relatively large time constants are calculated for ϕ_o-values lower than 10% (v/v) as a consequence of the then prevailing low values for the specific surface area (*e.g.* $\tau_0 = 47$ s for HCF 3 at 20°C and a $\phi_o = 1\%$ (v/v)). In Fig. 5B the time constant is plotted versus the energy capacity at two ϕ_o-values of 10 and 25% (v/v) for HCF 1 and HCF 3. It can be inferred for Fig. 5B that especially at $\phi_o = 25\%$ (v/v) low values for the time constant prevail.

Sensitivity analysis of diffusion coefficient and droplet diameter estimation

Diffusion coefficients of DBT mass transfer in an organic solvent can be estimated using the Wilke-Chang equation (Appendix 2), with an accuracy in the range of 20 to 30% around the mean value. The influence of variations in the diffusion coefficient on the relative time constant is presented in Fig. 6A. The relative value of the diffusion coefficient varied from 0.4 up to 1.6 times the estimated mean value. The diffusion

41

coefficients of DBT at 20°C in HCF 1 and 3 are $7.8 \cdot 10^{-10}$ m^2/s and $1.1 \cdot 10^{-10}$ m^2/s, respectively. In the model an underestimation of the diffusion coefficient of 25%, gives a 20% lower time constant. When the diffusion coefficient is 25% overestimated, the time constant will be 33% too high.
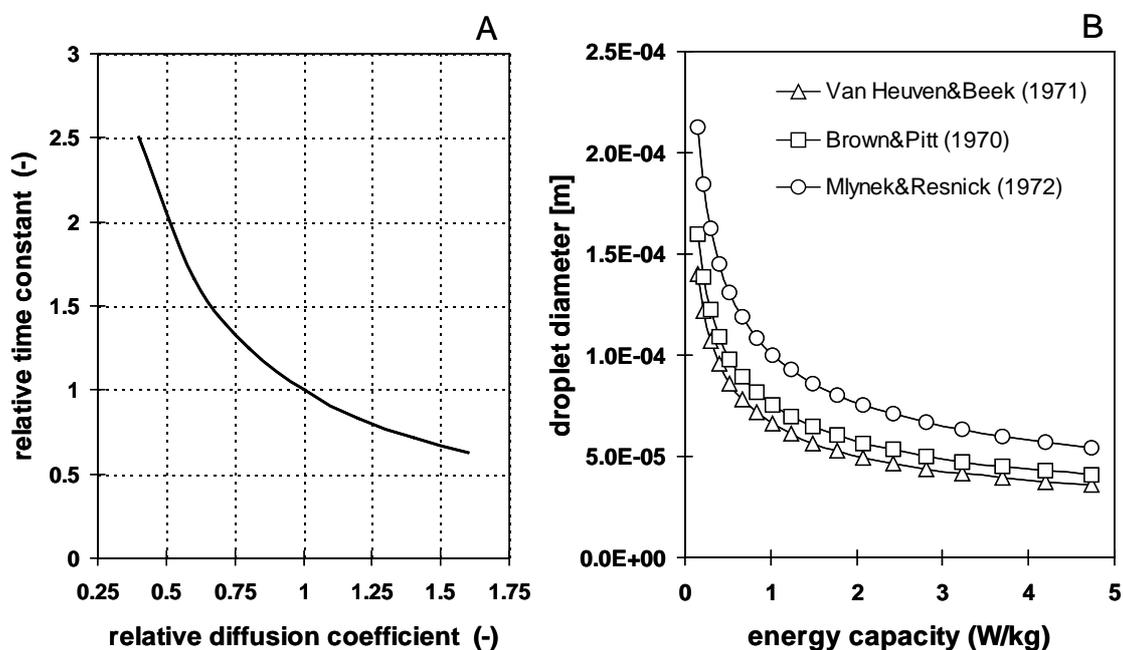

Fig. 6. 6A: Sensitivity of the relative time constant on the relative diffusion coefficient. 6B. Estimated droplet diameters vs. the energy capacity using different correlations to calculate d_{32} for HCF 3 droplets.

The calculated droplet diameter depends on accurate values for c_3 and c_4 in Eq. 7. Besides Van Heuven and Beek (1971) several other authors determined the correlation depicted in Eq. 7, resulting in different constants (see c_3 and c_4 values in Table 1). In Fig. 6B, the droplet diameters of HCF 3 had been calculated using values for c_3 and c_4 found by three different authors. Especially the values found by applying the Mlynek and Resnick (1972) correlation result in quite large droplet diameters. Deviations in the time constant can be expected and are acceptable in practice (data not shown). An important remark must be made regarding the time constant estimation with respect to the different d_{32} values found (Fig. 6B). The time constant is only used to compare different situations. Conclusions on the comparison of different time constants for various types of organic phases, the influence of the temperature and amount of organic phase are not influenced by possible deviations in estimations of the droplet diameter.

DBT mass transfer rate versus biological desulfurization rate

A time constant analysis of the two consecutive process steps (*i.e.* diffusion to the o/w surface and conversion of DBT) in biological desulfurization is a suitable tool to obtain insight in the rate-limiting step of the overall process. It is assumed that the transfer of DBT from the o/w-surface, via the water phase surrounding the microorganism is included in the overall time constant for the microbial desulfurization. Consequently, an apparent kinetic value is used that is composed of the DBT diffusion rate to the enzymes responsible for the conversion and the actual DBT conversion rate. It is not possible to determine DBT conversion kinetics as a sole parameter independent of diffusion. A direct comparison on the basis of time constants for DBT mass transfer and biological DBT conversion is feasible, when the DBT concentration ($[C]_{DBT}$) is known. To enable a comparison, we compared the flux of DBT to the o/w-surface ($J_o^{'}$) with aerobic conversion rates ($J_b^{'}$).

For the estimation of a range of time constants for the DBT flux, a dispersion with the following characteristics was used: 10% (v/v) HCF3 in water with a $[C]_{DBT}$ of 0.1, 1 or 10 mM at 20ºC. In case of an ideally mixed dispersion a homogeneous DBT concentration in the oil droplet can be assumed due to continuous formation and disruption of droplets. Consequently, the volumetric DBT flux to the o/w-interface ($J_o^{'}$) can be defined as:

$$J_0^{'} = \frac{[C]_{DBT}}{\tau_o} = k_o \cdot a_{ow} \cdot [C]_{DBT} \quad (\text{mol m}^{-3}\text{h}^{-1}) \tag{10}$$

The volumetric DBT flux must be compared to the DBT conversion rate ($J_b^{'}$). Significant work is performed on the aerobic conversion of DBT by several authors. Under aerobic conditions DBT is used as the sole source of sulfur and the carbon skeleton is conserved in a stepwise reaction as 2-hydroxybiphenyl as depicted in Fig. 7 (Kobayashi *et al.*, 2001; Folsom *et al.*, 1999; Ohshiro *et al.*, 1995; Izumi *et al.*, 1994).


DBT   2-HPB
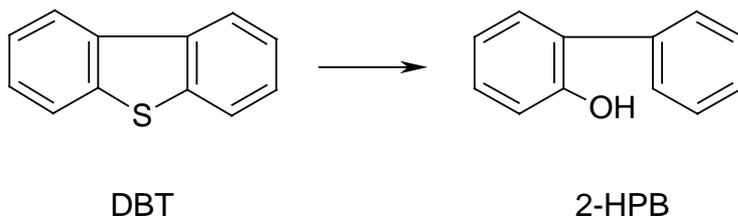
Fig. 7. 2-HBP (2-hydroxybiphenyl) is the end-product of aerobic DBT conversion.

An overview of DBT depletion rates for different types of biomass is presented in Table 3.

Table 3. Overview of aerobic degradation rates reported in literature.

strain / organism	DBT depletion rate $(mol \cdot m^{-3} \cdot h^{-1})$	Reference
Rhodococcus erythropolis I-19	5.0 [a]	(Folsom *et al.*, 1999)
R. erythropolis rKA2-5-1	2.4	(Kobayashi *et al.*, 2001)
R. erythropolis KA2-5-1	1.4	(Kobayashi *et al.*, 2001)
R. erythropolis H-2	1.2	(Ohshiro *et al.*, 1995)
R. erythropolis D-1	0.9 [b]	(Izumi *et al.*, 1994)

[a] Value used to calculate $J'_{b\,max}$, [b] Value used to calculate $J'_{b\,min}$.

For the comparison the range of 0.9 up to 5.0 mmol l^{-1} h^{-1} (see Table 3) is applied as the lowest ($J'_{b\,min}$) and highest ($J'_{b\,max}$) biological conversion rate. Generally, the DBT depletion rate data presented in Table 3 were obtained by following the DBT depletion in a resting cell reaction system, where cells pre-grown on alternative substrates (*e.g.* sugars) were added in high concentrations to a batch system, where DBT was present as the sole source of sulfur. The calculated microbiological DBT conversion rates are based on specific rates and the corresponding biomass concentrations given for the references cited in Table 3. In Fig. 8 the logarithmic value of the ratio of both fluxes (J'_o / J'_b) versus the energy capacity is presented.

As can be seen from the results in Fig. 8 the C_{DBT} determines the order of magnitude of $J'_o / J'_{b,max}$ up to $J'_o / J'_{b,min}$. At a energy capacity of 1.75 W/kg droplets of approximately 60 µm are formed (see Fig. 6B). At this energy capacity a factor 10 up to 10^4 is found for $J'_o / J'_{b,max}$ with a C_{DBT} of 0.1 mM and $J'_o / J'_{b,min}$ with a C_{DBT} of 10 mM, respectively (Fig 8). Therefore, it is evident that the aerobic biodesulfurization process is not mass transport limited with respect to the volumetric flux DBT to the o/w-interface.
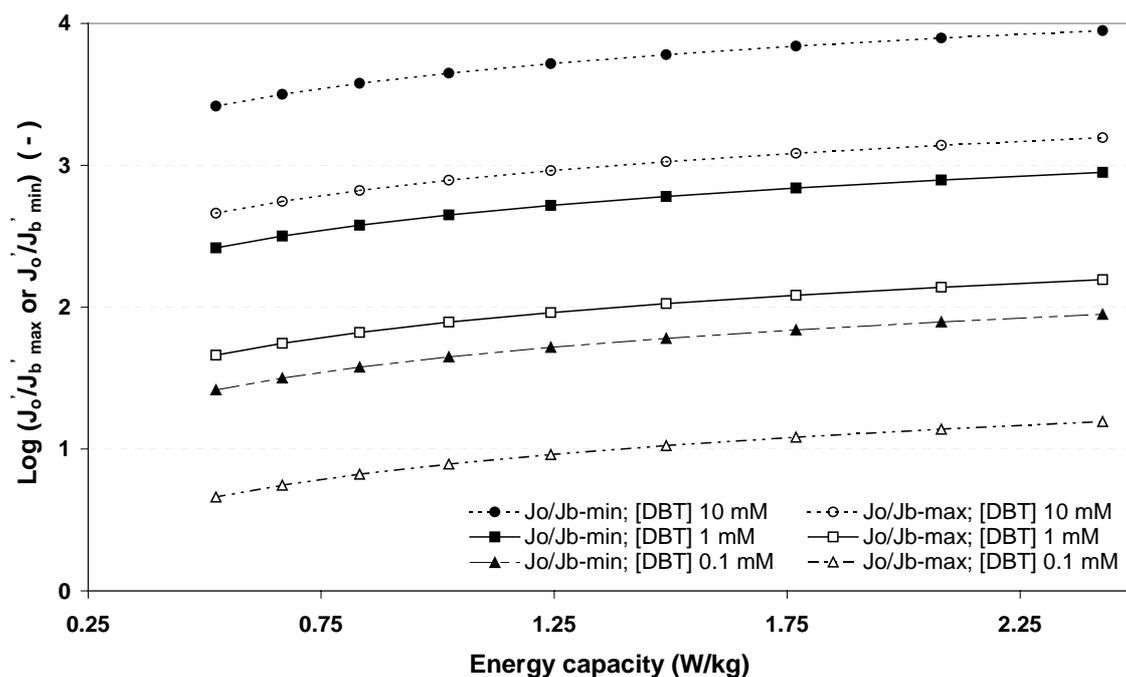
Fig. 8. Flux ratio $J'_o / J'_{b,max}$ or $J'_o / J'_{b,min}$ vs. the energy capacity at DBT concentrations of 0.1, 1 or 10 mM.

According to Kaufman *et al.* (1998), the mass transfer resistance is mainly located in the aqueous phase surrounding the bacteria. The bioavailability of DBT is low due to its minimal (≈ 0) solubility in the aqueous phase. Hitherto, a high specific surface area is not necessary to increase the DBT flux to the o/w interface, but it is essential to maximize the contact-area between the bacteria and the oil droplets. From the above results, it can be concluded that the microbial desulfurization rate is the main process that must be optimized to improve the aerobic process. A considerable amount of work to stimulate the oxidative conversion of DBT by altering genes is performed and maybe future developments can increase the DBT conversion activity further (Arensdorf *et al.*, 2002; Kobayashi *et al.*, 2001; Hirasawa *et al.*, 2001; Matsui *et al.*, 2001; Folsom *et al.*, 1999).

The formation of small droplets in a STR implies the application of high shear rates, which obviously will be a disadvantage for microorganisms. An alternative reactor type with less shear forces is an air lift reactor, but so far unfortunately little is known about the hydrodynamic behavior of such a three-phase system. Sajc *et al.* (1995) obtained a droplet diameter varying between 3.75 up to 5.0 mm at high gas flows ($U_g = 10^{-2}$ m·s^{-1}) using *n*-hexadecane as the organic phase. The calculated time constants for this system at volume fractions oil (ϕ_o) of 10 and 25% (v/v) are summarized for *n*-hexadecane, HCF 1 and HCF 3 in Table 4. Based on these calculations, this reactor configuration seems to be not very

promising. Due to the low specific surface area, high time constants are calculated and the amount of cells in direct contact with the o/w-interface is restricted.

Table 4. Calculation of the time constant at $\phi_o = 10$ and 25% (v/v) in an air lift system.

		$\phi_o = 10$ % (v/v)		$\phi_o = 0.25$ % (v/v)	
hydrocarbon phase	k [a] (m/s)	a [b] (m^2/m^3)	τ_o [c] (s)	a [b] (m^2/m^3)	τ_o [c] (s)
n-hexadecane	$5.6 \cdot 10^{-7}$	160	$11 \cdot 10^3$	400	$4 \cdot 10^3$
HCF 1	$1.5 \cdot 10^{-6}$	160	$4 \cdot 10^3$	400	$2 \cdot 10^3$
HCF 3	$2.0 \cdot 10^{-7}$	160	$31 \cdot 10^3$	400	$13 \cdot 10^3$

[a] Values calculated using Eq. 8 (see also Fig. 1)
[b] Calculation performed using Eq. 9 with the smallest d_{32} (best case; 3.75 mm) for the applied organic fractions (Sajc *et al.*, 1995).
[c] Time constant calculated according to Eq. 1.

Another approach described by Kaufman *et al.* (1997) concerns the use of an emulsion phase contactor (EPC), which is based on the formation of an emulsion of aqueous biocatalyst in the organic phase. The energy input is not imparted on the entire liquid bulk, but merely on the dispersed phase creating droplets of about 3 μm (Kaufman *et al.*, 1998). Although the EPC has a low power requirement no extra desulfurization capacity manifested when using *Rhodococcus sp*. IGTS8 as the biocatalyst. In a STR process under similar experimental conditions a droplet diameter of the same order of magnitude was created. The droplet diameter in the STR decreased considerably by interfacial active endogenously produced biosurfactants (Kaufman *et al.*, 1998). In processes where formation of biosurfactants is unlikely, a reactor type with an injection device to create small oil droplets might be advantageous, because of the high specific surface area and consequently low time constants that can be achieved.

CONCLUSIONS

A mathematical model was developed in order to study the time constant of dibenzothiophene mass transfer in a dispersed organic phase under a set of conditions using simulations. The model is based on theoretical and semi-empirical equations and it was used to compare the dibenzothiophene mass transfer in different hydrocarbon fractions in the temperature range of 20 up to 60°C. The calculated time constants depend mainly on the temperature dependent dynamic viscosity, the energy capacity, the hold-up organic phase (10 or 25% (v/v)) and were found to be in the order of seconds. At an increasing energy capacity the difference between the values of the time constants obtained for various simulated conditions becomes negligible. The dynamic viscosity has a profound impact on the estimation of the time constant. This is mainly due to the large influence of the dynamic viscosity on the value for the mass transfer coefficient. The temperature affects the time constant also via the mass transfer coefficient. The estimated diffusion coefficient depends directly on the temperature, but also indirectly via the viscosity. The specific surface area depends on the hold-up of the organic phase and the interfacial tension. The temperature dependency of the specific surface area is negligible. Minor variations in the interfacial tensions of the hydrocarbon fractions do not affect the time constant. Larger amounts of organic phase (>10% (v/v)) result in smaller time constants, due to the high specific surface area.

Sensitivity analysis on the estimations of the diffusion coefficients and droplet diameters demonstrates possible deviations in the prediction of the time constant, especially for viscous fractions.

A high specific surface area is favorable for a maximal contact between the bacteria and the oil phase. However, small droplets are not a prerequisite to enhance the DBT mass transfer in the oil phase, because the diffusion of DBT to the interface is relatively fast. The main mass transfer resistance is in the aqueous phase, influencing the DBT transport from the o/w-interface to the bacterium. The biological conversion rate is an important limiting factor, which exerts a large influence on the overall process.

NOMENCLATURE

a_{ow}	specific surface area ($m^2 m^{-3}$)
c_1	constant in Eq. 5
c_2	constant in Eq. 6
c_3, c_4	constants in Eq. 7
C_{DBT}	concentration dibenzothiophene in oil (mol/m^3)
D	impeller diameter (m)
d_{32}	Sauter droplet diameter (m)
d_{max}	maximal droplet diameter (m)
D_o	diffusion coefficient of DBT in the oil phase ($m^2 s^{-1}$)
H	liquid height in the tank (m)
J'_o	volumetric DBT flux in an organic phase ($mol\, m^{-3} s^{-1}$)
J'_b	DBT conversion rate ($mol\, m^{-3} s^{-1}$)
k_o	mass transfer coefficients in the oil phase ($m\, s^{-1}$)
N	stirrer speed (s^{-1})
N_p	power number (dimensionless)
P	power input (W)
Re	Reynolds number $\rho ND^2/\eta$ (dimensionless)
Sh	Sherwood number $k_o X/D_o$ (dimensionless)
T_S	tank diameter (m)
T	temperature (K or °C)
U_g	superficial gas velocity ($m\, s^{-1}$)
V_l	volume of liquid in the STR (m^3)
X	characteristic length (m)

Greek letters

ε	energy capacity ($W\, kg^{-1}$)
ϕ_o	volume fraction of oil in the mixture (dimensionless)
η_{ow}	dynamic viscosity of the total liquid phase ($kg\, m^{-1} s^{-1}$)
η_o	dynamic viscosity of the oil phase ($kg\, m^{-1} s^{-1}$)
η_w	dynamic viscosity of the aqueous phase ($kg\, m^{-1} s^{-1}$)
η_r	relative viscosity (dimensionless)

ρ_l density of the mixture ($kg \cdot m^{-3}$)

ρ_o density of the oil phase ($kg \cdot m^{-3}$)

ρ_w density of the water phase ($kg \cdot m^{-3}$)

σ_{ow} interfacial tension between the oil and water phase ($N \, m^{-1}$)

τ_o time constant for mass transfer of DBT to the oil-water interface (s)

Abbreviations

API   American Petroleum Institute

BP   boiling point (°C)

MeABP   mean average boiling point (°C)

MW   molecular weight ($g \, mol^{-1}$)

STR   stirred tank reactor

Acknowledgement

REFERENCES

American Petroleum Institute handbook (4th ed.). 1997. API procedure 10A3.2, 10A4.1 and 10A4.2.

Anabtawi J.A., Ali S.A., Ali M.A. 1996. Impact of gasoline and diesel specifications on the refining industry. Energ. Source 18: 203-214.

Arensdorf J.J., Loomis A.K., DiGrazia, P.M., Monticello, D.J., Pienkos P.T. 2002. Chemostat approach for the direct evolution of biodesulfurization gain-of-function mutants. Appl. Environ. Microbiol. 68: 691-698.

Aris R. 1969. Elementary Chemical Reactor Analysis, Prentice-Hall, Englewood Cliffs.

Brown D.E., Pitt K. 1970. Drop break up in a stirred liquid-liquid contactor. In: Proc. Chemeca 83, Melbourne and Sydney.

Calabrese R.V., Chang T.P.K., Dang P.T. 1986. Drop break-up in turbulent stirred-tank contactors, Part I: Effect of dispersed-phase viscosity. AIChE J. 32: 657-666.

Chang J.H., Chang Y.K., Cho K-S, Chang H.N. 2000. Desulfurization of model and diesel oils by resting cells of *Gordona* sp. Biotechnol. Lett. 22: 193-196.

De Gooijer C.D., Wijffels R.H., Tramper J. 1991. Growth and substrate consumption of *Nitrobacter agilis* cells immobilized in carrageenan: Part 1. dynamic modeling. Biotechnol. Bioeng. 38: 224-231.

European Union, E.U. 1998.Directive 98/70/EC.

Folsom B.R., Schieche D.R., DiGrazia P.M., Werner J., Palmer S. 1999. Microbial desulfurization of alkylated dibenzothiophenes from a hydrodesulfurized middle distillate by *Rhodococcus erythropolis* I19. Appl. Environ. Microbiol. 65: 4967-4972.

Gary J.H., Handwerk G.E. 1994. In: Introduction to petroleum refining. Marcel Dekker, New York.

Gogate P.R., Beenackers A.A.C.M., Pandit A.B. 2000. Multiple-impeller systems with a special emphasis on bioreactors: a critical review. Biochem. Eng. J. 6: 109-144.

Grossman M.J., Lee M.K., Prince R.C., Garrett K.K., George G.N., Pickering I.J. 1999. Microbial desulfurization of a crude oil middle-distillate fraction: analysis of the extent of sulfur removal and the effect of removal on remaining sulfur. Appl. Environ. Microbiol. 65: 181-188.

Hinze J.O. 1955. Fundamentals of the hydrodynamic mechanism of splitting in dispersion processes. AIChE J. 1: 289-295.

Hirasawa K., Ishii Y., Kobayashi M., Koizumi K., Maruhashi K. 2001. Improvement of desulfurization activity in *Rhodococcus erythropolis* KA2-5-1 by genetic engineering. Biosci. Biotechnol. Biochem. 65: 239-246.

Izumi Y. Oshiro T., Ogino H., Hine Y., Shimao M. 1994. Selective desulfurization of dibenzothiophene by *Rhodococcus erythropolis* D-1. Appl. Environ. Microbiol. 60: 223-226.

Kabe T., Ishihara A., Tajima H. 1992. Hydrodesulfurization of sulfur-containing polyaromatic compounds in light oil. Ind. Eng. Chem. Res. 31: 1577-1580.

Kaufman E.N., Harkins J.B., Borole A.P. 1998. Comparison of batch-stirred and electro-spray reactors for biodesulfurization of dibenzothiophene in crude oil and hydrocarbon feedstocks. Appl. Biochem. Biotechnol. 73: 127-144.

Kaufman E.N., Harkins J.B., Rodriguez M., Tsouris C., Selvaraj P.T., Murphy S.E. 1997. Development of an electro-spray bioreactor for crude oil processing. Fuel Process. Technol. 52: 127-144.

Kobayashi M., Horiuchi K., Yoshikawa O., Hirasawa K., Ishii Y., Fujino K., Sugiyama H., Maruhashi K. 2001. Kinetic analysis of microbial desulfurization of model and light gas oil containing multiple alkyl dibenzothiophenes. Biosci. Biotechnol. Biochem. 65: 298-304.

Maghsoudi S., Vossoughi M., Kheirolomoom A., Tanaka E., Katoh S. 2001. Biodesulfurization of hydrocarbons and diesel fuels by *Rhodococcus* sp. Strain P32C1. Biochem. Eng. J. 8: 151-156.

Maghsoudi S., Kheirolomoom A., Vossoughi M., Tanaka E., Katoh S. 2000. Selective desulfurization of dibenzothiophene by newly isolated *Corynebacterium* sp. Strain P32C1. Biochem. Eng. J. 5: 11-16.

Matsui T., Hirasawa K., Konishi J., Tanaka Y., Maruhashi K., Kurane R. 2001a. Microbial desulfurization of alkylated dibenzothiophene and alkylated benzothiophene by recombinant *Rhodococcus* sp. strain T09. Appl. Microbiol. Biotechnol. 56: 196-200.

Mlynek Y., Resnick W. 1972. Drop size in an agitated liquid-liquid system, AIChE J. 18: 122-127.

Moucha T., Linek V., Sinkule J. 1995. Measurements of $k_l a$ in multiple-impeller vessels with significant axial dispersion in both phases. Chem. Eng. Res. Des. 73A: 286-290.

Nocentini M., Fajner D., Pasquali G., Majeli F. 1993. Gas-liquid mass transfer and hold-up in vessels stirred with multiple Rushton turbines: water and water-glycerol solutions. Ind. Eng. Chem. Res. 32: 19-26.

Ohshiro T., Hirata T., Izumi Y. 1995. Microbial desulfurization of dibenzothiophene in the presence of hydrocarbon. Appl. Microbiol. Biotechnol. 44: 249-252.

Okada H., Numura N., Nakahara T., Muruhashi K. 2002. Analysis of substrate specificity of the desulfurizing bacterium *Mycobacterium* sp. G3. J. Biosc. Bioeng. 93: 228-233.

Onaka T., Konishi J., Ishii Y., Maruhashi K. 2001. Desulfurization characteristics of thermo-philic *Paenibacillus* sp. Strain A11-2 against asymmetrically alkylated dibenzothiophenes. J. Biosci. Bioeng. 92: 193-196.

Pinelli D., Nocentini M., Magelli F. 1994. Hold-up in low viscosity gas-liquid systems stirred with multiple-impellers: comparison of different agitator types and sets. Proc. Eur. Conf. Mix. 81: 8.

Perry R.H., Green D.W. 1997. Chemical engineers' handbook, 7th edition. McGraw-Hill, New York.

Polderman H.G. 1999.Personal communication. Shell Global Solutions International B.V. (Amsterdam).

Rall H.T., Thompson C.J., Coleman H.J., Hopkins R.L. 1972. In: Bulletin 659, Sulfur compounds in crude oil, U.S. Dept. of Interior, Bureau of Mines.

Sajc L., Obradovic B., Vukovic D., Urgarski B., Grubisic D., Vunjak-Novakovic G. 1995. Hydrodynamics and mass transfer in a four-phase external loop air lift bioreactor. Biotechnol. Prog. 11: 420-428.

Shafi R., Hutchings G. J. 2000. Hydrodesulfurization of hindered dibenzothiophenes: an overview. Catal. Today 59: 423-442.

Shennan J. L. 1996. Microbial attack on sulfur-containing hydrocarbons: implications for the biodesulfurization of oils and coals. J. Chem. Tech. Biotechnol. 67: 109-123.

Speight J.G. 1981. In: The Desulfurization of Heavy Oils and Residua (Heinz Hienemann, ed.), Marcel Dekker, New York.

Sweere A.P.J., Luyben K. Ch. A. M., Kossen N. W. F. 1987. Regime analysis and scale-down: tools to investigate the performance of bioreactors. Enzyme. Microb. Tech. 9**:** 386-398.

Van Heuven J.W., Beek W.J. 1971. In: Proc. Int. Solvent Extr. Conf.,The Hague, Soc. Chem. Ind. 70: Paper 51.

Wilke C.R., Chang P. 1955. Correlation of diffusion coefficients in dilute solutions. A.I.Ch.E. J. 1: 264-270.

Wang C.Y., Calabrese R.V. 1986. Drop breakup in turbulent stirred-tank contactors, Part II: Relative influence of viscosity and interfacial tension AIChE J. 32**:** 667-681.

Zhou G., Kresta S.M. 1998. Correlation of mean drop size and minimum drop size with the turbulence energy dissipation and the flow in an agitated tank. Chem. Eng. Sci. 53: 2063-2079.

Zuiderweg F.J. 1988. Physical scheidingsmethoden, deel 2. Delft, Technische Universiteit Delft.

APPENDICES

Appendix I

In appendix I the theoretical considerations for the calculation of the drop size are presented. The breakage of a drop depends on the balance between disruptive and restoring forces, expressed in the *We* number. As restoring forces the interfacial tension and the internal viscous stress can be considered. However, in this work the contribution of viscous stress is neglected and only the interfacial tension is considered as restoring force. This implies that the equations presented here are only applicable for dilute dispersions, where the average drop size is determined by the break-up of droplets. The break-up is dependent on external viscous shear stresses and turbulent pressure fluctuations. The external viscous stress is assumed to be negligible compared with the turbulent pressure fluctuations. Consequently, the diameter of a droplet is assumed to be much larger compared with the Kolmogoroff length scale (η_k, eq. A1.1), which is an estimate of the minimum eddy size (d, eq. A1.2). The Kolmogoroff length scale (η_k in m) is dependent on the kinematic viscosity (ν in m^2/s) and the turbulence kinetic energy dissipation rate (ε_k in m^2/s^3) The minimum eddy size is considered as the minimum drop size, since the remaining energy will dissipate in the continuous phase.

$$\eta_k = \left(\frac{v^3}{\varepsilon_k} \right)^{1/4}$$
(A1.1)

Taking all the assumptions mentioned above into account the resulting expression for the *We* number is presented in Eq. A1.2.

$$We = \frac{\rho_w \cdot \overline{u^2(d)} \cdot d}{\sigma_{ow}}$$
(A1.2)

Here $\overline{u^2(d)}$ corresponds to the energy in eddy size d. The turbulent forces break drops with diameters larger than d_{max}. Therefore, d_{max} is considered as the maximal attainable stable drop diameter and replaces d (Eq. A1.2). The characteristic velocity is proportional to the energy capacity per mass unit at turbulent conditions ($\varepsilon \propto \overline{u^2(d)}^{3/2} \cdot d^{-1}$). After rearrangement Eq. A1.3 is obtained (Hinze, 1955).

$$We = \frac{c_1 \cdot \rho_w \cdot \varepsilon^{2/3} \cdot d_{max}^{5/3}}{\sigma_{ow}}$$
(A1.3)

Since $\varepsilon \propto N^2 \cdot D^3$ the *We* number in the STR can be defined according to Eq. A1.4, more details are presented by Zhou and Kresta (1998).

$$\frac{d_{max}}{D} = c_2 \left(\frac{\rho_c \cdot N^2 \cdot D^3}{\sigma_{ow}} \right)^{-3/5} = c_2 (We_{STR})^{-3/5}$$
(A1.4)

Appendix II

The Wilke Chang equation (A2.1) is applied to estimate diffusion coefficients.

$$D_{A,B} = 7.4 \cdot 10^{-8} \cdot T \cdot \frac{\sqrt{\psi_B \cdot MW_B}}{\eta_B \cdot \overline{V}_A^{0.6}} \tag{A2.1}$$

Where A and B denote the solute and the solution, respectively, T is the temperature (K), MW_B the molecular weight of the solvent (g/mole), η_B is the dynamic viscosity of the solvent (cP), $\overline{V}_A$ is the molar volume of the solute at its normal boiling point (cm^3/mol) and ψ_B is the constant which accounts for the solvent interactions (2.6 for water, 1.9 for methanol, 1.5 for ethanol and 1 for non associating solvents). The diffusion coefficient has the unit (cm^2/s).

Appendix III

Convection within the oil droplet distributes DBT (homogeneously) over the organic phase. Whether internal circulation within the hydrocarbon droplets exists, is decided with the Levich criterion (eq. A3.1). Internal circulation will occur when:

$$r_{od} > \sqrt{\frac{3 \cdot \sigma_{ow}}{\left| \rho_w \cdot \rho_o \right| \cdot g}} \tag{A3.1}$$

Where σ_{ow} is the interfacial tension between the immiscible phases (N.m^{-1}), r_{od} is the radius of the oil droplets and ρ_w and ρ_o are the densities of the water and oil phase (kg.m^{-3}), respectively. In this work the use of the Levich criterion for the dispersion process resulted in the assumption that the oil droplets are rigid. Consequently, a Sherwood number of 6.6 for the dispersed phase was applied in the model.

Details of photographs depicting the experimental work that is described in Chapter 3.

ANAEROBIC DESULFURIZATION OF THIOPHENES
BY MIXED MICROBIAL COMMUNITIES FROM OILFIELDS

ABSTRACT

Anaerobic enrichment cultures obtained from oil fields degraded various thiophenic compounds *i.e.* thiophene, benzothiophene and dibenzothiophene, with the concomitant formation of sulfide using hydrogen, lactate and ethanol as possible electron donors. It was demonstrated that dibenzothiophene was converted to biphenyl. However, hydrocarbon products from benzothiophene and thiophene desulfurization could not be detected. After further enrichment on thiophenic compounds as the sole electron acceptor, the conversion activity disappeared while homo-acetogenic bacteria became abundantly present. In order to gain stable conversions of thiophenic compounds, attempts were made to isolate the sulfide-producing bacteria. Two highly enriched cultures were obtained, which converted thiophenic compounds, but the activity remained low and homo-acetogenesis remained dominant.

KEYWORDS

Anaerobic biodesulfurization, Sulfate reduction, Thiophenes

ABBREVIATIONS

BT - benzothiophene; DBT - dibenzothiophene; MSD - mass selective detection; SRB - sulfate reducing bacteria; T - thiophene

INTRODUCTION

Depending on its origin, crude oils may contain high quantities of organic sulfur compounds. When the organically bound sulfur is not sufficiently removed during the refining process, SO_2 will be formed during combustion. To minimize this environmental concern, stringent regulations on the sulfur content of fuels will come in place worldwide. In addition, low-sulfur crude oils are less available nowadays. Consequently, proper processes for the effective elimination of organic sulfur compounds are needed. The current physico-chemical methods to desulfurize hydrocarbon fractions rely on hydrodesulfurization using metal catalysts in the presence of hydrogen gas under high pressure and temperature. Total sulfur levels below 50 ppm (Anabtawi *et al.*, 1996) are difficult to reach, because of the steric hindrance of alkyl substitutions adjacent to the S-atom on especially the dibenzothiophene molecules (Kabe *et al.*, 1992; Shafi and Hutchings, 2000). Because bacterial enzymes may be very specific towards organic sulfur

compounds, biodesulfurization of fuels might be an attractive, complementary process to reach low sulfur levels.

Aerobic microbiological conversion of thiophenes has been studied extensively (Kobayashi *et al.*, 2001; Folsom *et al.*, 1999; Grossman *et al.*, 1999; Hirasawa *et al.*, 2001). However, only limited data are available in the literature concerning the sulfur specific anaerobic conversion of thiophenes. Furthermore, clear evidence for significant anaerobic desulfurization is scarce. It is proposed that thiophene molecules can be used as alternative electron acceptor leading to the formation of the remaining hydrocarbon molecule and H_2S (Kim *et al.*, 1990a). The main advantage of this reaction is the selective removal of the sulfur atom, thus retaining the caloric value of the hydrocarbon. The sulfate reducing bacterium *Desulfovibrio desulfuricans* M6 was reported to desulfurize various sulfur-containing organic compounds present in crude oils and distillates (Kim *et al.*, 1995). In an assay with methyl viologen as the artificial electron donor using a concentrated cell suspension of *D. desulfuricans* M6, biphenyl was found to be the major reaction product from dibenzothiophene desulfurization, suggesting specific cleavage of the C-S bond (Kim *et al.*, 1990a, b). This work suggested that sulfate reducing bacteria (SRB) have the potential of reducing organosulfur compounds. However, no conclusions could be drawn about the desulfurization capacity by these bacteria at growing conditions. Armstrong *et al.* (1997) tested several pure cultures of SRB and a sulfate reducing community on their ability to convert thiophenes using the method of Kim *et al.* (1995) and by using growing conditions in the absence of methyl viologen. None of these methods led to significant reductions in the sulfur content of dibenzothiophene or in total sulfur content of vacuum gas oil, deasphalted oil or bitumen.

In this study, the anaerobic conversion of thiophenes was examined under the conditions where growth can be expected. This strategy was chosen because in practical applications anaerobic biomass should grow in a continuously operated biodesulfurization reactor. In our experiments sulfate reducing enrichment cultures obtained from oilfields were used.

MATERIALS AND METHODS

Source of microorganisms and screening approach

Aqueous samples were collected from three Russian oilfields where sulfide formation occurred. The first inoculum was obtained from the Romashkinskoe oilfield (Tatarstan republic). The second biomass source was sampled at seven spots at the Binagady oilfields

(Baky region, Sabunchi). The third inoculum type was from the Talinskoe oilfield (Western Siberia). After activation of the initial samples with 3 mM sulfate, the sulfate reducing cultures were further cultivated on a combination of 3 mM sulfate and various thiophenic compounds in the primary enrichment. In parallel with the primary enrichment four highly enriched sulfate reducing cultures (designated Ap1 up to Ap4) were obtained from the Romashkinskoe oilfield sample using serial dilution. The occurrence of desulfurization was tested by the capability of the biomass to produce sulfide from organically bound sulfur in addition to sulfide formed from sulfate reduction. Only samples where more than 0.3 mM extra sulfide was formed were judged positive and were transferred to the secondary enrichment. This corresponds to 10% conversion of the thiophenic compounds. In the secondary enrichment the most promising enrichments were cultivated further in the presence of various combinations of thiophene (T), benzothiophene (BT), or dibenzothiophene (DBT) as the sole electron acceptor, while no sulfate was present. Furthermore, an attempt was made to obtain pure cultures from biomass of the secondary enrichments.

Media and cultivation

A bicarbonate-buffered medium was prepared as described by Stams *et al.* (1993). Bacteria were cultured at 30°C in 120-ml serum vials closed with Viton stoppers and aluminium crimp seals. The vials contained 50 ml medium and 2.5 ml organic phase. The desulfurization reactions of complex alkylated derivates from T, BT and DBT present in fuels are simplified by investigating the degradation of the parent molecules as model compounds. Due to the limited aqueous solubility of the thiophenes, these compounds were added to the cultures in an organic overlay of *n*-dodecane. This solvent has physical properties (boiling point 215˚C and a viscosity of 1.27 mPas at 30˚C) that are representative of diesel fuel distillates. Different concentrations T, BT or DBT were applied ranging from 20 up to 160 mM in *n*-dodecane. The gas phase consisted of 200 kPa of N_2-CO_2 (80:20 %v/v) when 10 mM lactate or 10 mM ethanol was applied as carbon- and energy source. In the experiments with H_2 as the main electron donor, a H_2-CO_2 mixture (200 kPa, 80:20 %v/v) supplemented with 0.7 mM acetate as carbon source was used.

Additional experiments under bicarbonate-limiting conditions were buffered using 15 mM HEPES (N-[2-hydroxyethyl]piperazine-N'-[ethane-sulfonic acid]). A 100% (v/v) 200 kPa

H_2 atmosphere, 1 mM HCO_3^- and 1 mM acetate were applied as the sole carbon and energy sources.

The electron donors (lactate or ethanol or acetate) and acceptors (sulfate or thiosulfate or organic sulfur) were added separately by syringe from sterile anoxic stock solutions. The inoculum size was 5% (v/v). Uninoculated controls and controls inoculated with autoclaved-killed biomass were included to ascertain the biological nature of the desulfurization reaction. Strict anaerobic techniques were used throughout all steps of the culture preparation. For isolation experiments using biomass from the secondary enrichments bicarbonate-buffered medium was solidified using 1.5 % (w/v) agar (Bacto difco). Combinations of thiosulfate or sulfate with thiophene mixtures or thiophene mixtures solely were applied as potential electron acceptors.

Chemicals

All chemicals were of analytical grade and commercially available.

Analytical methods

The concentrations of organic sulfur compounds were determined using a HP 6890 gas chromatograph (GC) equipped with a flame ionisation detector (FID) and a CP-Sil 5 CB (25 m x 0.25mm x 0.25 μm) column. The column temperature was programmed from 80°C (held 2.1 min) with an increasing rate of 25°C/min up to 260°C (hold 3 min). The injector and FID temperature were 280 and 300°C, respectively. The flow of the helium carrier gas was 1.0 ml/min.

Identification of desulfurization products present in the organic phase was carried out using mass selective detection (MSD). A HP 5890 series II GC was used, equipped with a HP 5971 Series MS detector. The *n*-dodecane sample was diluted with *n*-hexane and one microliter of sample was subjected to analyses. A HP-5MS capillary column (30 m x 0.25 mm) and a helium carrier gas flow of 0.7 ml/min was applied. The column temperature was programmed from 40°C (held 3.5 min) with an increasing rate of 20°C/min to a final temperature of 250°C. The injector temperature was 250°C and the detector temperature was 280°C.

Volatile alkanes and alkenes were analysed using a HP 5890 GC equipped with FID and a Chrompack Al_2O_3/KCl PLOT column (50 m x 0.32 mm x 5.2 μm) at a helium carrier flow

of 1.6 ml/min. The column temperature was 80°C (isotherm), the injector and detector temperature were 105°C and 250°C, respectively.

Possible water-soluble metabolites were monitored using high performance liquid chromatography (HPLC) equipped with a reversed-phase column as previously described by Van de Pas *et al.* (2001). The mobile phase consisted of acetonitril - 0.01 M H_3PO_4 (20:80 v/v) at a flow rate of 1 ml/min. Substrates were measured by HPLC as described by Stams *et al.* (1993) and for detection of sulfide a modified colorimetric method as described by Trüper and Schlegel (1964) was used.

RESULTS

Utilization of organic sulfur compounds in the presence of sulfate

To enrich for microorganisms capable of utilizing thiophenes, anaerobic cultures with lactate, ethanol or hydrogen as substrates, were cultivated in the presence of sulfate and different (combinations of) thiophenes (primary enrichment). The results of the capability to produce sulfide from thiophenes in the presence of sulfate are presented in Table 1. Several enrichments from each site showed a clear extra sulfide formation, indicating the conversion of thiophenes (Table 1). When the highly enriched sulfate reducing cultures (*viz.* Ap1 up to Ap4) were used as the inoculum, no additional sulfide formation could be observed. The biomass with positive results was used as inoculum for the secondary enrichment.

Table 1: Sulfide production from thiophenes by primary enrichments and pre-cultures from different oil fields.

Inoculum	Code	Substrate	Thiophene* (mM)	Sulfide formation**
Binagady oil field	A	EtOH	T 4 (160)	-
			T 2 (40) + BT 2 (40)	++
			DBT 4 (160)	++
Romashkinskoe oil field	B1	H_2/CO_2	T 4 (160)	-
			T 2 (40) + BT 2 (40)	+
			DBT 4 (160)	+
			DBT 2 (80)	+
Romashkinskoe oil field	B2	Lactate	T 4 (160)	-
			T 2 (40) + BT 2 (40)	++
			DBT 4 (160)	++
			DBT 2 (80)	++
Romashkinskoe oil field	B3	H_2/CO_2	T 4 (160)	-
			T 2 (40) + BT 2 (40)	++
			DBT 4 (160)	+

Table 1 (continued)

Romashkinskoe oil field	B4	Lactate	T 4 (160)	-
			T 2 (40) + BT 2 (40)	++
			DBT 2 (80)	+
Romashkinskoe oil field	B5	Lactate	T 4 (160)	- -
			T 2 (40) + BT 2 (40)	+
			DBT 2 (80)	+
Romashkinskoe oil field	B6	H_2/CO_2	T 4 (160)	+
			T 2 (40) + BT 2 (40)	++
			DBT 2 (80)	+
Romashkinskoe oil field	B7	Lactate	T 4 (160)	+
			T 2 (40) + BT 2 (40)	+
			DBT 4 (160)	+
Talinskoe oil field	C1	Lactate	T 4 (160)	+
			T 2 (40) + BT 2 (40)	++
			DBT 4 (160)	+
			DBT 2 (80)	++
Talinskoe oil field	C2	H_2/CO_2	T 4 (160)	+
			T 2 (40) + BT 2 (40)	++
			DBT 4 (160)	+
Romashkinskoe oil field	Ap1	Lactate	T 4 (160)	- -
			T 2 (40) + BT 2 (40)	- -
			DBT 4 (160)	- -
			DBT 2 (80)	- -
Romashkinskoe oil field	Ap2	EtOH	T 4 (160)	- -
			T 2 (40) + BT 2 (40)	+
			DBT 4 (160)	+
Romashkinskoe oil field	Ap3	Lactate	T 4 (160)	-
			T 2 (40) + BT 2 (40)	-
			DBT 4 (160)	+
			DBT 2 (80)	+
Romashkinskoe oil field	Ap4	H_2/CO_2	T 4 (160)	-
			T 2 (40) + BT 2 (40)	+
			DBT 4 (160)	+
			DBT 2 (80)	+

* T = thiophene, BT = benzothiophene, DBT = dibenzothiophene. Since bacteria thrive in the aqueous phase, the thiophene concentration is expressed in the medium phase using the applied oil-water phase ratio of 1:20. Consequently, *e.g.* 20 mM organically bound sulfur will give 1 mM sulfur present in the water phase (abbreviated as 1(20) mM), thus 1 mM of sulfide can be formed upon complete conversion.

** Sulfide formation: (+) complete 3 mM SO_4^{2-} reduction, (++) 0.3 mM extra sulfide in addition of sulfide from SO_4^{2-} reduction, (-) delayed incomplete SO_4^{2-} reduction, (- -) no SO_4^{2-} reduction observed.

Secondary enrichments

The main difference between the primary and the secondary enrichments is the absence of sulfate for the expression of sulfate reducing enzymes in the secondary enrichments. Thiophenes are the sole electron acceptor and sulfide formation must be the result of thiophene conversion. Enrichments A and B2, which showed a clear extra sulfide formation, were selected for further enrichment. Sulfide formation started after a lag phase of 10 up to 15 days (Fig. 1). The utilization of organic sulfur compounds is accompanied by growth and proceeds up to 45 days of incubation time. The growth was relatively slow compared to the sulfate reducing control experiments (see Fig. 1). Further enrichment of samples B3, B4 and B5 were less successful (data not shown), while enrichments C1 and C2 showed no growth at all.
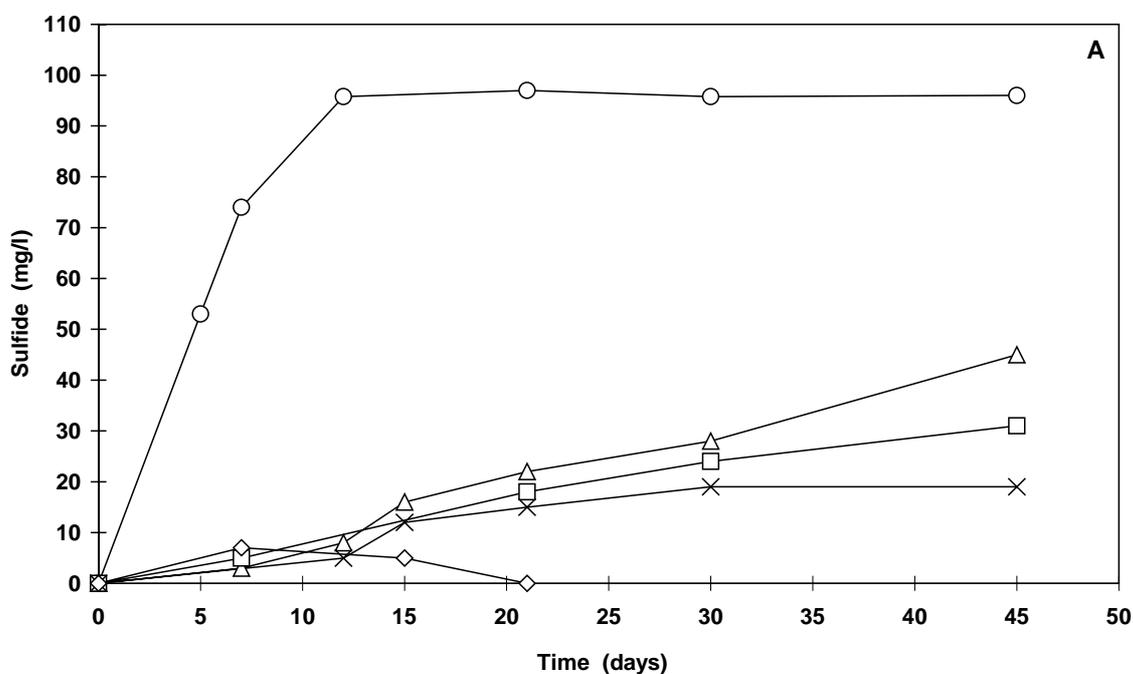

Fig. 1A. Profile of sulfide formation versus incubation time for the Binagady oilfield enrichment (enrichment A) on ethanol. Key: $\bigcirc$, 3 mM SO_4^{2-}; $\triangle$, 2(40) mM BT; $\square$, 2(40) mM DBT; $+$, 1(20) mM DBT; $\diamondsuit$, 1(20) mM T.
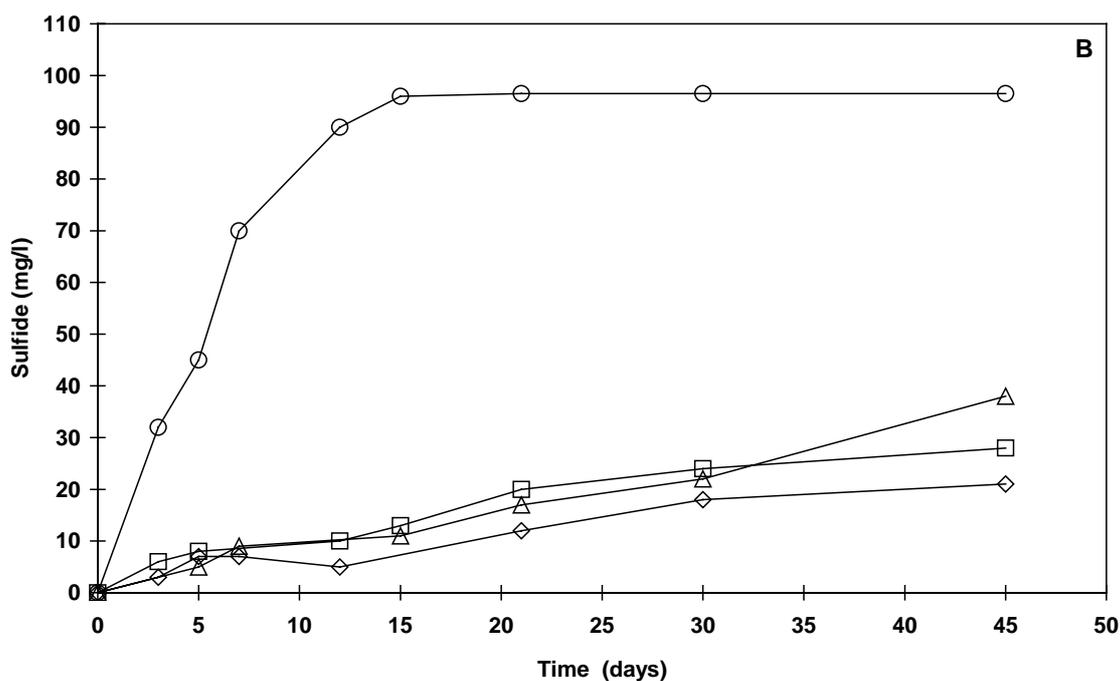
Fig. 1B. Profile of sulfide formation versus incubation time for the Romashkinskoe oilfield enrichment (enrichment B2) on lactate. Key: ○, 3 mM SO_4^{2-}; △, 2(40) mM BT; □, 2(40) mM DBT; ◇, 1(20) mM T.

The conversion efficiencies calculated on basis of thiophene depletion and sulfide formation for the incubations in Fig. 1 are presented in Table 2. The sulfide formation was compared to the maximum theoretical values that could be obtained from complete conversion. The efficiency on the basis of thiophene depletion was calculated by comparison with a matching control experiment containing autoclaved biomass.

Table 2: Conversion of thiophenes by enrichments A and B2.

		Conversion based on	
Enrichment A	Concentration water (organic) phase	Thiophene conversion	Sulfide formation
DBT	2 (40) mM	12 %	13 %
DBT	1 (20) mM	37 %	48 %
BT	2 (40) mM	55 %	59 %
T	1 (20) mM	-	-
Enrichment B2			
DBT	4 (80) mM	-	-
DBT	2 (40) mM	29 %	44 %
BT	2 (40) mM	48 %	59 %
T	1 (20) mM	49 %	65 %

The efficiencies obtained from thiophene depletion and sulfide formation are in relatively good agreement. On the basis of sulfide formation the desulfurization efficiency was somewhat overestimated (Table 2).

Conclusive evidence for the sulfur selective anaerobic conversion of DBT should be based on DBT depletion and the demonstration of product formation during the incubations. Besides sulfide the expected hydrocarbon product from DBT conversion is biphenyl. An example of a GC-MSD chromatogram showing biphenyl formation from DBT is presented in Fig. 2. The matching mass spectra for biphenyl and DBT are depicted in Fig. 3. The presence of biphenyl was demonstrated in every incubation where DBT was converted (Table 2).
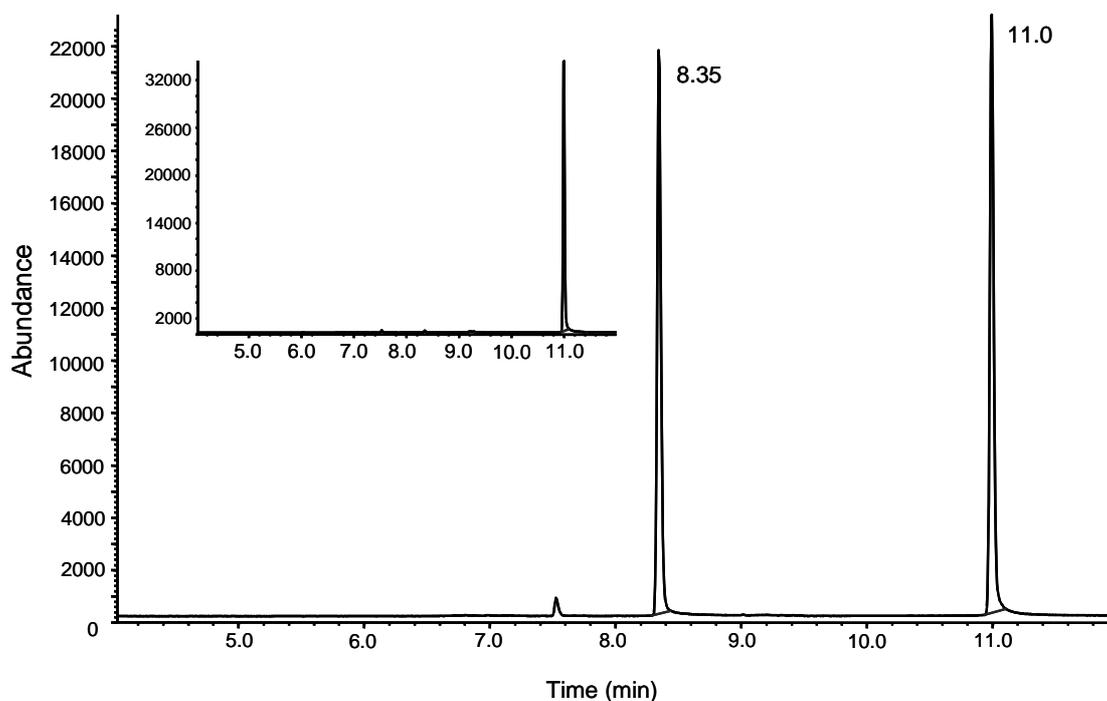

Fig. 2. Total ion chromatogram of the organic layer after incubation with 20 mM DBT, see Fig. 1A. DBT has a retention time of 11.00 min and BiPh has a retention time of 8.35 min. The inserted total ion chromatogram is obtained from the matching control vial. GC-MSD analysis was as described in Materials and Methods.
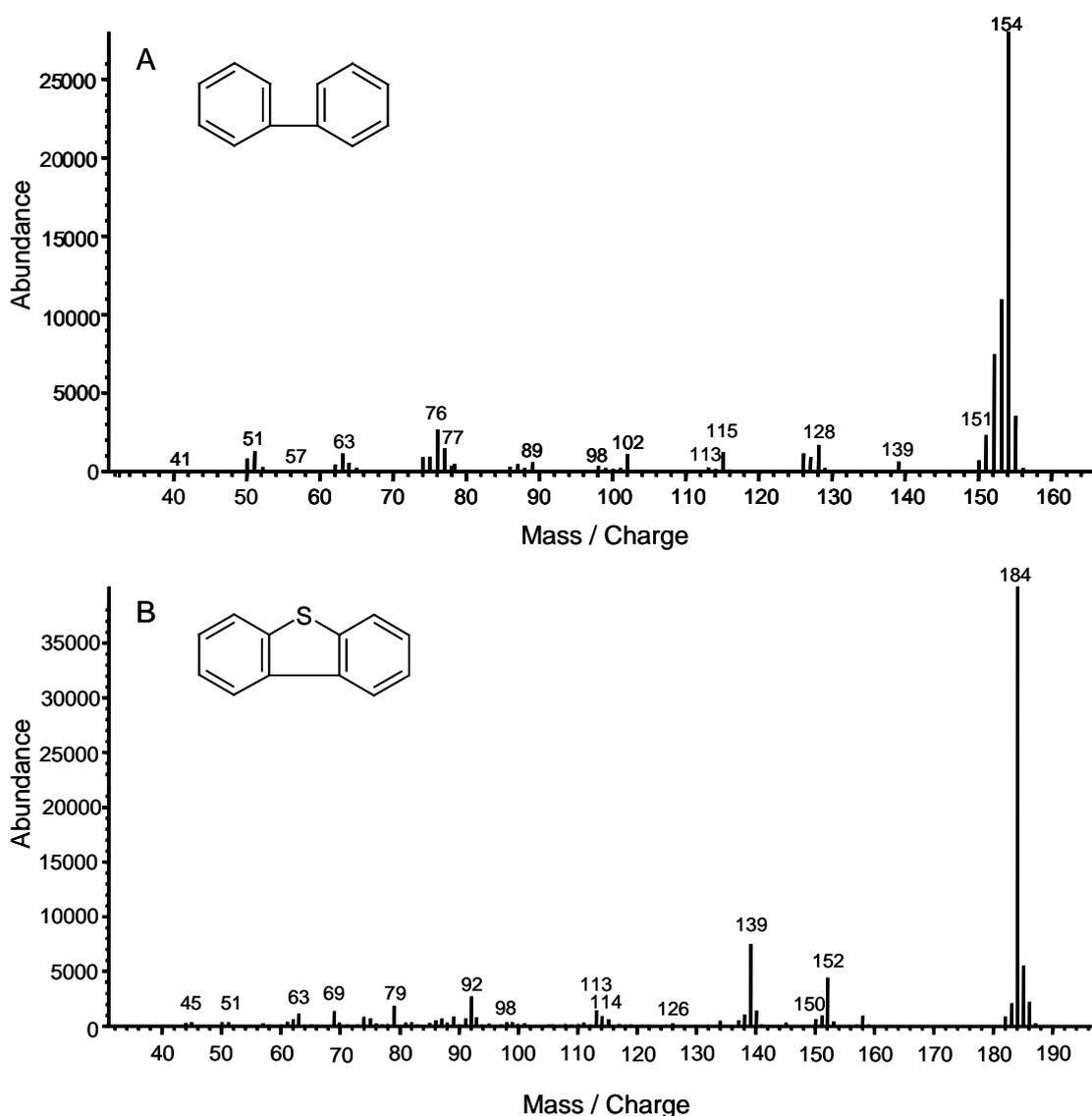
Fig. 3. Mass spectra of metabolite biphenyl (A, molecular weight of 154) and dibenzothiophene (B, molecular weight of 184) from Fig. 2.

Apart from the product identification of DBT desulfurization considerable effort was put in the identification of possible BT desulfurization products. Mass selective single ion monitoring could not reveal the presence of ethyl benzene or styrene as the most likely desulfurization products. Furthermore, MSD scans have excluded the presence of C_6 up to C_8 hydrocarbon fragments after desulfurization. To check if any water-soluble products were formed, HPLC measurements were applied. Also in the water phase no hydroxylated, carboxylated or oxygenated products were detected. For the incubation where T conversion was observed (Fig. 1B) an attempt was made to identify the desulfurization product of T by analysing the gas phase. Assuming that the mechanism of T conversion is

similar to that of DBT conversion (Kim *et al.*, 1990a), the most likely product would be a volatile C4 molecule; *e.g.* butane, butene or butadiene. However, none of these compounds were detected.

Follow up experiments

It was expected that microorganisms grown in the secondary enrichment would represent the best inocula for new batch experiments, leading to enhanced conversion efficiencies. Unfortunately, this was not the case. The biological desulfurization activity was lost due to growth of homo-acetogenic bacteria present in the biomass population. These bacteria apparently have better kinetic growth properties compared to desulfurizing bacteria. Therefore, an attempt was made to isolate the bacteria responsible for desulfurization. Various Romashkinskoe enrichment samples were diluted in agar roll tubes and incubated with different combinations of electron acceptors. In these isolation experiments the focus was on the utilization of H_2 as electron donor.

In the presence of sulfate or thiosulfate, mainly colonies of homo-acetogenic biomass were obtained. Only in the case of thiosulfate in combination with thiophene (T) as potential electron acceptors, suitable colonies developed after three months of incubation. Two colonies designated OSR1 and OSR2 were cultivated further. The sulfide formation as a function of time of OSR1 on thiophene [2(40) mM] and OSR2 on benzothiophene + dibenzothiophene [2(40) + 2(40) mM] is depicted in Fig. 4.

To demonstrate the sulfate reducing capacity the bacteria were also cultivated in the presence of 3 mM sulfate (Fig. 4). Cultures OSR1 and OSR2 were indeed sulfate reducing cultures and able to produce sulfide when thiophenes were present as the sole electron acceptor. However, the rate of sulfide formation was low (0.4 up to 0.8 mg/Lday). Because of the small scale of the experiment appropriate analysis of the organic layer was not practicable. Upon consecutive transfers in fresh medium acetate formation was observed again, indicating that homo-acetogens were still present.
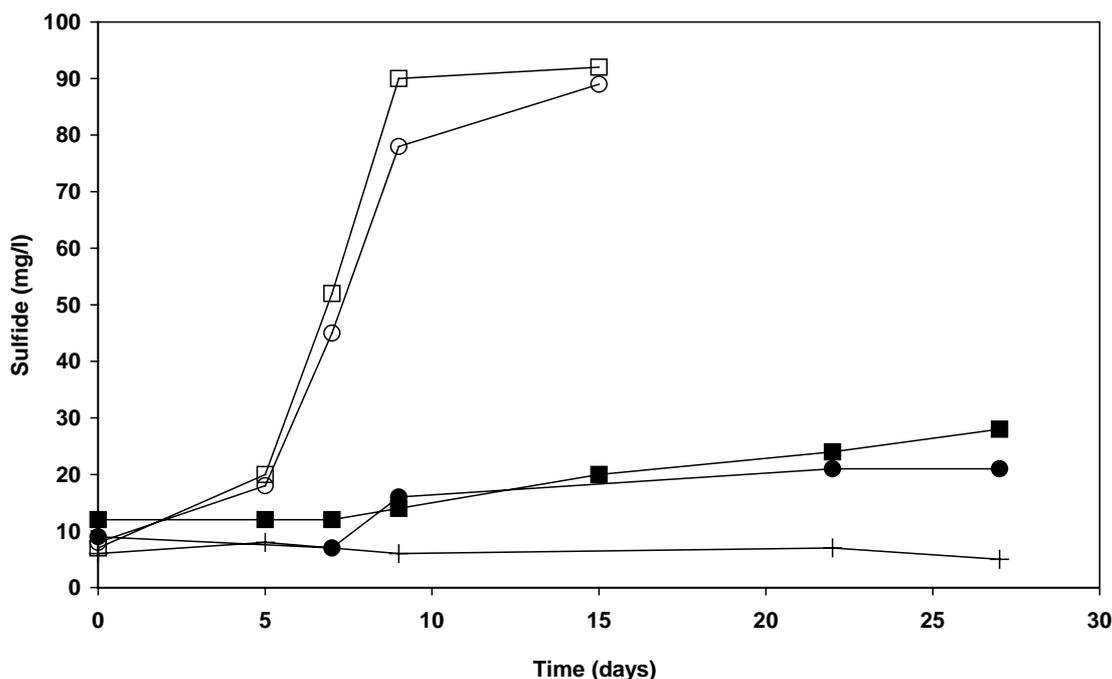
Fig. 4. Profile of sulfide formation versus incubation time for the highly enriched cultures OSR1 and OSR2 cultivated in the presence of H_2/CO_2. Key: □, OSR1, 3 mM SO_4^{2-}; ○, OSR2, 3 mM SO_4^{2-}; ■, OSR1, 2(40) mM T; ●, OSR2, 2(40) mM BT and 2(40) mM DBT; +, Control experiment).

To limit the growth of homo-acetogens, a medium low in bicarbonate (1 mM) was used. Growth of homo-acetogens was prevented effectively, a pH increase due to the consumption of protons was absent and no acetate formation occurred (data not shown). However, this approach did not result in a higher conversion efficiency of thiophenes. Addition of a sulfate pulse (2.5 mM) during growth on thiophenes did not result in a stimulation of the thiophene conversion (data not shown). This indicates that thiophene conversion occurs independent from sulfate reduction.

DISCUSSION

The objective of our research was to obtain a suitable biomass population that is able to use thiophenes as the terminal electron acceptor for growth. From the secondary enrichments several lines of evidence for anaerobic conversion of DBT were obtained. Apart from the depletion of DBT also the products sulfide and biphenyl were demonstrated conclusively. Recently, Bahrami *et al.* (2001) reported a 98% degradation of DBT using a thermophilic anaerobic consortium. That study demonstrated that there was no correlation of DBT conversion with biphenyl and sulfide formation. Biphenyl or other

possible metabolic products were not detected, indicating that a still unknown reaction occurred.

Results of this study revealed that measurable amounts of sulfide were formed from thiophene and benzothiophene. In addition, thiophene and benzothiophene depletion was observed, but no hydrocarbon products could be demonstrated. Anweiler *et al.* (2001) reported that a sulfate reducing enrichment culture growing with naphthalene as the sole source of carbon and energy was not able to grow with benzothiophene as the primary substrate. In that study, selective removal of organically bound sulfur could not be demonstrated, but carboxybenzothiophenes were formed cometabolically. In the present study, significant amounts of sulfide were formed from benzothiophene in the absence of sulfate. No polar derivatives (like carboxybenzothiophenes) could be revealed, thus carboxylation of benzothiophene is not an initial activating process. Rueter *et al.* (1994) reported that alkylbenzenes from crude oil can serve as electron donors by sulfate reducing enrichments. In another previous study (Harms *et al.*, 1999) oxidation of *o*-xylene and *p*-xylene by sulfate reducing bacteria was observed. In our experiments, complete oxidation to CO_2 by bacteria of the secondary enrichments is not likely, since sulfate was not present as electron acceptor. Consequently, it was expected that the metabolites should be excreted.

From the results of the secondary enrichment it is difficult to draw unambiguous conclusions about the concentration effects of the thiophenes. Results obtained by Londry and Suflita (1998) indicated that the inhibitory effects of thiophene and benzothiophene on sulfate reduction at the levels used in this study are not very pronounced. Their study was conducted with oily sludge as inoculum and lactate as carbon and energy source. A concentration effect caused by a change in the solvent due to the action of bacteria is not likely. The anaerobic oxidation of *n*-dodecane has been reported (Kropp *et al.*, 2000; Aeckersberg *et al.*, 1998; Aeckersberg *et al.*, 1991), but this reaction cannot occur in the absence of the electron acceptor sulfate.

In the primary enrichment experiments thiophene had a large effect on growth, which may be explained by the water solubility of thiophene. An inhibiting effect on the growth of biomass could explain the low activities. The solubility of benzothiophene and dibenzothiophene in the water phase can be neglected under the applied experimental conditions and a direct influence on the biomass is not likely. Highly enriched sulfate-reducing cultures (Ap1 up to Ap4) obtained from the Romashkinskoe oilfield were not

capable of desulfurizing thiophenes in the primary enrichment. Probably, the bacteria capable of converting thiophenes were lost during the consecutive transfers.

We did not succeed to obtain pure cultures of the desulfurizing bacteria pre-grown in secondary enrichment experiments, but two highly enriched cultures were obtained. The main problem was that homo-acetogens remained present. Omission of bicarbonate buffer from the medium using an alternative HEPES prevented homo-acetogenesis. However, the desulfurization efficiency compared to secondary enrichment cultures was still low.

From the different experiments the relation between sulfate reduction and the reduction of organic sulfur remains unclear. The expression of sulfate reducing enzymes has no direct link with the conversion of thiophenes and therefore the expression of another enzyme system is necessary.

Sulfide can have large effects on the performance of sulfate reducers converting aromatic hydrocarbons. Edwards *et al.* (1992) have demonstrated a severe inhibition of sulfate reduction at a concentration of only 1 mM Na_2S, when aromatic compounds (*e.g.* toluene, xylene) were used as the carbon- and energy source. This phenomenon indicates that even in the presence of a favorable electron acceptor the conversion of aromatic compounds is not an ubiquitous capacity of sulfate reducing bacteria.

In conclusion, this study shows that thiophenes can be anaerobically converted. They are however poor electron acceptors to stimulate growth. The use of enrichments resulted in a proof of principle, but the activity could not be enhanced. Isolation experiments yielded highly enriched cultures. Additional studies are necessary to get a better understanding of the conversion of thiophenic compounds.

REFERENCES

Aeckersberg F., Bak F., Widdel F. 1991. Anaerobic oxidation of saturated hydrocarbons to CO_2 by a new type of sulfate reducing bacterium. Arch. Microbiol. 156: 5-14.

Aeckersberg F., Rainey F.A., Widdel F. 1998. Growth, natural relationships, cellular fatty acids and metabolic adaptation of sulfate reducing bacteria that utilize long-chain alkanes under anoxic conditions. Arch. Microbiol. 170: 361-369.

Anabtawi J.A., Ali S.A., Ali M.A. 1996. Impact of gasoline and diesel specifications on the refining industry. Energ. Source 18: 203-214.

Annweiler E., Michaelis W., Meckenstock R.U. 2001. Anaerobic cometabolic conversion of benzothiophene by a sulfate reducing enrichment culture and in a tar-oil-contaminated aquifer. Appl. Environ. Microbiol. 67: 5077-5083.

Armstrong S.M., Sankey B.M., Verdouw G. 1997. Evaluation of sulfate reducing bacteria for desulfurizing bitumen or its fractions. Fuel Process. Technol. 76: 223-227.

Bahrami A., Shojaosadati S.A., Mohebali G. 2001. Biodegradation of dibenzothiophenes by thermophilic bacteria. Biotechnol. Lett. 23: 899-901.

Edwards E.A., Wills L.E., Reinhard M., Grbić-Galić D. 1992. Anaerobic degradation of toluene and xylene by aquifer microorganisms under sulfate reducing conditions. Appl. Environ. Microbiol. 58: 794-800.

Folsom B.R., Schieche D.R., DiGrazia P.M., Werner J. Palmer S. 1999. Microbial desulfurization of alkylated dibenzothiophenes from a hydrodesulfurized middle distillate by *Rhodococcus erythropolis* I19. Appl. Environ. Microbiol. 65: 4967-4972.

Grossman M.J., Lee M.K., Prince R.C., Garrett K.K., George G.N., Pickering I.J. 1999. Microbial desulfurization of a crude oil middle-distillate fraction: analysis of the extent of sulfur removal and the effect of removal on remaining sulfur. Appl. Environ. Microbiol. 65: 181-188.

Harms G., Zengler K., Rabus R., Aeckersberg F., Minz D., Rosselló-Mora R., Widdel F. 1999. Anaerobic oxidation of *o*-xylene, *m*-xylene, and homologous alkylbenzenes by new types of sulfate reducing bacteria. Appl. Environ. Microbiol. 65: 999-1004.

Hirasawa K., Ishii Y., Kobayashi M., Koizumi K., Maruhashi K. 2001. Improvement of desulfurization activity in *Rhodococcus erythropolis* KA2-5-1 by genetic engineering. Biosci. Biotechnol. Biochem. 65: 239-246.

Kabe T., Ishihara A., Tajima H. 1992. Hydrodesulfurisation of sulfur-containing polyaromatic compounds in light oil. Ind. Eng. Chem. Res. 31: 1577-1580.

Kim H.Y., Kim T.S., Kim B.H. 1990a. Degradation of organic sulfur compounds and the reduction of dibenzothiophene to biphenyl and hydrogen sulfide by *Desulfovibrio desulfuricans* M6. Biotechnol. Lett. 12: 761-764.

Kim T.S., Kim H.Y., Kim B.H. 1990b. Petroleum desulfurization by *Desulfovibrio desulfuricans* M6 using electrochemically supplied reducing equivalent. Biotechnol. Lett. 12: 757-760.

Kim B.Y., Kim H.Y., Kim T.S., Park D.H. 1995. Selectivity of desulfurization activity of *Desulfovibrio desulfuricans* M6 on different petroleum products. Fuel Process. Technol. 43: 87-94.

Kobayashi M., Horiuchi K., Yoshikawa O., Hirasawa K., Ishii Y., Fujino K., Sugiyama H., Maruhashi K. 2001. Kinetic analysis of microbial desulfurization of model and light gas oil containing multiple alkyl dibenzothiophenes. Biosci. Biotechnol. Biochem. 65: 298-304.

Kropp K.G., Davidova I.A., Suflita J.M. 2000. Anaerobic oxidation of *n*-dodecane by an addition reaction in a sulfate reducing bacterial enrichment culture, Appl. Environ. Microbiol. 66: 5393-5398.

Londry K.L., Suflita J.M. 1998. Toxicity effects of organosulfur compounds on anaerobic microbial metabolism. Environ. Toxicol. Chem. 17: 1199-1206.

Rueter P., Rabus R., Wilkes H., Aeckersberg F., Rainey F.A., Jannasch H.W., Widdel F. 1994. Anaerobic oxidation of hydrocarbons in crude oil by new types of sulfate reducing bacteria. Nature 372: 455-458.

Shafi R., Hutchings G. J. 2000. Hydrodesulfurisation of hindered dibenzothiophenes: an overview. Catal. Today 59: 423-442.

Stams A.J.M., Van Dijk J.B., Dijkema C., Plugge C.M. 1993. Growth of syntrophic propionate-oxidizing bacteria with fumarate in the absence of methanogenic bacteria. Appl. Environ. Microbiol. 59:1114-1119.

Trüper H.G., Schlegel H.G. 1964. Sulfur metabolism in *Thiorhodaceae*. Quantitative measurements on growing cells of *Chromatium okenii*. Antonie van Leeuwenhoek J. Microbiol. Ser. 30: 225-238.

Van de Pas B.A., Jansen S., Dijkema C., Schraa G., De Vos W.M., Stams A.J.M. 2001. Energy yield of respiration on chloro-aromatic compounds in *Desulfitobacterium dehalogenans*. Appl. Environ. Microbiol. 67: 3958-3963.
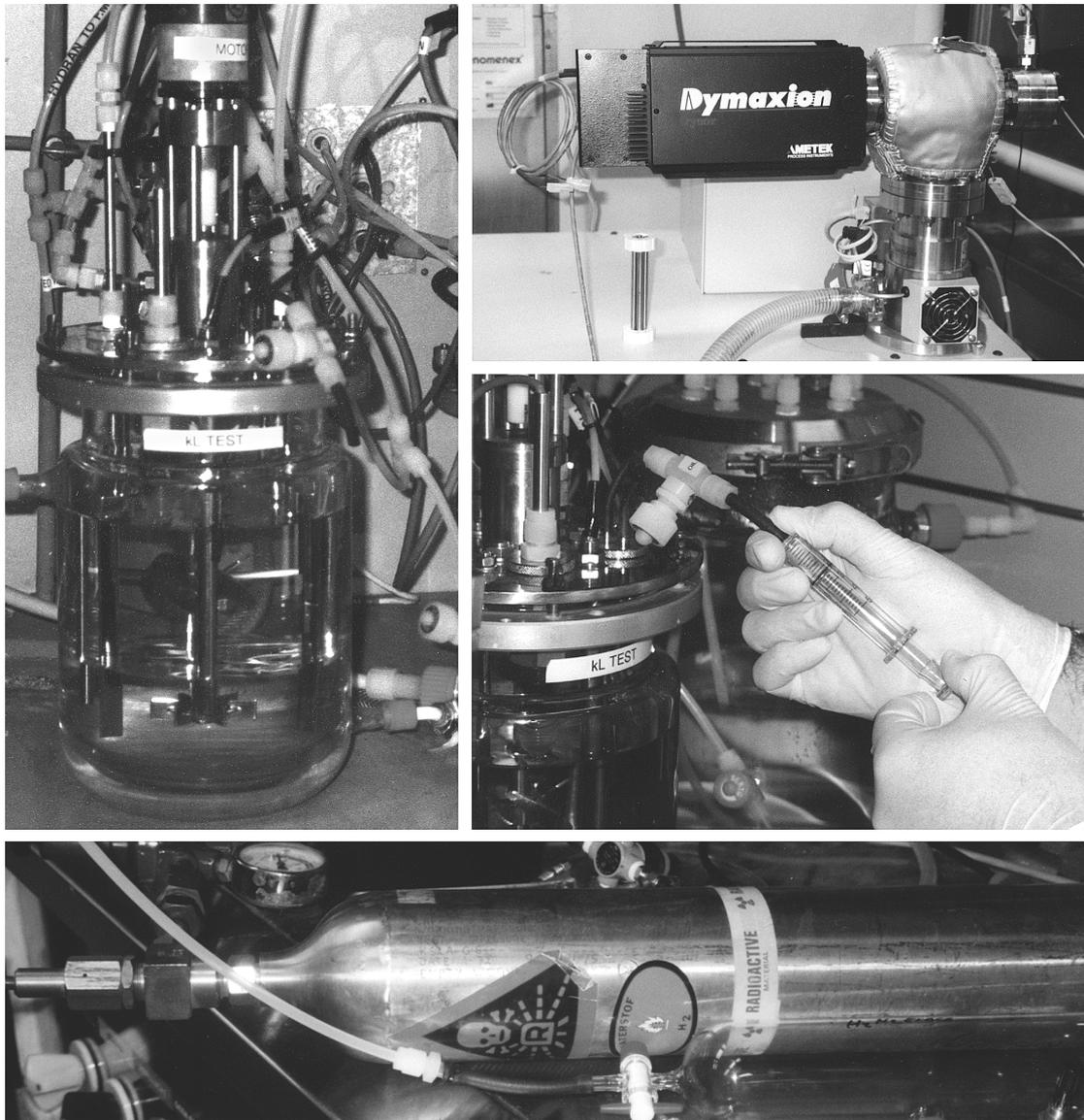
Details of photographs depicting the experimental work with tritium-hydride that is described in Chapter 4.

HYDROGEN MASS TRANSFER FROM *N*-DODECANE TO WATER, DETERMINATION OF THE MASS TRANSFER COEFFICIENTS IN A THREE-PHASE SYSTEM

ABSTRACT

Physical experiments were performed to determine the mass transfer coefficients from pure H_2 gas to *n*-dodecane (k_d) and from *n*-dodecane to water (k_{dw}). The dissolved H_2 can then be used to biologically convert organic sulfur compounds such as dibenzothiophene. To enable a comparison of using an organic phase to supply H_2 to the aqueous phase to direct H_2 gas supply to the water phase also the mass transfer coefficient between pure H_2 gas and water (k_w) was determined. The mass transfer coefficients k_d and k_w were determined using a dynamic method. The overall mass transfer coefficient k_{dw} was assessed using a steady state method. The resulting values for k_d, k_w and k_{dw} at 30ºC were: (2.89 ± 0.12) x 10^{-5} ms^{-1}, (9.7 ± 0.2) x 10^{-5} ms^{-1} and (5 ± 0.6) x 10^{-6} ms^{-1}, respectively. From the calculation of the maximally attainable H_2 flux it was concluded that the specific surface area between *n*-dodecane and water is the determining parameter for sufficient H_2 mass transfer compared to direct H_2 sparging.

KEYWORDS

Bioprocess design, Diffusion, Hydrogen, Mass transfer

INTRODUCTION

Many bioconversions involve hydrophobic reactants, such as aliphatic and aromatic hydrocarbons. To optimize these conversions two-phase liquid-liquid bioreactor systems have been widely studied and applied (Van Sonsbeek *et al.*, 1993; Woodley and Lilly, 1990; Van den Meer *et al.*, 1986; Wubbolts *et al.*, 1994). A major bottleneck of these systems can be the mass transfer rate of reactants and products between the hydrophobic and aqueous phase as it will affect the conversion efficiency (Baldascini *et al.*, 2001). However, this type of conversion is still relatively simple compared to three-phase liquid-liquid-gas systems. A characteristic example of such a bioprocess is the anaerobic biodesulfurization of dibenzothiophenes and analogs thereof that are present in fuels using hydrogen gas as the reducing agent. Hydrogen gas is an attractive electron donor for anaerobic bioprocesses on a relatively large scale (Van Houten *et al.*, 1994). Anaerobic biodesulfurization of dibenzothiophenes dissolved in the hydrocarbon phase occurs at the interface of the oil droplets and water, where the anaerobic bacteria thrive. A high specific surface area is necessary to transfer sufficient H_2 into the aqueous phase and to maximize the contact between the biomass and the hydrocarbon phase (Chapter 2). We encountered experimentally that direct gas sparging in a hydrocarbon in water dispersion is not a

practical option because it results in severe foaming. To cope with this constraint, it is proposed to saturate the hydrocarbon phase with H_2 gas before it is dispersed into the bioreactor. Using this approach the requirement of a high specific surface area to maximize the conversion of dibenzothiophenes is combined with the optimization of H_2 availability. To provide insight in the feasibility of designing such a system the mass transfer coefficients involved are assessed in this work. The solvent *n*-dodecane is applied as model organic phase.

THEORY OF GAS SOLUBILITY AND MASS TRANSFER COEFFICIENTS

In Fig. 1 the diffusive transport of H_2 from the gas (g) to the water (w) phase via an intermediate *n*-dodecane (d) phase is presented schematically. A common way to model diffusive transport is to consider the presence of hypothetical stagnant films in which the resistances to mass transfer are located (Fig. 1).
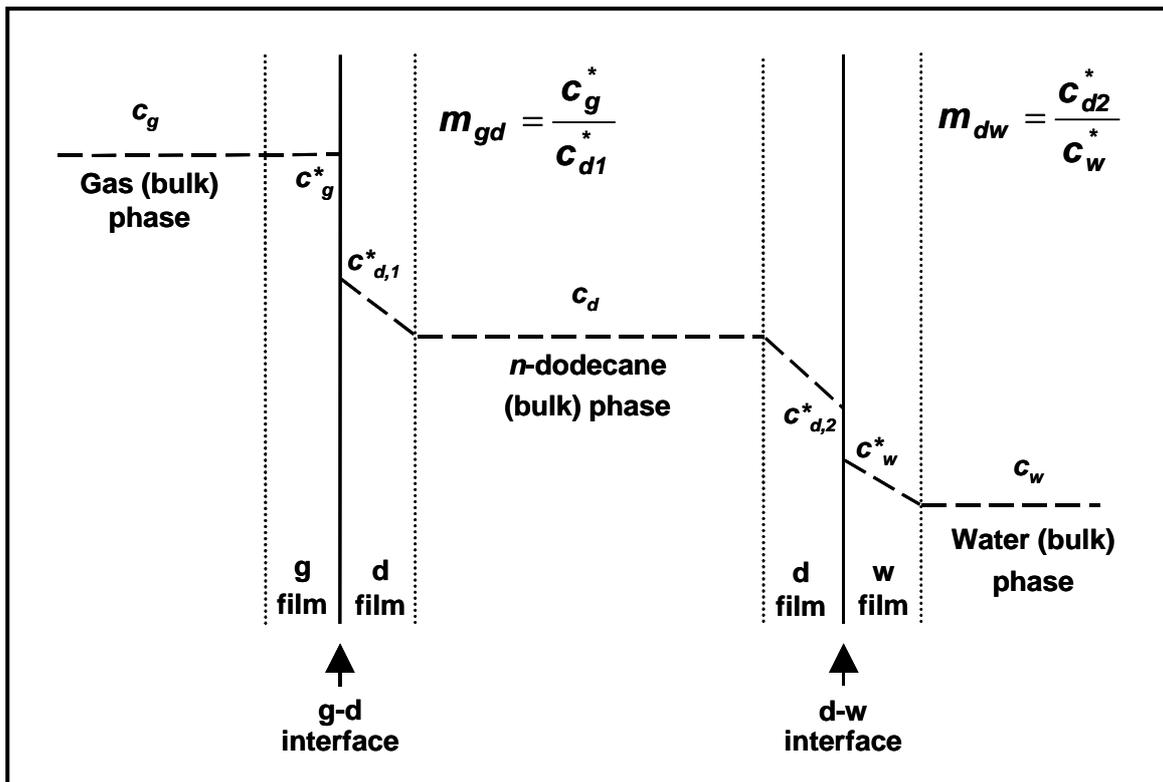

Fig 1: Schematic representation of the stagnant film model describing the H_2 mass transfer from gas (g) to water (w) via *n*-dodecane (d) as carrier phase.

When no equilibrium situation exists, a flux from one phase to another will occur. The flux depends on the concentration gradient ($c^* - c_{bulk}$) and the overall mass transfer coefficient (k_{gd}, ms^{-1}). The flux over a specific surface area (a) can be calculated according to:

75

$$J = k_{gd} \cdot \left(c^* - c_{bulk} \right) \qquad \text{(mol/m}^2\text{s)} \qquad (1)$$

Where the overall mass transfer coefficient k_{gd} in Eq. 1 is defined as:

$$\frac{1}{k_{gd}} = \frac{1}{mk_g} + \frac{1}{k_d} \qquad (2)$$

For our situation the value of gas-side mass transfer coefficient (k_g) in Eq. 2 is very large compared to the liquid-side mass transfer coefficient (k_d), due to the much higher diffusion coefficient in the gas phase and the value of m (12 for a g/d-system at 30ºC), which results in a negligible $1/(mk_g)$-term in Eq. 2 (Van Sonsbeek *et al.*, 1992). Consequently, the overall mass transfer coefficient (k_{gd}) is mainly determined by the partial mass transfer coefficient in the liquid phase (k_d). An analogue derivation can be made for g/w systems, where the effect is more pronounced because m equals 60 (at 30ºC).

When equilibrium exists, *i.e.* when the net diffusion between the phases (g/w/d) is 0, the [H$_2$] in each phase can be related by the partition coefficients involved (see m_{gd} and m_{dw} in Fig. 1).

For the diffusion of H$_2$ from the gas phase into *n*-dodecane it is assumed that the mass transfer resistance is entirely in the liquid film at the g/d interface. The [H$_2$] in the gas film at the g/d interface (c^*_g) is equal to the [H$_2$] in the bulk gas phase (c_g) as we use a pure gas: $c^*_g \approx c_g$ (see Fig. 1, g/d interface). The [H$_2$] in the *n*-dodecane film at the g/d interface (c^*_d) can be calculated as follows:

$$c_d^* = \frac{c_g}{m_{gd}} = \frac{P/RT}{m_{gd}} \qquad (3)$$

For the calculation of c_g it is assumed that the ideal gas law is valid and that the vapor pressure of *n*-dodecane can be neglected. If the headspace is not pure H$_2$, the pressure must be corrected by considering the H$_2$ partial pressure ($p_{H_2} = y_{H_2} \cdot P$).

In case of a g/w system the solubility of H$_2$ and therefore the mass transfer can be affected by the presence of dissolved ions, altering the partition coefficient. The effect of the presence of NaCl on *He* can be described with the Sechenov relation as depicted in Eq. 4 (Schumpe, 1993).

$$\log\left(\frac{c_{g,0}^*}{c_g^*}\right) = \log\left(\frac{He}{He_0}\right) = \sum_{i=1}^{N_i}(h_i + h_g)c_i^{ion} \qquad (4)$$

Here $c^*_{g,0}$ is the H$_2$ solubility in the demineralized water, c^*_g is the H$_2$ solubility in the salt solution, N_i is the number of ionic species, and c_i^{ion} is the molar concentration of ion i. The ion-specific parameters (h_i) in Eq. (4) for the NaCl solution used were $h_{Na^+} = 0.1143$ m^3/kmol and $h_{Cl^-} = 0.0318$ m^3/kmol (Weisenberger and Schumpe, 1996). The gas-specific parameter (h_g) is assumed to be a linear function of the temperature for 273K < T < 363 K, according to Eq. 5:

$$h_g = h_{g,0} + h_T (T - 298.15)$$
(5)

To calculate h_g the gas-specific salting-out parameters for H$_2$: $h_{H2,0} = -0.0218$ m^3/kmol at 298.15 K and $h_T = -2.99.10^{-4}$ m^3/(kmol·K) were used (Weisenberger and Schumpe, 1996).

Usually, the mass transfer capacity of a system is measured as the $k \cdot a$-value, where a denotes the specific surface area (m^{-1}) for mass transfer. When the mass transfer coefficient (k) needs to be calculated from $k \cdot a$, the value for a needs to be known very accurate. However, in case of a hydrocarbon in water dispersion the specific surface area available for mass transfer is very dependent on the droplet size distribution and the hold-up of the hydrocarbon phase. In order to avoid these uncertainties, it was decided to determine k separately using systems with an exactly known specific surface area (a). A stirred cell with a defined flat surface was used instead of a dispersion system. By using a stirred cell the minimal value for the mass transfer rate is assessed, because the film thickness is maximal at the low power input that is necessary to create a flat surface (Fillion and Morsi, 2000).

Generally, there are two well-known methods to determine the mass transfer coefficient: (*i*) the dynamic and (*ii*) the steady state method. Using method (*i*) the rate of change of H$_2$ concentrations in each phase involved is followed after a step-wise change in the H$_2$ inlet concentration. In method (*ii*) the concentrations in the phases involved are measured after a steady state is reached. Steady state is achieved by addition of H$_2$ to the first phase and removal of H$_2$ from the end-phase of the mass transfer sequence (Van Sonsbeek *et al.*, 1991). The dynamic method is commonly applied (Gogate and Pandit, 1999), but some restrictions have to be taken into account. When the response time of the probe is in the same order as $1/(k \cdot a)$, the probe dynamics have to be taken into account to avoid underestimation of $k \cdot a$ (Merchuk *et al.*, 1990). Apart from that it can be rather difficult to accomplish a proper step change in the inlet concentration.

The dynamic method was used to determine the mass transfer coefficients between the gas and *n*-dodecane phases (k_d) and between the gas and water phases (k_w). The H_2 mass transfer could be followed and analyzed from the pressure drop of the headspace.

The k_d-value was determined because this parameter is necessary to be able to solve mass balances over *n*-dodecane/water systems. The k_w-value was determined to enable a comparison of a gas/water system with a *n*-dodecane/water system. Finally, the overall mass transfer coefficient of *n*-dodecane to water (k_{dw}) was assessed using a steady state method.

MATERIALS AND METHODS

Experimental set-up, determination of k_d

To enable the calculation of k_d values at temperatures of 30, 40 and 50°C, the pressure drop of H_2 in the headspace in a gas/*n*-dodecane system was followed in time. The [H_2] in *n*-dodecane followed from mass balance calculations. This could not be measured directly, because a H_2 probe with a suitable low response time was not available.

Experiments were carried out in a jacketed Stirred Cell (SC) made of glass and stainless steel. In Fig. 2, a schematic drawing is given. Both the gas and *n*-dodecane phase were mixed to ensure homogeneous bulk phase concentrations. The stirrer shaft was equipped with three impellers (Fig. 2) and the stirrer speed was 50 rpm throughout the experiments. The whole system was thermostated by putting it in an incubator to prevent cooling of the gas phase by the metal lid. The SC (Applicon) used had an exact volume of 2.965 L and a cross sectional area of 126.32 cm^2. A pressure indicator (PI) Cerabar T PMC 131 with a 0.8×10^5 up to 1.2×10^5 Pa range, a Pt-100 thermocouple and a Brooks 5850S Mass Flow Controller (MFC) with a 0 up to 50 mL/min capacity were connected to the computer for automatic operation and data collection.

A zero H_2 starting concentration in the liquid phase at the beginning of the experiment is desirable to achieve a maximal pressure drop. However, this could not be obtained because due to the strength of the SC material it was not possible to operate at values below 0.8×10^5 Pa. Therefore, an alternative method was used. After filling the SC with 2 L of *n*-dodecane the headspace was exchanged with pure H_2. This was performed by alternating degassing and filling the headspace 12 times up to values of 0.8×10^5 and 1.2×10^5 Pa, respectively. Subsequently, the system was allowed to reach equilibrium at a

pressure of 0.8 x 10^5 Pa. Then, H$_2$ was added using the MFC until a pressure of 1.19 x 10^5 Pa. From this moment onwards, the depletion of H$_2$ from the headspace was followed in time by measuring the pressure drop until equilibrium was reached.
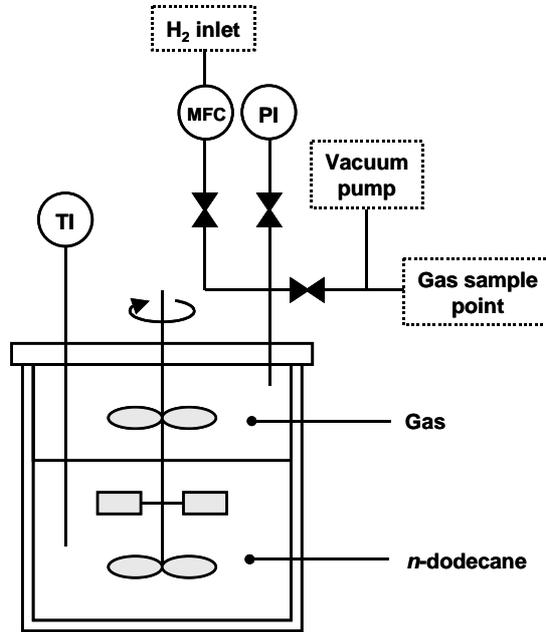
Fig. 2: Experimental set-up used for the experiments to determine k_d.

Calculation of k_d

From the data obtained k_d was calculated according to the equations presented below. In a short period of time dt, the amount of H$_2$ diffusing from the gas to the *n*-dodecane phase can be described by:

$$\int J \cdot a \cdot V_{SC} dt = \int k_d \cdot a \cdot V_{SC} \left(c_{d,t}^* - c_{d,t} \right) dt \tag{6}$$

where: $a \cdot V_{SC} = A$ (cross sectional area SC)

The amount of moles H$_2$ transferred to the *n*-dodecane phase at a certain time step (dt) is equal to the change of amount of moles H$_2$ in the gas phase:

$$-\int J \cdot A dt = \left(P_{t+dt} - P_t \right) \cdot V_g \Big/ RT \tag{7}$$

Combining Eq. 6 an Eq. 7 gives:

$$\frac{P_1 - P_2}{RT} \cdot V_g = \int_{t1}^{t2} k_{d,1} \cdot A \cdot (c_d^* - c_d) dt \tag{8}$$

When d$t \rightarrow 0$, the Eq. 8 can be solved numerically for a certain time period d$t = t_2 - t_1$:

$$\frac{P_1 - P_2}{RT} \cdot V_g \approx k_{d,1} \cdot A \cdot \left(\frac{(c_{d,t1}^* + c_{d,t2}^*)}{2}(t2 - t1) - \frac{(c_{d,t1} + c_{d,t2})}{2}(t_2 - t_1) \right) \tag{9}$$

The H_2 concentration in the n-dodecane phase was derived from the mass balance calculation:

$$c_{d,t} \cdot V_d = c_{d,t=0} \cdot V_d + \int_0^t J_A \cdot A \cdot dt = c_{d,t=0} \cdot V_d + \frac{P_0 - P_t}{RT} \cdot V_g \tag{10}$$

$$\therefore c_{d,t} = c_{d,t=0} + \frac{P_0 - P_t}{RT} \cdot \frac{V_g}{V_d}$$

where $c_{d,t=0}$ is the initial H_2 concentration in the n-dodecane phase.

A certain amount of H_2 already diffused into the n-dodecane phase during the H_2 addition at the start up. A lower gas pressure was measured than expected based on the dosage with the MFC. We corrected for this error.

After substitution of Eq. 3 and Eq. 10 into Eq. 9 and further rearrangement, k_d can be calculated according to:

$$k_{d,1} = \frac{(P_1 - P_2) \cdot V_g}{A \cdot \left(\frac{P_2 + P_1}{m_{gd}} + (P_1 + P_2 - 2P_0)\frac{V_g}{V_o} - 2 \cdot c_{d,t=0} \cdot RT \right) \cdot \frac{(t_2 - t_1)}{2}} \tag{11}$$

where k_{d1} is the k_d determined for the first time step. The detailed derivation to Eq. 11 is given in Appendix 1. The average k_d can be calculated as follows:

$$k_d = \frac{1}{n} \sum_{j=1}^n k_{d,j} \tag{12}$$

Check on He_d

The partition coefficients for gas liquid systems can be expressed as m (m^3_{liquid} / m^3_{gas}) or as He ($MPa/(mol/m^3)$) when the liquid properties are taken into account. In the calculation of k_d the partition coefficient between gas and n-dodecane (m_{gd}) is used to determine c_d^*. Therefore, accurate values for m_{gd} are necessary. We applied partitioning data obtained at 30, 40 and 50°C using the Soave-Redlich-Kwong model (results not shown). To check their validity, a control experiment was set-up in order to verify the H_2 partitioning at 30°C. Measurements were conducted using a similar procedure as for the determination of k_d. First the system was degassed and allowed to reach equilibrium at a

pressure of approximately 0.8 x 10^5 Pa (P_{eq1}). Subsequently, H$_2$ gas was added up to an initial headspace pressure (P_0) of approximately 1.2 x 10^5 Pa and the system was allowed to reach equilibrium again (P_{eq2}). Then m_{gd} can be calculated from Eq. 13 using the P_{eq1}, P_o and P_{eq2} data.

$$m_{gd} = \frac{V_d(P_{eq2} - P_{eq1})}{V_g(P_0 - P_{eq2})} \tag{13}$$

The complete derivation of Eq. 13 can be found in Appendix 2.

Experimental set-up, determination of k_w

The solubility of H$_2$ in water is low compared to the solubility in *n*-dodecane (0.66 vs. 3.3 mM at 30°C and 10^5 Pa). To obtain a sufficient pressure drop as a result of H$_2$ absorption it was necessary to start from a zero initial H$_2$ concentration. This can be achieved by operating near vacuum, thus a modified SC (as depicted in Fig. 3) was used.
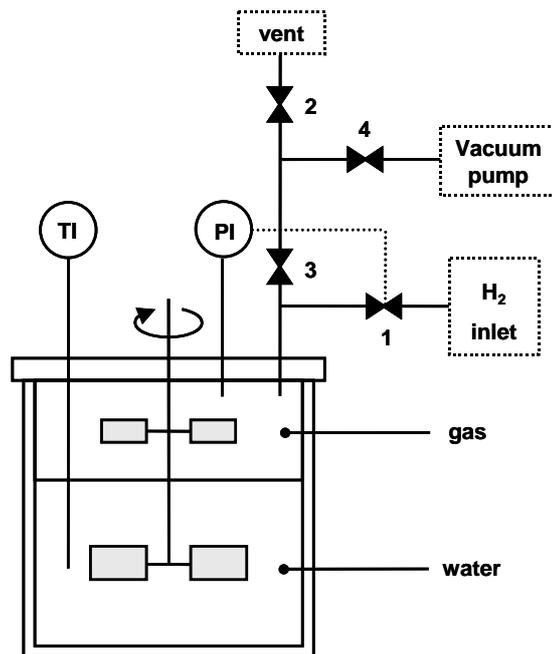
Fig. 3: Experimental set-up used for the experiments to determine k_w.

The volume of the SC was 1.9 L and the cross sectional area was 91.92 cm^2. After vacuumizing the headspace for 5 minutes the gas phase only contained water vapor, while the water phase was degassed. After closing valves 3 and 4 to the vacuum pump, H$_2$ was introduced by opening valve 1 until a pressure of approximately 0.97 x 10^5 Pa (see Fig. 3).

After closing valve 1, the stirring was started and the H_2 absorption was followed in time. In addition to the variation of temperature (30, 40 or 50ºC), the effect of the presence of salt (0, 25, 125 or 250 mM NaCl) on k_w was studied.

Calculation of k_w

During the absorption of H_2 in water over a defined specific surface area (a), the pressure decreases in time (t) according to Eq. 14 as derived by Demmink and Beenackers (1997):

$$P_t = P_{eq} + (P_{t=0} - P_{eq})exp\left[-\frac{\left(\frac{RTV_L}{He}\right) + V_g}{V_g} k_w \cdot a \cdot t\right] \tag{14}$$

The *He*-value depicted in Eq. 14 can be described with Eq. 15 (Demmink and Beenackers, 1997).

$$He = \left(\frac{P_{eq} - P_{H_2O}}{P_{t=0} - P_{eq}}\right)\frac{RTV_L}{V_g} \tag{15}$$

Since no other gas except water vapor was present at the beginning of each experiment, the initial H_2 concentration in the water phase was zero. Only, a correction for the water vapor pressure (P_{H_2O}) needs to be made (see Eq. 15). To enable the calculation of k_w using Eq. 14, the final pressure (P_{eq}) has to be calculated first using Eq. 15 when *He* and the initial pressure ($P_{t=0}$) are known. This leads to:

$$P_{eq} = \frac{bP_{t=0} + P_{H_2O}}{1+b} \quad \text{with } b = \frac{HeV_g}{RTV_L} \tag{16}$$

This relation is combined with Eq. 14 resulting in:

$$\frac{1}{a} \cdot \frac{1}{1+b} \ln\left(\frac{P_{t=0} - P_{eq}}{P_t - P_{eq}}\right) = k_w \cdot t \tag{17}$$

Now k_w can be determined by plotting the term on the left side of Eq. 17 against t. Again, the validity of *He*-values used in the calculation was checked using the equilibrium conditions as defined in Eq. 15.

Determination of k_{dw} using a steady state method

The detailed set-up is presented schematically in Fig. 4. The SC used was a 3L Applikon jacketed vessel equipped with 3 symmetrically placed baffles, a 2 L Applikon vessel with a heating coil inside was used as the stripping vessel and a 4 L vessel with jacket was used as the degassing vessel. The whole system was placed in an incubator for accurate temperature control. The SC was filled with *n*-dodecane and demineralized water. Hydrogen gas was introduced continuously to the SC by the MFC. The pressure in the headspace was kept atmospheric by removing excess gas through the gas outlet. Dissolved H$_2$ was continuously removed from the water phase by circulating the water phase through a stripper vessel, where H$_2$ was stripped using N$_2$. The degassing vessel was necessary to keep the water entering the SC free of N$_2$ bubbles, which were dragged together with the outcoming water flow from the stripper vessel.
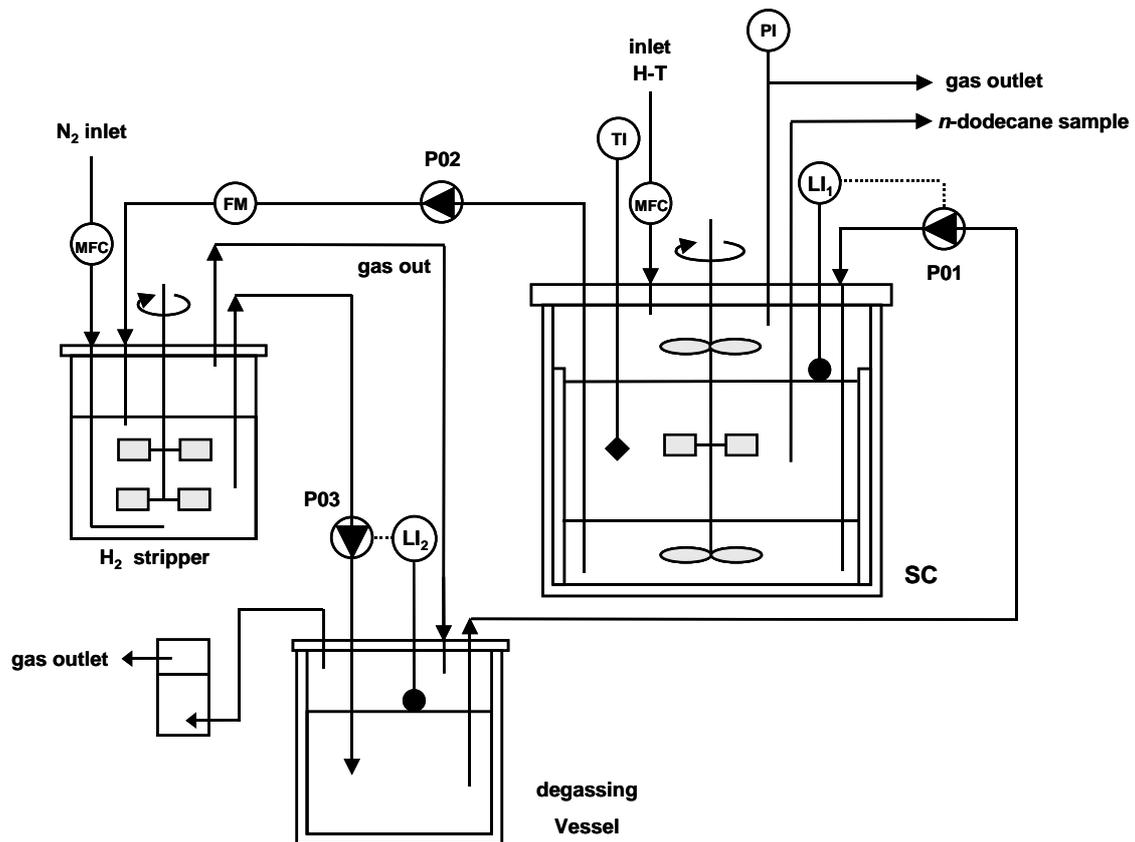
Fig. 4: Steady state configuration used to determine k_{dw}-values at 30, 40 and 50°C.

A flow meter (Kobold DPL-005 PKR) was placed after pump P-02 to check the stability of the flow. The liquid levels in the SC and the degassing vessel were kept constant by level controllers (LI$_1$ and LI$_2$, Fig. 4). A pressure indicator (PI) Cerabar T PMC 131, a Pt-

100 thermocouple (TI) and a flow meter (FM) were connected to the computer for automated data collection.

The overall mass transfer coefficient at the oil-water interface (k_{dw}) can be calculated using the mass balance depicted in Eq. 18. At steady state the net transfer from *n*-dodecane to water equals the H_2 removal rate (3rd term, Eq. 18) and the H_2 absorption rate (1st term, Eq. 18). One of these terms can be used to calculate k_{dw}. A detailed derivation of 2nd term of Eq. 18 to describe the mass transfer from *n*-dodecane to water is presented in Appendix 3.

$$k_d(c^*_d - c_d)A = k_{dw}(c_d - m_{dw} \cdot c_w)A = \Phi_w(c_w - c_{w,out}) \quad \text{(mol/s)} \quad (18)$$

In order to calculate k_{dw}, the [H_2] in the *n*-dodecane phase (c_d) and the [H_2] in the water phase (c_w) have to be measured accurately. Furthermore, the outlet [H_2] from the stripper ($c_{w,out}$) must be known to calculate the removal rate.

Using a Hydran 202 probe the c_w was estimated to be around 0.03 mM. An accurate measurement at this low concentration was not possible, since this device can only be calibrated with H_2 saturated water. To cope with the inability to measure c_w accurately, it was necessary to perform the experiments in such a way that the c_w can be considered as negligible, assuming an insignificant value of $m_{dw}.c_w$ in comparison with c_d (Eq. 18). Consequently, it was not possible to perform independent steady state experiments using the 3rd term in Eq. 18. The calculation of k_{dw} is then based on only the first two terms of Eq. 18, meaning that the mass balance is reduced to:

$$k_d(c^*_d - c_d) = k_{dw} \cdot c_d \quad (19)$$

The calculation of k_{dw} relies entirely on the accurate measurement of c_d and the use of calculated k_d-values from previous experiments (Eq. 19). To obtain a negligible c_w, the water residence time was minimized to 3.3 min and the H_2 removal efficiency of the stripper was optimized to 95% efficiency by operating at a N_2 flow rate of 500 ml/min at a stirring speed of 800 rpm. The water flow rate was 18 L/h and the H_2 flow rate over the headspace of the SC was 25 ml/min.

The dissolved H_2 concentration in *n*-dodecane (c_d) could not be measured with a probe. Therefore, radioactive tritium hydride (T-H) was used that could be measured by a scintillation counter. The use of T-H implies the assumption that the diffusion behavior of T-H is similar to that of H_2. To check this assumption the diffusion coefficients of H_2 and T-H in water and *n*-dodecane are compared. The Wilke-Chang equation was used to estimate the diffusion coefficient (Wilke and Chang, 1955), implying that the molar volume of H_2, T_2, or T-H at the normal boiling point is the most important physical

parameter that determines the diffusion coefficient. The calculated diffusion coefficients are summarized in Table 1.

Table 1: Comparison of the H$_2$, T-H and T$_2$ diffusion coefficients in water (D_w) and *n*-dodecane (D_d).

	H$_2$	T-H	T$_2$
V_m x 10^{-3} L/mol	29.39 [a]	24.41 [b]	20.45 [b]
D_w x 10^{-9} m^2/s at 30/40/50°C	2.53 / 3.19 / 3.93	2.83 / 3.57 / 4.4	3.15 / 3.97 / 4.89
D_d x 10^{-9} m^2/s at 30/40/50°C	3.04 / 3.4 / 4.41	3.4 / 4.13 / 4.94	4.41 / 4.93 / 5.49

([a] Kirk-Othmer, 1993; [b] Kirk-Othmer, 1995)

From Table 1 it follows that for both water and *n*-dodecane as the solvent the diffusion coefficient of T-H is 12% larger compared to the value for H$_2$. This falls within the predictive power of the Wilke-Chang equation (errors of 10 up to 20% are reported). Therefore, the deviation is regarded as acceptable and the diffusion behavior of both compounds is considered to be similar.

The use of T-H (see further description in section analytical techniques) was not applicable to measure c_w, because tritium atoms exchange with hydrogen atoms from water molecules, giving rise to an increasing background signal for radioactivity.

During the experiments, a steady state was maintained for three hours and every 30 min a sample was withdrawn from the oil layer in the stirred cell and immediately subjected to analysis to assess c_d. All experiments were conducted in duplicate at each temperature. Since, c_d* is dependent on the composition of the gas phase, an analysis was carried out to determine the fraction of H$_2$ in the headspace during steady state.

Stripper performance

The stripping performance was checked by adding oxygen-saturated water at a flow rate of 15 l/h to the vigorously stirred stripping vessel. The O$_2$ concentration of the incoming and outgoing flows were measured using O$_2$ probes (OXI 196, WTW). The stripping gas (N$_2$) was supplied using an MFC (Brooks 5850S, capacity 0 – 2000 ml/min). The stripper efficiency for H$_2$ was modeled according to the considerations presented in appendix 4.

Analytical techniques

Tritium hydride (T-H) was obtained by adding tritium (T_2) to H_2 until gas with an activity of 22.5 kBq/mmol H_2 was obtained. Tritium hydride was obtained by the following reaction at room temperature: $H_2 + T_2 \rightarrow 2TH$. A sample to measure c_d was prepared by adding approx. 3 ml sample to 17 ml scintillation liquid. The exact amounts added were determined gravimetrically. The scintillation liquid consisted of 4 g 2,5-diphenyloxazole as the primary scintillator and 0.2 g dimethyl-POPOP (phenyl-oxygen-phenyl-oxygen-phenyl) as the secondary scintillator, dissolved in a liter of toluene. The scintillation vial was completely filled to prevent partitioning of H_2 to the headspace. The fluorescence quantum yield was measured using a Packard Tri-Carb 2500 TR Liquid scintillation counter and compared to a standard (^{3}H-*n*-hexadecane, Packard) with a known activity. Every sample was counted 3 times for 5 minutes, to obtain a 95% confidence level. Control experiments revealed that no tritium exchange with *n*-dodecane occured. The activity of the samples decreased less than 3% in one hour after sampling.

During steady state the off gas from the SC was flown over a gas bulb containing a sample valve. The composition of the gas was verified by subjecting gas from the bulb directly to analyis in an Ametek Process Instruments mass selective detector.

RESULTS AND DISCUSSION

k_d measurements

The results from the experiments to determine k_d are summarized in Table 2. The value of k_d increases with temperature. This is in accordance with the decreasing viscosity at increasing temperatures (Table 2).

Table 2: k_d –values obtained at 30, 40 and 50°C.

T ($^\circ$C)	η (mPas)	k_d x 10^{-5} (ms^{-1})	SD [1] x 10^{-5} (ms^{-1})
30 [2]	1.27	2.89	0.12
40	1.08	3.89	0.13
50	0.93	4.27	0.21

[1]SD= standard deviation.

[2]At 30ºC 6 instead of 3 experiments were performed.

The data processing to determine k_d is illustrated in Fig. 5. The H$_2$ concentration at the g/d-interface and in the bulk *n*-dodecane phase were calculated from the pressure drop (Fig. 5A). The k_d -value was calculated for a time interval of 120 s (Fig. 5B) and an average k_d was obtained from data up to 4000 s. At that time the pressure drop became too small (< 5 Pa). The criterion used was that a difference of 5 Pa in the PI reading resulted in a 5% error in the calculated k_d.

Commonly, the solubility in the liquid phase is assumed to be constant to estimate k_L (Gaddis, 1999). The advantage of using our numerical calculation method is that the gas phase is not necessarily assumed to be at constant pressure, thus the solubility is corrected for the decreased pressure.
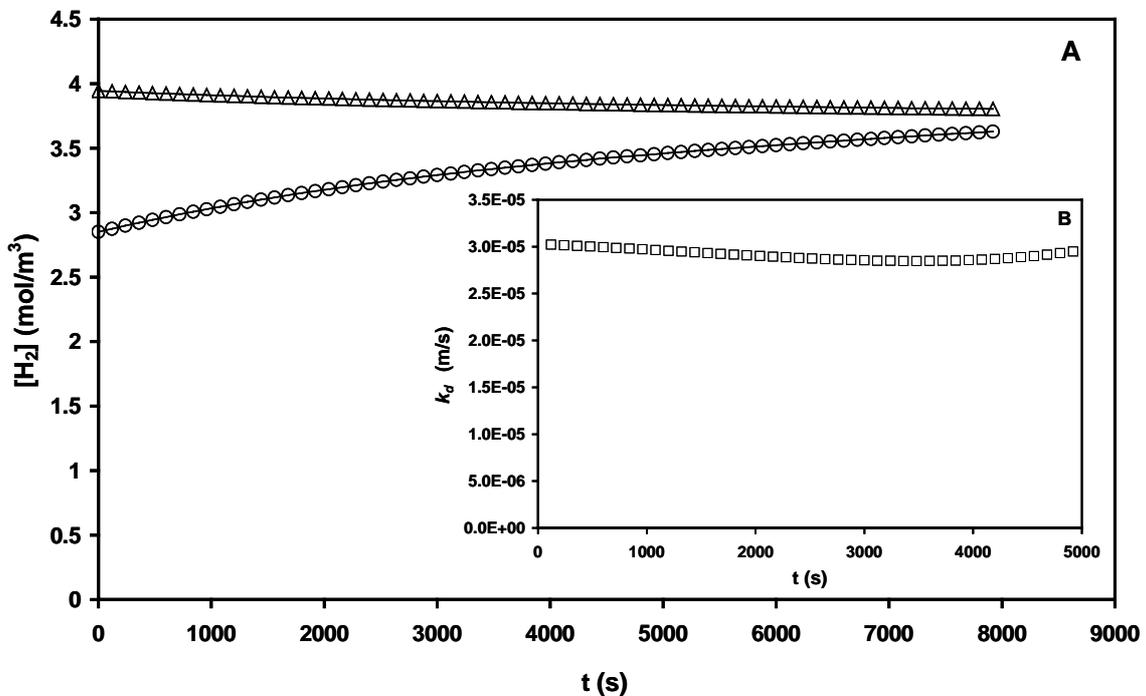
Fig. 5. A: Calculated H$_2$ concentrations on the *n*-dodecane g/d-interface ($\triangle$) and *n*-dodecane bulk ($\bigcirc$) during the pressure drop and B: the calculated k_d-values up to 4000 s ($\square$) for a typical experiment at 30°C.

In order to assess the accuracy of the k_d calculation method the average k_d-value obtained from 6 experiments at 30°C (Table 1) was used to predict the pressure drop (P_2) using P_0 and P_1 data from an independent experiment (see Eq. 11). The difference between the predicted pressure profile and the measured data is not more that 0.7% (data not shown) and the accuracy of the experimental method applied is considered to be very good. Several experiments were conducted to verify the partitioning data at 30, 40 and 50°C

obtained with the theoretical Soave-Redlich-Kwong model, using Eq. 13. The collected data of P_0, P_{eq1} and P_{eq2} and the results are presented in Table 3.

Table 3: Results of measured pressures (P_0, P_{eq1} and P_{eq2}) and calculated He_d.

P_0	P_{eq1}	P_{eq2}	m	K	He_d
(x10^2 Pa)	(x10^2 Pa)	(x10^2 Pa)	(m^{3}g / m^{3}d)	(-)	(MPa.m^3/kmol)
176	-163.7	124.5	12.04	1326.94	30.44
192	-176.6	132.8	12.25	1349.15	30.97
166	-133.2	121	12.15	1339.45	30.72

Comparing the He_d-values obtained to the model value (30.38 MPa.m^3/kmol) the experimental results are slightly higher. This is due to the sensitivity of the experimental method to pressure fluctuations. A difference of only 100 Pa in the pressure reading gives an offset of 0.8 MPa·m^3/kmol.

k_w measurements

In Table 4 the results of the determination of k_w at 30, 40 and 50°C at different NaCl concentrations are summarized.

Table 4: Results of k_w and the effect of the presence of NaCl on the k_w-value.

T	[NaCl]	η	k_w	SD in k_w
(°C)	(mM)	(mPa s)	x 10^{-5} (ms^{-1})	x 10^{-5} (ms^{-1})
30	0	0.85	9.66	0.19
	25		9.04	0.10
	125		8.77	0.22
	250		8.07	0.51
40	0	0.7	14.82	0.53
	25		14.81	0.04
	125		13.22	0.67
	250		11.75	0.27
50	0	0.58	21.11	0.99
	25		21.90	0.31
	125		18.28	0.32
	250		18.32	0.83

Again the value of k_w increases with temperature due to the lower viscosity (Table 4). The influence of the presence of salt results in a slightly decreasing k_w at every temperature (Table 4). This effect can be explained by an increase of the viscosity with higher salt concentrations (Mahiuddin and Ismail, 1996; Beenackers and Van Swaaij, 1993).

An example of the method applied to find the k_w-values summarized in Table 4 is presented in Fig. 6. In the regression only data up to approx. 100 s was used, after 100 s the pressure drop of the headspace was to small to enable accurate calculations.
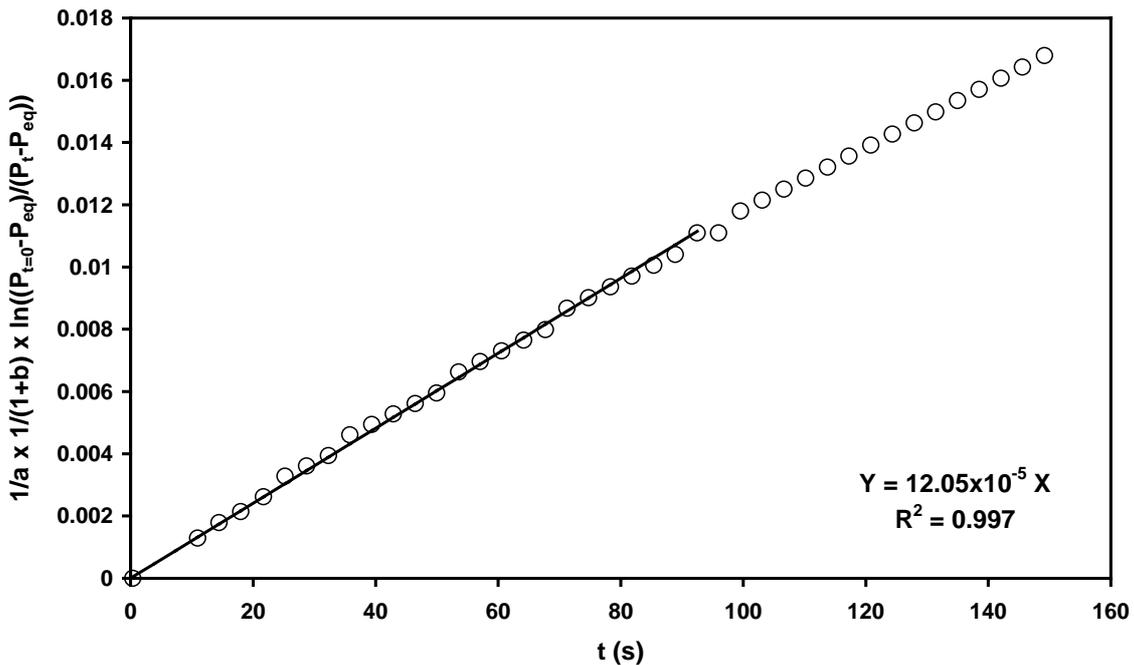
Fig. 6. Typical example of a plot to determine k_w using Eq. 16 and Eq. 17 and the data obtained at 40°C and a [NaCl] of 250 mM.

Typical k_w-values for oxygen transfer in bubble columns are in the order of 1 up to 5 x 10^{-4} ms^{-1}, depending on the bubble diameter (Heijnen and Van 't Riet, 1984). The results depicted in Table 4 are within the lower part of this range. This might be explained by the smaller film thickness present in bubble columns compared to the stirred cell system.

In Table 5 the He_w-values at different temperatures (30, 40 and 50°C) and NaCl concentrations (0 up to 250 mM) used in the k_w determinations are summarized.

Table 5: Dependency of the *He*-value on temperature and the presence of NaCl, comparison of measured with predicted *He*-values.

T	[NaCl]	He_S**	He_{exp}	Deviation	$\gamma(He_S / He_{demi})$
(°C)	(mM)	MPa/(kmol/m³)	MPa/(kmol/m³)	(%)	(-)
30	0	151.77*	151.59	0.12	1.00
	25	152.69	154.00	0.86	1.01
	125	156.45	156.03	0.26	1.03
	250	161.27	160.86	0.25	1.06
40	0	146.14*	143.23	1.99	1.00
	25	147.08	144.07	2.05	1.01
	125	150.91	148.52	1.58	1.03
	250	155.83	147.63	5.26	1.07
50	0	140.59*	135.05	3.94	1.00
	25	141.54	141.75	0.15	1.01
	125	145.42	143.23	1.51	1.03
	250	150.42	143.28	4.75	1.07

*He-value of deionized water. **He_s at different salt concentrations were calculated according to Eq. 4.

From the comparison of the values listed in Table 5, it is obvious that the *He*-value increases as a result of the decreased solubility of H_2 in water due to the presence of salt. The salting out effect is not very pronounced, the values of *He* deviated less than 10% from the *He* of demineralized water (γ<1.1, Table 5). This means that the H_2 solubility is not significantly affected up to NaCl concentrations of 250 mM. Nevertheless, the corrected *He*-values in the presence of NaCl were used in the calculations of k_w. The experimental *He*-values and the theoretical *He$_s$*-values according to Weisenberg and Schumpe (1996) have a minor deviation (Table 5), indicating that the experimental conditions during the measurements of k_w were optimal.

k_{dw} measurements

Table 6 provides the results of the steady state experiments performed at 30, 40 and 50°C. In Table 6, c_d is calculated from 6 measurements during the steady state. The [H$_2$] in the headspace was found to be 99% pure in every experiment, this value was used to calculate c_d^* (Eq. 3). The k_{dw}-values obtained when the maximal and minimal value for c_d were applied using the mass balance described in Eq. 19 are depicted in Table 6.

Table 6: Results of the calculated k_{dw}-values from steady state experiments.

T	c_d	c_d^*	k_{dw} variable c_d	k_{dw} variable k_d	k_{dw} including $m_{dw} \cdot 0.05 \cdot c_w^*$
($^\circ$C)	(mM)	(mM)	(x 10^{-6} ms^{-1})	(x 10^{-6} ms^{-1})	(x 10^{-6} ms^{-1})
30	2.79 ± 0.05	3.3	5.15 ± 0.61	5.15 ± 0.21	5.42
	2.83 ± 0.04	3.3	4.82 ± 0.45	4.82 ± 0.2	5.08
40	2.84 ± 0.06	3.4	7.62 ± 1.05	7.62 ± 0.25	8.03
	2.83 ± 0.06	3.4	7.91 ± 0.97	7.91 ± 0.26	8.33
50	2.92 ± 0.05	3.54	9.13 ± 0.88	9.11 ± 0.45	9.61
	2.92 ± 0.02	3.54	9.12 ± 0.43	9.13 ± 0.45	9.60

It can be inferred from Table 6 that the duplicate measurements of c_d are in very good agreement and show a slight increase with temperature. The calculated k_{dw}-values appear to be quite sensitive to minor differences in the c_d-measurements. Consequently, an accurate measurement of c_d is absolutely necessary for an exact determination of k_{dw}. When calculations are performed with the maximal and minimal k_d-values (see Table 2) at constant average c_d-values using Eq. 19, the deviations in the resulting k_{dw}-values are smaller (Table 6). The accuracy of the k_{dw} calculation method by assuming a negligible c_w was assessed by performing calculations using the stripper efficiency. As depicted in Fig. 7 the efficiency for stripping H$_2$ at the experimental conditions is 95%.
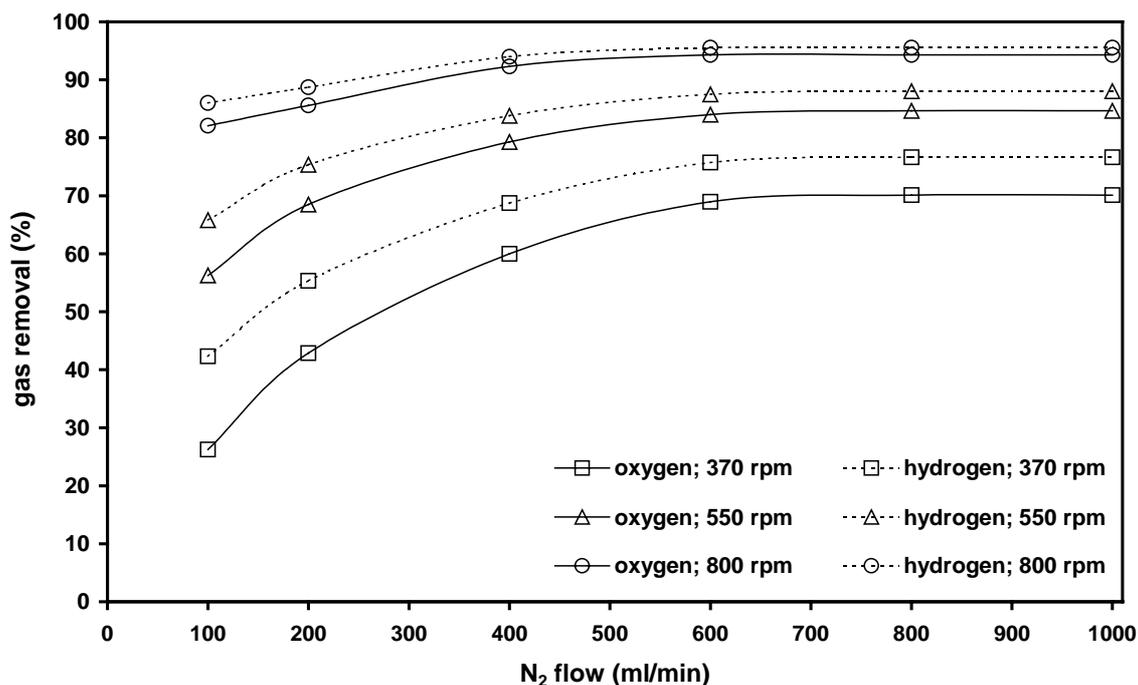
Fig. 7. Stripping efficiency at different operating conditions (variable N_2 flow and stirrer speed).

For the calculation of the k_{dw}-values using Eq. 19, it was assumed that a 95% stripping efficiency leads to a c_w of 0.05 x c_w^* (Table 6). The k_{dw}-values thus calculated are in accordance with the other values summarized in Table 6. Hitherto, neglecting the steady state c_w did not lead to unacceptable errors.

Generally, the value of k_{dw} increases with temperature, as can be explained by the non-linear viscosity decrease of water and *n*-dodecane with temperature (see Table 2 and 4).

Cesário *et al.* (1995) also determined an overall mass transfer coefficient for dichloromethane as the diffusing compound in a dodecene/water system using empirical relations to describe mass transfer in two-phase bioreactors. Calculations with a known specific surface area for a liquid impelled loop reactor and a packed bed reactor containing immobilized bacteria revealed a value of 16×10^{-6} ms^{-1} for the mass transfer of dichloromethane (Cesário *et al.*, 1995; Van Sonsbeek *et al.*, 1992). The k_{dw}-values found in the current study are in the same order, confirming their validity.

CONCLUSIONS

In this work the feasibility of using *n*-dodecane as a carrier phase for H$_2$ transfer is assessed. Therefore, the mass transfer coefficient from *n*-dodecane to water is compared to mass transfer coefficient from gas to water directly.

From this study it can be concluded that the value for k_w [(9.7 ± 0.2) x 10^{-5} ms^{-1} at 30ºC]) is a factor 3.3 higher than for k_d [(2.89 ± 0.12) x 10^{-5} ms^{-1} at 30ºC)] because of the lower viscosity. The presence of salt (up to 250 mM NaCl) has no major influence on the k_w-value. The k_{dw}-value determined in the steady state experiments at 30ºC is (5 ± 0.6) x 10^{-6} ms^{-1} and 19.4 times smaller than what can be attained in a gas/water system. The considerably smaller value for k_{dw} is due to the additional mass transfer resistance introduced by the second liquid phase.

Based on the measured k_{dw}-values, the concept of using an organic phase to supplement H$_2$ to the bacteria does not seem attractive. Furthermore, when comparing the H$_2$ flux from *n*-dodecane to water to the flux from gas to water also the driving force must be considered. Calculations revealed a flux of 0.016 x 10^{-3} mol/m^{2}s for a *n*-dodecane/water system and 3.9 x 10^{-3} mol/m^{2}s for a gas/water system, respectively (using Eq. 1 with $c_{bulk} \approx 0$). To obtain a maximal concentration gradient the [H$_2$] in the aqueous phase was assumed to be negligible, because of the immediate H$_2$ consumption by the bacteria. However, the driving force for a g/w system is much bigger than the one for a d/w system (40.2 mM vs. 3.3 mM, using Eq. 3 to calculate c^* at 30°C and 10^5 Pa).

In conclusion it can be said that the feasibility of supplying H$_2$ via the oil phase to the bacteria is completely dependent on the specific surface area available for mass transfer. To compensate for the smaller flux in the *n*-dodecane/water system, the specific surface area must be a factor 244 larger than for a g/w-system.

In the following chapter we will pay attention to the estimation of the specific surface area in a dispersion system by investigating the droplet size distribution to make a final judgment on the feasibility to use *n*-dodecane as a carrier phase for H$_2$ transfer. A system equipped with a nozzle to create very fine droplets (< 15 µm) will be used. Apart from that the k_{dw}-values determined in this chapter will be verified in a three-phase bioreactor system at 30°C. To approach the practical situation more exactly sulfate reducing bacteria that consume H$_2$ will be used.

NOMENCLATURE

A	interfacial area (m^2)
a	specific surface area ($m^2 m^{-3}$)
C	concentration ($kmol\,m^{-3}$)
D	Diffusivity ($m^2 s^{-1}$)
h_i	ion-specific salting-out parameter, see Eq. 4 ($m^3 kmol^{-1}$)
h_g	gas-specific salting-out parameter, see Eq. 5 ($m^3 kmol^{-1}$)
$h_{g,0}$	gas-specific salting-out parameter at 298.15 K, see Eq 5. ($m^3 kmol^{-1}$)
He	Henry coefficient ($Pa\,m^3 mol^{-1}$)
J	Mass transfer flux ($mol\,m^{-2} s^{-1}$)
k_d	liquid side mass transfer coefficient gas/*n*-dodecane (ms^{-1})
k_w	liquid side transfer coefficient gas/water (ms^{-1})
k_{dw}	overall mass transfer coefficient *n*-dodecane/water (ms^{-1})
K	partition coefficient based on mole fractions (dimensionless)
m_{gd}	partition coefficient between gas and *n*-dodecane (m_d^3 / m_g^3)
P	pressure (Pa)
p_{H2}	partial H_2 pressure $y_{H2} \cdot P$ (Pa)
Q	volumetric flow ($m^3 s^{-1}$)
R	ideal gas constant ($8.314\ J\,mol^{-1} K^{-1}$)
T	temperature (K or °C)
T	time (s)
V	volume (m^3)
V_m	Molar volume at normal boiling point ($Lmol^{-1}$)

Greek symbols

η	Viscosity (Pa s)
Φ	Flow ($m^3 s^{-1}$)

Super and subscripts

* or eq	at equilibrium
w	water phase
d	n-dodecane phase
g	H_2 gas phase
s	salt
t	at time t

Abbreviations

LI	Level indicator
MFC	Mass Flow Controller
PI	Pressure Indicator
SC	Stirred cell
TI	Temperature Indicator

ACKNOWLEDGEMENTS

REFERENCES

Baldascini H., Ganzeveld K.J., Janssen D.B., Beenackers A.A.C.M. 2001. Effect of mass transfer limitations on the enzymatic kinetic resolution of epoxides in a two-liquid-phase system. Biotechnol. Bioeng. 73: 44-54.

Beenackers A.A.C.M., Van Swaaij W.P.M. 1993. Mass transfer in gas-liquid slurry reactors. Chem. Eng. Sci. 48: 3109-3139.

Cessário M.T., Beeftink H.H., Tramper J. 1995. Feasibility of using water-immiscible organic solvents in biological waste-gas treatment. Bioprocess Eng. 12: 55-63.

Demmink J.F., Beenackers A.A.C.M. 1997. Oxidation of ferrous NTA with oxygen, A model for oxygen mass transfer in parallel to reaction kinetics. Ind. Eng. Chem. Res. 36: 1989-2005.

Fillion B., Morsi B.I. 2000. Gas-liquid mass-transfer and hydrodynamic parameters in a soybean oil hydrogenation process under industrial conditions. Ind. Eng. Chem. Res. 39: 2157-2168.

Gaddis E.S. 1999. Mass transfer in gas-liquid contactors. Chem. Eng. Process. 38: 503-510.

Gogate P.R., Pandit A.B. 1999. Survey of measurement techniques for gas-liquid mass transfer coefficient in bioreactors. Biochem. Eng. J. 4: 7-15.

Heijnen J.J., Van 't Riet K. 1984. Mass transfer, mixing and heat transfer phenomena in low viscosity bubble column reactors. Chem. Eng. J. 28: 21-42.

Kirk-Othmer. 1993. Encyclopedia of Chemical Technology. 4th Ed. Vol.8: Deuterium & Tritium to Elastomers, Polyethers. John Wiley & Sons.

Kirk-Othmer. 1995. Encyclopedia of Chemical Technology. 4th Ed. Vol.13: Helium Group to Hypnotics. John Wiley & Sons.

Merchuk J.C., Yona S., Siegel M.H., Ben Zvi A. 1990. On the first-order approximation to the response of dissolved oxygen electrodes for dynamic $k_L a$ estimation. Biotechnol. Bioeng. 35:1161-1163.

Mahiuddin S., Ismail K. 1996. Temperature and concentration dependence of the viscosity of aqueous sodium nitrate and sodium thiosulphate electrolytic systems. Fluid Phase Equilibr. 123: 231-243.

Schumpe A. 1993. The estimation of gas solubilities in salt solutions. Chem. Eng. Sci. 48: 153-158.

Van den Meer A.B., Beenackers A.A.C.M., Stamhuis E.J. 1986. Microbial production of epoxides from alkenes in continuous multi-phase reactors. Chem. Eng. Sci. 41: 607-616.

Van Houten R.T., Hulshoff Pol L.W., Lettinga G. 1994. Biological sulfate reduction using gas-lift reactors fed with hydrogen and carbon dioxide as energy and carbon source. Biotechnol. Bioeng. 44: 586-594.

Van Sonsbeek H.M., Beeftink H.H., Tramper J. 1993. Two–liquid phase bioreactors. Enzyme Microb. Technol. 15: 722-729.

Van Sonsbeek H.M., De Blank H., Tramper J. 1992. Oxygen transfer in liquid-impelled loop reactors using perfluorcarbon liquids. Biotechnol. Bioeng. 40: 713-718.

Van Sonsbeek H.M., Gielen S.J., Tramper J. 1991. Steady-state method for *ka* measurements in model systems. Biotechnol. Tech. 5: 157-162.

Weisenberger S, Schumpe A. 1996. Estimation of gas solubilities in salt solutions at temperatures from 273 K to 363 K. AIChE J. 42: 298-300.

Wilke C.R., Chang P. 1955. Correlation of diffusion coefficients in dilute solutions. AIChE J. 1: 264-270.

Woodley J.M., Lilly M.D. 1990. Extractive biocatalysis: The use of two-liquid phase biocatalytic reactors to assist product recovery. Chem. Eng. Sci. 45: 2391-2396.

Wubbolts M.G., Hoven J., Melgert B., Witholt B. 1994. Efficient production of optically active styrene epoxides in two liquid-phase cultures. Enzyme Microb. Technol. 16: 887-894.

APPENDICES

Appendix 1

Substitution of the expression for c^* (according to Eq. 1) and the expression for $c_{d,t}$ (according to Eq. 9) in Eq. 8 results in an expression that can be rearranged to Eq. 12 as presented below.

$$\frac{P_1 - P_2}{RT} \cdot V_g = k_{d,1} \cdot A \cdot \left(\frac{\dfrac{P_2}{m_{gd}RT} + \dfrac{P_1}{m_{gd}RT}}{2} - \frac{c_{d,t=0} + \dfrac{P_0 - P_2}{RT} \cdot \dfrac{V_g}{V_o} + c_{d,t=0} + \dfrac{P_0 - P_1}{RT} \cdot \dfrac{V_g}{V_o}}{2} \right)(t_2 - t_1)$$

$\Leftrightarrow$

$$\frac{P_1 - P_2}{RT} \cdot V_g = k_{d,1} \cdot A \cdot \left(\frac{P_2}{m_{gd}} + \frac{P_1}{m_{gd}} - (P_0 - P_2)\frac{V_g}{V_o} - (P_0 - P_1)\frac{V_g}{V_o} - 2 \cdot c_{d,t=0} \cdot RT \right) \cdot \frac{(t_2 - t_1)}{2RT}$$

$\Leftrightarrow$

$$\frac{P_1 - P_2}{RT} \cdot V_g = k_{d,1} \cdot A \cdot \left(\frac{P_2 + P_1}{m_{gd}} + (P_1 + P_2 - 2P_0)\frac{V_g}{V_o} - 2 \cdot c_{d,t=0} \cdot RT \right) \cdot \frac{(t_2 - t_1)}{2RT}$$

$\Leftrightarrow$

$$k_{d,1} = \frac{(P_1 - P_2) \cdot V_g}{A \cdot \left(\dfrac{P_2 + P_1}{m_{gd}} + (P_1 + P_2 - 2P_0)\dfrac{V_g}{V_o} - 2 \cdot c_{d,t=0} \cdot RT \right) \cdot \dfrac{(t_2 - t_1)}{2}} \qquad \text{(Eq. 12)}$$

The same procedure can be followed for $k_{d,2}$, $k_{d,3}$ and so on.

Appendix 2

Consider $c_{eq1,g}$ and $c_{eq1,d}$ as the equilibrium H_2 concentrations in the gas and *n*-dodecane phase after degassing when the 1st equilibrium is reached at a pressure of approximately 0.8×10^5 Pa (P_{eq1}). Their relations with the pressure in the headspace are:

$$c_{eq1,d} = \frac{c_{eq1,g}}{m_{gd}} = \frac{P_{eq1}}{m_{gd}RT} \qquad \text{(A2.1)}$$

Subsequently, H_2 gas was added up to an initial headspace pressure (P_0) of approximately 1.2×10^5 Pa. Then, the total amount of H_2 gas in the system after the H_2 gas addition is:

$$H_{2,tot} = (H_{2,g} + H_{2,d})_{eq1} + H_2 \, added \, by \, MFC \qquad \text{(A2.2)}$$

$$H_{2,tot} = \left(\frac{P_{eq1} V_g}{RT} + \frac{P_{eq1} V_d}{m_{gd} RT} \right) + \frac{\left(P_0 - P_{eq1} \right) V_g}{RT} \tag{A2.3}$$

When the 2nd equilibrium is reached (after the pressure drop), the H$_2$ concentration in the gas ($c_{eq2,g}$) and the *n*-dodecane phase ($c_{eq2,d}$) are related by m_{gd}:

$$m_{gd} = \frac{c_{eq2,g}}{c_{eq2,d}} \tag{A2.4}$$

Then $c_{eq2,d}$ can be calculated from the mass balance:

$$H_{2,tot} = (H_{2,g} + H_{2,d})_{eq2} = c_{eq2,d}.V_d + c_{eq2,g}.V_g \tag{A2.5}$$

Since $c_{eq2,g} = \frac{P_{eq2}}{RT}$, $\quad c_{eq2,d} = \frac{H_{2,tot} - \dfrac{P_{eq2} V_g}{RT}}{V_d} \tag{A2.6}$

Substitution of Eq. (A2.6) into Eq. (A2.4), yields:

$$m_{gd} = \frac{c_{eq2,g}}{\dfrac{H_{2,tot} - \dfrac{P_{eq2} V_g}{RT}}{V_d}} \Leftrightarrow m_{gd} \left(H_{2,tot} - \frac{P_{eq2} V_g}{RT} \right) = \frac{P_{eq2}}{RT} V_d \tag{A2.7}$$

Substitution of Eq. (A2.5) into Eq. (A2.7) yields:

$$m_{gd} \left(\frac{P_{eq1} V_g}{RT} + \frac{P_{eq1} V_d}{m_{gd} RT} + \frac{\left(P_0 - P_{eq1} \right) V_g}{RT} - \frac{P_{eq2} V_g}{RT} \right) = \frac{P_{eq2}}{RT} V_d \tag{A2.8}$$

$$m_{gd} \left(\frac{P_{eq1} V_d}{m_{gd}} + P_0 V_g - P_{eq2} V_g \right) = P_{eq2} V_d \tag{A2.9}$$

$$m_{gd} = \frac{V_d \left(P_{eq2} - P_{eq1} \right)}{V_g \left(P_0 - P_{eq2} \right)} \tag{13}$$

Appendix 3

The mass transfer process in the steady state process is depicted schematically in Fig. A3.1.
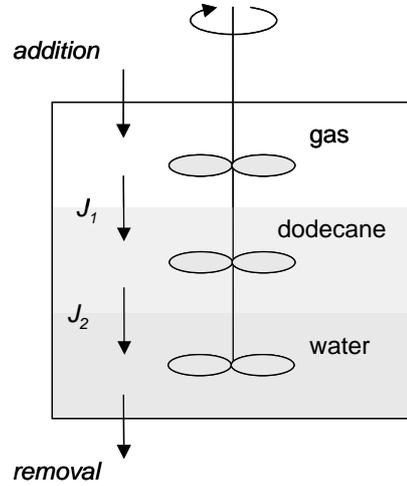
Fig. A3.1: Steady State method: the arrows show the direction of H_2 diffusion.

The rate of H_2 mass transfer at the *n*-dodecane-water interface is represented by:

$$J_2 = k_{d,2}(c_d - c^*_{d,2}) = k_{w,2}(c^*_w - c_w) \qquad \text{(mol/m}^2\text{.s)} \qquad \text{(A3.1)}$$

with $k_{d,2}$ and $k_{w,2}$ as the mass transfer coefficients in the *n*-dodecane and in the water phase, respectively, at the *n*-dodecane/water interface. $c^*_{d,2}$ and c^*_w are related by m_{dw} according to: $c^*_{d,2} = m_{dw} \cdot c^*_w$, consequently:

$$k_{d,2}(c_d - m_{dw} \cdot c^*_w) = k_{w,2}(c^*_w - c_w) \qquad \text{(A3.2)}$$

$$c^*_w = \frac{k_{d,2} \cdot c_d + k_{w,2} \cdot c_w}{k_{w,2} + k_{d,2} \cdot m_{dw}} \qquad \text{(A3.3)}$$

Substitution of Eq. (A3.3) into Eq. (A3.1) and introduction of the overall oil-water mass transfer coefficient (k_{dw}) results in the following expression for J_2:

$$J_2 = k_{w,2} \left(\frac{k_{d,2} \cdot c_d + k_{w,2} \cdot c_w}{k_{w,2} + k_{d,2} \cdot m_{dw}} - c_w \right) \qquad \text{(A3.4)}$$

$$J_2 = \frac{1}{\frac{1}{k_{d,2}} + \frac{m_{dw}}{k_{w,2}}}(c_d - m_{dw} \cdot c_w) = k_{dw}(c_d - m_{dw} \cdot c_w) \qquad \text{(A3.5)}$$

Appendix 4

The stripper was modeled as an ideally mixed system ($c_{out}=c$) according to the following mass balance:

Molar flux of (H_2 gas)$_{in}$ –Molar flux of (H_2 gas)$_{out}$ = desorption rate from the liquid phase to the gas phase, or:

$$Q_L \cdot (c_{gas,in} - c_{gas,out}) = k_L \cdot (c_{gas,out} - c^*) \cdot A \qquad \text{(mol/s)} \qquad \text{(A4.1)}$$

Since N_2 flows continuously through the stripper, the concentration of O_2 or H_2 in the gas phase can be assumed to be negligible ($c^* = 0$), resulting in:

$$Q_L \cdot (c_{gas,in} - c_{gas,out}) = k_L \cdot c_{gas,out} \cdot A \qquad \text{(A4.2)}$$

Eq. A4.2 can be rearranged to:

$$\frac{c_{gas,out}}{c_{gas,in}} = \frac{Q_L}{Q_L + k_L.A} \qquad \text{(A4.3)}$$

The gas removal is defined as:

$$\text{Removal} = \frac{c_{in} - c_{out}}{c_{in}} = 1 - \frac{c_{out}}{c_{in}}, \text{ thus: } \frac{c_{out}}{c_{in}} = 1 - \text{Removal} \qquad \text{(A4.4)}$$

Comparing the removal of O_2 and H_2 using Eq. A4.3 results in:

$$\frac{\dfrac{c_{H_2,out}}{c_{H_2,in}}}{\dfrac{c_{O_2,out}}{c_{O_2,in}}} = \frac{Q_L + k_{O_2}.A}{Q_L + k_{H_2}.A} \qquad \text{(A4.5)}$$

When $Q_L << k_L.A$, Eq. A4.5 reduces to:

$$\frac{c_{H_2,out}}{c_{H_2,in}} = \frac{k_{O_2}}{k_{H_2}} \frac{c_{O_2,out}}{c_{O_2,in}} \qquad \text{(A4.6)}$$

The liquid side mass transfer coefficients (k_L) of H_2 and O_2 can be calculated from their diffusion coefficients $D_{H2} = 3.81.10^{-9}$ m^2/s at 21°C and $D_{O2} = 2.33.10^{-9}$ m^2/s at 21°C, according to:

$$k_{L,O_2} = k_{L,H_2} * \sqrt{\frac{D_{O_2}}{D_{H_2}}} \qquad \text{(A4.7)}$$

Substitution of Eq. A4.4 and Eq. A4.7 in Eq. A4.6 results in:

$$1 - H_2 Removal = \sqrt{\frac{D_{O_2}}{D_{H_2}}} \cdot \left(1 - O_2 \ Removal\right) \tag{A4.8a}$$

Inserting the *D* values gives:

$$H_2 Removal = 0.218 + 0.782 * O_2 \ Removal \tag{A4.8b}$$

Using the removal data for O$_2$, the H$_2$ removal can be calculated with Eq. A4.8b.

When $Q_L \gg k_L A$, equation (A4.5) reduces to: $H_2 Removal = O_2 \ Removal$

Details of photographs depicting the experimental work that is described in Chapter 5.

DETERMINATION OF HYDROGEN MASS TRANSFER
IN A THREE-PHASE SULFATE REDUCING BIOREACTOR

ABSTRACT

This work provides an extensive analysis of the feasibility to use *n*-dodecane as carrier phase for H_2 mass transfer. A *n*-dodecane/water dispersion is considered as a model system for a new anaerobic biodesulfurization process. In this process H_2 gas is used as electron donor to reduce organic or inorganic sulfur compounds. Steady state experiments with hydrogenotrophic sulfate reducing bacteria were performed to determine the mass transfer coefficient for a *n*-dodecane/water system (k_{dw}). A value of $(4\pm0.24)\times10^{-6}$ m·s^{-1} was found, which is close to the values found in previous non-biological steady state experiments using tritium hydride, *i.e.* $(5\pm0.6)\times10^{-6}$ m·s^{-1}. In order to compensate for the low flux attained in a *n*-dodecane/water system compared to a H_2 gas/water system, 0.16 x 10^{-6} versus 3.9 x 10^{-6} mol/m^{2}s, respectively, a high specific surface area of *n*-dodecane droplets in water is a prerequisite. A nozzle appeared to be a very effective tool in creating very fine droplets resulting in a Sauter mean diameter (d_{32}) of only 10.3 ± 0.9 μm as a net result of disruptive forces and coalescence. The droplet size was found to be independent of the sodium ion concentration and the applied pressure drop over the nozzle. The hold-up of *n*-dodecane in the aqueous medium though is clearly affected by the sodium ion concentration. The hold-up decreases rapidly (from 0.14 to 0.04) with increasing sodium ion concentrations due to coagulation; from 94 mM onwards the hold-up becomes 0.04. The effectiveness of using *n*-dodecane droplets as a carrier phase for H_2 mass transfer was demonstrated in batch tests for sulfate reduction. During operation biomass flotation was observed caused by injection of *n*-dodecane to create a fine dispersion. Calculations show that the volumetric H_2 mass transfer rate from *n*-dodecane to water is comparable to values found for gas lift reactors.

KEYWORDS

Biodesulfurization, Bioprocess design, Dispersion, Droplet size, Hydrogen, Mass transfer, Sulfate reduction

INTRODUCTION

Biotechnological processes where hydrophobic substrates and products are involved are challenging. Mostly, the water immiscible organic solvent is dispersed in the continuous aqueous phase where whole cells are cultivated (Van Sonsbeek *et al.*, 1993; Woodley and Lilly, 1990; Van den Meer *et al.*, 1986; Wubbolts *et al.*, 1994). Nevertheless, several

alternative bioprocess concepts such as immobilized cell and membrane bioreactors are also reported in literature. In these cases, the absence of direct contact between the aqueous and organic phase offers advantages in downstream processing because no emulsion formation occurs. However, mass transfer limitations do represent a major problem (Kawakami *et al.*, 1990, 1992; Brink and Tramper, 1986a, b; Doig *et al.*, 1998, 1999).

When apart from hydrophobic compounds also gaseous compounds are involved in the bioconversion, a more complex gas-water-hydrocarbon system needs to be considered. This situation is typical for the anaerobic biodesulfurization of dibenzothiophenes and analogs thereof (Chapter 3; Kim *et al.*, 1995). In this novel bioprocess dibenzothiophenes are converted to hydrogen sulfide and the remaining hydrocarbon as outlined in Fig. 1.
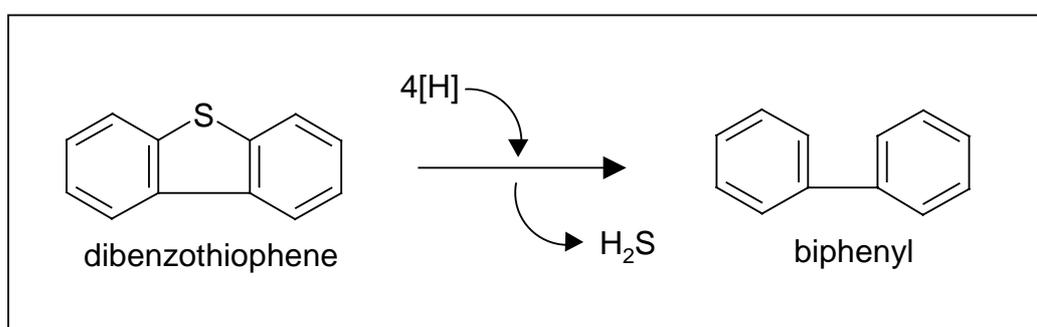

Fig. 1. Anaerobic conversion of dibenzothiophene to biphenyl and sulfide.

Looking at the design of this process, a high specific surface area of the hydrocarbon phase is a prerequisite as the solubility of dibenzothiophenes in the aqueous phase is negligible (Shennan, 1996). The anaerobic bacteria thrive in the aqueous phase, consequently conversion reactions are supposed to occur at the interface of the hydrocarbon and aqueous phase (see Chapter 2). Hydrogen gas is an suitable electron donor for anaerobic bioprocesses, especially on a relatively large scale (Van Houten *et al.*, 1994). However, preliminary laboratory tests showed that direct addition of H_2 gas to a dispersion of *n*-dodecane in water is not feasible because of severe foaming problems. When foaming occurs, the concept of a high specific surface area of the hydrocarbon phase is disturbed and a non-robust system with respect to H_2 mass transfer and biomass wash out is created. Therefore, an alternative approach was chosen resulting in a supply of dissolved H_2 gas to the bacteria via the hydrocarbon phase. The hydrocarbon phase is saturated with H_2 gas before the dispersion is formed in the bioreactor. Thus, the

hydrocarbon phase is applied as a carrier phase for H_2 in addition to the role of solvent for dibenzothiophenes.

In this Chapter, we determined the feasibility of this set-up using a real three-phase bioreactor system with hydrogenotrophic sulfate reducing bacteria (SRB) to impose a driving force for mass transfer. Microbiological aspects of the anaerobic conversion of dibenzothiophenes are hardly investigated (Armstrong *et al.*, 1997; Kim *et al.*, 1995). However, previous research pointed out that dibenzothiophene can be converted specifically to biphenyl, but growth proceeded slowly and cultivation is not straightforward (Chapter 3). To avoid cultivation problems while determining the H_2 mass transfer, hydrogenotrophic SRB were used in our investigations. Moreover, the mass transfer coefficient (k_{dw} at 30°C) determined in previous work was verified (Chapter 4). The extra determination of k_{dw} using SRB was performed because the non-biological experiments were carried out with tritium hydride (H-T) instead of hydrogen. Furthermore, this approach resembles the practical situation because SRB are involved that consume H_2, which is comparable to conditions in the anaerobic biodesulfurization process.

In our previous work we found that the specific surface area for H_2 mass transfer must be sufficiently large to overcome the lower flux in a *n*-dodecane/water system compared to a gas/water system, *i.e.* 0.16 x 10^{-6} and 3.9 x 10^{-6} mol/m^{2}s, respectively (Chapter 4). To create a high specific surface area of the *n*-dodecane phase a high pressure nozzle was applied. The main advantage of a nozzle is the possibility to create very fine droplets, while the mixing energy is only imparted on the hydrocarbon phase and not on the whole liquid phase like in a stirred system (Kaufman *et al.*, 1998). Besides the droplet size, the specific surface area is also dependent on the hold-up of the organic phase.

A second objective of this study is to obtain an initial insight into the behavior of the *n*-dodecane in water dispersion by carrying out two different experiments. At first, the H_2 availability for bacteria when *n*-dodecane is dispersed and applied as a carrier phase is investigated by performing batch tests using hydrogenotrophic SRB. The SRB are present as free cells and the question arises which effects on the biomass-organic phase contact occur during operation. Secondly, the dispersion behavior, *i.e.* droplet size distribution, hold-up of the organic phase and the stability, is determined in the absence of biomass at a range of different salt concentrations. These data can be used to estimate the specific surface area available for H_2 mass transfer. Finally, the H_2 mass transfer rate in a

dispersion system is estimated and compared to the H_2 mass transfer rate obtained in gas lift bioreactors.

MATERIAL AND METHODS

Determination of k_{dw}

In this work *n*-dodecane is used as a hydrocarbon phase because of its similar physical properties compared to diesel fuel distillates (boiling point 215˚C and a viscosity of 1.27 mPas at 30˚C).

A determination of the $k_{dw} \cdot a$-value in a dispersion system implies that the droplet size distribution and the hold-up of the organic phase must be exactly known and that these parameters remain constant in time. To avoid uncertainties caused by these parameters in the experiments to determine k_{dw}, a non-mixed three-phase system with a defined specific surface area for H_2 mass transfer was used. The *n*-dodecane floats on the aqueous phase providing a constant surface for H_2 mass transfer from the H_2 headspace to the aqueous phase via the intermediate *n*-dodecane phase.

In the k_{dw} verification experiments a steady state method is applied as described by Van Sonsbeek *et al.* (1991). The concentration of H_2 in *n*-dodecane (c_d) cannot be measured directly with a probe and must be calculated from the steady state mass balance describing the H_2 mass transfer process. At steady state, the net H_2 transport from gas to *n*-dodecane equals the transport from *n*-dodecane to the aqueous phase containing the SRB that consume the H_2. Sulfate is reduced by hydrogenotrophic SRB according to Eq. 1 ($H_2S_{(aq)}$ + $HS^-_{(aq)}$; 1:1 at pH of 7).

$$2SO_4^{2-} + 8H_2 \rightarrow H_2S + HS^- + 5H_2O + 3OH^- \qquad (1)$$

The steady state sulfate consumption is measured to enable the calculation of the overall mass transfer coefficient (k_{dw}), according to the following mass balance, which is valid at steady state (Chapter 4):

$$R_H = k_{gd} \left(c_d^* - c_d \right) \cdot A = k_{dw} \cdot \left(c_d - m_{dw} \cdot c_w \right) \cdot A = 4 \cdot R_S \qquad \text{(mol/s)} \qquad (2)$$

Where: R_s is the rate of sulfate consumption (mol/s) that equals 1/4 of the rate of H_2 consumption (R_H), according to Eq.1; k_{gd} is the overall mass transfer coefficient from gas to *n*-dodecane (m/s); m_{dw} is the partition coefficient between *n*-dodecane and water (m^3_w/m^3_d); c_a^* is the equilibrium H_2 concentration (mol/m³); A is the specific surface area

(m^{-1}); c_d and c_w are the bulk H_2 concentrations in the *n*-dodecane and water phases (mol/m^3), respectively. It is assumed that SRB will consume H_2 instantaneously, because at steady state the system operates under H_2 limiting conditions. Therefore, c_w is assumed to be zero and Eq. 2 can be simplified to:

$$k_{gd}\left(c_d^* - c_d\right) \cdot A = k_{dw} \cdot c_d \cdot A = 4 \cdot R_S \qquad (3)$$

The 3rd term of Eq. 3 is determined by measuring the inlet and outlet SO_4^{2-} concentrations. Then c_d can be calculated using the 1st term of Eq. 3 and the known k_{gd} and c_d^* values. The value of c_d^* is calculated according to:

$$c_d^* = \frac{c_g}{m_{gd}} = \frac{P/RT}{m_{gd}} \qquad (4)$$

Where: P is the pressure of the headspace (Pa) and m_{gd} is the partition coefficient between gas and *n*-dodecane (m^3_d/m^3_g). The ideal gas law is used for the calculation of the H_2 concentration in the headspace (c_g) and the vapor pressure of *n*-dodecane is neglected. If the headspace is not pure H_2, the pressure must be corrected by considering the H_2 partial pressure ($p_{H_2} = y_{H_2} \cdot P$).

Finally, the value for k_{dw} can be calculated using the 2nd and 3rd term of Eq. 3. By stepwise increasing the sulfate loading rate (SLR), the maximum amount of H_2 that can be transferred to the aqueous phase is assessed. At this point, the H_2 transfer rate becomes the process limiting step, provided that no biomass limitation or sulfide toxicity is present. When the SLR was increased also the SO_4^{2-} concentration in the bioreactor was spiked to the same level as the influent SO_4^{2-} concentration to prevent a SO_4^{2-} concentration gradient in the bioreactor. Above the maximal attainable H_2 mass transfer rate, the sulfate reduction rate (SRR) will not increase any further and SO_4^{2-} reduction becomes incomplete. When H_2 limitation occurs the steady state situation is reached and Eq. 3 is valid. This experiment was carried out in triplicate. In the third experiment a constant SLR above the maximal attainable SLR was applied to verify the maximal SRR again.

A schematic representation of the configuration used to determine the k_{dw}-value is depicted in Fig. 2.
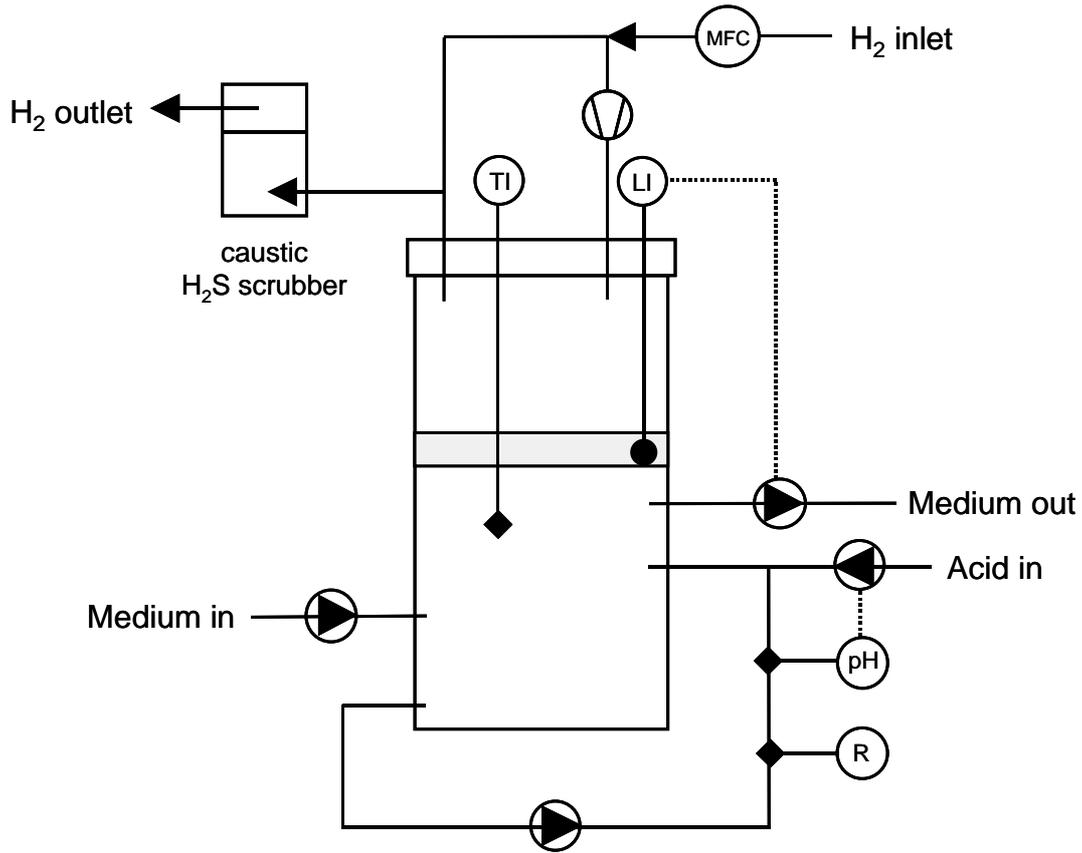
Fig. 2. Schematic representation of the experimental set-up used to verify the k_{dw}-value. Key: LI = level indicator, MFC = mass flow controller, pH = pH electrode, R = redox electrode, TI = temperature indicator.

Medium was pumped continuously into the bioreactor. The HRT was set at 55 h, because at lower HRT values no complete sulfate reduction was found, due to the limiting conditions of acetate (1 mM) and bicarbonate (1 mM). A level indicator to maintain an exact volume of the aqueous phase (1.74 L) controlled the effluent pump. The volume of the *n*-dodecane phase floating on top of the aqueous phase was 0.2 L (Fig. 2). To ensure the homogeneity of the aqueous phase a mixing loop (flow of 50 L/h) was incorporated. The loop also contained the pH and redox potential sensors, while HCl was added to the loop to control the pH. The gas phase was recycled with a compressor (Verder, type PM8536) at a flow rate of 360 L/h. A mass flow controller (MFC, Brooks 5850S) was applied to control the influent H_2 gas flow at 0.6 L/h. The off gas was scrubbed using a 5% (w/w) NaOH solution to enable measurement of the sulfide removal with the off-gas.

The growth medium contained (mM): $Na_2HPO_4 \cdot 2H_2O$ (3); KH_2PO_4 (3); NH_4Cl (5.6); $MgCl_2 \cdot 6H_2O$ (0.59); NaCl (5.13); $CaCl_2 \cdot 6H_2O$ (0.5) as the macronutrients. Trace elements and vitamins were added according to Stams *et al.* (1993). The pH was maintained at 7.3 ± 0.1, while the medium was not buffered. Acetate and bicarbonate were added in limiting amounts (1 mM) as the carbon and energy source. Pure H_2 was supplied as electron donor, while sulfate was added as electron acceptor.

The hydrogenotrophic sulfate reducing biomass used throughout the experiments was obtained from Romashkinskoe oil field (Russia) and cultivated by serial dilution under the conditions mentioned above (Chapter 3). The resulting sulfate reducing enrichment was used as the inoculum for the initial reactor experiment.

Sulfate reduction in a batch wise operated dispersion reactor

To study the feasibility of using *n*-dodecane as a carrier phase for H_2 transfer the sulfate reducing capacity was determined in a batch wise operated dispersion reactor. A nozzle (Spraybest, Pinjet 10) was applied to create small *n*-dodecane droplets in the aqueous phase. The *n*-dodecane was saturated with H_2 prior to injection in the bioreactor. A schematic drawing of the system is presented in Fig. 3. Batch tests were performed with 1.3 L biomass suspension supplemented with 0.2 L fresh medium giving identical medium conditions as described above. The biomass used in the batch tests was obtained from a continuously operated fermentor (Applikon) using a similar set-up as depicted in Fig. 2, with the modification that H_2 was sparged continuously at a flow of 0.02 L/min. The sulfate reducing biomass appeared to have a specific conversion capacity of 0.07 mmol SO_4^{2-}/(L·day·mg biomass) at a HRT of 55 h and a SLR of 10.2 mmol/L·day.

A total of 1.5 L *n*-dodecane was present in the system: 0.5 L on top of the aqueous phase in the bioreactor and 1 L in the H_2 saturation vessel. The *n*-dodecane was saturated with a constant H_2 flow of 6 L/h using a MFC, while mixing at 600 rpm. The H_2S present in the *n*-dodecane was removed via the off gas. After saturation the *n*-dodecane was injected in the bioreactor. The pressure drop over the nozzle was 19 bar. Coalescenced *n*-dodecane was pumped to the saturation vessel controlled by a level sensor, maintaining constant volumes in time (Fig. 3).
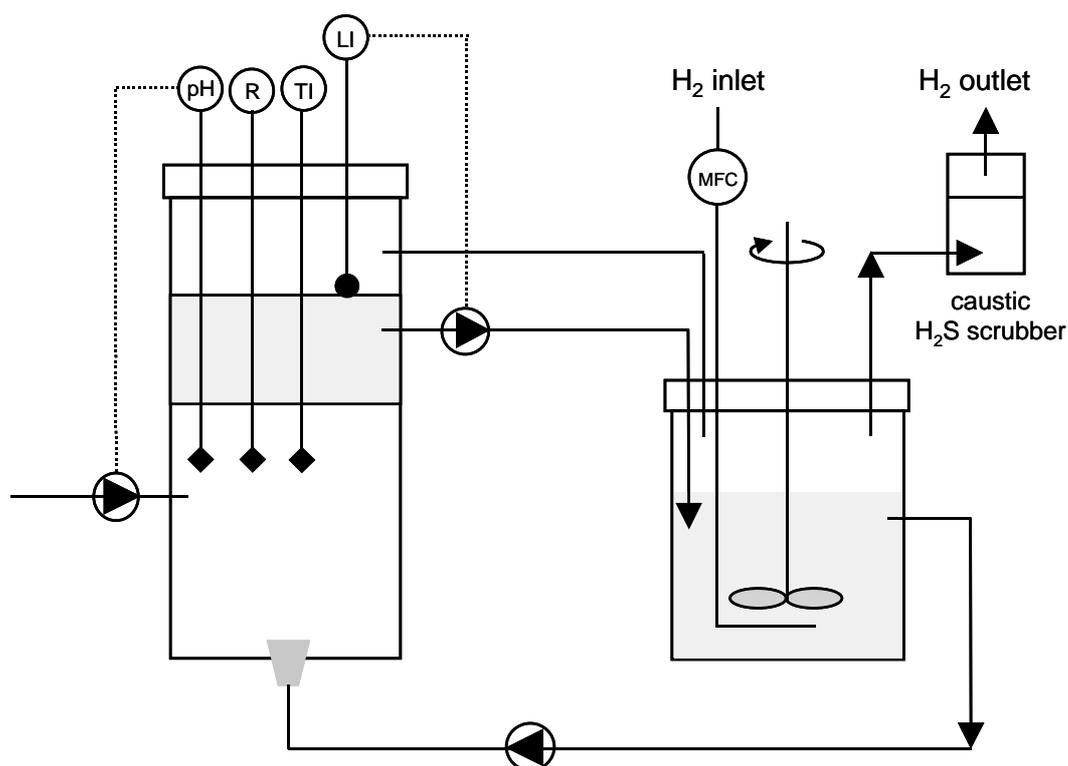
Fig. 3: Schematic representation of the experimental set-up of the bioreactor. Key: LI = level indicator, MFC = mass flow controller, pH = pH electrode, R = redox electrode, TI = temperature indicator.

Three batch experiments were performed with an initial SO_4^{2-} concentration of approximately 5 mM. The SO_4^{2-} depletion was followed in time and the experiments were stopped after 1, 3 and 4 h of operation. After each experiment the biomass concentration was determined. We observed that during the course of the experiments biomass flotated to the upper *n*-dodecane phase. In order to quantify the loss of biomass, two additional experiments were carried out that were stopped after 2 and 6 h of operation.

Analytical methods bioreactor experiments

The total sulfide concentration was measured using a colorimetric method based on the formation of methylene blue (Dr Lange kit LCW053, Germany), which is a modified procedure of the method described by Trüper and Schlegel (1964). Centrifuged samples were diluted to an end-concentration between 0.5 up to 1.5 mg/L and measured at $\lambda = 666$ nm (Cadas30 spectrophotometer).

The sulfate concentrations in samples were determined using a (Waters) HPLC, equipped with an IC-Pak anion column (50 mm x 4.6 mm x 10 µm). The mobile phase contained 35 mL concentrate (containing: 9.1 g Na-gluconate, 25.5 g H_3BO_3, 4.4 g $LiOH \cdot H_2O$, 90 ml glycerol per L milli-Q-water) and 120 mL acetonitril per liter milli-Q-water. A flow rate of 1.2 mL/min was applied. The injection volume was 10 µL (Waters 717 autosampler), sulfate was quantified by a conductivity detector (Waters 431). Samples were diluted in 30 mM mannitol to an end-concentration of approximately 100 mg/l total sulfate.

Acetate concentrations were determined using a HP 5890 gas chromatograph (GC) equipped with a flame ionization detector and an Alltech AT-wax (30 m x 0.25 mm x 0.5 µm) column. Samples were prepared by adding 0.1 ml 85% w/w formic acid to 1.6 mL centrifuged sample. The column temperature was programmed from 60°C (held 5 min) with an increasing rate of 20°C/min up to 210°C (hold 5 min). The injector and FID temperature were 280 and 300°C, respectively. The flow of the helium carrier gas was 0.8 mL/min. The biogas composition was measured using the GC methods previously described by Van Houten *et al.* (1994). The biomass concentration was derived from the Kjeldahl-nitrogen corrected for ammonium present in the growth medium, according to the general formula ($CH_{1.8}O_{0.5}N_{0.2}S_{0.02}P_{0.01}$) for biomass composition (Roels, 1983).

Chemicals

All chemicals used were of the highest grade commercially available.

Determination of the specific surface area and dispersion characterization

The specific surface area available for H_2 transfer determines the mass transfer rate to a great extent. This parameter is estimated by measuring the droplet sizes. The Sauter mean diameter (d_{32}) represents the volume surface mean droplet diameter and is defined as the droplet diameter of a monodisperse dispersion. Ideally, this theoretical dispersion has the

same interfacial area per liquid volume as the actual dispersion sample. The d_{32} value obtained can be used to calculate the specific surface area (*a*) according to:

$$a = \frac{6\varepsilon}{d_{32}} \tag{5}$$

The organic phase hold-up (ε) is defined as the ratio of the *n*-dodecane volume to the total liquid volume. A simplified system without biomass was used to investigate the behavior of the emulsion. A reactor (as depicted in Fig. 2 without saturation vessel) was filled with 1.55 L demineralized water, 1 L *n*-dodecane and supplemented with salt. A range of concentrations was prepared using Na_2SO_4 or $NaCl$. The whole system was maintained at 30°C. The flow over the nozzle was varied by applying different pressure drops over de nozzle; *i.e.* 19, 22 and 24 bar. Samples to determine the organic phase hold-up (ε) were taken during steady state, *i.e.* when the volume of *n*-dodecane on top of the dispersion remained constant in time. Samples were taken by using gravity, tubing with an internal diameter of 4 mm was used to minimize the disturbance of the droplet size distributions by shear. Volume based droplet size distributions were measured in triplicate using a laser diffraction method with a Beckman Coulter LS 230. The Sauter mean diameters (d_{32}) were calculated from the volume based droplet size distributions.

The stability of the dispersion was characterized by allowing dispersion samples to separate under gravity. The backscattering of the dispersion sample during the gravity settling was followed using a Turbiscan MA6000 device. For this, 6 mL of sample was transferred to a tube and subjected to analysis one minute after the sample was withdrawn from the reactor. Every minute the dispersion sample was scanned from the bottom to the top of the liquid phase in the tube. During the scan along the tube, data was acquired every 40 µm and the backscattered light was detected under an angle of 135° at $\lambda = 850$ nm.

RESULTS AND DISCUSSION

Determination of k_{dw}

The value of the overall mass transfer coefficient (k_{dw}) is verified in a three-phase bioprocess, containing hydrogenotrophic SRB. The results obtained in run 2 are shown in Fig. 4. The system was operated continuously at a HRT of 55h. When the sulfate reduction rate (SRR) equated the sulfate loading rate (SLR), it was increased stepwise, *viz.* from 0.66 to 0.98 and from 0.98 to 1.31 mmol/L·day, respectively (Fig. 4). The dotted line plotted in Fig. 4 is the predicted maximum SRR using the average k_{dw}-value (4.98 x 10^{-6} m·s^{-1}) obtained from the previous experiments using tritium hydride.
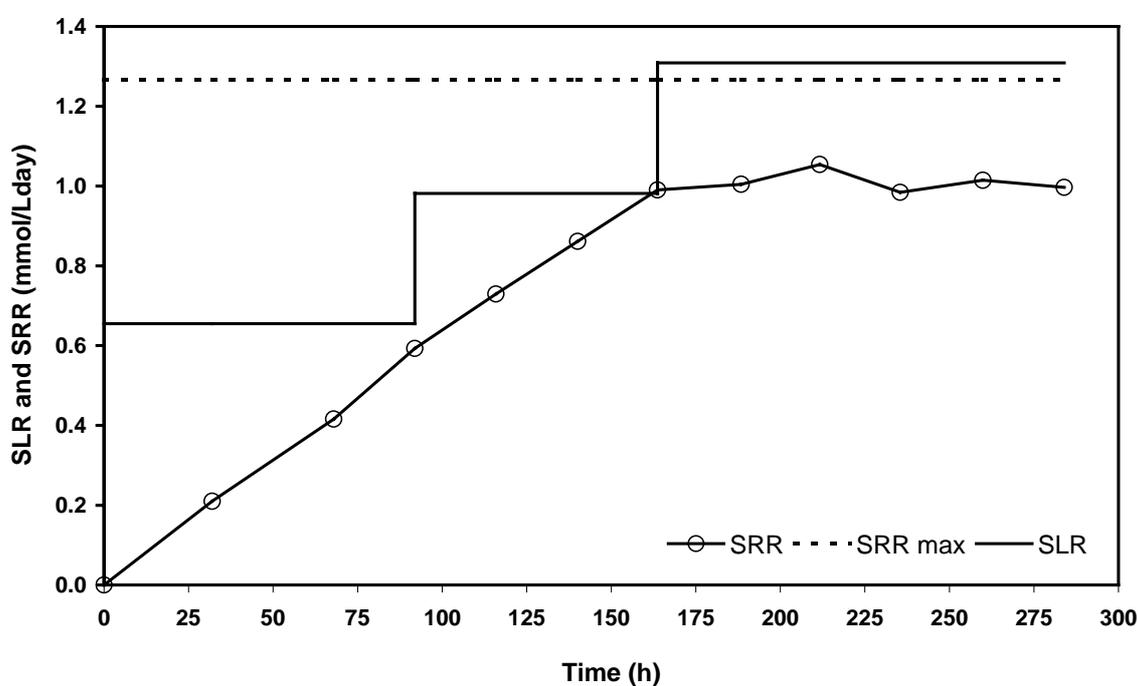

Fig. 4: Profile of SLR and SRR versus time in the hydrogenotrophic sulfate reducing bioreactor during run 2.

As can be seen from Fig. 4 the SRR reaches a plateau value of about 1 mmol/L·day. The SRR cannot increase further, because the H_2 transfer rate becomes the process limiting factor. From 164 h onwards, Eq. 4 was used to calculate k_{dw}-values at the established steady state. Three independent experiments were performed leading to almost identical steady state SRR values and consequently k_{dw}-values, as presented in Table 1. The second biological run had a similar SLR profile and SRR trend as run 1 (results not shown). Run 3 was performed at a constant SLR throughout the experiment, *viz.* 1.27 mmol/L·day, corresponding to the dotted line in Fig. 4.

Table 1: Overview of the k_{dw}-values found in physical and biological experiments.

| Experiment type	SRR (mmol/L·day)	k_{dw} (x 10^{-6} m·s^{-1})
Abiotic 1*	-	5.15 ± 0.61
Abiotic 2*	-	4.82 ± 0.45
Biological, run 1	1.01	4.03 ± 0.24
Biological, run 2	1.04	3.97 ± 0.24
Biological, run 3	1.03	4.04 ± 0.24

*using tritium hydride (Chapter 4).

From the results depicted in Table 1, it can be concluded that the k_{dw}-values found are in good agreement with the values determined in previous abiotic experiments. The results obtained indicate that tritium hydride can be used as an appropriate model compound to measure H_2 diffusion because it has comparable diffusion characteristics as hydrogen (Chapter 4).

There is no indication that inhibition on hydrogenotrophic sulfate reduction due to sulfide toxicity played a significant role and in this way would affect the steady state SRR. The total sulfide concentration (H_2S + HS^-)$_{aq}$ found during the steady state of run 2 was 1.2 ± 0.1 mM. This level remained well below the toxicity values reported by O'Flaherty *et al.* (1998). They found that the chemolithotrophic activity with sulfate decreased 50% at total sulfide levels of 22 up to 26 mM (for a pH of 7.2). Van Houten *et al.* (1994) reported that growth of hydrogenotrophic SRB is still possible at free H_2S levels of 13.2 mM.

A parameter sensitivity analysis showed that R_s impinges the largest influence on the calculation of k_{dw} via the sulfate measurements (see Eq. 3). A deviation of 0.24 x 10^{-6} m·s^{-1} was found when the 95% confidence level for the sulfate measurements was taken into account (Table 1). A change of +/- 5% in k_{gd} resulted in a minor influence (<1 %) on the outcome of the k_{dw} calculation. During the experiments the H_2 concentration in the headspace (see Eq. 4) was measured to be at least 99% pure. A variation of +/- 1%, results in a deviation of 4.7 x 10^{-8} m·s^{-1}, which is negligible. The temperature and specific surface area were considered as constant values for the system.

The sulfidogenic biomass that developed in the bioreactor utilizes H_2 as the electron donor. A relevant aspect of using a mixed culture is the possible occurrence of competition for H_2 by different species present in the biomass. Apart from SRB also methanogenic

archaea (MA) and homo-acetogenic bacteria (HAB) are able to consume H_2, according to the following equations:

$$4H_2 + HCO_3^- + H^+ \rightarrow CH_4 + 3H_2O \quad (MA) \tag{6}$$

$$4H_2 + 2HCO_3^- + H^+ \rightarrow CH_3COO^- + 4H_2O \quad (HAB) \tag{7}$$
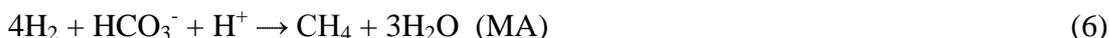
This means that when apart from sulfate reduction H_2 consumption according to reaction 6 or 7 occurs, the k_{dw}-value will be underestimated because the calculations are only based on sulfate depletion with H_2 (see Eq. 4). Three independent k_{dw} verification experiments revealed identical steady state SRR values (Table 1). This would not have been possible if hydrogenotrophic SRB had no competitive advantage. Furthermore, a limiting bicarbonate concentration (1 mM) hampered the activity of MB and HAB. In Fig. 5 the results of the sulfide mass balance are depicted, which were obtained during the steady state of run 2 (see Fig. 4 and Table 1).
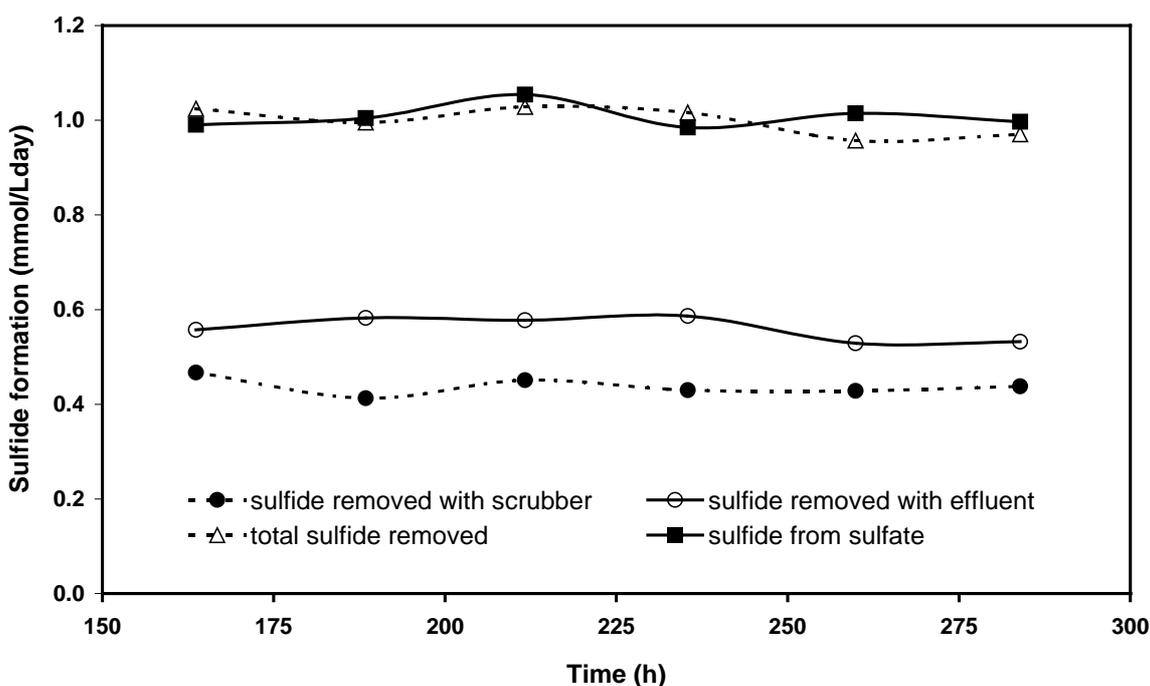

Fig. 5: Sulfide balance obtained during the steady state from run 2.

As can be seen from Fig. 5 the sum of the sulfide removed with the effluent ($HS^- + H_2S)_{aq}$ and via the off gas (H_2S captured as S^{2-} in the scrubber) corresponds perfectly well with the total amount of sulfide expected on the basis of sulfate conversion. The revealed exact stoichiometry (Fig. 5) supports the assumption that H_2 was only used for sulfate reduction. This is also in line with the fact that hydrogenotrophic sulfate reduction predominates over

methanogenes, because of the more favorable reaction kinetics and thermodynamics (Oude Elferink *et al.*, 1994).

As in this continuous set-up (Fig. 2) methane production was difficult to assess, complementary batch tests were carried out under the same experimental conditions (medium, pH, T). No methane production was observed, while an exact SO_4^{2-}/S^{2-} stoichiometry according to Eq. 1 was found (data not shown).

Therefore, it can be concluded that methanogenic activity was not present in the hydrogenotropic sulfate reducing biomass that was used. From a thermodynamic point of view acetotrophic sulfate reduction could occur (Oude Elferink *et al.*, 1998; Widdel, 1988). However, reported growth rates of acetotrophic SRB are low, indicating that it is unlikely that acetotrophic sulfate reduction does occur.

For run 2 and 3 the time course of the acetate concentration in the influent and effluent was followed. It was found that the acetate consumption in both experiments amounted to 0.15 mmol/L·day during steady state H_2 consumption. To elucidate any biological activity of HAB, the concentrations of the carbon sources were changed in run 3. To stimulate growth of HAB, the influent bicarbonate concentration was increased to 5 mM, while the acetate concentration was lowered to 0.6 mM at t = 189 h. The profile of acetate concentrations in the influent and effluent is presented in Fig. 6.
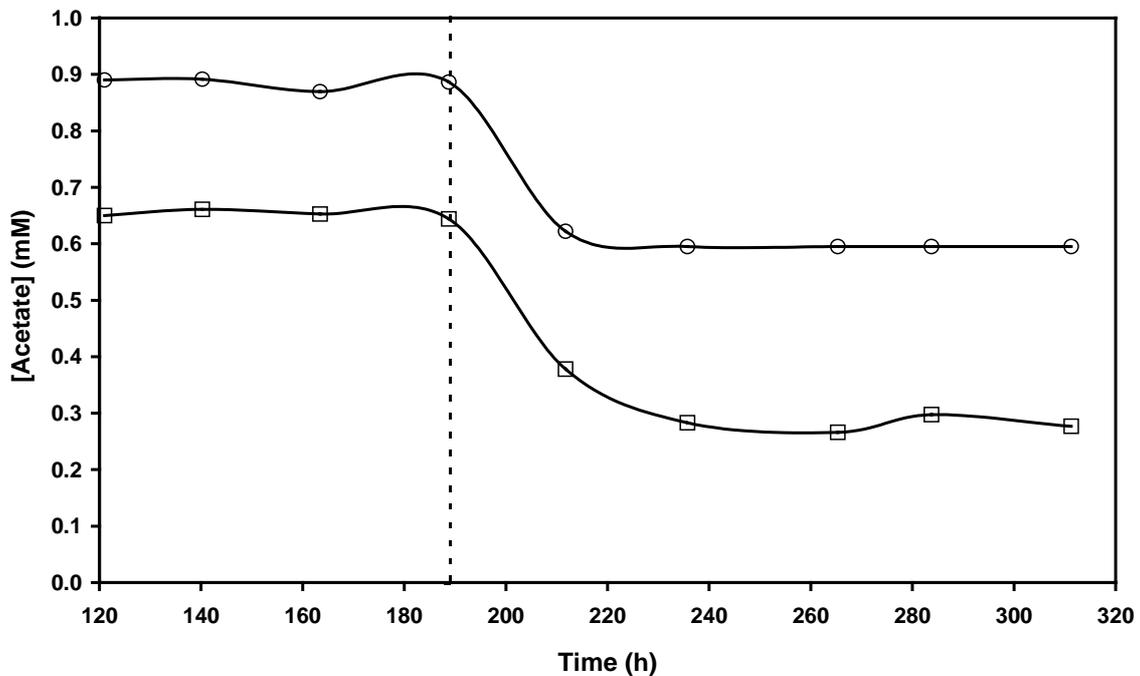

Fig. 6: Response of the acetate effluent concentration (□) upon a decrease in the influent acetate concentration (○) at t=189 h during run 3.

From the results depicted in Fig. 6, it can be inferred that a decrease in the influent acetate is accompanied by a corresponding decrease in the acetate effluent concentration. If HAB were active in this system it would not be likely that such a response would occur; an increased acetate concentration could have been expected. In run 3 a steady state H_2 consumption was achieved from 235 h onwards.

Based on the aforementioned results, it is postulated that acetate is used solely by H_2 utilizing SRB for biomass synthesis. This confirms the results by Van Houten *et al.* (1994), who demonstrated that hydrogenotrophic SRB use acetate and bicarbonate as carbon sources.

In the calculations the relation $R_H = 4R_S$ was applied (see Eq. 2). However, a small part of the electrons is used for the synthesis of biomass instead of sulfate reduction. This amount can be estimated by using the yield obtained in the continuously operated fermentor system (HRT 55 h). The steady state biomass concentration of 144 mg and SLR of 10.2 mmol/L·day gives a yield of 6.2 g cells/mol SO_4^{2-}. This yield value is in the same order of magnitude as values reported for hydrogenotrophic *Desulfovibrio* species (Robinson and Tiedje, 1984; Brandis and Thauer, 1981). Assuming that acetate, CO_2 and NH_3 are required for biomass synthesis; Eq. 8 can be applied to estimate the H_2 use (Roels, 1983).

$$C_2H_4O_2 + 2CO_2 + NH_3 + 4.5\ H_2 \rightarrow\ <C_4H_8O_2N> + 4H_2O \qquad (8)$$

Using a value of 102 g/mol biomass and the estimated yield, it can be calculated that approximately $(6.2/102) \times 4.5$ mol $H_2 = 0.27$ mol H_2 is necessary for biomass synthesis. Consequently, the estimated stoichiometry is: $R_H = 4.27 \cdot R_S$ that results in a deviation of 6%. Using the adjusted stoichiometry k_{dw}-values of: 4.3×10^{-6}, 4.24×10^{-6} and 4.31×10^{-6} m·s^{-1} can be calculated for run 1, run 2 and run 3, respectively. The values obtained are close to the values depicted in Table 1.

Performance of SRB in a *n*-dodecane/water dispersion using H_2 as the electron donor
The H_2 mass transfer was further investigated by following the sulfate reduction rate in batch when H_2 saturated *n*-dodecane was dispersed using a nozzle (see Fig. 3). In Fig. 7A the three sulfate depletion curves obtained are presented. Fig. 7B provides the results of the biomass measurements performed at the end of each experiment to reveal the flotation of SRB during the batch experiments.
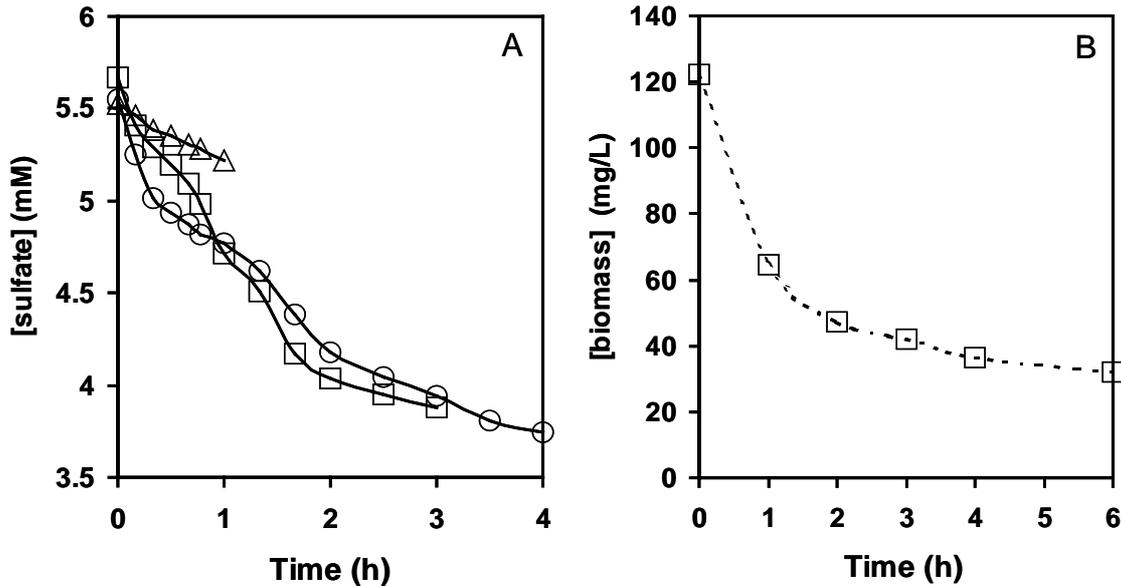
Fig. 7A: Observed sulfate depletion during batch experiments that were stopped after 1 (△), 3 (□) or 4 (○) hours of operation, using the experimental configuration depicted in Fig. 2. Fig. 7B: Amount of biomass (□) that was measured initially or after 1, 2, 3, 4 or 6 h of operation, the dashed line provides the trend of biomass flotation.

From the experimental results presented in Fig. 7A it can be concluded that *n*-dodecane can be used effectively as carrier phase for H$_2$ transfer. The specific activity during the 3 hours incubation (□ in Fig. 7A) was 0.25 mmol SO$_4^{2-}$/ L·day·mg biomass in the first hour and decreases to 0.083 mmol SO$_4^{2-}$/L·day·mg biomass during the last hour of the incubation. For the calculation the average biomass concentration is used assuming a linear decrease in biomass concentration in the first and last hour of the incubation. This results in 93 and 44.5 mg biomass/L, respectively (see Fig. 7B). Moreover, it is assumed that biomass growth during the short batch period can be neglected. Both calculated values exceed the performance of the initial cell suspension that had a specific activity of 0.07 mmol SO$_4^{2-}$/(L·day·mg biomass). It must be noticed here that the biomass concentration is a difficult parameter to determine in this system. From the trend depicted in Fig. 7B it is clear that the biomass concentration decreases in time, because the addition of H$_2$ saturated *n*-dodecane causes flotation of the biomass. During the batch experiments a large part of the biomass accumulates just under and in the lower part of the *n*-dodecane phase, but no emulsification occurred. During the first hour of operation 47% of the biomass concentration was removed due to flotation while after 6 hours 74% of the initial amount was flotated. It is obvious that this is an undesirable situation because the biocatalyst

disappeared and less biomass is present in the zone were the *n*-dodecane is injected causing a lower sulfate reducing capacity (Fig. 7A).

Determination of hold-up and dispersion stability

Hydrocarbon droplets in dispersion are negatively charged (Lyklema, 2002). This might affect the amount of *n*-dodecane that can be dispersed in the aqueous phase, because cations are present and electrostatic effects occur. Since many biosystems are buffered with $NaHCO_3$, we analysed the effect of increasing Na^+ concentrations on the hold-up of the *n*-dodecane phase. As depicted in Fig. 8A, the hold-up of *n*-dodecane (ε) is clearly dependent on the Na^+ concentration that is supplied as Na_2SO_4 or NaCl.
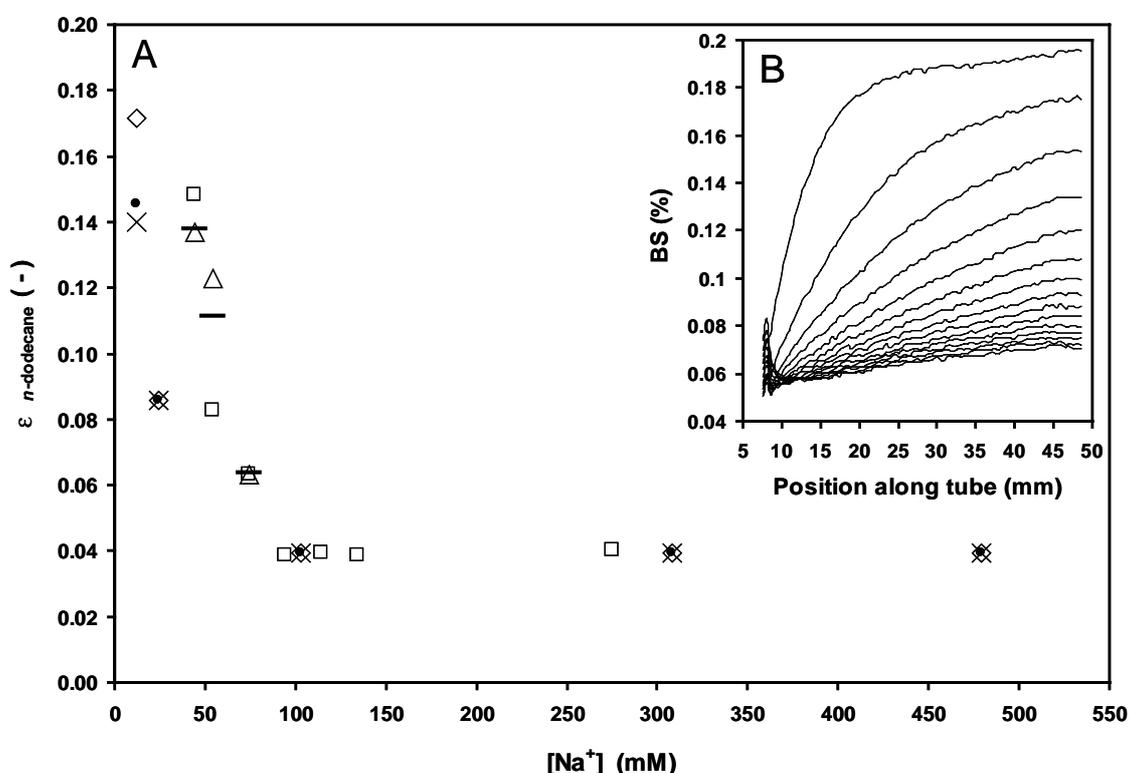

Fig 8A: Hold-up (ε) of *n*-dodecane at different [Na^+] and pressure drops over the nozzle: (x) NaCl, ΔP of 19 bar; (●) NaCl, ΔP of 22 bar; (◇) NaCl, ΔP of 24 bar; (□) Na_2SO_4, ΔP of 19 bar; (-) Na_2SO_4, ΔP of 22 bar; (△) Na_2SO_4, ΔP of 24 bar. Fig. 8B: Profile generated during the turbiscan, vs. backscattering time for a dispersion sample containing 45 mM Na^+.

For every pressure drop (ΔP) over the nozzle (19, 22 or 24 bar), ε decreases from approximately 0.14 to 0.04 at an increase in the Na^+ concentration from 12 up to 94 mM (Fig. 8A). Generally, the increased pressure drop over the nozzle had no measurable effect

on the hold-up. Above 94 mM, ε stabilizes around a value of 0.04. The trend observed in Fig. 8A can be explained by coagulation of *n*-dodecane droplets due to the presence of Na$^+$-ions (Hiemenz and Rajagopalan, 1997). The coagulation promotes coalescence because the destabilization of a dispersion is considered as a combined process of droplet coagulation and coalescence (Dukhin *et al.*, 2001). The Na$^+$-ions effectively relieve the repulsion between the negatively charged *n*-dodecane droplets, according to the DLVO theory (Overbeek, 1969). Apparently, Na$^+$ concentrations higher than 94 mM do not contribute anymore to this effect. Furthermore, the type of cation will influence the rate of coagulation, because bivalent cations are more effective in screening the negative surface charges. It was observed that in the absence of salt no steady state *n*-dodecane layer is formed and all the *n*-dodecane was dispersed. This means that in the absence of salt, disruptive forces predominate and coagulation followed by coalescence is a minor process. The dispersion stability was assessed by following the separation under gravity of a dispersion sample taken during steady state in the hold-up. In Fig. 8B a backscattering profile of a dispersion sample containing 45 mM Na$^+$ is presented. During the sampling the system operated at a pressure drop (ΔP) of 22 bar over the nozzle leading to a hold-up of 0.137 in the presence of 22.5 mM Na$_2$SO$_4$ (Fig. 8A). The profile was generated by following the backscattering along the sample tube, every minute a new profile was measured. As can be inferred from Fig. 8B the dispersion separates very rapidly when the disruptive forces are absent and no *n*-dodecane is added to the dispersion. When the amount of dispersed *n*-dodecane was constant in time, the same level of backscattering could be expected along the height of the tube and also the backscattering would be constant in time. However, from Fig. 8B it is clear that the dynamic pattern changes very rapidly, the backscattering increases along the position in the tube indicating that the *n*-dodecane migrates from the bottom to the top of the tube. This effect decreases in time, after 9 minutes almost complete separation was observed (*n*-dodecane content < 2%). For the dispersion sample containing 55 mM Na$^+$ complete separation was observed after only 4 minutes. Here, the system operated at a ΔP of 22 bar generating a hold-up of 0.11 in the presence of 110 mM Na$_2$SO$_4$ (Fig. 8A).

The results indicate a considerable effect of Na$^+$ ions on the separation rate in the interval of 45 up to 55 mM Na$^+$. This effect can also be observed from Fig 8A. No suitable backscattering profiles could be measured at a Na$^+$ concentration above 55 mM, due to the rapid separation.

Droplet size determinations

For every data point depicted in Fig. 8A, volume-based droplet size density distributions were measured. Different pressure drop settings over the nozzle of 19, 22 or 24 bar, did not result in significant differences in volume-based droplet size density distributions. The d_{32}-values obtained were: 10.8 ± 1.3 µm, 9.9 ± 0.6 µm and 10.0 ± 0.9 µm for a ΔP of 19, 22 or 24 bar, respectively. Combining these d_{32}-values gives an overall d_{32}-value of 10.3 ± 0.9 µm. In the system used, no difference in the d_{32}-values were observed along the height of the dispersion. With respect to the d_{32}-values obtained it should be noted that for systems with larger volumes other hydrodynamic conditions are present. It can be expected that at a larger distance from the nozzle higher d_{32}-values are found due to increased coalescence.

The results show an insignificant influence of the presence of salts on the volume-based droplet size density distributions obtained. This is illustrated in Fig. 9A (next page) where three examples of measured volume-based droplet size density distributions are presented: *i.e.* for Na^+ concentrations of 55 mM or 480 mM and in the presence of mineral medium with SRB. In Fig. 9B the results of two calculated number-based droplet size density distributions are presented, which were calculated from the measured volume-based droplet size density distributions for Na^+ concentrations of 55 and 480 mM, respectively. For these calculations it was assumed that the *n*-dodecane droplets are completely spherical. From the results depicted in Fig. 9 it is clear that Na^+ ions up to concentrations of 500 mM have no major influence on the drop sizes measured. Apparently, Na^+ determines mainly the coagulation of *n*-dodecane and the effect on coalescence is minor.

The droplet size distributions depicted in Fig. 9A are bimodal. This can be explained by the coalescence of primary droplets (< 10 µm) formed by the nozzle, which occurs during the handling of the sample. From the comparison of Fig. 9A with Fig. 9B it follows that the amount of large drops (10 - 100 µm) is relatively small, but corresponds to a relatively large fraction of the total volume. In spite of the limited stability of the dispersion formed in the reactor, we regard the droplet diameters measured off-line as a reasonable representation of the actual mean droplet size distribution within the reactor. However, it should be noted that the d_{32}-value calculated represents a maximal value, because coalescence cannot be avoided completely during sample handling.
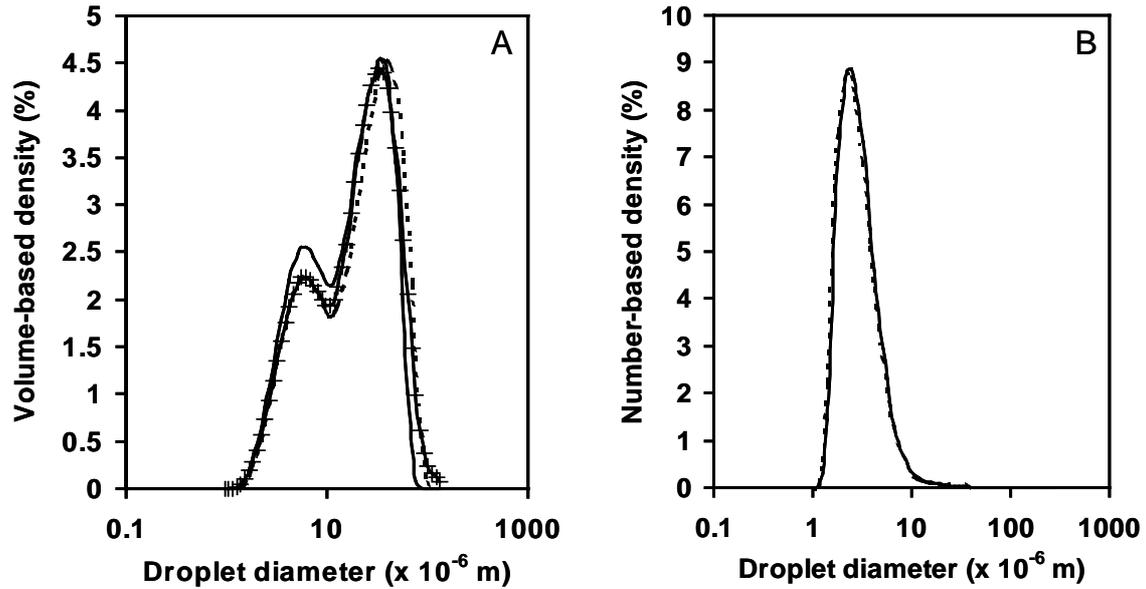
Fig. 9A: Measured volume-based droplet size density distributions: (Dashed line), $[Na^+]$ of 55 mM and ΔP of 19 bar; (Solid line), $[Na^+]$ of 480 mM and ΔP of 19 bar; (+++), sulfate reducing cell suspension with salts present according to the mineral medium and a ΔP of 19 bar. Fig. 9B: Number-based droplet size density distributions calculated from the measured volume-based droplet size density distributions, same key as Fig. 9A.

The presence of bacteria has no clear effect on the volume based droplet size distribution and the d_{32}-value (11.6 μm) compared to the situation where bacteria are absent (Fig. 9A). This result can be explained by the absence of any emulsifying compound produced by the sulfate reducing biomass. The sulfate reducing hydrogenotrophic biomass consisted of a vibrio type of SRB, which are generally gram-negative. It is known that gram-positive bacteria are capable of producing biosurfactant that results in fine emulsions. During the aerobic biodesulfurization of dibenzothiophene using *Rhodococcus erythropolis* cells, stable emulsions with droplet sizes of 2 up to 50 μm are generated in a stirred system (Borole *et al.*, 2002). This is attributed to the hydrophobic nature of the outer cell membrane of the gram-positive *R. erythropolis* cells. When however gram-negative *E. coli* cells were used, unstable dispersions were formed with droplet sizes in the range of 100 up to 1000 μm at the same hydrodynamic conditions (Borole *et al.*, 2002). This is in line with the effects observed in this work. Schmid *et al.* (1998) reported d_{32} values between 10-13 μm for *Pseudomonas oleovorans* biosurfactant stabilized decane/water emulsions in a stirred system, which is the same order of magnitude as described here.

Comparison of the H$_2$ mass transfer capacity in *n*-dodecane/water dispersion compared to a H$_2$-sparged gas lift system

To estimate the mass transfer capacity for H$_2$ (mol/m^3·s) in a bioreactor where H$_2$ is transferred using *n*-dodecane as a carrier phase, the H$_2$ flux at variable droplet sizes and volume fractions of *n*-dodecane was calculated. In the calculations a k_{dw}-value of 4 x 10^{-6} m·s^{-1} at 30°C was used, as was verified in this work. A range of values for the specific surface area was calculated, using d_{32} values from 4 up to 15 μm (see Eq. 4). The H$_2$ flux is compared to a gas lift system where H$_2$ is sparged directly in the aqueous phase, using a k_La value of 0.026 s^{-1} as reported by Van Houten *et al.* (1994) for a hydrogenotrophic sulfate reducing bioreactor. The volumetric H$_2$ flux (*J'*) can be calculated according to Eq. 9.

$$J' = ka\left(c^* - c_{bulk}\right) \qquad \text{(mol/m}^3\text{·s)} \qquad (9)$$

Where c^* denotes the H$_2$ solubility in the gas or *n*-dodecane phase for a gas lift or dispersion system, respectively. The concentration gradient was maximal by assuming a zero liquid bulk H$_2$ concentration, because of instantaneous biological consumption in the H$_2$ limited system. The results of the calculations are shown in Fig. 10.
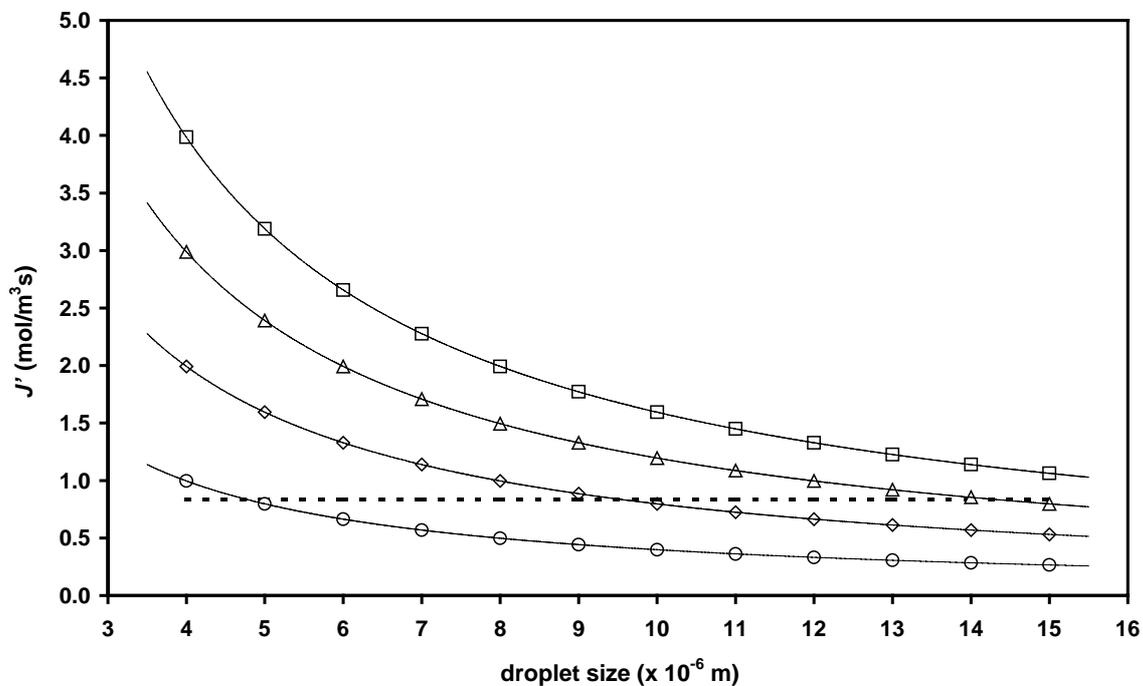

Fig. 10: Estimated values for the volumetric H$_2$ flux as function of the dispersion droplet size: (○) ε = 0.05; (◇) ε = 0.1; (△) ε = 0.15; (□) ε = 0.2. Dashed line represents the volumetric H$_2$ flux in a gas lift system.

From Fig. 10 it can be seen that the volumetric H_2 flux increases with a decreasing droplet size and a larger hold-up of *n*-dodecane. For a droplet size of 10 µm the hold-up should be at least 0.1 to reach the H_2 mass transfer performance of a gas lift system (0.84 mol/m^3·s). However, from results presented earlier (Fig. 8A) it became clear that the hold-up depends on the cation concentration. In this work a model system was used to reveal the dispersion behavior in the absence of bacteria. It was not possible to measure the hold-up in the presence of SRB very precise, because no distinct steady state *n*-dodecane layer could be found anymore due to the flotation of biomass. Nevertheless, the order of magnitude of the hold-up was found to be in the range of 0.04 up to 0.08, indicating that the volumetric H_2 flux is in the order of 0.32 up to 0.64 mol/m^{3}s at a droplet diameter of 10 µm (Fig. 9A), which is lower (a factor 2.6 or 1.3) than H_2 mass transfer rate obtained in gas lift systems. The amount of H_2 transferred in the gas lift system was sufficient to convert 13 mmol S/L·h (Van Houten *et al.*, 1994). Fedorovich *et al.* (2000) applied a hydrophobic membrane to supply H_2 to a sulfate reducing bioreactor and reported a maximal H_2 mass transfer that was enough to convert 0.4 mmol S/L·h. Based on the range of hold-up values found in the presence of SRB, the potential amount of S that can be converted in the dispersion system would be between 5 and 10 mmol S/L·h. This is quite acceptable and exceeds the performance of using a hydrophobic membrane.

It should be noted that the k_{dw}-values used in the volumetric flux calculation represent a minimum value, because the power input during the experiments to measure k_{dw} was low to maintain a flat surface and a constant film thickness for mass transfer. Consequently, at more favorable hydrodynamic conditions the value will be larger. The $k_L a$ value used to calculate the H_2 mass transfer rate in the gas lift system was measured under well mixed conditions (Van Houten *et al.*, 1994). Finally, it must be remarked that the d_{32}-value used in the calculation was a maximal value because the measurements were done offline. In practice possibly smaller droplet sizes can be attained resulting in a larger volumetric H_2 flux because of a larger specific surface area (Fig. 10).

In case of a practical biodesulfurization process it would be desirable to work at minimum salt requirements for the bacteria in order to minimize the coagulation of the organic phase. In that way the hold-up of the organic phase will be maximized (Fig. 8A) and consequently the volumetric H_2 flux will be increased (Fig. 10). However, the presence of biomass may play also a role on the overall coagulation and coalescence processes, which is not taken into account here. This effect should be investigated in more detail together

with the biomass flotation process and these phenomena constitute a technological challenge.

CONCLUSIONS

The verification of the H_2 mass transfer coefficient from *n*-dodecane to water using a steady state approach with H_2 consuming sulfate reducing bacteria was successfully carried out. The value found [$(4\pm0.24) \times 10^{-6}$ m·s^{-1}] was comparable to the value found in previous abiotic steady state experiments [$(5\pm0.6) \times 10^{-6}$ m·s^{-1}] using tritium hydride, indicating that the radio active compound is a good model compound to follow H_2 diffusion. It was shown that the specific surface area resulting from the tiny droplets [10.3 ± 0.9 μm] produced by a nozzle can be sufficiently small to overcome the smaller H_2 flux [0.16×10^{-6} mol/m^{2}s] compared to direct H_2 gas addition [3.9×10^{-6} mol/m^{2}s] to a large extent. The hold-up of the organic phase has a large effect on the H_2 mass transfer and is dependent on the cation (Na^+) concentration. It appeared that the amount of *n*-dodecane that can be dispersed decreases from 0.14 to 0.04 with increasing Na^+ concentrations, at Na^+ concentrations higher than 94 mM the hold-up was found to be 0.04.

In case of a practical biodesulfurization process the H_2 mass transfer is not expected to be a rate limiting factor. However, the flotation of biomass due to the injection of *n*-dodecane in the aqueous phase limits the potential of this approach, because the intimate contact of dibenzothiophene with biomass is disturbed.

These type of systems are relatively unexplored and research on coagulation and coalescence of hydrocarbon droplets and biomass flotation in dispersions should be addressed in the future.

NOMENCLATURE

A interfacial area (m^2)

a specific surface area ($m^2\ m^{-3}$)

c concentration ($mol\ m^{-3}$)

J Mass transfer flux ($mol\ m^{-2}\ s^{-1}$)

J' Volumetric mass transfer flux ($mol\ m^{-3}\ s^{-1}$)

k_{dw} overall mass transfer coefficient *n*-dodecane/water ($m\ s^{-1}$)

k_{gd} overall mass transfer coefficient gas/*n*-dodecane ($m\ s^{-1}$)

m_{gd} partition coefficient between gas and *n*-dodecane ($m^3_{\ d}/m^3_{\ g}$)

P pressure (Pa)

p_{H2} partial H_2 pressure $y_{H2} \cdot P$ (Pa)

R_H rate of hydrogen consumption

R_S rate of sulfate consumption

T temperature (°C)

t time (s)

V volume (m^3)

Super and subscripts

$*$ at equilibrium

w water phase

d *n*-dodecane phase

g H_2 gas phase

Abbreviations

HAB   Homo-Acetogenic Bacteria

HRT   Hydraulic retention time

LI   Level indicator

MA   Methanogenic Archaea

MFC   Mass Flow Controller

PI   Pressure Indicator

SLR   Sulfate Loading Rate

SRB   Sulfate Reducing Bacteria

SRR   Sulfate Reduction Rate

Acknowledgements

The authors wish to thank H. Baptist of the Food Physics Group Wageningen University and F.D. Zoet and G. van Aken from the Wageningen Centre for Food Sciences (WCFS) for their advise on the dispersion characterization.

REFENRENCES

Armstrong S.M., Sankey B.M., Verdouw G. 1997. Evaluation of sulfate-reducing bacteria for desulfurizing bitumen or its fractions. Fuel Process. Technol. 76: 223-227.

Borole A.P., Kaufman E.N., Grossman M.J., Minak-Bernero V., Bare R., Lee M.K. 2002. Comparison of the emulsion characteristics of *Rhodococcus erythropolis* and *Escherichia coli* SOXC-5 cells expressing biodesulfurization genes. Biotechnol. Progr. 18: 88-93.

Brandis A., Thauer R.K. 1981. Growth of *Desulfovibrio* species on hydrogen and sulfate as sole energy source. J. Gen. Microbiol. 126: 249-252.

Brink L.E.S., Tramper J. 1986a. Modeling the effects of mass transfer on kinetics of propene epoxidation of immobilized *Mycobacterium* cells: 1. Pseudo-one-substrate conditions and negligible product inhibition. Enzyme Microb. Technol. 8: 281-288.

Brink L.E.S., Tramper J. 1986b. Modeling the effects of mass transfer on kinetics of propene epoxidation of immobilized *Mycobacterium* cells: 2. Product inhibition. Enzyme Microb. Technol. 8: 334-340.

Doig S.D., Boam A.T., Leak D.I., Livingston A.G., Stuckey D.C. 1999. Epoxidation of 1,7-octadiene by *Pseudomonas oleovorans* in a membrane bioreactor. Biotechnol. Bioeng. 58: 601-611.

Doig S.D., Boam A.T., Leak D.I., Livingston A.G., Stuckey D.C. 1998. A membrane bioreactor for biotransformations of hydrophobic molecules. Biotechnol. Bioeng. 58: 587-594.

Dukhin S.S., Sjöblom J., Wasan D.T., Sæther Ø. 2001. Coalescence coupled with either coagulation of flocculation in dilute emulsions. Colloid Surface A 180: 223-234.

Fedorovich V., Greben M., Kalyuzhnyi S., Lens P., Hulshoff Pol L.W. 2000. Use of hydrophobic membranes to supply hydrogen to sulfate reducing bioreactors. Biodegradation 11: 295-303.

Hiemenz P.C., Rajagpalan R. 1997. Principles of colloid science and surface chemisty. Marcel Dekker Inc. New York.

Kaufman E.N., Harkins J.B., Borole A.P. 1998. Comparison of batch-stirred and electro-spray reactors for biodesulfurization of dibenzothiophene in crude oil and hydrocarbon feedstocks. Appl. Biochem. Biotech. 73: 127-144.

Kawakami K., Tsuruda S., Miyagi K. 1990. Immobilization of microbial cells in a matrix of silicone polymer and calcium alginate gel: Epoxidation of 1-octane by *Nocardia coralina* B-276 in organic media. Biotechnol. Progr. 6: 357-361.

Kawakami K., Takeshi A., Yoshida T. 1992. Silicone immobilized biocatalysts for bioconversions in nonaqueous media. Enzyme Microb. Technol. 14: 371-375.

Kim B.Y., Kim H.Y., Kim T.S., Park D.H. 1995. Selectivity of desulfurization activity of *Desulfovibrio desulfuricans* M6 on different petroleum products. Fuel Process. Technol. 43: 87-94.

Lyklema H. 2002. Laboratory for physical chemistry and colloid science, Wageningen University. Personal communication.

O'Flaherty V., Mahony T., O'Kennedy R., Colleran E. 1998. Effect of pH on growth kinetics and sulfide toxicity thresholds of a range of methanogenic syntrophic and sulfate-reducing bacteria. Process Biochem. 33: 555-569.

Overbeek J.Th.G. 1969. In: H.R. Kruyt (Ed.) Colloid Science, Part I, Elsevier, Amsterdam.

Oude Elferink S.J.W.H., Visser A., Hulshoff Pol L.W., Stams A.J.M. 1994. Sulfate reduction in methanogenic bioreactors. FEMS Microbiol. Rev. 15: 119-136.

Oude Elferink S.J.W.H., Luppens S.B.I, Marcelis C.L.M., Stams A.J.M. 1998. Kinetics of acetate oxidation by two sulfate reducers isolated from anaerobic granular sludge. Appl. Environ. Microbiol. 64: 2301-2303.

Robinson J.A., Tiedje J.M. 1984. Competition between sulfate-reducing and methanogenic bacteria for H_2 under resting and growing conditions. Arch. Microbiol. 137: 26-32.

Roels J.A. 1983. Energetics and kinetics in biotechnology. Elsevier Biomedical Press, Amsterdam.

Schmid A., Kollmer A., Witholt B. 1998. Effects of biosurfactant and emulsification on two-liquid phase *Pseudomonas oleovorans* cultures and cell-free emulsions containing *n*-decane. Enzyme Microb. Technol. 22: 487-493.

Shennan J.L. 1996. Microbial attack on sulfur-containing hydrocarbons: implications for the biodesulfurization of oils and coals. J. Chem. Technol. Biotechnol. 67: 109-123.

Stams A.J.M., Van Dijk J.B., Dijkema C., Plugge C.M. 1993. Growth of syntrophic propionate-oxidizing bacteria with fumarate in the absence of methanogenic bacteria. Appl. Environ. Microbiol. 59: 1114-1119.

Trüper H.G., Schlegel H.G. 1964. Sulfur metabolism in *Thiorhodaceae*. Quantitative measurements on growing cells of *Chromatium okenii*. Antonie van Leeuwenhoek J. Microbiol. Ser. 30: 225-238.

Van den Meer A.B., Beenackers A.A.C.M., Stamhuis E.J. 1986. Microbial production of epoxides from alkenes in continuous multi-phase reactors. Chem. Eng. Sci. 41: 607-616.

Van Houten R.T., Hulshoff Pol L.W., Lettinga G. 1994. Biological sulfate reduction using gas-lift reactors fed with hydrogen and carbon dioxide as energy and carbon source. Biotechnol. Bioeng. 44: 586-594.

Van Sonsbeek H.M., Beeftink H.H., Tramper J. 1993. Two-liquid phase bioreactors. Enzyme Microb. Technol. 15:722-729.

Van Sonsbeek H.M., Gielen S.J., Tramper J. 1991. Steady-state method for *ka* measurements in model systems. Biotechnol. Technol. 5: 157-162.

Widdel F. 1988. Microbiology and ecology of sulfate and sulfur reducing bacteria, In Biology of anaerobic microorganisms, ed. AJB Zehnder. Wiley & Sons, New York 469-586.

Woodley J.M., Lilly M.D. 1990. Extractive biocatalysis: The use of two-liquid phase biocatalytic reactors to assist product recovery. Chem. Eng. Sci. 45: 2391-2396.

Wubbolts M.G., Hoven J., Melgert B., Witholt B. 1994. Efficient production of optically active styrene epoxides in two liquid-phase cultures. Enzyme Microb. Technol. 16: 887-894.

Details of photographs depicting the experimental work that is described in Chapter 6.

CHAPTER 6

PARTITIONING OF HYDROGEN SULFIDE

IN A THREE-PHASE SYSTEM

ABSTRACT

The partitioning of gaseous hydrogen sulfide has been studied for a three-phase system consisting of hydrocarbon, water and gas. To enable a comparison of this system with the partitioning in gas/water systems also the latter was described in a mathematical model. The model predictions were evaluated and validated by laboratory measurements. Furthermore, attention was paid to the importance of salt on the partitioning of H_2S. A sensitivity analysis was carried out to investigate the effect of changes in model parameters to the outcome of the models. With the models developed it is possible to calculate the sulfide concentrations in each of the phases involved.

KEYWORDS

Biodesulfurization, Modeling, Partitioning, Sulfide

INTRODUCTION

Gaseous hydrogen sulfide ($H_2S_{(g)}$) is the characteristic end-product of sulfate and sulfur reducing bacteria (SRB) and it is known to be an inhibitory compound for bacterial growth (Reis *et al.*, 1991; Hao *et al.*, 1996). The neutrality of the H_2S-molecule allows easy diffusion through the lipid membrane into the cytoplasm (O'Flaherty *et al.*, 1998). In the cell the H_2S dissociates in bisulfide (HS^-) and a proton (H^+). Essential cell components might react with H_2S or HS^- leading to less viable conditions for the bacterium. In addition, the protons resulting from the H_2S dissociation dissipate the proton gradient across the cell membrane.

Several authors reported that sulfide inhibition is reversible, speculating that irreversible reactions of sulfide with cell components are of minor importance (Okabe *et al.*, 1992; Reis *et al.*, 1992; Van Houten *et al.*, 1994). The influence of H_2S levels on growth of mesophilic SRB is reviewed elsewhere (Colleran *et al.*, 1995; Oude Elferink *et al.*, 1994; Maillacheruvu *et al.*, 1993). Less in known about thermophilic SRB, but they seem to be more sensitive to H_2S (Min and Zinder, 1990). Still a lot is unclear regarding sulfide inhibition in mixed anaerobic biosystems. Especially when mixed anaerobic consortia consisting of sulfate reducing bacteria, methane producing bacteria and acetogenic bacteria are present. Sometimes the tolerance towards sulfide of methanogens is higher than for sulfate reducing bacteria (Uberoi and Bhattacharya, 1995; McCartney and Oleszkiewicz, 1991). Sulfide exerts a different influence on each group, depending on the species present in the biomass and the type of substrate (O'Flaherty *et al.*, 1998; Omil *et*

al., 1996). Furthermore, the effect of sulfide inhibition greatly depends on the pH and this effect is not always taken into account (O'Flaherty *et al.*, 1998). When biomass grows in aggregates or flocs, the sensitivity towards sulfide is less, because sulfide gradients will exist along a biofilm (Lens *et al.*, 1993; Koster *et al.*, 1986).

When in the bioprocess an additional hydrocarbon phase is involved, an extra factor to describe the influence of H_2S should be taken into account. H_2S is soluble in the hydrocarbon phase and therefore will partition over the gas/water/hydrocarbon phases. This situation is characteristic for the anaerobic biodesulfurization process. In this bioprocess, sulfur is removed specifically from organosulfur compounds that are present in fuels. The model reaction for the anaerobic desulfurization of dibenzothiophene (DBT) is depicted in Fig. 1. Sulfide is formed concomitantly with the remaining hydrocarbon product. From Fig. 1 it can be seen that the sulfur is removed specifically and the fuel value of the hydrocarbon remains. The DBT molecules are insoluble in the aqueous phase and this implies that the conversion should occur at the water/hydrocarbon interface (Shennan, 1996).
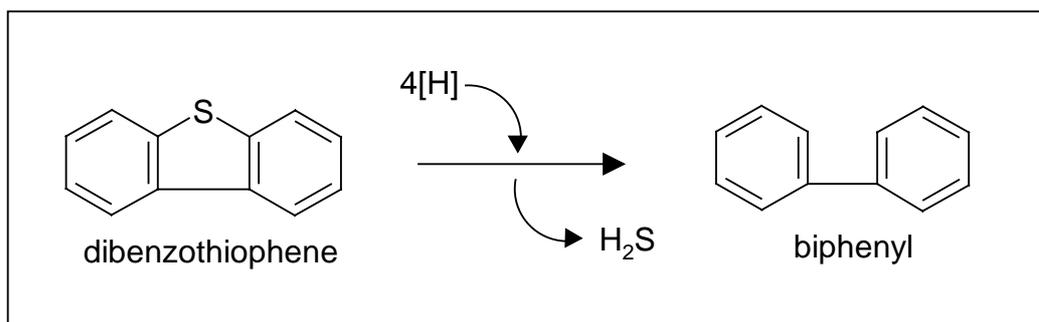

Fig. 1. Anaerobic conversion of dibenzothiophene to biphenyl and sulfide.

The anaerobic conversion of dibenzothiophene proceeds slowly because it is a less favorable electron acceptor compared to sulfate (Chapter 3; Armstrong *et al.*, 1997; Kim *et al.*, 1995). Furthermore, the reaction is also not very favorable from an energetic point of view. Consequently, an effective removal of sulfide is important to avoid inhibiting effects caused either by product inhibition or reversible toxicity.

The objective of this work is to model the partitioning of $H_2S_{(g)}$ for a three phase system consisting of a gas, water and hydrocarbon phase. In this work *n*-dodecane is used as a typical model solvent for the hydrocarbon phase, because it has similar physical properties as diesel fuel distillates (boiling point 215°C and a viscosity of 1.27 mPas at 30°C). To reveal the influence of the hydrocarbon phase and to enable a comparison also the H_2S

partitioning in a two-phase gas/water system had to be evaluated. The pH, temperature and volume fractions of each phase were considered as variables. The model predictions for the two and three phase systems were validated by measuring the sulfide concentrations in each phase at various pH values. In addition, a parameter sensitivity analysis was performed with respect to the key parameters applied in the model. Furthermore, the possible influence of the salting out effect on the $H_2S_{(g)}$ solubility in the aqueous phase is estimated and investigated experimentally.

The model predictions presented in this work show the dissolved sulfide concentration in each phase for a gas/water and gas/water/*n*-dodecane system, respectively.

THEORY

Sulfide species in water and the effect of pH and temperature

For the modeling of sulfide partitioning the effect of pH and temperature on the presence of various sulfide species in the water phase is important. The H_2S present in the water phase is in equilibrium with HS^- en S^{2-}, according to the following acid-base equilibrium:

$$H_2S \underset{k_{-1}}{\overset{k_1}{\rightleftarrows}} HS^- + H^+ \underset{k_{-2}}{\overset{k_2}{\rightleftarrows}} S^{2-} + 2H^+ \tag{1}$$

Where: $K_1 = \dfrac{k_1}{k_{-1}} = 1.0\text{x}10^{-7}$ and $K_2 = \dfrac{k_2}{k_{-2}} = 0.7\text{x}10^{-17}$ defined at 20ºC (Steudel, 2000).

Except for solutions with a pH near 14, the occurrence of S^{2-} ions can be excluded because of the extremely low value of K_2 (Steudel, 2000). However, it should be noted that in older literature pK_2 values around 12 are reported (*e.g.* Sillén and Martell, 1964), suggesting the occurrence of S^{2-} at lower pH values. Nevertheless, the pH range chosen in this work was from 6.4 up to 8, because of its relevance for most biological systems. Therefore, the second part of Eq. 1 is not considered and only HS^- and H_2S are involved as relevant sulfide species. The concentration of each sulfide species depends on the value of the chemical equilibrium constant $K_1 = K^{H_2S}$, which is defined as:

$$K^{H_2S} = \frac{C_w^{H^+} \cdot C_w^{HS^-}}{C_w^{H_2S}} \tag{2}$$

Where: $C_w^{H^+}$, $C_w^{HS^-}$ and $C_w^{H_2S}$ denote the H⁺, HS⁻ and H₂S concentration in the water phase, respectively. The temperature dependency of the K^{H_2S} can be well described by a Van 't Hoff-type expression:

$$\ln K' = c_1 - \frac{c_2}{T} - c_3 \cdot \ln T + c_4 \cdot T \tag{3}$$

Where K' is expressed in mol/mol. The constants c_1 (214.6), c_2 (-12995.4), c_3 (-33.55) and c_4 (0) applied in the model were reported originally by Edwards *et al.* (1978) and are widely used by other authors (Xia *et al.*, 2000; Kuranov *et al.*, 1996; Weiland *et al.*, 1993; Gas Research Institute, 1991).

To relate K' to K^{H_2S} we used the following relation:

$$K^{H_2S} = K' \cdot \frac{\rho_w}{MW_w} \tag{4}$$

Where MW_w (kg/kmol) denotes the molecular weight of the pure water phase and ρ_w (kg/m³) the density of the water phase. To determine the pK^{H_2S} Eq. 5 was set-up:

$$pK^{H_2S} = -log(K^{H_2S}) \tag{5}$$

Partitioning

A gas/water/*n*-dodecane (g/w/d) system at a defined temperature and pressure is in equilibrium when the net diffusion of H₂S over the phases involved equals zero. At this condition the partition coefficients can be defined, according to Eq. 6:

$$m_{dw} = \frac{C_d^{H_2S}}{C_w^{H_2S}} = \frac{1}{m_{wd}}$$

$$m_{dw} = \frac{C_d^{H_2S}}{C_w^{H_2S}} = \frac{C_d^{H_2S}}{C_g^{H_2S}} \cdot \frac{C_g^{H_2S}}{C_w^{H_2S}} = \frac{m_{gw}}{m_{gd}} \qquad (m_w^3/m_d^3) \tag{6}$$

The partition coefficient is also called the 'dimensionless' Henry's coefficient (He') when a gas phase is involved. Usually, the Henry's coefficient (*He*) is expressed as the proportionality constant between the partial pressure of H₂S (p_{H_2S}) and the H₂S concentration in the liquid phase at equilibrium ($C_l^{H_2S}$) under constant pressure as:

$$He = \frac{p_{H_2S}}{C_l^{H_2S}} \qquad \text{(Pa)} \qquad (7)$$

When the liquid properties are taken into account the Henry's coefficient (He'') has the units: MPa/(kmol/m^3). At standard conditions and dilute chemical concentrations m and He can be related according to (Peng and Wan, 1997):

$$m_{gl} = He \cdot \frac{MW_l}{\rho_l RT} \qquad \text{(-)} \qquad \text{or} \qquad m_{gl} = \frac{He''}{RT} \qquad (m_l^3/m_g^3) \qquad (8)$$

Where MW_l (kg/kmol) denotes the molecular weight of the pure liquid phase and ρ_l (kg/m^3) the density of the liquid phase.

The partition coefficients for the gas/water system m_{gw} and gas/n-dodecane system m_{gd} were calculated using a thermodynamic method according to the Soave-Redlich-Kwong model (Reid *et al.*, 1987). The predictions were compared to reported values and verified under the experimental conditions.

Volatile compounds such as H$_2$S have a lower solubility in electrolytes and consequently the value for He_w might increase (the salting out effect). In practical situations these ions are present in the cultivation medium or in the influent that has to be treated in a bioreactor. In this work, NaCl is used to study the importance of the salting out effect of H$_2$S.

The salting out coefficient (κ, expressed in m^3/kmol) can be determined by plotting $\log \gamma$ against I according to the following relationship:

$$\log\gamma = \kappa \cdot I \qquad (9)$$

In Eq. 9 γ is the activity coefficient (-) and I is the ionic strength (kmol/m^3), which is calculated according to:

$$I = \frac{1}{2}\sum\left(C_i^{ion} \cdot z_i^2\right) \qquad (10)$$

In this equation C_i^{ion} denotes the concentration of ion i (kmol/m^3) and z_i is the charge of ion i. The Henry's law coefficient for water with ions (He_s') can be described by:

$$He_s' = \gamma \cdot He_0' \qquad (11)$$

Where $He_s' = m_{gw,s}$ is the dimensionless Henry's constant in 'salted' water and $He_0' = m_{gw,0}$ is the dimensionless Henry's constant for 'unsalted' pure water. When the salting out coefficient is close to zero and γ close to unity, the system will show ideal behavior.

At moderately high salt concentrations (up to 2 *M*), the effect of the presence of NaCl on $He_w^{'}$ can be estimated with the Sechenov relation as depicted in Eq. 12 (Schumpe, 1993).

$$log\left(\frac{He_s^{'}}{He_0^{'}}\right) = log\left(\frac{m_{gw,s}}{m_{gw,0}}\right) = \kappa^{''} \cdot C_s = \sum_{i=1}^{N_i}(h_i + h_g)C_i^{ion} \qquad (12)$$

Here C_s is the salt concentration (kmol/m³) and the parameter $\kappa^{''}$ is called the Sechenov constant, which is specific for the system used (Weisenberger and Schumpe, 1996). The ion-specific parameters (h_i) used in Eq. 12 were: h_{Na^+} = 0.1143 m³/kmol, h_{Cl^-} = 0.0318 m³/kmol and h_{HS^-} = 0.0851 m³/kmol, N_i is the number of ionic species and C_i^{ion} is the molar concentration of ion *i* (data obtained from Weisenberger and Schumpe, 1996). The gas-specific parameter (h_g) is assumed to be a linear function of the temperature for 273K < T < 363 K, according to Eq. 13:

$$h_g = h_{g,0} + h_T(T - 298.15) \qquad (13)$$

Unfortunately, no value for the h_T parameter for H₂S is reported and the value used for h_g corresponds to $h_{g,0}$, thus: $h_{H_2S} = h_{H_2S,0} = -0.0333$ m³/kmol defined at 25ºC (Weisenberger and Schumpe, 1996). Applying Eq. 12 and 13 for values of the similar CO_2/HCO_3^- equilibrium at 35ºC (*viz.* pK = 6.31; h_T = -0.338x10⁻³ m³/(kmol·K); $h_{HCO_3^-}$ = 0.0967 m³/kmol) results in a minor change of 0.2% in the calculated value for $He_s^{'}$ (Gas Research Institute, 1991; Weisenberger and Schumpe, 1996). Therefore, the use of h_{H_2S} defined at 25ºC without temperature correction will not result in unacceptable errors. The values predicted according to Eq. 12 are verified experimentally for NaCl concentrations up to 0.5 *M* in g/w systems.

Set-up of the model

The partitioning of H₂S(g) over a g/w or g/w/d system is dependent on the following parameters: pH, volume fractions of each phase, temperature and pressure. Since biosystems mostly operate at atmospheric pressure this parameter is considered to be constant. It is assumed that H₂S partitions over the gas, water and *n*-dodecane phase and can only dissociate in the aqueous phase. This is a realistic assumption because no bisulfide can exist in the gas or *n*-dodecane phase.

The basic expression that was used to derive an equation that relates the HS⁻ concentration in the aqueous phase ($C_w^{HS^-}$) to the H_2S concentrations in each phase for a g/w/d system is presented below:

$$C_w^{HS^-} = \frac{C^{S,TOT}}{\left(C_w^{S,TOT} + C_g^{H_2S} + C_d^{H_2S}\right)\Big/ C_w^{HS^-}} \qquad \text{(kmol/m}^3) \qquad (14)$$

In Eq. 14 $C^{S,TOT}$ is the total amount of moles sulfide species added to the system, $C_w^{S,TOT}$ denotes the sum of $C_w^{HS^-}$ and $C_w^{H_2S}$, because these sulfide species cannot be measured independently in the aqueous phase with our analytical tools. Parameters $C_g^{H_2S}$ and $C_d^{H_2S}$ denote the H_2S concentration in the gas and *n*-dodecane phase respectively. Rearrangement results in Eq. 15, which is incorporated in the model to relate K^{H_2S} and the partition coefficients to find $C_w^{HS^-}$:

$$C_w^{HS^-} = \frac{\dfrac{C_w^{S,Tot}}{1000} \cdot \dfrac{1}{MW_S}}{\left(\dfrac{C_w^{H^+}}{K^{H_2S}} + 1\right) + \left(\dfrac{C_w^{H^+}}{K^{H_2S}} \cdot m_{gw} \cdot \dfrac{V_g}{V_w}\right) + \left(\dfrac{C_w^{H^+}}{K^{H_2S}} \cdot \dfrac{1}{m_{wd}} \cdot \dfrac{V_d}{V_w}\right)} \qquad (15)$$

Where $C_w^{S,Tot}$ denotes the amount of milligrams of sulfur introduced to the system per liter of aqueous phase and MW_S is the molecular weight of the sulfur. When $C_w^{HS^-}$ is known, $C_w^{H_2S}$ is calculated according to Eq. 16.

$$C_w^{H_2S} = C_w^{HS^-} \cdot \frac{C_w^{H^+}}{K^{H_2S}} \qquad (16)$$

Finally, $C_g^{H_2S}$ and $C_d^{H_2S}$ can be calculated from $C_w^{H_2S}$ using the partition coefficients (m_{gw} and m_{wd}). For the two phase system, the third term in the denominator of Eq. 15 describing the water/*n*-dodecane partition is left out. In case of a gas/*n*-dodecane system Eq. 17 was applied, because then only H_2S is present.

$$C_d^{H_2S} = \frac{n_{H_2S}}{\left[\left(m_{gd} \cdot \dfrac{V_g}{V_d}\right) + 1\right] \cdot V_d}$$

(17)

Where n_{H_2S} denotes the total amount of moles $H_2S_{(g)}$ added to the (g/d) system.

The fraction of total sulfide was calculated for each phase involved to enable a comparison of the amount of sulfide in each phase of a g/w and g/w/d system. As an example; the fraction of total sulfide in *n*-dodecane in a g/w/d system can be calculated according to Eq. 18:

$$\Phi_d^{H_2S} = \frac{C_w^{S,Tot} \cdot V_w}{C_w^{S,Tot} \cdot V_w + C_g^{H_2S} \cdot V_g + C_d^{H_2S} \cdot V_d}$$

(18)

Basic data for He_w, He_d and pK^{H_2S}

The temperature dependent basic data for He_w, He_d and pK^{H_2S} used throughout the calculations are presented in Fig. 2. In Fig. 2A, a comparison is made between literature data and calculations based on the Soave Redlich Kwong (SRK) model.
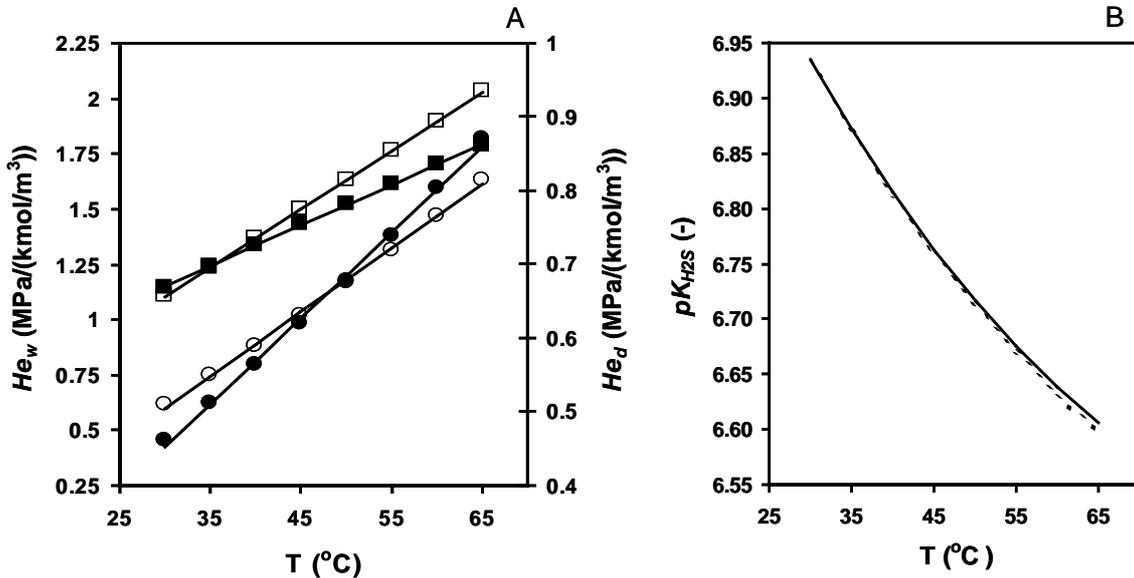
Fig. 2: Temperature dependencies of He_d, He_w and pK^{H_2S}. Fig. 2A: ■, He_w data obtained with the SRK model, y = 0.0184x + 0.599; □, He_w data adapted from Edwards *et al.* (1978), y = 0.0264x + 0.313; ●, He_d data obtained with the SRK model, y = 0.0117x + 0.102; ○, He_d data adapted from King *et al.* (1977), y = 0.0087x + 0.244. Fig. 2B: solid line, pK^{H_2S} data obtained from Edwards *et al.* (1977); dashed line, pK^{H_2S} data obtained from Tsonopolis *et al.* (1976).

As can be seen from the plots of Fig. 2A, somewhat different predictions for He_d and He_w with temperature were found. In the partition models, the He_d and He_w values based on the SRK equations were applied. At 65°C the difference between literature values and the SRK equations are in the order of only 10%. Variations in pK^{H_2S} with temperature are considerable (see Fig. 2B). Several investigators (Xia *et al.*, 2000; Weiland *et al.*, 1993) adapted the values from Edwards *et al.* (1978), the values reported by Tsonopoulus *et al.* (1976) were very similar (Fig. 2B). To obtain insight in the impact of variations in He_w, He_d and pK^{H_2S} a sensitivity analysis needs to be made (as will be presented further on).

MATERIALS AND METHODS

Experimental procedure model validation

The validation experiments carried out in this study can be divided in three sets:

Set I refers to the validation of He_d,

Set II-a refers to the validation of He_w and the gas/water partition model at a range of pH values (6.6, 7.0, 7.4, 7.8), while in Set II-b measurements to study the importance of salting out effects were performed at a range of NaCl concentrations (15, 50, 100, 150, 200, 250, 300, 350, 400, 450 and 500 mM at a pH of 7).

Set III refers to the validation of the gas/water/*n*-dodecane partition model at a range of pH values (6.6, 7.0, 7.4, 7.8).

All experiments with pH as the sole variable were carried out in triplicate, except the experiments of Set II-b that were performed once for each salt concentration. The validation experiments were conducted in a stirred cell (Applikon) equipped with three, disk flat blade, Rushton turbines for efficient mixing. All metal internals were coated with chemically resistant epoxy resin to prevent any reaction with sulfide. During all experiments the temperature was maintained at 35°C by circulating water through the jacket surrounding the glass vessel. To prevent cooling of the gas phase by the steel head plate the whole system was placed in an incubator (at 35°C). The experimental set-up is depicted schematically in Fig. 3.
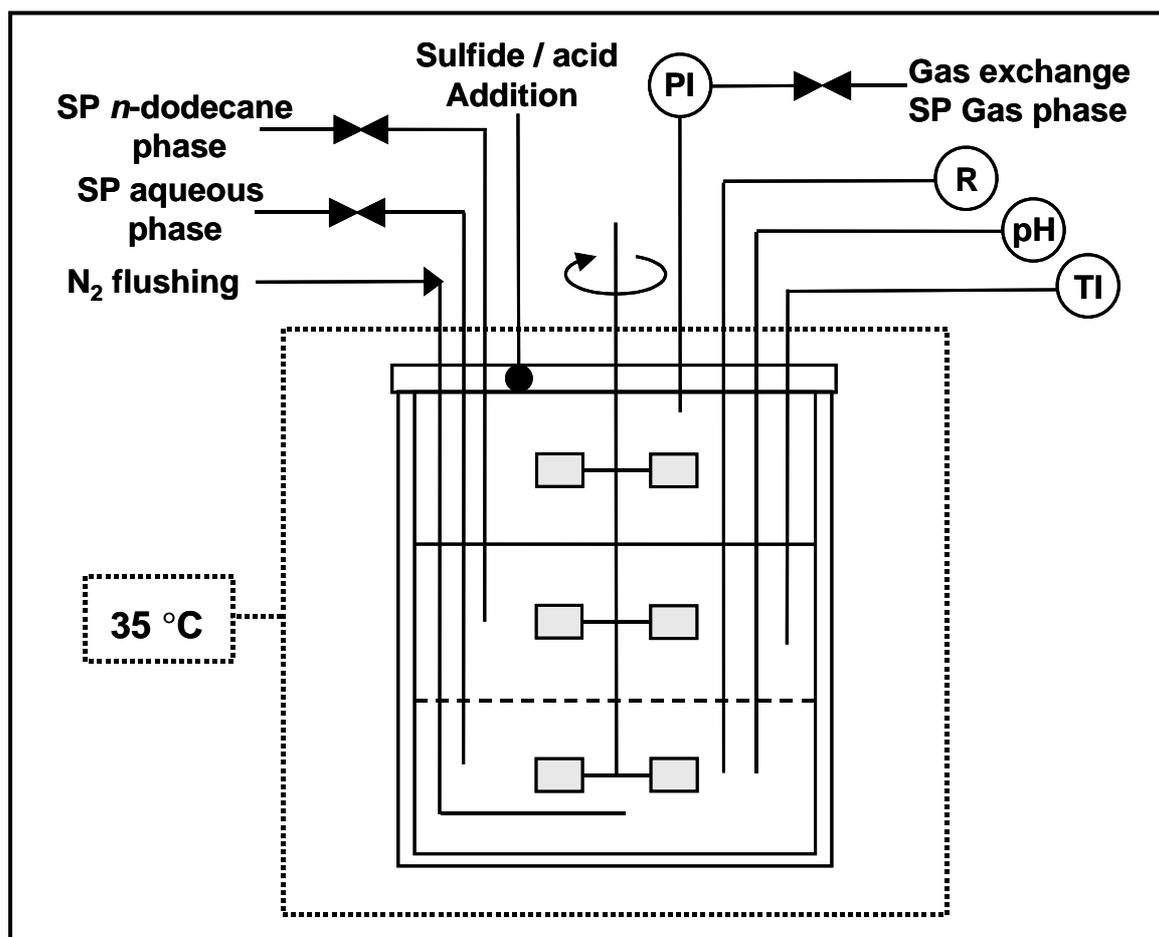
Fig. 3. Schematic presentation of the configuration used in the validation experiments. TI: temperature indicator, PI: pressure indicator, R: redox probe, pH: pH probe, SP: sampling point.

The approximate working volumes for set I, set II-a and set II-b were 2.25 L for the liquid and 1 L for the gas phase, respectively. For set III the approximate working volumes were 1.2 L for the water as well as the *n*-dodecane phase and 0.85 L for the gas phase. Calculations were performed with the exact volume of each phase involved and of the stirred cell (*i.e.* 3.325 L). Before addition, of sulfide the oxygen present in the liquids was removed thoroughly by N_2 flushing. The liquids were transferred to the stirred cell by using N_2 overpressure, while the stirred cell was flushed with N_2 during the addition to avoid any entrance of O_2 to the system. After closing the system, the headspace was exchanged 60 times (from 0.8×10^5 up to 1.2×10^5 Pa, alternately to ensure a complete (100%) N_2 atmosphere. Sulfide was added to the system using a 625 mM solution of $Na_2S \cdot 9H_2O$. In case of Set I, pure H_2S gas was added using a gas tight syringe equipped with a mini inert teflon valve. The pH was set at the desired value by titration with 1M HCl. Additions of sulfide and HCl were made via a viton septum. In the experiments of Set IIb NaCl was added with the aqueous phase. All the liquid additions were performed

gravimetrically to obtain accurate data for the calculations. During the experiments a slight overpressure was present to facilitate the sampling. The mixing speed was set at 900 rpm for 0.5 h to ensure complete mixing of all the liquid additions. Afterwards the system was allowed to equilibrate for 3.5 h at 350 rpm, at this speed the phases were separated. The pH, redox, temperature and pressure trends were measured to observe equilibrium and enable a check for leakage. At stable values for the pH and redox trends (equilibrium), two independent samples were taken from each phase involved and subjected to analysis.

Analytical methods

The total sulfide in the water phase is measured by a spectrophotometric method based on the formation of methylene blue (Dr Lange kit LCW053, Germany). Samples were diluted with O_2 free water to the range of 0,5 up to 1,5 mg S/L. The H_2S concentration in the gas phase was determined by adding 50 ml gas sample with a gas tight syringe to a sealed vial containing 20 ml of 1 M NaOH under a 100 % N_2 atmosphere. The caustic S^{2-} sample was sufficiently diluted to avoid any influence with the methylene blue assay, because the reactants in the assay need an acidic environment to yield the methylene blue colour. Consequently, standard addition using a calibrated sulfide stock solution was necessary to gain a 95% confidence level.

The H_2S dissolved in the *n*-dodecane was determined using a (Hewlet Packard 6890) gas chromatograph equipped with a sulfur chemoluminescence detector (Antek 704E) and a (Supelco) Sulfur SPB-1 column (length 30m, inner diameter 0.32 mm, film thickness 4 µm). Helium was used as the carrier gas, at a flow rate of 5.5 ml/min. The initial oven temperature of 35°C was ramped to 275°C with a rate of 3°C/min during analysis. The injector temperature was 250°C, while the furnace temperature of the detection system was 950°C. Samples were prepared by adding 0.98 ml H_2S containing sample to 0.98 ml benzothiophene solution (2.8 mmol/L *n*-dodecane) using a positive displacement pipette. Benzothiophene was used as the internal standard to enable an exact calculation of the amount of H_2S present in the *n*-dodecane.

Chemicals

All chemicals used were of the highest grade commercially available.

RESULTS AND DISCUSSION

Model evaluation

Fig. 4A up to 4D present the fraction of total sulfide present in each phase against pH and temperature for a two- and three phase system, respectively. The predictions were calculated at atmospheric pressure with equal volumes of each phase involved, *i.e.* $V_g = V_w$ for the g/w-system and $V_g = V_w = V_d$ for the g/w/d-system. In Fig. 4A and 4B the pH was varied between 6.4 and 8 at a constant temperature of 35ºC, while in Fig. 4C and 4D the temperature was varied between 20 and 65 ºC at a constant pH of 7.2.

It can be seen from Fig. 4A and 4B that the total sulfide fraction in the water phase increases along with increasing pH values, while the amount of H₂S in each phase decreases. This effect must be explained by the pronounced influence of the increasing $C_w^{HS^-}$ at the expense of $C_g^{H_2S}$, $C_w^{H_2S}$ and $C_d^{H_2S}$ in this pH range. At pH values above 6.87 (pK^{H_2S} at 35ºC), $C_w^{HS^-}$ is larger than $C_w^{H_2S}$ (see Fig. 4A and 4B). Since $C_w^{H_2S}$ decreases with increasing pH the amount of H₂S that can partition between the other phases becomes less (see Eq. 16). The presence of a third *n*-dodecane phase has a marked influence on the trend depicted in Fig. 4B compared to Fig. 4A. This indicates that the *n*-dodecane phase acts as sink for H₂S because the amount of H₂S in the aqueous and gas phase is lowered considerably (Fig 4B). Consequently, $C_w^{S,Tot}$ is smaller at lower pH values.

From Fig. 4C and 4D, it follows that also temperature affects the sulfide partitioning. For the g/w system depicted in Fig. 4C, the prediction shows almost constant values for $C_g^{H_2S}$ and $C_w^{S,Tot}$ upon an increase in temperature. The slight decrease of $C_g^{H_2S}$ cannot be explained by the trend of He_w with temperature, because He_w increases with temperature, suggesting a higher $C_g^{H_2S}$. The major factor acting here is the temperature dependence of pK_{H_2S}. This parameter decreases considerably at increasing temperature (see Fig. 2B).

Consequently, at a constant pH of 7.2 the $C_w^{HS^-}$ will increase while $C_w^{H_2S}$ must decrease with temperature (see Eq. 16). For the g/w/d system depicted in Fig. 4D a similar trend can be observed. However, the $C_d^{H_2S}$ imparts a great influence on the trend.
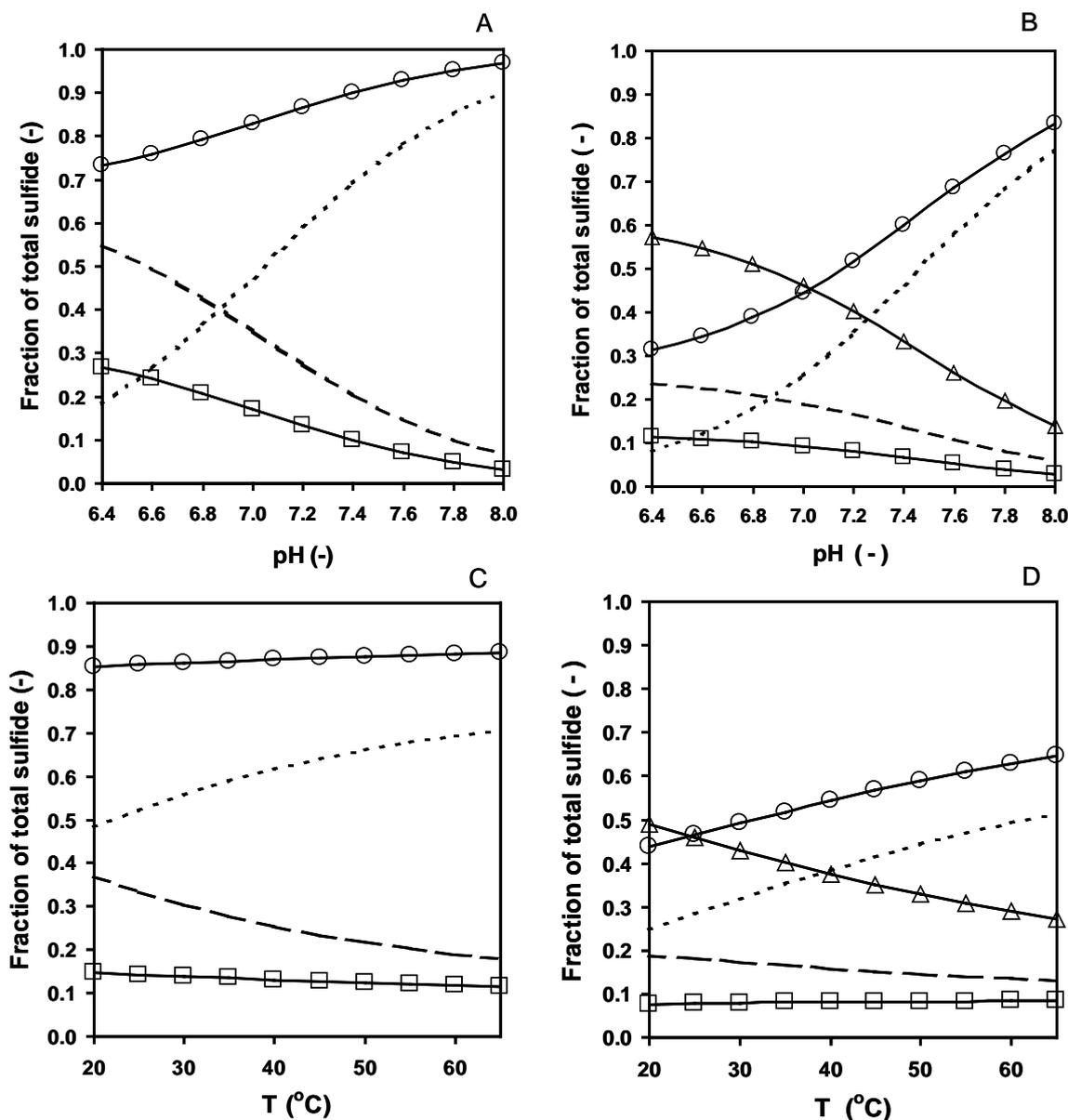
Fig. 4: Predicted profiles of sulfide species for the g/w-system and g/w/d-system. Fig 4A and 4B: fraction of total sulfide vs. pH for the g/w and g/w/d model, respectively. Fig. 4C and Fig. 4D, fraction of total sulfide vs. temperature for the g/w and g/w/d model, respectively.

Legend key: $\bigcirc$, prediction $C_w^{S,Tot}$; $\square$, prediction $C_w^{H_2S}$; $\triangle$, prediction $C_d^{H_2S}$; large dotted line, prediction model $C_g^{H_2S}$; small dotted line, prediction model $C_w^{HS^-}$.

The majority of H_2S that goes to HS^- comes from the *n*-dodecane phase, this clearly demonstrates again that *n*-dodecane acts as a sink for H_2S at pH values below 7. Both the solubility of H_2S in *n*-dodecane and water decrease at higher temperature, but the

dependency of m_{gd} in Eq. 15 is reciprocal compared to m_{gw} indicating that m_{gd} has a larger effect on the partitioning (m_{gw} = 0.49, while $1/m_{gd}$ = 1/0.2 = 5). Consequently, a larger effect for $C_d^{H_2S}$ can be observed upon an increase in temperature.

Model validation

Validation of partition coefficients

Validation experiments (Set I and Set II-a) were performed in order to check the values for $He_d^{'}$ and $He_w^{'}$ applied in the models. The average result from triplicate measurements at 35ºC for $He_d^{'}$ (Set I) was 0.202, with a maximal deviation from the SRK equation of 2.5%. The deviation from the $He_d^{'}$ value predicted by King *et al.* (1977) at 35ºC was -6.2%. The results of the validation experiments for $He_w^{'}$ (Set II-a) are presented in Table 1.

Table 1: Results experimental validation $He_w^{'}$, Set II-a.

pH	I*	$He_w^{'}$	Deviation**
(-)	(mM)	$\left(m_w^3/m_g^3\right)$	(%)
6.58	19	0.464	-4.3
6.61	18	0.468	-3.5
6.65	15	0.505	4.1
6.88	19	0.464	-4.3
7.03	17	0.475	-2.1
7.04	16	0.469	-3.3
7.26	20	0.452	-6.8
7.37	18	0.465	-4.1
7.42	18	0.458	-5.6
7.83	21	0.464	-4.3
7.83	20	0.497	2.5
7.86	20	0.490	1.0
average	18	0.473	-2.5

* Ionic strength is calculated according to Eq. 10.
** Deviation compared to prediction with SRK model.

From the results summarized in Table 1 it can be concluded that the average $He_w^{'}$ obtained (*viz.* 0.473) is in good agreement with the values predicted according to the SRK equation

(*viz.* 0.465, Fig. 2A), the deviation is -2.5%. From literature references the calculated He'_w at 35ºC is 0.476, giving a deviation of only –0.6% with the SRK prediction. Although the experiments were carried out at different pH values and different (trace) ionic strengths, He'_w is clearly independent on these variations (Table 1). Consequently, it was justified to average the He'_w results. The fact that the values found experimentally are generally lower than expected can be explained by slightly lower values found for $C_g^{H_2S}$. For this measurement additional steps during the analysis procedure (*viz.* dilution and standard addition) are necessary, which could result in a small systematic error.

Salting out effect

The expected and measured values of He'_w at various ionic strengths (Set II-b) are summarized in Table 2.

Table 2: Results of the predicted and measured He'-values (Set II-b) salting out experiments.

I	$He'_{w,salt}$	$He'_{w,exp}$	$\gamma_1 = \dfrac{He'_s}{He'_0}$	$\gamma_2 = \dfrac{He'_{exp}}{He'_{trace}}$
(mM)	(-)	(-)	(-)	(-)
19	0.485	0.464	1.004	1.000
69	0.489	0.469	1.012	1.012
119	0.493	0.470	1.021	1.015
166	0.496	0.475	1.027	1.025
216	0.500	0.475	1.035	1.024
267	0.502	0.477	1.039	1.029
316	0.508	0.477	1.052	1.030
366	0.511	0.483	1.058	1.042
417	0.514	0.489	1.064	1.054
467	0.517	0.494	1.070	1.065
516	0.521	0.499	1.079	1.075

To reveal the influence of salt on He'_w, the activity coefficients were calculated in two different ways (Table 2). The activity coefficient based on predicted values (γ_1) is calculated as the ratio of He'_s and He'_0 using Eq. 11. The ratio (γ_2) of He'_{exp} and He'_{trace} is calculated to estimate the activity coefficient based on measurements, where He'_{exp}

denotes the value found at the experimental ionic strength (*I* in Table 2) and He'_{trace} denotes the value at an ionic strength of 19 mM.

As can be seen from Table 2 the He'_w values increase with higher salt concentrations as a result from the lower H₂S solubility. However, at an ionic strength of 516 mM only a 8% higher He'_w was found for both the Sechenov-Schumpe prediction at 25ºC and the experimentally determined value found at 35ºC. Therefore, the system can be assumed to be ideal (γ near unity) and a correction for the salting out effect can be neglected.

The H₂S salting-out coefficient for the g/w-system was estimated to enable a comparison of the salting out effect of H₂S with other volatile compounds. The data for log γ_1 and log γ_2 were plotted against the ionic strength (*I*), the results are shown in Fig. 5.
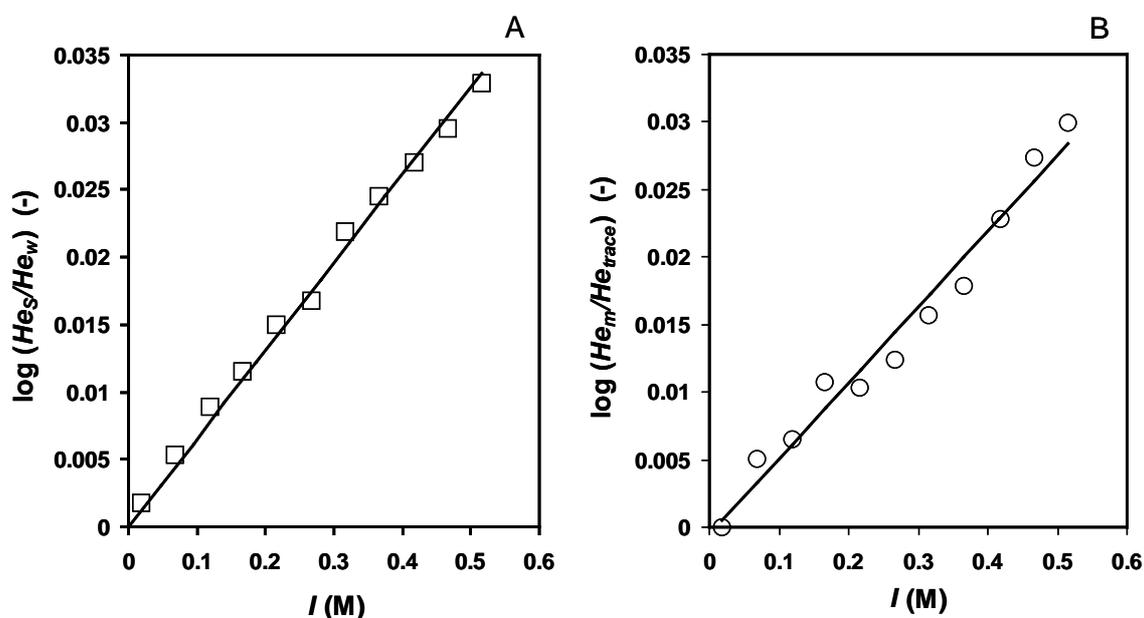
Fig. 5: Estimation of salting out coefficient. Fig. 5A: □, calculated data according to Eq. 12 at 25ºC, trendline: y = 0.0653x. Fig 5B: ○, experimental data at 35ºC, trendline: y = 0.0562x - 0.0006.

As can be seen from the results depicted in Fig. 5, the estimated salting out parameters are 0.065 L/mol and 0.056 L/mol based on the Sechenov Schumpe model and experimental data, respectively. According to Eq. 12 the trendline in Fig. 5B should cross the y-axis at zero. Nevertheless, after linear regression the intercept with the y-axis was found to be slightly negative. This small deviation is present because He'_{trace} was used instead of He'_0

in the calculations, assuming that γ equals 1 at 18 mM. This approach is acceptable, because the difference between He'_{trace} and He'_0 is only 0.4%.

Peng and Wan (1997) reported salting out coefficients at 20ºC for benzene, toluene trichloroethene and tetreachloroethylene of: 0.202, 0.24, 0.224 and 0.217 L/mol, respectively. Gosset (1987) reported the following values for chlorinated hydrocarbons determined at 20ºC (L/mol): 0.213 (tetrachloroethylene), 0.186 (trichloroethylene), 0.193 (1,1,1-trichloroethane), 0.145 (1,1-dichloroethane), 0.14 (chloroform) and 0.107 (dichloromethane), respectively. The increase of He_w for volatile organic compounds was reported to be at least 10% for ionic strengths greater than 200 mM (Peng and Wan, 1997). The experimental salting out parameter found for H_2S is considerably lower compared to the values for (chlorinated) hydrocarbons, indicating that the partitioning of H_2S into the gas phase is not greatly favored by the presence of NaCl up to values of 516 mM.

Validation of g/w and g/w/d models

The predictions of the H₂S partitioning model were validated (Set III) by comparing experimental data with model simulations (Fig. 6). Three independent experiments were performed at 4 different pH values for both the g/w and the g/w/d systems. The pH difference in the triplicates was due to differences in the initial amount of sulfide added to each system, the rest of the set points were identical for each experiment.
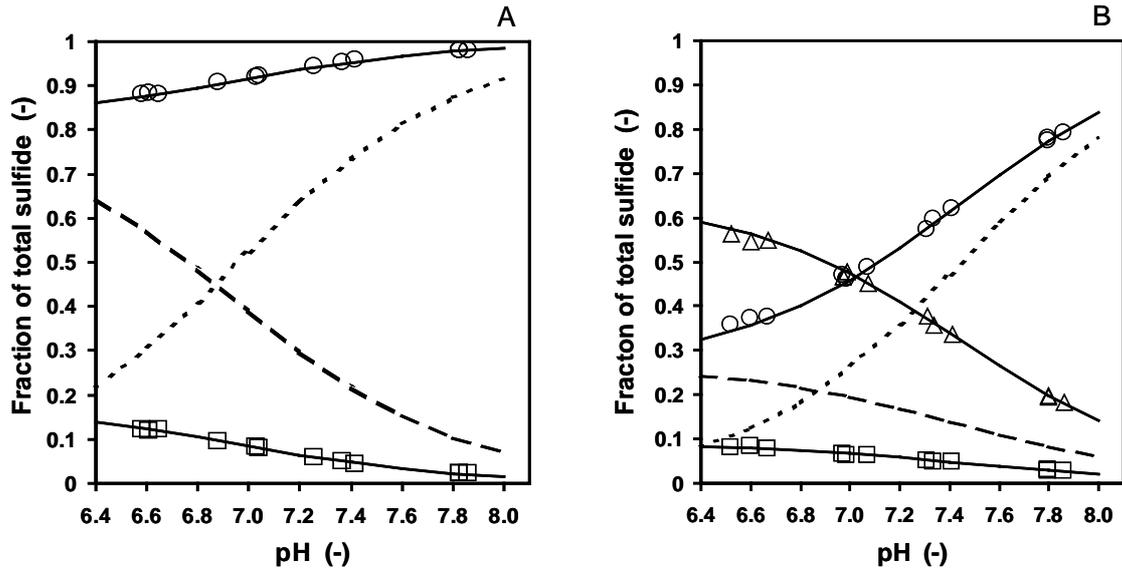
Fig. 6: Validation of sulfide partitioning models: Fraction of total sulfide vs. pH for the g/w and g/w/d model Fig. 6A and Fig. 6B, respectively.

Legend key: ○, experimental data $C_w^{S,Tot}$; □, experimental data $C_w^{H_2S}$; △, experimental data $C_d^{H_2S}$; Solid lines, values predicted according to the model; large dotted line, prediction model $C_g^{H_2S}$; small dotted line, prediction model $C_w^{HS^-}$.

It appeared that both models gave a realistic description of the H₂S partitioning, because the fractions found experimentally and the fractions predicted are very close to each other. Deviations between predictions and measurements were within 5% error.

Sensitivity analysis of the g/w and g/w/d models

To establish the sensitivity of the g/w and g/w/d models for variations in the partition coefficients involved and the pK_{H_2S} value used, a sensitivity analysis was made around the following set points: $V_g = V_w$ for the g/w-system and $V_g = V_w = V_d$ for the g/w/d-system, a constant temperature of 35ºC and a pH of 7.0 (near pK^{H_2S}). In the sensitivity analysis one parameter was varied at a chosen offset, while the other variables were kept constant. For the partition coefficients a variation of +/- 10% was chosen, because this was the maximal deviation in the predictions presented in Fig. 2A. Since the data on pK^{H_2S} is very consistent variations of +/- 1% or +/- 2% were applied (Fig. 2B). The results of the sensitivity analysis are depicted in Table 3 for the g/w system and in Table 4 for the g/w/d system, respectively.

Table 3: Sensitivity analysis of the He'_w and pK^{H_2S} used in the g/w model. Percentage change in sulfide concentrations in each phase involved, resulting from -10% or + 10% change in He'_w and a -1% / -2% or +1% / +2% change in pK^{H_2S}.

Parameter	He'_w		pK^{H_2S}	
% change	- 10%	+10 %	-1% / -2%	+1% / +2%
$C_w^{S,Tot}$ (%)	1.7	-1.7	1.8 / 3.2	-1.5 / -3
$C_g^{H_2S}$ (%)	-8.4	8.1	-7.7 / -15.2	7.4 / 14.6
$\varphi_w^{S,Tot}$ (%)	1.8	-1.6	1.7 / 3.3	-1.5 / -3
$\varphi_w^{H_2S}$ (%)	1.7	-1.7	-7.7 / -15.2	7.4 / 14.6
$\varphi_w^{HS^-}$ (%)	1.7	-1.7	8.5 / 16.8	-8.2 / -16.1
$\varphi_g^{H_2S}$ (%)	-8.4	8.1	-7.7 / -15.2	7.4 / 14.6

Varying the He'_w in the g/w-system did not result in a large response (Table 3), except for the prediction for the gas phase. As expected, a positive change in He'_w leads to an augmented $\varphi_g^{H_2S}$. A decrease in $\varphi_g^{H_2S}$ gives rise to increased sulfide concentrations in the water phase. However, overall the model response does not exceed the variation in He'_w, indicating that the model can predict the sulfide concentrations rather well.

Table 4: Sensitivity analysis of the $He_w^{'}$, m_{wd} and pK^{H_2S} used in the g/w/d model. Percentage change in sulfide concentrations in each phase, resulting from -10% or + 10% change in $He_w^{'}$ or m_{wd} and a -1% / -2% or +1% / +2% change in pK^{H_2S}.

Parameter	$He_w^{'}$		m_{wd}		pK^{H_2S}	
% change	- 10%	+ 10%	- 10%	+ 10%	-1% / -2%	+1% / +2%
$C_w^{S,Tot}$ (%)	0.9	-0.9	-4.9	4.4	5.5 / 11.0	-4.8 / -9.2
$C_d^{H_2S}$ (%)	0.9	-0.9	5.7	-5.1	-4.4 / -8.8	3.8 / 7.4
$C_g^{H_2S}$ (%)	-9.1	9.0	-4.9	4.3	-4.3 / -8.8	3.9 / 7.4
$\phi_w^{S,Tot}$ (%)	0.9	-0.9	-4.9	4.3	5.4 / 10.8	-4.9 / -9.2
$\phi_w^{H_2S}$ (%)	1.1	-1.1	-4.7	4.7	-4.2 / -8.9	3.7 / 7.4
$\phi_w^{HS^-}$ (%)	1.2	-0.8	-4.7	4.7	12.9 / 25.5	-11.0 / -21.2
$\phi_d^{H_2S}$ (%)	0.9	-0.9	5.6	-5.0	-4.3 / -8.8	3.9 / 7.4
$\phi_g^{H_2S}$ (%)	-9.1	9.5	-4.9	4.3	-4.3 / -8.8	3.9 / 7.4

A similar response to variations in $He_w^{'}$ was found for the g/w/d system (Table 4). In conclusion a deviation of 10% in $He_w^{'}$ possibly caused by variations in temperature or due to a salting out effect will not affect the model prediction to a large extent. A change of 10% in m_{wd} for the g/w/d model generally caused a deviation of only 5% in the predictions summarized in Table 4, thus the model is rather insensitive for variation in this parameter. However, the results presented in Table 3 and 4 clearly show a high sensitivity of both models for variations of only 1 or 2% in the value of pK^{H_2S}. Consequently, a correct value for pK^{H_2S} is essential to gain adequate model predictions. The pH of the g/w or g/w/d system exerts a great influence upon the sulfide concentrations present in each phase. To access the influence of a 2% error in the pK^{H_2S} at a range of pH values, the expected deviations in each phase were calculated, as depicted in Fig. 7 on the next page. From the results presented in Fig. 7A it becomes clear that the errors are most pronounced in the vicinity of pK^{H_2S} and diminish if the pH < 6.4 or pH > 8. For the three phase system presented in Fig. 7B the errors reduce fast for pH < 6.4, but remain quite high at increasing pH.
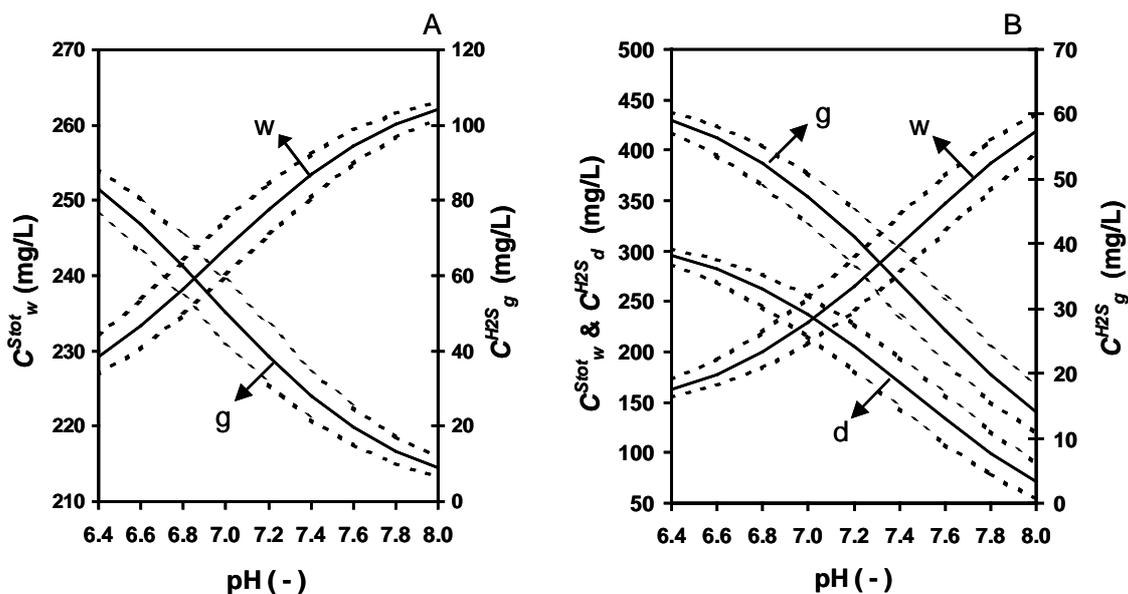
Fig. 7: Sensitivity analysis of the model predictions for a g/w system (A) and g/w/d system (B), respectively. Variation in the predicted concentrations in each phase involved upon a deviation of +/- 2% in the pK^{H_2S} value plotted versus the pH. The solid lines represent the original predictions, while the dashed lines represent the predictions using the positive and negative offset.

CONCLUSIONS

The modeling of the sulfide partition in gas/water and gas/water/*n*-dodecane systems was carried out successfully. Experimental results matched well with the model predictions. Furthermore, it was demonstrated that the influence of salting out effects on H_2S can be neglected up to salt concentrations of 500 mM. The model was only sensitive for variations in the pK^{H_2S} value, whilst changes in partition coefficients had no large effect on the model predictions.

The effect of the presence of a third, *i.e.* hydrocarbon phase (*n*-dodecane), notably decreased the total sulfide concentration in the water phase and the H_2S fraction in the gas phase. The *n*-dodecane phase apparently serves as a sink for H_2S molecules. This phenomenon can be used to remove H_2S in the anaerobic biodesulfurization process, *e.g.* by scrubbing the hydrocarbon phase to lower the H_2S concentration and lower the toxicity of H_2S towards microbiological conversion reactions.

NOMENCLATURE

$C_d^{H_2S}$	concentration of H₂S in the *n*-dodecane phase [kmol/m³]
$C_g^{H_2S}$	concentration of H₂S in the gas phase [kmol/m³]
$C_w^{H^+}$	concentration of H⁺ in the water phase [kmol/m³]
$C_w^{H_2S}$	concentration of H₂S in the water phase [kmol/m³]
$C_w^{HS^-}$	concentration of HS⁻ in the water phase [kmol/m³]
$C_w^{S,Tot}$	concentration of total sulfide (H₂S + HS⁻) in the water phase [kmol/m³]
C_s	concentration of salt, see Eq. 12 [kmol/m³]
c_1, c_2, c_3, c_4	constants defined in Eq. 3
C_i^{ion}	concentration of ion *i*, see Eq. 10 and 12 [kmol/m³]
$He_d^{'}$	dimensionless Henry's law coefficient for *n*-dodecane [-]
$He_w^{'}$	dimensionless Henry's law coefficient for water [-]
$He_0^{'}$	dimensionless Henry's law coefficient for water without ions, see Eq. 12 [-]
$He_s^{'}$	dimensionless Henry's law coefficient for water with ions, see Eq. 12 [-]
$He"$	Henry's law coefficient [MPa/(kmol/m³)]
h_i	ion-specific parameters with $i = Na^+$, Cl⁻ or HS⁻, see Eq. 12 [m³/kmol]
h_g	gas-specific parameter, see Eq. 12 and 13 [m³/kmol]
h_T	gas-specific parameter for the temperature effect, see Eq. 13 [m³/(kmol·K)]
I	ionic strength (kmol/m³)
K^{H_2S}	equilibrium constant for H₂S equilibrium [-]
K'	equilibrium constant, see Eq. 3 [mol/mol]
m_{dw}	partition coefficient between *n*-dodecane and water [m_w^3 / m_d^3]
m_{gw}	partition coefficient between gas and water [m_w^3 / m_g^3]
m_{gd}	partition coefficient between gas and *n*-dodecane [m_d^3 / m_g^3]
m_{gl}	partition coefficient between gas and liquid [m_l^3 / m_g^3]

MW_l	molecular weight of the liquid phase [kg/kmol]
n_{H_2S}	total amount of moles H_2S [mol]
N_i	number of ionic species, see Eq. 12 [-]
p_{H_2S}	partial pressure of H_2S [Pa]
R	gas constant [J/molK]
T	temperature (K or °C)
V_g	volume of the gas phase (m^3)
V_d	volume of the *n*-dodecane phase (m^3)
V_w	volume of the water phase (m^3)
z_i	charge of ion *i* [-]

greek

γ	activity coefficient [-]
$\phi_d^{H_2S}$	fraction of H_2S in the *n*-dodecane phase compared to the total sulfide [-]
$\phi_g^{H_2S}$	fraction of H_2S in the gas phase compared to the total sulfide [-]
$\phi_w^{H_2S}$	fraction of H_2S in the water phase compared to the total sulfide [-]
$\phi_w^{HS^-}$	fraction of HS^- in the water phase compared to the total sulfide [-]
$\phi_w^{S,Tot}$	fraction of total sulfide (H_2S + HS^-) in the water phase compared to the total sulfide [-]
κ	salting out coefficient [m^3/kmol]
$\kappa^{"}$	Sechenov constant [-]
ρ_l	density of the liquid phase [kg/m^3]

REFERENCES

Armstrong S.M., Sankey B.M., Verdouw G. 1997. Evaluation of sulfate reducing bacteria for desulfurizing bitumen or its fractions. Fuel Process. Technol. 76: 223-227.

Colleran E., Finnegan S., Lens P. 1995. Anaerobic treatment of sulfate-containing waste streams. Antonie van Leeuwenhoek 67: 29-46.

Edwards T.J., Maurer G., Newman J., Prausnitz J.M. 1978. Vapor-liquid equilibria in multicomponent aqueous solutions of volatile weak electrolytes. AIChE J. 24: 966-976.

Gas Research Institute. 1991. Research needs for acid gas kinetics and equilibria in alkanolamine systems. Chicago.

Gosset J.M. 1987. Measurement of Henry's law constants for C_1 and C_2 chlorinated hydrocarbons. Environ. Sci. Technol. 21: 202-208.

Hao J.H., Chen J., Huang L., Buglass R.L. 1996. Sulfate-reducing bacteria. Crit. Rev. Environ. Sci. Technol. 26: 155-187.

Kim B.Y., Kim H.Y., Kim T.S., Park D.H. 1995. Selectivity of desulfurization activity of *Desulfovibrio desulfuricans* M6 on different petroleum products. Fuel Process. Technol. 43: 87-94.

King M.B., Al-Najjar H. 1977. The solubilities of carbon dioxide, hydrogen sulfide and propane in some normal alkane solvents. I. Experimental determinations in the range 15-70ºC and comparison with ideal solution values. Chem. Eng. Sci. 32: 1241-1246.

Koster I.W., Rinzema A., de Vegt A.L., Lettinga G. 1986. Sulfide inhibition of the methanogenic activity of granular sludge at various pH-levels. Water Res. 20: 1561-1567.

Lens P.N.L., de Beer D., Cronenberg C.C.H., Houwen F.P., Ottengraf, S.P.P. 1993. Heterogeneous distribution of microbial activity in methanogenic aggregates: pH and glucose profiles. Appl. Environ. Microbiol. 59: 3803-3815.

Maillacheruvu K.M., Parkin G.F., Peng C.Y., Kuo W.C., Oonge, Z.I., Lebduschka V. 1993. Sulfide toxicity in anaerobic systems fed sulfate and various organics. Water Environ. Res. 65: 100-109.

McCartney D.M., Oleszkiewicz J.A. 1991. Sulfide inhibition of anaerobic degradation of lactate and acetate. Water Res. 25: 203-209.

Min H., Zinder S.H. 1990. Isolation and characterization of a thermopilic sulfate-reducing bacterium *Desulfotomaculum thermoacetoxidans* sp. nov. Arch. Microbiol. 153: 399-404.

O'Flaherty V., Mahony T., O'Kennedy R., Colleran E. 1998. Effect of pH on growth kinetics and sulfide toxicity thresholds of a range of methanogenic, syntrophic and sulfate-reducing bacteria. Process Biochem. 33: 555-569.

Okabe S., Nielsen P.H., Characklis W.G. 1992. Factors affecting microbial sulfate reduction by *Desulfovibrio desulfuricans* in continuous culture: limiting nutrients and sulfide concentration. Biotechnol. Bioeng. 40: 725-734.

Omil F., Lens P., Hulshoff Pol L.W., Lettinga G. 1996. Effect of upward velocity and sulfide concentration on volatile fatty acid degradation in a sulfidogenic granular sludge reactor. Process Biochem. 31: 699-710.

Oude Elferink S.J.W.H., Visser A., Hulshoff Pol L.W., Stams A.J.M. 1994. Sulfate reduction in methanogenic bioreactors. FEMS Microbiol. Rev. 15: 119-136.

Peng J., Wan A. 1997. Measurement of Henry's constants of high-volatility organic compounds using a headspace auto sampler. Environ. Sci. Technol. 31: 2998-3003.

Reid, Prausnetz, Poling. 1987. The properties of gases and liquids, 4th edition, McGraw-Hill, 341-351 and 597-600.

Reis M.A.M., Almeida J.S., Lemos P.C., Carrondo, M.J.T. 1992. Effect of hydrogen sulfide on growth of sulfate reducing bacteria. Biotechnol. Bioeng. 40: 593-600.

Reis M.A.M., Lemos P.C., Almeida J.S., Carrondo M.J.T. 1991. Evidence for the intrinsic toxicity of H₂S to sulfate reducing bacteria. Appl. Microbiol. Biotechnol. 36: 145-147.

Shennan J.L. 1996. Microbial attack on sulfur-containing hydrocarbons: implications for the biodesulfurization of oils and coals. J. Chem. Technol. Biotechnol. 67: 109-123.

Sillén L.G., Martell A.E. 1964. Stability constants of metal-ion complexes. The Chemical Society, Burlington House.

Steudel R. 2000. The chemical sulfur cycle. In: Environmental technologies to treat sulfur polution, principles and engineering. (Lens P.N.L., Hulshoff Pol L.W., eds.), 1 - 31 IWA Publishing, London.

Tsonopoulus C. 1976. Ionisation constants of water pollutants. J. Chem. Eng. Data 21: 190-193.

Uberoi V., Bhattacharya S.K. 1995. Interactions among sulfate reducers, acetogens and methanogens in anaerobic propionate systems. Water Environ. Res. 67: 330-339.

Van Houten R.T., Hulshoff Pol L.W., Lettinga G. 1994. Biological sulfate reduction using gas-lift reactors fed with hydrogen and carbon dioxide as energy and carbon source. Biotechnol. Bioeng. 44: 586-594.

Weiland R.H., Chakravarty T., Mather A.E. 1993. Solubility of carbon dioxide and hydrogen sulfide in aqueous alkanolamines. Ind. Eng. Chem. Res. 32: 1419-1430.

Xia J., Pérez-Salado Kamps Á., Rumpf B., Maurer G. 2000. Solubility of hydrogen sulfide in aqueous solutions of single strong electrolytes sodium nitrate, ammonium nitrate, and sodium hydroxide at temperatures from 313 to 393 K and total pressures up to 10 MPa. Fluid Phase Equilibr. 167: 263-284.

CHAPTER 7

SUMMARY AND
CONCLUDING REMARKS

SUMMARY

Distillates from crude oil such as diesel and fuel oil may contain significant amounts of dibenzothiophenes and their alkylated derivatives, containing organically bound sulfur. Combustion of those fossil fuels leads to the release of polluting sulfur dioxide into the atmosphere, where it causes 'acid rain'. Due to stricter environmental legislation and depletion of crude oil reserves with low organic sulfur contents, effective desulfurization processes are becoming increasingly important. For instance: beginning in 2005 the maximal allowable sulfur content in gas oil in the European Community will be 0.005 wt.%. Currently, the refining industry applies the energy intensive physico-chemical hydrodesulfurization (HDS) process in order to reduce the sulfur content. Due to the high costs and inherent chemical limitations associated with HDS, biodesulfurization of hydrocarbon streams might represent an attractive complementary method to obtain sufficiently low sulfur levels. Bacteria require relatively mild process conditions (pressure and temperature) and bacterial enzymes are very selective in converting target molecules. The objective of this thesis was to develop an anaerobic biodesulfurization process. The thesis is build up around the reductive desulfurization reaction presented below.
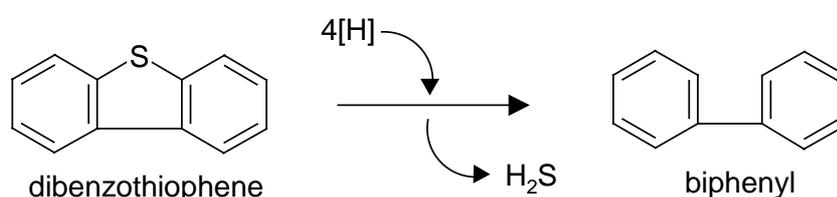
Dibenzothiophene (DBT) is converted under anaerobic conditions to biphenyl and sulfide with the concomitant conversion of reduction equivalents. The caloric value of the fuel molecule is retained and the sulfur is removed specifically.

Chapter 1 presents a general introduction on physico-chemical and microbiological methods to desulfurize organic sulfur compounds.

In Chapter 2 the DBT mass transfer rate within hydrocarbon droplets is compared to aerobic DBT conversion rates. The apolar DBT must diffuse to the hydrocarbon/water interface where bacteria prevail. The calculated values for the DBT mass transfer rate were compared to those found for aerobic DBT conversion rates, as reported in the literature. Temperature dependent data (ranging from 20 up to 60°C) of viscosity, density, and interfacial tension of various hydrocarbon distillates were incorporated in the model. The model simulated the DBT diffusion in hydrocarbon droplets as obtained in a stirred

tank reactor. Based on these calculations, we estimated that the mass transfer rate of DBT within the hydrocarbon droplet to the hydrocarbon/water interface is at least a factor 10 to 10^4 higher than the specific DBT conversion rates. However, the presence of a high specific surface area is essential to enhance the surface contact between bacteria and the hydrocarbon phase.

The availability of a suitable biomass is crucial to develop this new bioprocess. In Chapter 3 a screening method is described to enrich biomass from mixed bacterial populations obtained from oil-polluted environments. The enriched cultures were able to grow in the presence of thiophenes as the sole electron acceptor. A proof of principle was obtained; the formation of sulfide and biphenyl from dibenzothiophene was shown conclusively. Also thiophene and benzothiophene depletion with concomitant sulfide formation was observed. However, apart from sulfide no thiophene nor benzothiophene desulfurization products could be demonstrated. The main problem during consecutive enrichments was the loss of biological activity after transferring the desulfurizing biomass. A mixed population was present and the active desulfurizing biomass was easily overgrown by acetogenic bacteria. Therefore, it was attempted to isolate the desulfurizing bacteria. The isolation procedure resulted in the availability of highly enriched cultures able to desulfurize thiophenes when cultivated using a selective medium with H_2 as electron donor and limiting amounts of bicarbonate and acetate (1 mM each).

Based on process considerations H_2 gas is the most suitable electron donor for the reductive desulfurization process. In Chapters 4 and 5 attention is paid to the mass transfer rate of H_2 in a gas/water/hydrocarbon three-phase system using *n*-dodecane as model solvent. Because vigorous foam formation occurs when H_2 gas is directly added to a *n*-dodecane in water dispersion, it was proposed to saturate the *n*-dodecane with H_2 gas prior to disperse it into the water phase. Experiments to determine the H_2 mass transfer coefficients involved using physical methods are described in Chapter 4. The H_2 mass transfer coefficients between the gas and the *n*-dodecane phase (k_d) and between the gas and the water phase (k_w) were determined using a dynamic method by following the pressure decline in time, whilst the overall H_2 mass transfer coefficient between *n*-dodecane and water (k_{dw}) was determined using a steady state method. The value for k_{dw} was assessed using tritium-hydride (T-H instead of H-H) as the tracer. The effects of the temperature (30, 40 and 50°C) and salt concentrations (0-250 mM) were studied. The value for k_w [$(9.7 \pm 0.2) \times 10^{-5}$ ms^{-1} at 30°C] was found to be a factor 3.3 higher than for k_d [$(2.89 \pm 0.12) \times 10^{-5}$ ms^{-1} at 30°C] because of the lower viscosity of water. No effect was

found for the presence of salts (up to 250 mM NaCl) on the k_w-value. The k_{dw}-value determined in the steady state experiments at 30ºC was $(5 \pm 0.6) \times 10^{-6}$ ms^{-1} which is 19.4 times smaller than the above-mentioned k_w-value. The considerable smaller value for k_{dw} must be attributed to the additional mass transfer resistance introduced by the second liquid phase. Calculations of the maximal attainable H$_2$ flux revealed values of 0.016 x 10^{-3} mol/m^{2}s and 3.9 x 10^{-3} mol/m^{2}s for a *n*-dodecane/water and gas/water system, respectively. Therefore, the specific surface area between *n*-dodecane and water is the determining parameter for sufficient H$_2$ mass transfer. In Chapter 5, the H$_2$ mass transfer is described further using a bioreactor equipped with a nozzle to create very fine *n*-dodecane droplets. The specific surface area is dependent on the maximum attainable hold-up of *n*-dodecane and the diameter of the droplets. These parameters were studied in a model system consisting of *n*-dodecane and water supplemented with NaCl. The use of the nozzle resulted in droplets with a Sauter mean diameter of only 10.3±0.9 µm. The droplet size was found to be independent of the applied pressure drop over the nozzle. The hold-up of *n*-dodecane in the aqueous medium is clearly dependent on the sodium ion concentration. The hold-up decreases rapidly (from 0.14 to 0.04) with increasing sodium ion concentrations due to coagulation; from 94 mM onwards the hold-up becomes 0.04. The application of *n*-dodecane droplets as carrier phase for H$_2$ mass transfer was demonstrated in batch tests for biological sulfate reduction. During operation of the bioreactor, biomass attached to the rising *n*-dodecane droplets and eventually flotated from the system.

In addition biological steady state experiments were performed with hydrogenotrophic sulfate reducing bacteria to determine the H$_2$ mass transfer coefficient for a *n*-dodecane/water system (k_{dw}). A value of $(4.0\pm0.24) \times 10^{-6}$ ms^{-1} was found, which is close to the values found in the experiments using tritium hydride. Final calculations showed that the volumetric H$_2$ mass transfer rate (mol/m^{3}s) from *n*-dodecane to water can be comparable to values found for gas lift reactors, thus the high specific surface area that can be created by applying a nozzle can overcome the lower value of the H$_2$ flux (mol/m^{2}s) to a large extent.

Chapter 6 addresses the role of sulfide on anaerobic biodesulfurization. The presence of increased sulfide concentrations is undesirable because it is expected that sulfide will inhibit the DBT conversion. Therefore, insight in the partitioning of gaseous hydrogen sulfide (H$_2$S) over a three-phase gas/water/hydrocarbon system is required. The

partitioning of H_2S over a gas/water/*n*-dodecane system is described. Experimental results matched well with the model predictions. The effect of the presence of an extra hydrocarbon phase (*n*-dodecane) notably decreased the total sulfide in the water phase and the H_2S fraction in the gas phase. The hydrocarbon phase serves as a sink for H_2S molecules and by scrubbing the H_2S in a separate process step (*e.g.* during H_2 saturation) the sulfide concentration can be lowered to favor the anaerobic biodesulfurization.

CONCLUDING REMARKS

Microbiological aspects

Still many aspects on anaerobic desulfurization of organic sulfur compounds need to be clarified in future research. To date, no pure cultures have been described that show growth on thiophenic compounds. This is a prerequisite to study the physiology and genomics of anaerobic desulfurizing bacteria and to obtain insight in the formation of metabolites by characterization of products and conversion kinetics. The use of isolates is of less importance with respect to a practical biodesulfurization process. Sterile operation of a biodesulfurization system on a relevant scale is difficult to achieve and undesirable with respect to the investment costs. Furthermore, isolation procedures not only select for the capability of bacteria to convert organic sulfur compounds but *e.g.* also for the capability to grow in colonies on solid media. This can result in selecting for a strain with a lower activity compared to the original enrichment. Another approach mentioned in the current literature on aerobic desulfurization processes is the use of directed evolution by altering genes in such a way that the metabolic flux through the sulfur specific metabolic pathway is enhanced (see Chapter 1). Based on the current knowledge of anaerobic biodesulfurization genetic modification is not an option. Probably the best option is to use highly enriched biomass obtained from naturally occurring biomass as present in oil wells. The desulfurization capacity can be enhanced by the use of a concentrated cell suspension. Growth of bacteria that do not contribute to the desulfurization activity (*e.g.* acetogenic bacteria) must be prevented by the use of selective media (*i.e.* H_2 gas with limiting amounts of acetate and bicarbonate). The best way to further develop the process is to continuously search for suitable biomass, *i.e.* by enrichment on thiophenes as the sole electron acceptor. When the molecular mechanism of anaerobic desulfurization is known, molecular tools can also be used to facilitate the screening of samples by checking the presence of certain genes in a bacterial community (Duarte *et al.* 2001).

Engineering aspects

The potential of three-phase gas/water/hydrocarbon bioprocesses has not been realized in practice up to now, because the underlying engineering principles have not been sufficiently developed to allow further process development and scale-up. Generally, interphase mass transfer is considered as one of the most critical engineering parameters (*e.g.* Schmid *et al.*, 1998). Also, the effect of biomass on the performance of gas/water/hydrocarbon bioprocesses is still poorly understood.

In this thesis, the choice of the bioreactor configuration was based on the requirement of a high specific surface area of the hydrocarbon phase to enable an intimate biomass/substrate contact. Furthermore, the hydrocarbon phase was used as the carrier phase for the addition of H_2 gas. Unfortunately, thiophene reduction was insufficient to start up a desulfurization reactor. Therefore, hydrogenotrophic sulfate reducing bacteria were used in short-term batch experiments in order to demonstrate the principle of using *n*-dodecane as carrier phase for H_2. It was found that biomass started to flotate during operation, however no emulsification occurred. The flotation of biomass causes a reduced biomass/substrate contact. The addition of a recycle loop to the bioreactor configuration possibly can restore the biomass/substrate contact by continuously pumping flotated biomass to the lower region of the bioreactor. The question remains what happens with respect to emulsification when long-term continuous experiments are performed. The presence of proteins that accumulate at the liquid-liquid interface might prevent coalescence of the oil droplets, resulting in emulsification of the reactor content (Borole *et al.*, 2002). Consequently, separation of the hydrocarbon/water/biomass mixture will be very difficult and continuous operation is not possible.

As an alternative for the direct-contact system a membrane bioreactor could be considered. Although the problem of emulsification can be avoided because the phases are not mixed, operational difficulties will exist at a relevant scale. A careful control of the transmembrane pressure to avoid phase breakthrough is difficult, because the membrane properties are altered by the biocatalyst that adheres to the membrane (Schroen *et al.*, 1994; Vaida *et al.*, 1994a, b). Furthermore, clogging of the membranes will occur during operation (Srijaroonrat *et al.*, 1999; Fedorovich *et al.*, 2000). In addition, the mass transfer of organic sulfur compounds and H_2 over the membrane to the aqueous phase containing the bacteria should be sufficient. Based on the aforementioned disadvantages, a direct contact system where mixing of the hydrocarbon and aqueous phase occurs seems to be

the only feasible option and a downstream separation step treating a hydrocarbon/water/biomass mixture cannot be avoided.

The main condition set for the work described in this thesis was that the anaerobic biomass should utilize the thiophenes as the sole electron acceptor. Consequently, the activity on thiophenes is coupled to growth. Because of the slow conversion rates under anaerobic conditions, the water phase was chosen to be the continuous phase. A similar approach could be followed for the anaerobic conversion of water insoluble mercaptanes and chlorinated compounds.

If a concentrated cell suspension with a high activity would be available, a different process configuration could be considered. To optimize the process performance it is recommended to use water in hydrocarbon dispersions instead of hydrocarbon in water dispersions.

Kaufman *et al.* (1997) used a water in hydrocarbon dispersion to carry out aerobic biodesulfurization. Here, the aqueous biomass suspension is dispersed at the top of the vessel and flows downward through the hydrocarbon bulk phase by gravity. The tubular reactor (emulsion phase contactor) consists of a nozzle region and an operating region. In the nozzle region very fine aqueous droplets (3 up to 5 µm) are created using a vertical electrical field. The operating region contains a pair of parallel plate electrodes and controls the vertical motion of the aqueous droplets by a horizontal electrical field. Droplets are accelerated into the operating region and coalescence and redisperse continuously, while they shuttle between the plates (Byers and Amarnath, 1995). The droplets maintain their size and the net flow of the droplets is downward caused by gravity. The use of the electrical field enables in-situ separation.

Provided that no emulsification occurs this could be a technically feasible bioreactor set-up for anaerobic biodesulfurization. The in-situ separation allows continuous operation to maintain growth of the bacteria. The use of a water in hydrocarbon dispersion has the advantage that the bioavailability of reactants (organic sulfur compounds and H_2 gas) is optimal, while desulfurization products partition back into the hydrocarbon phase. Furthermore, the load of organic sulfur compounds can be varied easily. This is not possible in hydrocarbon in water systems, because the hold-up of the hydrocarbon phase is limited.

Another possibility to set-up a desulfurization process is the application of immobilization techniques, which entrap anaerobic bacteria in a support, such as: κ-carrageenan,

polyurethane and calcium alginate (*e.g.* Wijffels, 1994). Then, an active concentrated cell suspension should be available that is able to maintain the desulfurization activity in the support material using gaseous substrates (H_2 and CO_2). In this manner a two-phase system consisting of immobilized cells in a hydrocarbon phase is created and a complicated separation step is avoided, because emulsion formation is not possible. The process liquid should pass the biocatalyst bed (consisting of spherical beads where the bacteria are entrapped) at such a velocity that the beads are fluidized. Biodesulfurization should occur in the biocatalyst film simultaneously with mass transfer between the film and the hydrocarbon phase. Gaseous substrates (H_2 and CO_2) and products (H_2S) can be added and removed via the hydrocarbon phase. After reaction the beads can be separated from the hydrocarbon phase using a cyclone-type separator enabling the reuse of the biocatalyst, as described by Yu (1998). The success of this approach will be determined by performance of the immobilized biocatalyst. The activity of the biocatalyst should be stable over a longer time and the immobilization support must be able to handle the mechanical strength during separation to allow reuse. The main disadvantage of this approach is mass transfer limitation, because the reaction rate will be limited by the diffusive resistance of substrates (H_2, CO_2 and organic sulfur compounds) and products (hydrocarbon product after desulfurization and H_2S) over the support material (Brink and Tramper, 1986a, b). Naito *et al.* (2001) tested the DBT desulfurization using immobilized *Rhodococcus erythropolis* KA2-5-1 cells according to the aforementioned approach and found that the conversion rate was slower than what can be attained in a hydrocarbon/water/cell system.

The direct use of purified enzymes obtained from anaerobic biomass would take away constraints concerning biomass activity and mass transfer limitations. The approach of using enzymes in nearly anhydrous environments is followed in biocatalytic reactions such as chiral resolution and enantioselective synthesis of valuable organic compounds to produce pharmaceuticals and fragrance and flavor compounds (Griebenow *et al.*, 1999; Ke and Klibanov, 1999). However, a sequence of enzymes is probably involved in the conversion and oxido-reductases need to be added to sustain electron transport to the thiophenic compound that acts as the electron acceptor. Therefore, the use of enzymes seems not very promising in the reductive conversion of thiophenic compounds.

Potential of biodesulfurization

The location within the refinery where biodesulfurization may be applicable depends on the composition of the hydrocarbon stream. Refineries are quite different in the way the crude oil is processed. Generally, refineries in the USA are focused on the production of gasoline, while less gas oil is produced. The higher boiling point fractions (220 up to 350ºC) formed in the gas oil range after atmospheric distillation are treated in the Fluid Catalytic Cracker (FCC) unit to generate hydrocarbons in the gasoline range (boiling points of 95 up to 220ºC. In European refineries more distillates in the gas oil range are produced.

The question arises if biodesulfurization is an interesting technology to apply at a refinery and which hydrocarbon streams can be treated. As outlined in Chapter 1 there is a multitude of developments on physico-chemical techniques regarding catalyst performance and hydrodesulfurization (HDS) process configurations. It is obvious that biodesulfurization cannot be an alternative process to remove the bulk of sulfur present in various distillates, because HDS has a significant larger conversion capacity. This leaves two types of hydrocarbon streams where the bulk of sulfur is removed already during HDS, *viz.* (*i*) FCC gasoline and (*ii*) gas oil containing alkylated dibenzothiophenes that are refractory to HDS.

(*i*) Gasoline fractions predominantly contain: thiophene, 2-methyl- and 3-methyl thiophene as the sulfur species, which are not very amenable for biodesulfurization. In the aerobic 4S-pathway thiophene seems not to be converted (Izumi *et al.*, 1994; McFarland *et al.*, 1998). The results in this thesis (Chapter 3) show that conversion of thiophene under anaerobic conditions is likely to occur. In practice high amounts of low-weight hydrocarbons (*e.g.* benzene, toluene) are present, which are toxic to the bacteria (McFarland *et al.*, 1998). Currently, the refinery industry aims at removing the sulfur in the FCC feedstock to prevent the formation of organic sulfur compounds during the FCC process (Leflaive *et al.*, 2002).

Based on these arguments biodesulfurization of gasoline seems not an attractive option.

(*ii*) Very deep desulfurization of gas oil towards a zero sulfur content is very difficult to achieve with HDS, leaving refractory alkylated dibenzothiophene derivatives (see Chapter 1). Since bacterial enzymes are very specific, biodesulfurization could be a complementary method to polish the distillate fraction after HDS. A possible drawback for application is that large volumes with a low sulfur content must be treated. Consequently, high catalytic rates are important.

REFERENCES

Borole A.P., Kaufman E.N., Grossman M.J., Minak-Bernero V., Bare R., Lee M.K. 2002. Comparison of the emulsion characteristics of *Rhodococcus erythropolis* and *Escherichia coli* SOXC-5 cells expressing biodesulfurization genes. Biotechnol. Progr. 18: 88-93.

Brink L.E.S., Tramper J. 1986a. Modeling the effects of mass transfer on kinetics of propene epoxidation of immobilized *Mycobacterium* cells: 1. Pseudo-one-substrate conditions and negligible product inhibition. Enzyme Microb. Technol. 8: 281-288.

Brink L.E.S., Tramper J. 1986b. Modeling the effects of mass transfer on kinetics of propene epoxidation of immobilized *Mycobacterium* cells: 2. Product inhibition. Enzyme Microb. Technol. 8: 334-340.

Byers C.H., Amarnath A. 1995. Understanding the potential of electroseparations. Chem. Eng. Prog. 107: 63-69.

Duarte G.B., Rosado A.S., Seldin L., De Araujo W., Van Elsas J.D. 2001. Analysis of bacterial community structure in sulfurous-oil-containing soils and detection of species carrying dibenzothiophene desulfurization (*dsz*) genes. Appl. Environ. Microbiol. 67: 1052-1062.

Fedorovich V., Greben M., Kalyuzhnyi S., Lens P., Hulshoff Pol L.W. 2000. Use of hydrophobic membranes to supply hydrogen to sulfate reducing bioreactors. Biodegradation 11: 295-303.

Izumi Y., Oshiro T., Ogino H., Hine Y., Shimao M. 1994. Selective desulfurization of dibenzothiophene by *Rhodococcus erythropolis* D-1. Appl. Environ. Microbiol. 60: 223-226.

Kaufman E.N., Harkins J.B., Rodriguez M., Tsouris C., Selvaraz P.T., Murphy S.E. 1997. Development of an electro-spray bioreactor for crude oil processing. Fuel Process. Technol. 52: 127-144.

Leflaive P., Lemberton J.L., Pérot G., Mirgain C., Carriat J.Y., Colin J.M. 2002. On the origin of sulfur impurities in fluid catalytic cracking gasoline - reactivity of thiophene derivatives and of their possible precursors under FCC conditions. Appl. Catal. A-Gen. 227: 201-215.

McFarland B.L., Boron D.J., Deever W., Meyer J.A, Johnson A.R., Atlas R.M. 1998. Biocatalytic sulfur removal from fuels: applicability for producing low sulfur gasoline. Crit. Rev. Microbiol. 24: 99-147.

Naito M., Kawamoto T., Fujino K., Kobayashi M., Mauruhashi K., Tanaka A. 2001. Long-term repeated biodesulfurization by immobilized *Rhodococcus erythropolis* KA2-5-1 cells. Appl. Microbiol. Biotechnol. 55: 374-378.

Schmid A., Sonnleitner B., Witholt B. 1998. Medium chain length alkane solvent-cell transfer rates in two-liquid phase, *Pseudomonas oleovorans* cultures. Biotechnol. Bioeng. 60: 10-23.

Schroen C.G.P.H., Cohen Stuart M.A., Van der Padt A., Van 't Riet K. 1994. Minimum breakthrough pressure as a measure for wettability changes caused by protein adsorption at hydrophobic membranes. Bioseparation 4: 151-163.

Srijaroonrat P., Julien E., Aurelle Y. 1999. Unstable secondary oil/water emulsion treatment using ultrafiltration: fouling control by backflushing. J. Mem. Sci. 159: 11-20.

Vaidya A.M., Halling P.J., Bell G. 1994a. Surfactant induced breakthrough effects during the operation of two-phase biocatalytic membrane reactors. Biotechnol. Bioeng. 44: 765-771.

Vaidya A.M., Halling P.J., Bell G. 1994b. Aqueous-organic membrane bioreactors, Part. 2. Breakthrough pressure measurement. J. Mem. Sci. 97: 13-26.

Wijffels R.H. 1994. Nitrification by immobilized cells. PhD-thesis, Wageningen University.

Yu L.Q. 1998. Oil/water/biocatalyst three-phase separation process U.S. Patent 5,772,901.

SAMENVATTING

Oliedestillaten (bijvoorbeeld diesel) kunnen grote hoeveelheden dibenzothiofeen en met name gealkyleerde derivaten van dit molecuul bevatten. Deze dibenzothiofenen bevatten organisch gebonden zwavel. Om het milieu te beschermen is het van belang om het organisch gebonden zwavel te verwijderen, voordat het destillaat als brandstof wordt gebruikt. Op deze manier wordt de vorming van zwaveldioxide tijdens de verbranding voorkomen en het ontstaan van zure regen tegengegaan. Steeds strenger wordende normen met betrekking tot toelaatbare zwavelgehaltes in destillaten, alsmede een afname van de voorraad ruwe olie met lage zwavelgehaltes, zijn de oorzaak van een vergrote vraag naar effectieve ontzwavelingsprocessen. Op dit moment wordt in de raffinage-industrie het fysisch-chemische 'hydrodesulfurization' (HDS) proces toegepast om organisch gebonden zwavel te verwijderen. Het zwavel wordt met behulp van H_2 katalytisch omgezet naar H_2S bij hoge temperatuur en druk. Belangrijke nadelen van HDS zijn de hoge kosten en de intrinsieke chemische limitaties die ervoor zorgen dat het zwavel niet volledig kan worden verwijderd. Daarom is het van belang de mogelijkheden van biologische ontzwaveling als complementaire techniek te onderzoeken. Bacteriën voeren conversies uit bij milde proces condities (lage druk en temperatuur). Daarnaast zijn bacteriële enzymen in staat om conversies zeer specifiek te katalyseren.

Het doel van het onderzoek dat staat beschreven in dit proefschrift is het ontwikkelen van een anaëroob biologisch ontzwavelingsproces. De keuze voor een anaëroob (reductief) reactiemechanisme is gebaseerd op het behoud van de calorische waarde van de organische zwavelverbindingen na conversie. Dit kan worden geïllustreerd aan de hand van het volgende reactiemechanisme voor dibenzothiofeen (DBT):
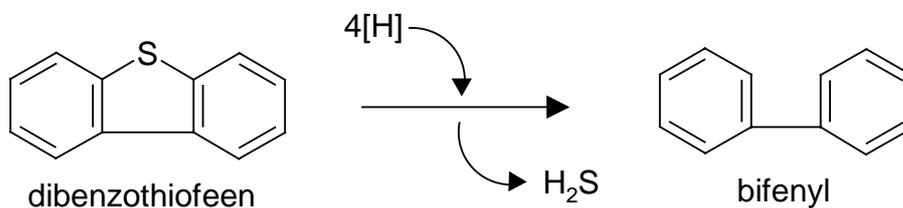
Het DBT wordt onder anaërobe condities omgezet naar bifenyl en sulfide waarbij reductie-equivalenten worden verbruikt. De calorische waarde van het DBT blijft behouden omdat geen koolstof-koolstof bindingen worden verbroken en het zwavel wordt specifiek verwijderd.

In Hoofdstuk 1 wordt een algemene introductie gegeven over bestaande fysisch-chemische en microbiologische methoden om organische zwavelverbindingen te ontzwavelen.

In Hoofdstuk 2 is de stofoverdrachtssnelheid van DBT in oliedruppels naar het olie/water-grensvlak beschreven voor verschillende oliefracties. Omdat DBT niet oplosbaar is in water, moet het apolaire DBT naar het olie/water-grensvlak diffunderen waar de bacteriën leven. De DBT stofoverdrachtssnelheid is vergeleken met in de literatuur gerapporteerde aërobe DBT conversiesnelheden, om te kunnen beoordelen of de diffusie van DBT naar het olie/water-grensvlak limiterend zou kunnen zijn voor het proces. In een model is de DBT stofoverdrachtssnelheid in verschillende typen destillaten beschreven. Hiertoe zijn temperatuursafhankelijke data voor de viscositeit, dichtheid en grensvlakspanning in het gebied van 20 tot 60°C gebuikt. Het model simuleert de DBT diffusie in oliedruppels zoals die worden gevormd in een geroerde tank reactor. De vergelijking van de DBT diffusiesnelheid in elke destillaatfractie is gemaakt op basis van een tijdsconstante analyse. De berekende tijdsconstanten voor DBT diffusie hebben een ordegrootte van seconden en zijn met name afhankelijk van de dynamische viscositeit (mPa s), de energiecapaciteit (W/kg) en de volumefractie oliefase (10 of 25% (v/v)). Op basis van berekeningen is geschat dat de DBT stofoverdrachtssnelheid in de oliedruppel naar het olie/water-grensvlak minimaal een factor 10 tot 10^4 hoger is in vergelijking met specifieke microbiële DBT omzettingssnelheden. Het is echter wel van belang kleine oliedruppels te maken om zo het specifieke oppervlak zo groot mogelijk te maken en daardoor het contact van bacteriën met de oliefase te maximaliseren.

Een voorwaarde voor toepassing van een anaëroob ontzwavelingsproces is de beschikbaarheid van biomassa. In Hoofdstuk 3 staat de gebruikte 'screeningsmethode' beschreven, waarbij gebruik is gemaakt van bacteriële mengpopulaties die zijn opgehoopt uit monsters van Russische olievelden. De cultures waren in staat te groeien met thiofenen als enige elektronacceptor. Hierbij is het principe van anaërobe ontzwaveling bewezen voor dibenzothiofeen, omdat de vorming van sulfide en bifenyl duidelijk is aangetoond. Tevens is afname in de thiofeen en benzothiofeen concentraties gevonden, waarbij ook sulfidevorming is aangetoond. De aanwezigheid van koolwaterstoffen na verwijdering van zwavel uit thiofeen en benzothiofeen kon echter niet worden aangetoond. Het grootste probleem tijdens de opeenvolgende ophopingsexperimenten was het verlies van de biologische activiteit na het door-enten van de biomassa. De biomassa die verantwoordelijk was voor de omzetting van thiofenen werd snel overgroeid door

acetogene bacteriën die ook in de mengpopulatie aanwezig waren. Om toch een stabiele conversie te krijgen is geprobeerd om de ontzwavelende bacteriën te isoleren. De uitgevoerde isolatieprocedure heeft geleid tot het vinden van twee cultures die thiofenen kunnen ontzwavelen. Omdat de cultures echter niet volledig rein waren, moest wel een selectief medium worden toegepast met H_2 als elektrondonor en limiterende hoeveelheden bicarbonaat en acetaat (1 mM) om groei van acetogene bacteriën te voorkomen. In deze studie is bewezen dat thiofenen anaëroob kunnen worden omgezet, maar de groei van de bacteriën is helaas beperkt.

Uit het oogpunt van een effectieve procesvoering is H_2 gas de meest geschikte elektrondonor. In de Hoofdstukken 4 en 5 wordt de stofoverdrachtssnelheid van H_2 in een gas/water/olie drie-fase systeem beschreven, waarbij *n*-dodecaan is gebruikt als model oliefractie. Wanneer H_2 gas direct aan een dispersie van *n*-dodecaan in water wordt toegevoegd ontstaat ongewenste schuimvorming. Daarom is voorgesteld het *n*-dodecaan eerst met H_2 te verzadigen, voordat het als kleine druppels wordt gedispergeerd in de waterfase. Het H_2 wordt dan overgedragen via de *n*-dodecaanfase. Het toepassen van deze strategie resulteert in een goede beschikbaarheid van H_2 en in een optimale beschikbaarheid van de organische zwavelcomponenten. Om een inschatting te maken van de effectiviteit van deze methode zijn de betrokken H_2 stofoverdrachtscoëfficiënten bepaald.

In Hoofdstuk 4 staan fysische experimenten beschreven waarmee de H_2 stofoverdrachtscoëfficiënten zijn afgeleid. De H_2 stofoverdrachtscoëfficiënt tussen de gas en de *n*-dodecaanfase (k_d) en tussen de gas en de waterfase (k_w) zijn bepaald met een dynamische methode waarbij de drukval in de tijd is gemeten. De H_2 stofoverdrachtscoëfficiënt tussen de *n*-dodecaan- en de waterfase (k_{dw}) is bepaald aan de hand van een 'steady-state' methode. Hierbij is gebruik gemaakt van tritium-hydride (T-H in plaats van H_2) als 'tracer', omdat H_2 in *n*-dodecaan niet rechtstreeks kan worden gemeten. Verder is de invloed van temperatuur (30, 40 and 50°C) en zoutconcentratie (0-250 mM NaCl) op de k_w-waarde bestudeerd. De berekende waarde voor k_w [(9.7 ± 0.2) x 10^{-5} ms^{-1} bij 30ºC] is een factor 3.3 groter dan die voor k_d [(2.89 ± 0.12) x 10^{-5} ms^{-1} bij 30ºC], wat kan worden toegeschreven aan de lagere viscositeit. De aanwezigheid van NaCl (tot 250 mM) heeft geen grote invloed op de waarde voor k_w. De k_{dw}-waarde die is bepaald in 'steady-state' experimenten bij 30ºC bedraagt (5 ± 0.6) x 10^{-6} ms^{-1} en is een factor 19.4 kleiner dan de waarde die is gevonden voor een gas/water-systeem (k_w). De lagere waarde voor k_{dw} is het resultaat van de extra weerstand voor de stofoverdracht die

169

wordt geïntroduceerd door de aanwezigheid van een extra vloeistoffase. Uit berekeningen voor de maximaal haalbare H_2-flux volgen waarden van respectievelijk: 0.016 x 10^{-3} mol/m^{2}s of 3.9 x 10^{-3} mol/m^{2}s voor een *n*-dodecane/water- of gas/water-systeem. Hieruit blijkt duidelijk dat het specifiek oppervlak tussen *n*-dodecaan en water bepalend is voor de effectiviteit van de totale H_2 stofoverdracht. Deze waarde moet groot genoeg zijn om te compenseren voor de lagere stofoverdrachtssnelheden.

In Hoofdstuk 5 wordt verder ingegaan op de H_2 stofoverdracht. Hier wordt een bioreactor systeem beschreven dat is uitgerust met een 'nozzle' waarmee de oliefase (*n*-dodecaan) als zeer kleine druppels in de continue waterfase kan worden gedispergeerd (='vernevelen'). Het specifiek oppervlak dat beschikbaar is voor stofoverdracht is afhankelijk van de maximale volume fractie *n*-dodecaan die in de vorm van druppels in de waterfase aanwezig kan zijn en de diameter van deze druppels. Deze parameters zijn bestudeerd in een modelsysteem waarbij *n*-dodecaan met een 'nozzle' is gedispergeerd. De waterfase bevatte NaCl om de invloed van zout op de oliedruppels te bestuderen, bacteriën waren afwezig. De gemiddelde diameter van de gevormde druppels in het systeem was 10.3±0.9 μm. De volumefractie *n*-dodecaan die het water kan bevatten ('hold-up') is afhankelijk van de natrium-ion concentratie. De hold-up neemt af (van 0.14 tot 0.04) met een toenemende natrium-ion concentratie. Dit effect wordt veroorzaakt door coaggulatie (uitvlokken) van de oliedruppels. Voor natrium-ion concentraties groter dan 94 mM stabiliseert de hold-up rond de waarde 0.04.

Het concept om H_2 via *n*-dodecaan over te dragen naar de waterfase is ook getest in een bioreactor. De H_2 stofoverdracht is bestudeerd in een batch-experiment met hydrogenotrofe sulfaatreducerende bacteriën, waarbij continu H_2 verzadigd *n*-dodecaan in de waterfase werd gedispergeerd. Gedurende deze test werd waargenomen dat de biomassa floteerde als gevolg van de continue injectie van het *n*-dodecaan.

Verder is de H_2 stofoverdrachtscoëfficiënt van *n*-dodecaan naar water onderzocht met behulp van hydrogenotrofe sulfaatreducerende bacteriën. Dit biologische 'steady-state' experiment heeft een k_{dw}-waarde opgeleverd van (4.0±0.24) x 10^{-6} m·s^{-1}. Deze waarde heeft dezelfde ordegrootte als de waarden die zijn gevonden in de fysische 'steady-state' experimenten met tritium-hydride. Uit berekeningen van de volumetrische H_2 flux (mol/m^{3}s) van *n*-dodecaan naar water kon worden afgeleid dat het grote specifieke oppervlak dat kan worden gecreëerd door *n*-dodecaan met een 'nozzle' te dispergeren de

lagere waarde voor de H_2 flux (mol/m^{2}s) voor een groot deel kan compenseren, waardoor een vergelijkbare volumetrische flux kan worden bereikt.

De aanwezigheid van sulfide in het medium waar de anaërobe ontzwavelingsreacties plaatsvinden is niet gewenst, omdat hierdoor remming van de omzetting kan optreden. Daarom is het van belang om inzicht te hebben in de partitie van sulfide in een gas/water/olie-systeem. In Hoofdstuk 6 is de partitie van H_2S over een gas/water/*n*-dodecaan-systeem modelmatig beschreven. De modelvoorspellingen zijn gecontroleerd door middel van experimenten en hieruit komt naar voren dat de voorspellingen goed aansluiten bij de meetwaarden. Het effect van de aanwezigheid van een extra oliefase (*n*-dodecaan) heeft een grote invloed op de totale sulfideconcentratie in de waterfase en de H_2S fractie in de gasfase. Het H_2S lost goed op in de oliefase en dit effect kan worden gebruik om het H_2S effectief te verwijderen. In een aparte processtap kan het H_2S gestript worden, bijvoorbeeld tijdens de H_2 verzadiging van de oliefase.

DANKWOORD

Het proefschrift is af! Een grote club van collega's en andere betrokkenen hebben bijgedragen aan dit werk en zonder hun hulp zou het proefschrift niet zijn geworden zoals het nu is. Natuurlijk wil ik iedereen voor deze samenwerking bedanken (nu ben ik dus niemand vergeten). Toch wil ik de gelegenheid aangrijpen een aantal mensen speciaal te noemen. Albert, jij hebt je rol als co-promotor meer dan serieus genomen. Jouw kritische blik, je vermogen om complexe materie te doorzien en het genereren van creatieve ideeën zijn het onderzoek zeker ten goede gekomen. Verder heb je veel energie gestoken in het corrigeren van mijn schrijfsels. Voor dit alles ben ik je zeer erkentelijk en ik heb er veel van geleerd. Gatze, vanaf het begin was jij mijn promotor en je hebt mij het belang van de toepasbaarheid van wetenschap bijgebracht. Fons, ik ben erg blij dat ik altijd welkom bij je was om over ideeën te discussiëren en jouw begeleiding tijdens de schrijffase heb ik zeer gewaardeerd. Bedankt voor je inzet en interesse in mijn werk, fijn dat je ook mijn promotor wil zijn. Look, bedankt voor het mede begeleiden van de milieutechnologie studenten. Ineke, jouw inbreng en verhelderende kijk op zaken in het stofoverdracht en partitie onderzoek had ik niet willen missen. Tenslotte Cees, bedankt dat je dit project aan mij hebt toevertrouwd.

Mijn directe collega's bij Paques in het lab en de proefhal hebben mij een prettige werksfeer en de mogelijkheden geboden om dit onderzoek uit te voeren. Dus: Bob, Hans, Jane, Hillie, Klaas, Marga, Mark (2x), Meine, Olga, Pascal, Ramon, Sake, Sandra, Simon, Welmoed, Wim en Wobby, bedankt allemaal! Een aantal jokers uit het rijtje hierboven waarmee ik 's middags na de lunch ging wandelen zal ik voorlopig niet vergeten. Verder natuurlijk de mensen van de 'pilot groep' en het secretariaat die altijd voor mij/ons klaar stonden ter ondersteuning van het project, bedankt hiervoor!

Gelukkig heb ik nog een aantal studenten onder mijn hoede gehad. Jullie werk is helaas niet allemaal in het proefschrift terechtgekomen, maar dat maakt het niet minder belangrijk. Michiel, Yvonne, Sjoerd, Clemens, Bart, Mark, Annereinou, Josina, Jack, Christa, Hans, Poppy, Claudia en John; bedankt voor alles wat jullie mij hebben geleerd.

Door de jaren heen ben ik veel te gast geweest bij het Laboratorium voor Microbiologie en ik wil iedereen daar bedanken voor de gastvrijheid. Om beesten zo gek te krijgen thiofenen te gebruiken als elektronacceptor heb ik lange tijd mogen samenwerken met Anna Ivanova. Anna, thanks for all the work you did on this topic and for your cooperation. I am still amazed about the amount of experiments you can perform in a short time.

Ik heb ook nog mogen samenwerken met industriële partners. De samenwerking met Sjoerd Kijlstra en Pierre van Grinsven van Shell Global Solutions en Blaise Arena van UOP is zeer waardevol geweest voor het project. Sjoerd; bedankt voor alle data, oliedestillaten en contacten met mensen die je voor me geregeld hebt. Zonder deze waardevolle informatie waren veel experimenten anders gelopen. Blaise; thanks for all your ideas, suggestions and analyses of oil samples you have arranged for me.

Natuurlijk wil ik ook mijn familie en vrienden bedanken voor de steun en interesse die ze hebben getoond. Als laatste wil ik mijn vrouw Sandra bedanken voor de onvoorwaardelijke steun van de afgelopen jaren. Wij zijn er samen voor gegaan en buiten dit proefschrift zijn we nog een veel groter 'project' begonnen: onze twee fantastische kinderen!

CURRICULUM VITAE

De schrijver van dit proefschrift werd op 10 februari 1971 geboren te Best. Na het doorlopen van de middelbare school, begon hij met een studie Bioprocestechnologie aan de Landbouwuniversiteit Wageningen. Tijdens de doctoraalfase heeft hij afstudeervakken gedaan bij de vakgroepen Microbiologie, Organische Chemie en Proceskunde. Een stage werd afgelegd bij de vakgroep Enzymologie en Microbiologie van de Technische Universiteit Delft. Na het afronden van zijn studie eind 1996, begon hij in april 1997 aan een promotieproject bij Paques B.V. in Balk waar hij tot en met mei 2002 heeft gewerkt als onderzoeker. Het promotieonderzoek werd uitgevoerd in samenwerking met het Laboratorium voor Microbiologie en de Sectie Milieutechnologie van Wageningen Universiteit, het Cluster Technische Scheikunde van Rijksuniversiteit Groningen en de bedrijven Shell Global Solutions B.V. en Universal Oil Products (USA). De resultaten van dit onderzoek staan beschreven in dit proefschrift. Van juni tot en met november 2002 heeft hij als post-doc gewerkt aan de schuimvorming in sulfide-oxiderende bioreactorsystemen bij het Laboratorium voor Fysische Chemie en Kolloïdkunde (Wageningen Universiteit). Vanaf december 2002 is hij werkzaam als 'program-officer' bij de technologiestichting STW in Utrecht.

List of publications

Oude Elferink S.J.W.H., Luppens S.B.I, Marcelis C.L.M., Stams A.J.M. 1998. Kinetics of acetate oxidation by two sulfate reducers isolated from anaerobic granular sludge. Applied and Environmental Microbiology 64: 2301-2303.

Heinsman N.W.J.T., Orrenius S.C., Marcelis C.L.M., De Sousa Teixeira A., Franssen M.C.R., Van de Padt A., Jongejan J.A., De Groot Ae. 1998. Lipase mediated resolution of γ-branched chain fatty acid methyl esters. Biocatalysis and Biotransformation. 16: 145-162.

Janssen A.J.H., Marcelis C.L.M., Buisman C.J.N. 1999. Industrial applications of new sulfur biotechnology. Water21-nov/dec

Marcelis C.L.M., Van Leeuwen M., Polderman H.G., Janssen A.J.H., Lettinga G. Model description of dibenzothiophene mass transfer in oil/water dispersions with respect to biodesulfurization. *Accepted for publication in Biochemical Engineering Journal.*

Marcelis C.L.M., Ivanova A.E., Janssen A.J.H., Stams A.J.M. Anaerobic biodesulfurization of thiophenes by mixed microbial communities from oilfields. *Accepted for publication in Biodegradation.*

Marcelis C.L.M., Sutanto-Versteeg, P.J., Janssen A.J.H., Ganzeveld K.J. Hydrogen mass transfer from *n*-dodecane to water, determination of the mass transfer coefficients in a three-phase system. *Submitted for publication in Biotechnology and Bioengineering.*

Marcelis C.L.M., Kuitert S., Gielen J.G.M., Ganzeveld K.J., Stams A.J.M., Janssen A.J.H. Determination of the hydrogen mass transfer in a three-phase sulfate reducing bioreactor. *Submitted for publication in Biotechnology and Bioengineering.*

Marcelis C.L.M., Cifuentes-Varona C.X., Stams A.J.M., Ganzeveld K.J., Janssen A.J.H. Partitioning of hydrogen sulfide in a three-phase system. *Submitted for publication in Bioprocess and Biosystems Engineering.*

De grote tragedie van de wetenschap

is het omverwerpen van een schone

hypothese door een akelig feit.

T.H. Huxley, Collected Assays.

Front cover thesis: manipulated picture of a *n*-dodecane 'cloud' emerging from a nozzle.

Work on photographs: Gert Buurman